Investigation of type 2 cytokine pathways as modulators of haematopoiesis during chronic inflammation

James William Swann

St Edmund Hall

A thesis submitted for the degree of Doctor of Philosophy

December 2020

Abstract

Chronic inflammatory diseases often promote bone marrow (BM) myelopoiesis at the expense of erythropoiesis and lymphopoiesis, facilitating production of mature myeloid cells to sustain the inflammatory response. In previous studies, type 2 cytokines, including IL-4, IL-5, and IL-33, have been suggested as possible regulators of haematopoiesis, but their role in modulation of haematopoiesis during inflammation was unknown. Spondyloarthritis (SpA) is a chronic inflammatory disease of people that has systemic sequelae, including anaemia. Although associated with type 17 immune responses, there is evidence of a concurrent type 2 response in the intestine of people with SpA. In this thesis, I sought to bring these areas of investigation together by asking if a possible type 2 immune module in murine SpA might be implicated in changes in haematopoiesis, and whether this would be important for progression of disease.

I find inflammation perturbs haematopoiesis in murine SpA, causing a marked bias towards myelopoiesis in the BM, as well as accumulation of myeloid progenitors in spleen and inflamed joints. Conversely, BM erythropoiesis is suppressed, resulting in anaemia. I find that mice also have evidence of a type 2 immune module in the intestine, with increased numbers of cells producing IL-4 and IL-5, and increased production of IL-33. Of these cytokines, IL-4 has pro-myelopoietic effects *in vivo* and *ex vivo*, but my results suggest this pathway is not important for development of clinical disease or expansion of myelopoiesis in SpA. Conversely, I find that IL-33 specifically suppresses differentiation of erythroid progenitors. This effect is implicated in development of anaemia in SpA, with IL-33 also causing resistance to the effects of erythropoietin (EPO). Interleukin-33 also promotes myelopoiesis through a combination of direct and indirect effects on progenitor stages, indicating that IL-33 has co-ordinated effects in different parts of the haematopoietic system that may be consistent with its role as an alarmin.

Collectively, my work reveals IL-4 and IL-33 as regulators of myelopoiesis, which may be important in disease settings associated with increased production of these cytokines. I further identify IL-33 as a mediator of anaemia of inflammatory disease and EPO resistance in murine SpA, suggesting that IL-33 could be a therapeutic target for this prevalent and debilitating comorbidity in people with chronic inflammation.

Acknowledgments

I am grateful to my supervisors, Dr Thibault Griseri and Professor Fiona Powrie, for their input in my studies and thesis. I also thank the members of my thesis committee, Dr Roy Drissen, Dr Emily Thornton, and Professor Paul Bowness for their advice on the project.

I wish to thank the Kennedy Trust for Rheumatology Research for funding my DPhil.

I am grateful to many members of staff and students at the Kennedy Institute of Rheumatology for their assistance with techniques and materials during this project.

Declaration

Except where stated, this thesis is the result of my own work. The following experiments were completed with assistance from others:

Dr Lada Koneva completed the RNA sequencing analysis of erythroid progenitors; her analysis is included in this thesis with her permission (chapter 5.2.7).

Fluorescence activated cell sorting was completed by Mr Jonathan Webber of the Kennedy Institute Flow Cytometry Core Facility.

Histological sections were produced by the Kennedy Institute Histology Core Facility.

Dr Daniel Regan-Komito, Dr Thibault Griseri, and Dr Stephen Sansom produced RNA sequencing data from purified stem and progenitor populations before I commenced by DPhil project; I consulted these data for my thesis.

Dr Daniel Regan-Komito and Dr Thibault Griseri assisted with set-up and culling of *in vivo* experiments described in chapters 3 and 4.

Dr Tal Arnon injected the chimeras described in chapter 3.2.2.

With the permission of the publishers and the other authors, some of the work in this thesis is reproduced from the papers ‘IL-33 promotes anemia during chronic inflammation by inhibiting differentiation of erythroid progenitors’ (2020) J Exp Med 217(9): e202000164 by JW Swann, LA Koneva, D Regan-Komito, SN Sansom, F Powrie, and T Griseri, and ‘GM-CSF drives dysregulated hematopoietic stem cell activity and pathogenic extramedullary myelopoiesis in experimental spondyloarthritis’ (2020) Nat Commun 11:155 by D Regan-Komito, JW Swann, P Demetriou, ES Cohen, NJ Horwood, SN Sansom, and T Griseri.

SARS-CoV-2 Statement

When the University of Oxford closed in March 2020, a number of mice were culled that I had intended to use for experiments in this thesis. Owing to delays in re-establishing some lines, I chose to produce mixed bone marrow chimeras using B6.SJL-*Ptprc*^{a} (i.e. CD45.1^{+}) recipient mice rather than the C57BL/6-*Ubc*^{GFP} mice I had wished to use. The results of this experiment are shown in chapter 6.2.4. This experiment has produced useful results, but these are difficult to interpret fully because erythroid cells do not express CD45. The limitations of this experiment are discussed further in chapter 6.

Abbreviations

5-FU	5-fluorouracil
7-AAD	7-aminoactinomycin D
AIA	Antigen-induced arthritis
AID	Anaemia of inflammatory disease
ANOVA	Analysis of variance
AS	Ankylosing spondylitis
BFU-E	Blast-forming unit - erythroid
BM	Bone marrow
BMP4	Bone morphogenetic protein 4
BrdU	Bromodeoxyuridine
BSA	Bovine serum albumin
CAR	CXCL12 abundant reticular cell
CDK	Cyclin-dependent kinase
C/EBP-α/β	CCAAT-enhancer binding protein alpha/beta
CFSE	Carboxyfluorescein succinimidyl ester
CFU-E	Colony-forming unit - erythroid
CFU-G	Colony-forming unit - granulocyte
CFU-M	Colony-forming unit - macrophage
CFU-GM	Colony-forming unit – granulocyte/macrophage
CIA	Collagen-induced arthritis
cMoP	Common monocyte progenitor
CMP	Common myeloid progenitor
DAPI	4’,6-diamidino-2-phenylindole
DC	Dendritic cell
DNA	Deoxyribonucleic acid
DSS	Dextran sodium sulphate
E	Embryonic day
ELISA	Enzyme-linked immunosorbent assay
EMH	Extramedullary haematopoiesis
EMSA	Electrophoretic mobility shift assay
EoP	Eosinophil progenitor
EPCR	Endothelial protein C receptor
EPO	Erythropoietin
EPO-R	Erythropoietin receptor
ERK	Extracellular signal-related protein kinase
ESAM	Endothelial cell-selective adhesion moledule
FACS	Fluorescence activated cell sorting
FCS	Fetal calf serum
Flt3	Fms-like tyrosine kinase 3
FMO	Fluorescence minus one
FOG-1	Friend of GATA 1
GALT	Gut-associated lymphoid tissue
G-CSF	Granulocyte colony stimulating factor
GFP	Green fluorescent protein
GM-CSF	Granulocyte macrophage colony stimulating factor
GMP	Granulocyte macrophage progenitor
GSEA	Gene set enrichment analysis
GWAS	Genome-wide association study

Gy	Gray
Hgb	Haemoglobin
HMBA	Hexamethylene bisacetamide
HSC	Haematopoietic stem cell
HSPC	Haematopoietic stem and progenitor cells
IGF-1	Insulin-like growth factor 1
IBD	Inflammatory bowel disease
IL	Interleukin
IL1RAP	IL-1 receptor accessory protein
IFN	Interferon
IKKγ	IκB kinase γ
ILC	Innate lymphoid cell
ILC2P	ILC2 progenitor
IMDM	Iscove's modified Dulbecco medium
IP	Intraperitoneal
IRAK4	IL-1 receptor associated kinase 4
IRS	Insulin receptor substrate
JAK2	Janus kinase 2
LepR	Leptin receptor
LK	Lineage$^-$, c-Kit$^+$ cells
LMPP	Lymphoid/myeloid progenitor
LPS	Lipopolysaccharide
LSK	Lineage$^-$, c-Kit$^+$, Sca-1$^+$ cells
M-CSF	Macrophage colony stimulating factor
MEL	Murine erythroleukaemia
MEP	Megakaryocyte/erythroid progenitor
MPP	Multipotent progenitor
MSC	Mesenchymal stem/stromal cell
mTORC	Mammalian target of rapamycin complex
MyD88	Myeloid differentiation primary response 88
NBD	NEMO domain binding
NG2	Neural-glial antigen 2
OBC	Osteoblastic lineage cell
PBS	Phosphate buffered saline
PDGFRα	Platelet-derived growth factor receptor alpha
PDK1	Protein-dependent kinase 1
PMA	Phorbol 12-myristate 13-acetate
Pre-CFU-E	Pre-colony-forming unit - erythroid
Pre-GM	Pre-granulocyte macrophage progenitor
Pre-MegE	Pre-megakaryocyte erythroid progenitor
PsA	Psoriatic arthritis
RA	Rheumatoid arthritis
RBC	Red blood cell
RNA	Ribonucleic acid
RORγt	RAR related orphan receptor γt
RT-qPCR	Reverse transcriptase quantitative polymerase chain reaction
S	Serine
SCF	Stem cell factor
SD	Standard deviation
SEM	Standard error of the mean

SFEM	Serum-free expansion medium
SpA	Spondyloarthritis
SPF	Specific pathogen free
STAT	Signal transducer and activator of transcription
ST2	Suppressor of tumorigenicity 2
T	Threonine
TCR	T cell receptor
TGF-β	Transforming growth factor beta
TLR	Toll-like receptor
TNBS	2,4,6-trinitrobenzene sulphonic acid
TNF-α	Tumour necrosis factor alpha
TNFR	TNF receptor
Treg	Regulatory T cell
TSLP	Thymic stromal lymphopoietin
Ub	Ubiquitin
VCAM-1	Vascular cell adhesion molecule 1
WBC	White blood cell
WT	Wild type

Contents

Figures

1 Introduction

1.1 Haematopoiesis

1.1.1 Definition

Haematopoiesis refers to the production of blood cells through orderly differentiation of haematopoietic stem cells (HSCs) and their progeny; all circulating blood cells are derived from HSCs. During murine embryogenesis, haematopoietic cells are first detected in the yolk sac around embryonic day (E)7 [1, 2], but cells with the properties of definitive HSCs arise by E10.5-11.5 in the aorta-gonad-mesonephros region [3, 4]. HSCs to circulate to the fetal liver by E12.5 [5] and fetal spleen by E14.5 [6]. Development of the fetus during gestation and early postpartum life are dependent on the haematopoietic cells produced at these locations but, beginning shortly after parturition, HSCs migrate to the medullary cavities of bone to produce the haematopoietic constituents of bone marrow (BM). After this time, definitive haematopoiesis is located principally in the BM in mammals, but haematopoietic cells are also produced in the spleen of healthy adult mice.

1.1.2 Structure and organisation

Haematopoietic stem cells self-renew throughout the life of animals, meaning they can divide in a manner that permits one or both daughter cells to retain the attributes of the parent stem cell. Additionally, HSCs are multipotent, with the ability to produce progeny of many, discrete lineages. Consequently, transplantation of single HSCs into lethally irradiated recipients is sufficient to restore a complete haematopoietic compartment [7-10], and the defining attribute of self-renewal of

HSCs is demonstrated by their ability to achieve similar reconstitution across 2-3 serial transplantations [11]. Despite these properties, most HSCs spend the majority of their time in a quiescent state, only dividing occasionally to produce highly proliferative multipotent progenitors (MPPs), which have limited capacity to self-renew but retain the ability to produce cells of many lineages. Most of the daily haematopoietic output of the BM is attributable to division of cells of this type [12, 13], which progressively differentiate into lineage-committed progenitors that produce a restricted range of mature cells. In this thesis, I use the term 'haematopoietic stem and progenitor cells' (HSPCs) to refer collectively to HSCs and all types of MPP and lineage-committed progenitor.

Owing to these features, others have described haematopoiesis as a pyramidal hierarchy capped by rare HSCs producing tiers of cells that are progressively more proliferative, abundant, and committed to particular lineages [14]. Traditionally, models describing this hierarchy have implied that HSPCs pass through discrete stages defined by expression of characteristic surface markers [14-16]. However, analysis of the transcriptome of single HSPCs indicates this process is continuous, with no discrete stages separating HSCs from mature progeny [17-20]. Consequently, although evaluation of surface marker expression is used frequently for identification of different HSPC populations, these definitions probably describe heterogeneous populations of cells that occupy different but propinquitous points in the same differentiation trajectory [21].

1.1.3 HSPC biology

At any time, the majority (~70%) of adult HSCs reside in a quiescent state outside the cell cycle [22, 23], as indicated by absence of proliferation markers like

Ki67 and failure to incorporate synthetic nucleotides that would indicate active DNA synthesis. This quiescence is not observed in fetal HSCs but prevails as definitive haematopoiesis emerges in the BM, possibly dependent on cell-intrinsic transcription factors [24] and interaction with the niche. Others have proposed that quiescence is a mechanism permitting HSCs to maintain the capacity to self-renew throughout the life of animals by providing time for DNA repair [25, 26] and removal of improperly folded proteins [27], and by alleviating metabolic stress associated with oxidative phosphorylation [28, 29] and exposure to reactive oxygen species [30, 31]. In support of this notion, exposure of HSCs to stimuli that cause emergence from quiescence, such as granulocyte colony stimulating factor (G-CSF) [32, 33], type I [34, 35] or II [36-39] interferons, or pathogen derivatives [40-43], decreases their fitness in repopulation assays that force them to compete against HSCs from healthy mice. The self-renewal potential of HSCs in transplantation assays is therefore correlated with the length of time spent in quiescence [23, 44], with repeated cell divisions in adulthood leading to irreversible loss of this attribute [45]. Artificial loss of quiescence caused by deletion of critical regulating factors produces a phenotype of BM failure owing to HSC exhaustion [46, 47], which is postulated but not proven to occur also in patients suffering from diseases that increase demand for haematopoietic cells or expose HSCs to inflammatory signals [48].

Label-retention assays, where HSCs are labelled with a marker such as bromodeoxyuridine (BrdU) that is incorporated into DNA [22, 33] or by labelling of chromatin with green fluorescent protein (GFP) [49], reveal that the pool of HSCs is heterogeneous with respect to its quiescence status. At any time, ~10% of cells appear to be persistently dormant, with no dilution of accumulated labels over long

periods of time [33, 49, 50]. Conversely, ~90% of HSCs form a 'homeostatic' or 'primed' pool, wherein cells divide occasionally to maintain the pool of MPPs [51] but still spend the majority of their time outside the cell cycle. Cells are able to transition between these populations [33, 52] and may even exist along a continuum of relative dormancy [53]. Further studies suggest the 'reserve/dormant' and 'homeostatic' populations may be distinguished among HSCs by expression of the surface markers CD34 [53], CD49b [54, 55], and endothelial protein C receptor (EPCR, CD201) [33, 56, 57], with 'reserve/dormant' HSCs being $CD34^{lo}$, $CD49b^{lo}$, and $EPCR^{+}$. As discussed in **section 1.2.3.1**, insult or injury may cause HSCs to emerge from quiescence, but it appears that a pool of 'reserve/dormant' HSCs still remains quiescent in some models, even in the face of these stimuli [56]. At a cellular level, quiescence is maintained in HSCs by expression of transcription factors [58], including retinoblastoma family members [59] and Foxo3a [31], which collectively prevent entry into the cell cycle, restrain protein synthesis [53], and maintain anaerobic metabolism [60, 61]. Conversely, increased expression of molecules such as cyclin-dependent kinase (CDK)6 [62, 63] and Myc [64, 65] cause HSCs to emerge from quiescence.

Alongside continued self-renewal, the other essential property of HSCs is multipotency, which refers to their ability to generate mature cells of several different lineages. As HSPCs differentiate, this multipotency is lost progressively as cells ultimately commit to a single lineage in a process endowed with illusory agency when cells are said to make 'lineage decisions'. However, defining the extent to which any individual cell is committed to a particular lineage is difficult because functional assays, such as BM transplantation and formation of colonies in methylcellulose medium, reveal the capability of cells to differentiate into particular

lineages but not the likelihood of their doing so if not disturbed [44]. These assays impose artificially stressful conditions on HSPCs, as illustrated by the differences observed in the output and proliferation of single bar-coded HSCs injected into either unconditioned recipient mice or myeloablated counterparts [66]. For these reasons, such assays probably indicate only into which lineages particular cells cannot differentiate. Lineage commitment may be predicted from the transcriptome of single cells using techniques that map their profiles onto a wider differentiation continuum [17]. However, the ability to define lineage commitment in this way is limited by the current impossibility of assessing the transcriptome and actual, undisturbed, output of the same cell [44]. More recently, cellular barcoding techniques have been used to track the progeny of individual HSC clones *in situ* [67-69]. Although this approach carries the substantial advantage of permitting observation of undisturbed haematopoiesis without disruption of the niche, it loses the strength of transplantation approaches by preventing phenotypic analysis of the cells from which clones derive. Consequently, it has not been possible to associate phenotypic features of founder cells with their behaviour in this experimental setting; this deficiency might be remedied in future using serial *in situ* imaging of cells expressing multiple fluorescent markers.

Various theories have been advanced to explain the mechanisms underpinning loss of multipotency with progressive haematopoietic differentiation. According to traditional models, all cells reaching branch points in the haematopoietic hierarchy would have a similar probability of pursuing either distributary, meaning that much of the haematopoietic compartment would be composed of multi- or oligo-potent progenitors [14] (**Fig. 1.1A**). According to this model, all HSCs should produce a balanced mixture of cells of the different lineages.

However, increasing application of single cell techniques reveals that individual HSCs have different patterns of reconstitution after transplantation, with some producing a restricted range of lineages [70-75]. Although others have suggested this lineage restriction is caused or revealed by pre-transplantation conditioning [66], similar observations have been made by those studying *in situ* haematopoiesis [67, 69]. This functional phenomenon of so-called 'lineage bias' is reflected in the transcriptome, with individual HSCs often having signatures reminiscent of the mature lineages towards which they are biased [71, 76, 77]. Importantly, cells with different signatures, described as 'lineage primed' HSCs, share expression of genes associated with stemness at similar levels [76], suggesting they are not differentiated contaminants of the HSC pool. A further form of this phenomenon has been described, in which HSCs may generate lineage-committed progenitors in a single asymmetrical cell division, omitting all MPP stages [78]. Similar lineage bias and associated priming are found among subsets of MPPs [79], which may derive from HSCs with the same features. These and similar observations derived from *in situ* labelling [67] develop former ideas by showing that there are few functionally multi- or oligo-potent progenitors in the haematopoietic compartment under homeostatic conditions. Instead, the apparent multipotency of previously defined progenitor stages probably derives from their incorporation of unipotent progenitors that are committed to different lineages but have the same surface phenotype [80, 81]. Collectively, these studies suggest lineage commitment may be enshrined in transcriptomic priming at the earliest stages of haematopoiesis, creating differentiation landscapes akin to those proposed by Waddington (**Fig. 1.1B**) [44, 82].

Figure 1.1

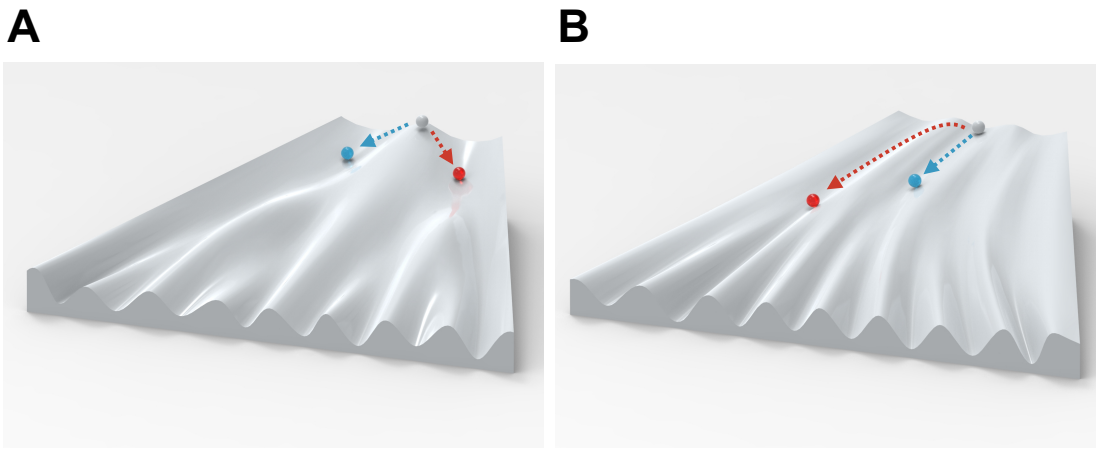

Figure 1.1: Waddington landscapes for haematopoietic differentiation
(**A**) If HSCs are equally likely to differentiate into any mature lineage, multipotent cells (white) will reach a series of division points with an equal likelihood of following any of the distributaries. Thus, the likelihood of differentiating towards either red or blue fates is equal.
(**B**) Recent data reveals evidence of lineage priming, meaning that HSCs (white) are predisposed to follow a particular path (shown by the blue cell and arrow). However, it has been proposed that extrinsic signals might cause these cells to change their priming, shifting into a different set of possible lineage fates (red).
Note that the final state of multiple discrete lineages is similar in both landscapes but the paths taken to reach them are different.

The molecular mechanisms causing lineage priming and bias are unknown but are likely to be related to epigenetic factors under homeostatic conditions. Definite loss of multipotency (e.g. when an oligopotent progenitor generates a unipotent cell) has been linked to the expression of critical, lineage-defining, transcription factors, which frequently form complex interacting networks. In some cases, pairs of transcription factors might exist as cross-antagonistic pairs, with previous theories suggesting that cell-intrinsic stochastic variations in their relative expression would be the determinant of the lineage commitment event [83]. Such a relationship was suggested between the transcription factor GATA1, associated with erythroid fate, and PU.1, associated with myeloid fate [84]. However, more recent work reveals that 1) the lineage decision point between GATA1^{+}

erythroid/megakaryoid and GATA1^{-} myeloid cells occurs before detectable changes in expression of PU.1, which is upregulated among the latter cells after subsequent cell divisions *in vitro* [85], and 2) that there is no true MPP stage that co-expresses PU.1 and GATA1, prior to the dominance of either factor [86], even though the factors are co-expressed in some progenitors and mature cells at more distal points in the haematopoietic hierarchy. Conceptually, the notion that lineage commitment would be enshrined exclusively in cell-intrinsic mechanisms is meretricious because it belies both the normal homeostatic consistency of haematopoietic output, which is presumably controlled by yet-to-be identified feedback mechanisms, and the responsiveness of HSPCs to signals signifying increased demand for haematopoietic cells, which is discussed in **section 1.2**.

Consequently, environmental influences are likely to affect the lineage commitment of HSPCs, although the exact mechanisms by which this might occur and the nature of interactions between cell-intrinsic and extrinsic factors have not been defined. For example, the cytokines macrophage colony stimulating factor (M-CSF) [87] and erythropoietin (EPO) [88] have lineage-instructive effects among multipotent HSPCs when their concentrations are increased owing to their ability to cause upregulation of lineage-defining transcription factors. However, it often remains unclear whether similar effects are important under homeostatic conditions, or whether cytokines are instructing genuinely multipotent cells or selecting cells that already have some bias.

Phenotypically, HSCs are enriched in the fraction of murine BM that does not express lineage markers but co-expresses c-Kit and Sca-1, often described as the 'LSK' population [89, 90] (**Fig. 1.2**). Exclusion of fms-like tyrosine kinase (Flt)3^{+} MPPs [91] and use of the SLAM markers CD150 and CD48 [9, 92, 93] identifies

cells enriched for long-term self-renewal potential as LSK, $Flt3^-$, $CD150^+$, and $CD48^-$ (hereafter referred to as 'HSCs' in this thesis): these cells are capable of maintaining haematopoietic reconstitution for >4 months after transplantation [9, 94]. Within this population, increasing expression of CD34 probably signifies erosion of self-renewal capacity [53], with $CD34^+$ cells having lesser reconstitution potential than $CD34^-$ [10]: these former cells are sometimes described as MPP1 progenitors [58, 95] or 'intermediate term' HSCs [54, 96] owing to their ability to maintain haematopoietic output for ~2-4 months after transplantation [72]. Additionally, most HSCs express endothelial cell-selective adhesion molecule (ESAM) [97, 98], EPCR [57], and *Fgd5* [99] and are able to expel intravital dyes [100]. Recently, differential expression of CD34 and EPCR has been used to identify four subsets of $ESAM^+$ HSCs, with $EPCR^+$, $CD34^-$ cells probably representing the 'reserve/dormant' pool with greatest self-renewal capacity [56].

Figure 1.2

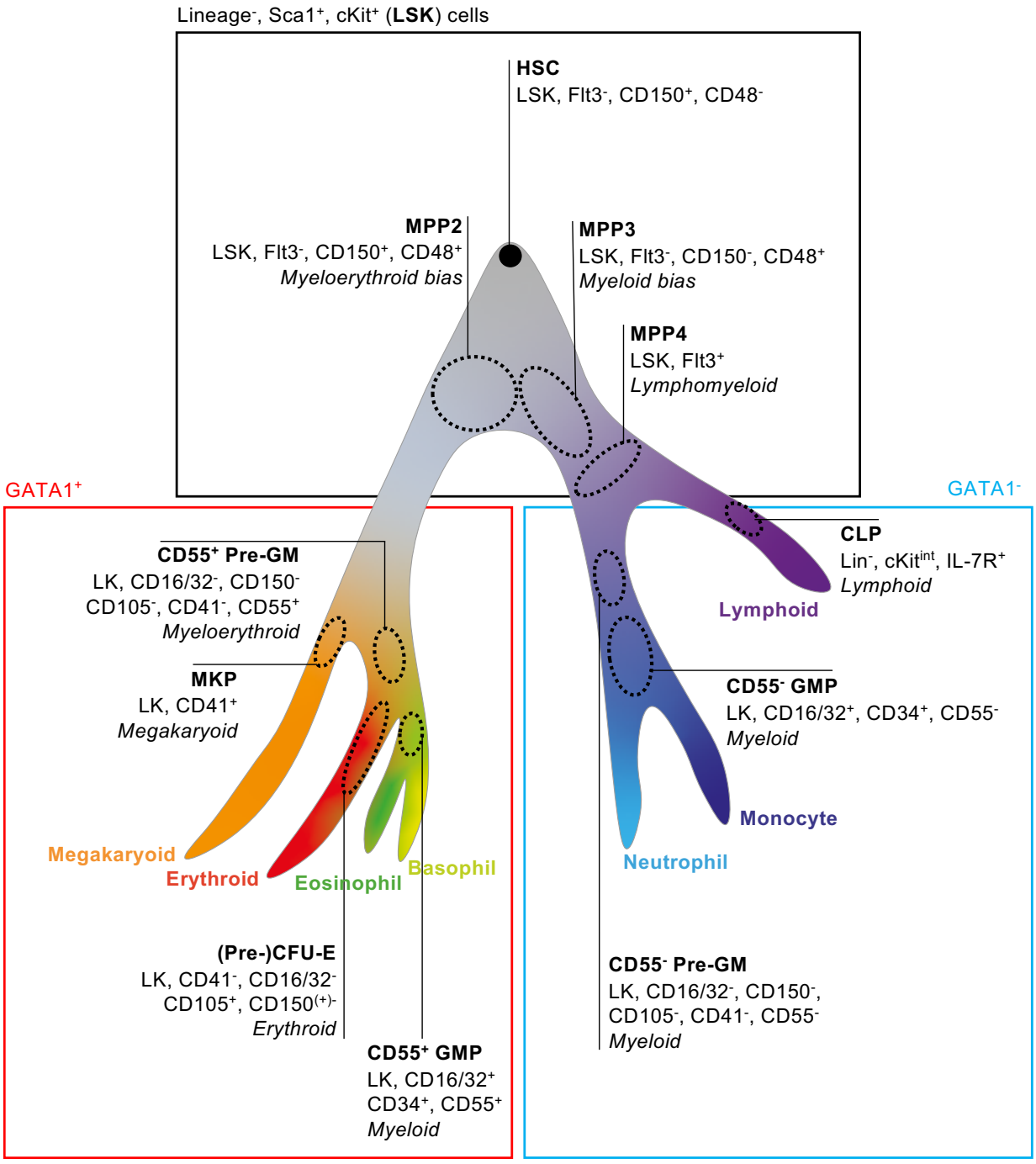

Figure 1.2: Haematopoietic hierarchy
Schematic diagram showing continuous differentiation from multipotent HSCs (top) to differentiated lineages of haematopoietic cells, marked in different colours. Within this continuum, surface markers can be used to identify progenitors passing through particular points, as indicated by dashed circles. The lineage restriction or bias of each progenitor stage is indicated in italic text. HSC: haematopoietic stem cell, MPP: multipotent progenitor, GMP: granulocyte macrophage progenitor, CLP: common lymphoid progenitor, CFU-E: colony forming unit erythroid, MKP: megakaryocyte progenitor.

Multipotent progenitors, which all express CD34, constitute the remainder of the LSK fraction not occupied by HSCs and may be divided into several subsets based on surface expression of CD48, CD150, and Flt3 (also called Flk2). The limited self-renewal capacity of MPPs is revealed by transplantation, with donor-derived blood cells detectable for only ~4 weeks [10, 79, 101, 102]. By evaluating the functional and transcriptomic properties of these subsets, others have found MPP2 cells (LSK, $Flt3^-$, $CD34^+$, $CD150^+$, $CD48^+$) are biased toward megarkyoid and myeloid lineages, though single MPP2s retain the ability to generate erythroid, megakaryoid, myeloid, and lymphoid lineages [79, 95]. Conversely, the more abundant MPP3 group (LSK, $Flt3^-$, $CD34^+$, $CD150^-$, $CD48^+$) is biased towards myelopoiesis [79, 95], whereas the MPP4 group (LSK, $Flt3^+$) is largely [103], though not absolutely [104], restricted to formation of either myeloid or lymphoid cells. Cells of this latter group have also been described as lymphoid/myeloid-biased MPPs (LMPPs). Recapitulating similar findings among HSCs, these studies show that the MPP pool is heterogeneous, with some cells already restricted or biased in their ability to form particular lineages. Because single cell sequencing studies indicate that differentiation from HSCs to MPPs is a continuous process, it has been hypothesised but not proven that particular subsets of MPP could derive from HSCs with similar lineage priming [21].

1.1.4 Bone marrow niche

Haematopoietic stem and progenitor cells exist in a niche in the BM composed of several cell types co-ordinated by soluble growth factors, cytokines, physical interactions, and neurohormonal factors [105-108]. Among the cellular contributors to the niche are mesenchymal stem or stromal cells (MSCs) and their

mature progeny, cells of the osteoblastic lineage, $CD31^+$ endothelial cells, and other haematopoietic cells resident in the BM, including macrophages and megakaryocytes. Several surface markers have been used to identify MSCs in BM, producing descriptions of different populations that overlap in their cellular biology and function. Specifically, MSCs located close to arterioles and identified by expression of neural-glial antigen (NG)2, myosin heavy chain 11, and high levels of nestin [109-111] are professional producers of CXCL12 and stem cell factor (SCF, also called Kit ligand), which maintain HSC numbers and prevent their egress from the niche. In addition to CXCL12 and SCF required for HSC quiescence and maintenance, these $NG2^+$ MSCs also produce angiopoietin-1, which appears to have a similar but non-redundant role [112]. Using surface markers, these $NG2^+$ MSCs may be identified by co-expression of CD51 and the platelet-derived growth factor receptor (PDGFR)α (CD140a) but low expression of Sca-1 among the population of non-haematopoietic BM $CD45^-$, $CD31^-$, $Ter119^-$ cells [113]; similar PαS cells in compact bone do express Sca-1 [114]. In addition, a more numerous population of MSCs localised adjacent to BM sinusoids has been identified by surface expression of the leptin receptor (LepR) [115, 116], low level expression of nestin [110], and by their production of CXCL12, leading to their description as CXCL12-abundant reticular (CAR) cells [117, 118]. However, whereas production of CXCL12 by $NG2^+$ MSCs was essential for HSC maintenance, conditional deletion of *Cxcl12* using a LepR-driven cre recombinase did not cause any change in HSC numbers [111]. Instead, SCF production by $LepR^+$ cells was required for HSC maintenance, suggesting different mesenchymal niche populations may be specialised for production of particular trophic factors in different spatial regions of the niche.

Although initial studies suggested osteoblastic lineage cells (OBCs) were critical determinants of the BM niche [119, 120], their role in regulation of HSCs is unclear, partly owing to the technical difficulty in separating the contribution of these cells from the MSCs from which they derive [105]. Although transplanted HSCs appear to home to locations close to the endosteal surface of BM in irradiated recipients [121], the importance of OBCs has been questioned because their numbers do not correlate with the number of HSCs in BM [55] and because ablation of CXCL12 and SCF under the control of osteoblast-specific cre recombinases has little effect on HSC number or function [115, 122]. Furthermore, whereas deletion of OBCs using the col2.3 promoter cre recombinase displaces HSCs to the spleen, the depletion of BM HSCs occurs only after a lag of 2-3 weeks, suggesting they are not entirely dependent on OBCs for maintenance in the BM [123, 124]. Conversely, OBCs are required for normal development of committed lymphoid progenitors, to the extent that their deletion in mice causes immediate defects in lymphopoiesis [125], possibly owing to their production of IL-7 [126] and/or CXCL12 [122, 127]. Cells of the osteoblastic lineage in BM may be identified by surface expression of CD51 without PDGFRα or Sca-1 within the population of $CD45^-$, $CD31^-$, $Ter119^-$ cells [128, 129] and by expression of the essential osteoblastic transcription factor Runx2 [130].

Endothelial cells in BM also have non-redundant roles in regulation of HSPCs through production of CXCL12 [122] and SCF [115] but they express these molecules at much lower levels than MSCs [111]. However, recent studies have identified considerable heterogeneity in the phenotype and activities of endothelial cells in different locations in the BM [131, 132], suggesting their contribution to HSPC regulation may vary accordingly.

Finally, progeny of HSPCs have a regulatory role in the niche. Production of CXCL4 and TGF-β by megakaryocytes has an important role in maintaining HSC quiescence [133, 134]. Resident macrophages in the BM also contribute to HSPC maintenance, partly through production of oncostatin M [135]; their depletion causes mobilisation of HSCs into the bloodstream [129]. A particular subset of $CD169^+$ ($Siglec\text{-}1^+$) macrophages forms erythroblastic islands by making direct contact with and supporting differentiation of erythroid progenitors [136], as described in **section 1.1.7**.

1.1.5 Myelopoiesis

According to traditional models, progenitors capable of producing myeloid cells exclusively would derive from MPPs through a series of increasingly lineage-restricted stages [14]. This appeared to be confirmed by the description of common myeloid progenitors (CMPs) in 2000, which had the potential to produce both myeloid-restricted progenitors, granulocyte-macrophage progenitors (GMPs: LK, $CD16/32^+$, $CD34^+$), and megakaryocyte-erythroid progenitors (MEPs: LK, $CD16/32^-$, $CD34^-$) [15]. These cells were identified by differential expression of the surface markers CD34 and CD16/32 within the pool of $lineage^-$, $Sca\text{-}1^-$, $c\text{-}Kit^+$ (LK) progenitors, and the lineage capabilities were confirmed at the population level by functional assays *in vivo* and *vitro*. Downstream of these progenitors, MEPs would produce megakaryocytes and committed erythroid progenitors, whereas GMPs would produce dedicated monocyte [137], dendritic cell (DC) [138], and neutrophil progenitors [139, 140].

More recent studies of myelopoietic progenitors have provided new insights into this process. First, as discussed in **section 1.1.3**, some MPPs are primed for

formation of myeloid progenitors [79], meaning that lineage biases are already established before emergence of the CMP stage. This contradicts the notion that all individual CMPs have a similar likelihood of producing either GMPs or MEPs, which was inferred from population level assays [15]. Building on this observation, single cell RNA sequencing analysis of cells possessing the surface phenotype of CMPs (i.e. LK, $CD34^+$, $CD16/32^{int}$) or similar pre-granulocyte-macrophage progenitors (pre-GMs, LK, $CD16/32^-$, $CD41^-$, $CD105^-$, $CD150^-$) shows that both populations are actually composed of a heterogeneous mixture of progenitors with restricted lineage potential [18, 80, 81]. For example, expression of the transcription factor GATA1 in pre-GMs identifies those cells with a greater likelihood of producing mast cells/basophils, eosinophils, erythrocytes, and platelets but lesser capacity to generate neutrophils or monocytes [80]. Conversely, expression of Flt3 identifies CMPs biased toward production of dendritic cells and monocytes but away from neutrophils [141]. These results suggest the surface definition of the CMP has insufficient resolution to identify lineage restrictions that are already manifest in progenitors at this stage of differentiation.

1.1.6 Differentiation of $GATA1^+$ progenitors

Recent work indicates that an early division occurs in haematopoiesis, which is marked by the expression of GATA1. Therefore, $GATA1^+$ pre-GM progenitors, which may be derived from myeloerythroid biased MPP2 cells, generate erythroid, megakaryoid, eosinophil, and basophil/mast cells lineages, whereas $GATA1^-$ progenitors generate monocytes, neutrophils, and lymphoid lineages (**Fig. 1.2**) [17, 80]. Comparison of RNA and surface protein expression between $GATA1^+$ and $GATA1^-$ pre-GM cells reveals that the IL-33 receptor ST2, the complement inhibitory

factor CD55, and the high affinity IgE receptor FcεRI are all expressed at higher levels on GATA1^{+} cells. This CD55^{+} group probably also encompasses the β7 integrin^{+} [142] and IL-4^{+} [143] myeloid progenitors described in other studies, which also expressed FcεRI and were committed to produce basophils and mast cells. Conversely, Flt3 and the transcription factors PU.1 and interferon regulatory factor (IRF)8 are expressed at higher levels among GATA1^{-} cells. These findings develop previous models of haematopoiesis by showing that some types of myeloid cell (eosinophils and basophils/mast cells) are more closely related to the erythroid and megakaryoid lineages than to other myeloid branches (monocytes and neutrophils); these findings have been confirmed independently in several laboratories [18, 144, 145].

Multipotent GATA1^{+} pre-GM progenitors express a number of additional transcription factors that affect lineage decisions, including GATA2, friend of GATA1 (FOG)-1, and CCAAT-enhancer binding protein (C/EBP)-α and β [80, 146]. Among these factors, GATA2 is expressed in early erythroid progenitors, basophils/mast cells and eosinophils. However, it is considered to be essential only for specification of mast cells because they were absent in GATA2$^{-/-}$ murine embryos, against a background of wider haematopoietic abnormalities related to the additional role of GATA2 in regulating HSC maintenance [147]. GATA1 is not required for formation of mast cells [148] but its deficiency causes complete absence of eosinophils, probably owing to failure to specify the lineage [149]. Conversely, C/EBP-α is required for specification of eosinophils [150]. Therefore, GATA2 is of primary importance in specifying mast cells/basophils, probably in co-operation with PU.1 and C/EBP-α [151, 152], whereas GATA1 (at intermediate levels of expression) and

C/EBP-α are essential to specify the eosinophil lineage [146, 153]. Beyond this, PU.1 is also required in eosinophils for formation of mature cells [154].

The decision of cells to commit to either mast cell/basophil and eosinophil or megakaryoid/erythroid lineages is determined by the balance of C/EBP factors and FOG-1. For commitment to the eosinophil lineage, MPPs must therefore downregulate FOG-1, which favours erythroid and megakaryoid differentiation [155]. Accordingly, overexpression of FOG-1 in either eosinophils [155] or mast cells [156] causes reversion to a multipotent state that can also generate erythrocytes, whereas FOG-1 deficiency eliminates erythroid/megakaryoid progenitors [157]. Conversely, C/EBP-α overexpression causes erythroid progenitors to differentiate into eosinophils [158].

1.1.7 Erythropoiesis

Definitive mammalian erythropoiesis is located in the BM, where erythroid progenitors derive from bipotent erythroid/megakaryoid progenitors (pre-MegEs: LK, CD16/32^{-}, CD41^{-}, CD105^{-}, CD150^{+}) in a process dependent on GATA1 expression [157]. The first committed erythroid progenitors are termed pre-CFU-Es, conventionally identified using flow cytometry by their co-expression of CD105 and CD150 [159] in mice among the pool of LK cells [17] (i.e. LK, CD16/32^{-}, CD41^{-}, CD105^{+}, CD150^{+}) (**Fig. 1.3**). Functionally, pre-CFU-E cells approximate the same stage of maturation as progenitors capable of forming large, ~500 cell, 0.5-1 mm diameter blast-forming unit – erythroid (BFU-E) colonies in methylcellulose medium under appropriate conditions [160]. Pre-CFU-Es express PU.1 in addition to GATA1, but this transcription factor is downregulated as the surface transferrin receptor (CD71) is upregulated to mark the transition to CFU-Es [161].

Overexpression of PU.1 prevents further differentiation beyond the pre-CFU-E stage [162]. The CFU-E stage is so named because these cells are able to form small, 8-32 cell, haemoglobinised colonies in methylcellulose medium after 2-3 days [163]. By flow cytometry, this stage is defined as LK, CD16/32^{-}, CD41^{-}, CD105^{+}, CD150^{-}.

From the CFU-E stage, murine cells begin to express the mature erythroid marker Ter119 [164]. The Ter19 antibody clone recognises an antigen unique to the erythroid lineage that is associated with, but not identical to, the surface glycophorin A molecule encoded by *Gypa* [165]: the specific antigen bound by Ter119 antibodies is unknown. The human paralogue of this molecule is glycophorin A, CD235a. Maturing cells initially express c-Kit and Ter119 at intermediate levels (proerythroblast) but progress to become c-Kit^{-}, Ter119^{+} mature erythroblasts, which are further subcategorised into stages A, B, and C as they lose expression of CD71 and become progressively smaller [166]. Ultimately, erythroblasts extrude their nucleus but initially retain their ribosomal RNA to become reticulocytes. Reticulocytes are released into circulation, losing the ribosomal RNA to become mature RBCs, which circulate in the blood for an average period of ~60 days in mice [167, 168] before senescent cells are removed by red pulp macrophages in the spleen.

Figure 1.3

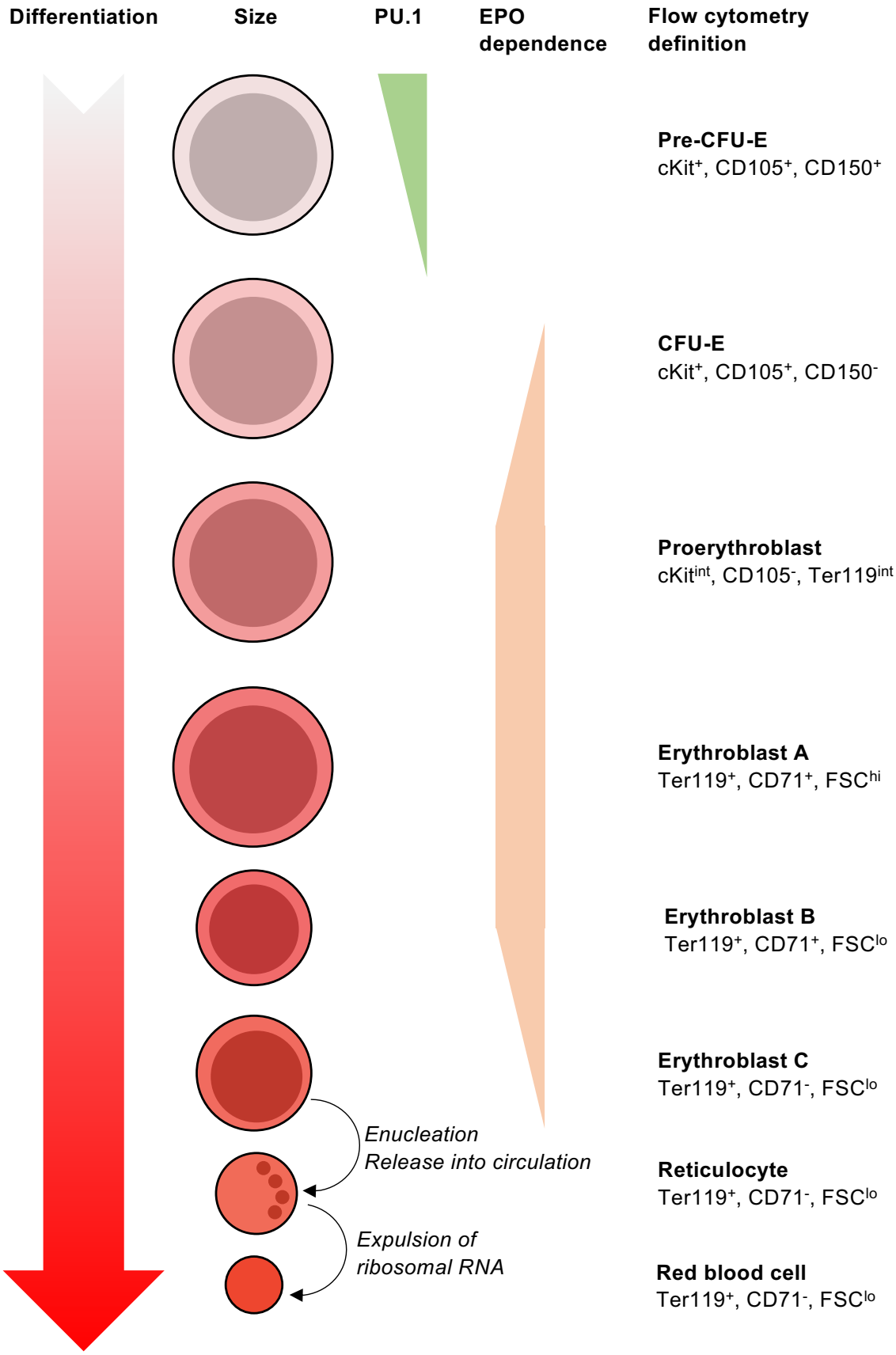

Figure 1.3: Outline of erythroid differentiation
Schematic diagram showing progressive differentiation of erythroid cells, from which various cell stages can be identified based on surface marker expression. Also shown are relative cell sizes (not to scale), nucleation, the period when the transcription factor PU.1 is expressed, and the period during which cells are dependent on erythropoietin (EPO). FSC: flow cytometric forward scatter.

During their development in the BM, erythroid progenitors associate around $CD169^+$, $F4/80^+$ resident macrophages to form so-called erythroblastic islands [169]. These structures are maintained by physical interactions between macrophage and progenitors using such molecules as vascular cell adhesion molecule (VCAM)-1 [170] and CD163 [171]. Additionally, erythroblastic island macrophages produce soluble factors, including insulin-like growth factor (IGF)-1, that facilitate maturation of erythroid progenitors [172], and they also phagocytose the nuclei of erythroblasts as they are extruded using the receptor MerTK [173]. Depletion of erythroblastic island macrophages by expression of diphtheria toxin under the control of the CD169 promoter causes anaemia related to decreased numbers of erythroid progenitors in BM [136], demonstrating the importance of these cells and their island structures in regulating erythropoiesis.

Differentiation of erythroid cells from the CFU-E to the early erythroblast stages is dependent on EPO, which is produced by peritubular cells in the kidneys in response to tissue hypoxia [174]. Erythropoietin is not required for formation of pre-CFU-Es and CFU-Es, even though the receptor starts to be expressed before these stages [175]. Although dispensable up to the CFU-E stage, EPO does have a lineage instructive effect on MPPs to promote erythroid differentiation, which is probably of greatest relevance in conditions of accelerated erythropoiesis created by anaemia [88]. Evidence for the critical role of EPO in terminal differentiation of erythroblasts comes from mice lacking either EPO or the EPO receptor (EPO-R), which strains both suffer embryonic mortality owing to anaemia, despite having normal numbers of CFU-Es [175].

The specific effect of EPO in erythroid progenitors has been difficult to define because differentiation and cell cycle events are closely linked. However, it appears

its chief role is to prevent apoptosis of proerythroblasts and erythroblasts, an effect mediated by Janus kinase (JAK)2/signal transducer and activator of transcription (STAT)5 phosphorylation downstream of the EPO-R, resulting in expression of the anti-apoptotic factor Bcl-xL [176, 177] and decreased expression of the pro-apoptotic surface molecules Fas and Fas ligand on the cell surface [164]. Although the EPO-R activates other signalling pathways, including extracellular signal-related protein kinase (ERK)1/2, p38, and Akt to produce other effects [178], it often remains unclear whether these pathways are essential for erythropoiesis or merely correlated with progressive differentiation. This principle is exemplified by EPO-R-induced Akt activation, for which the exact role in erythropoiesis is disputed [179].

When activated by the EPO-R, Akt is translocated to the plasma membrane and phosphorylated at two critical sites: threonine (T)308, mediated by protein-dependent kinase (PDK)-1, and serine (S)473, mediated by the mammalian target of rapamycin complex (mTORC)2 [180]. Importantly, although T308-phosphorylated Akt has some activity, concurrent S473 phosphorylation is required for full activation and for stability of the T308 event. Akt is further regulated by an interaction with the Pim-1 kinase, with Pim-1 inhibition decreasing phosphorylation of the Akt S473 residue [181, 182]. Among its pleiotropic effects on erythroid cells [179], EPO-induced Akt activation promotes differentiation [183] because Akt phosphorylates GATA1 at the S310 residue to cause activation [184]. This S310 phosphorylation appears to be essential for GATA1 interactions with its binding partner FOG-1, which co-operates with GATA1 to repress non-erythroid gene transcription [185]. Additionally, as in other cell types, Akt phosphorylates and activates the mTORC1 complex, which regulates protein translation and cell growth via the S6 kinase [186]. Importantly, many of these molecules have essential roles

in erythropoiesis. Whereas knockout of Akt itself does not impair erythropoiesis in mice [187], inhibition of Akt activity using the small molecule inhibitor LY294002 prevents terminal differentiation of erythroid cells from murine erythroleukaemia cells [188], the human K562 cell line [189], and from $CD34^+$ human progenitors [190, 191], suggesting the constitutive Akt knockout mice could be compensated by other changes. This notion is supported by the finding that combined deficiency of Pim-1 and Akt causes lethal anaemia in mice before or shortly after birth [192], with Pim-1 deficiency alone causing mild anaemia [193]. Furthermore, artificial activation of Akt independent of EPO is sufficient to induce erythroid differentiation of human pluripotent stem cells [194]. Downstream of Akt, mice with a mutant form of GATA1 that does not have the S310 phosphorylation site do not have an erythroid phenotype [195], though this might also be compensated. Conversely, mice lacking mTORC1 have impaired erythroid differentiation beyond the pre-MegE stage [196]. Collectively, this evidence suggests EPO-R-induced Akt activation has an essential role in erythroid differentiation, but the precise mechanism underlying this effect is not completely defined.

1.1.8 Extramedullary haematopoiesis and haematopoietic migration

Extramedullary haematopoiesis (EMH) refers to production of haematopoietic cells at any location outside the BM. In humans, splenic and other forms of EMH are generally taken as evidence of a pathological process, such as BM failure or increased demand for haematopoietic cells [197]. However, in domestic animals, several forms of EMH are observed in healthy individuals.

The spleen of normal mice is colonised by HSCs at E14.5 [6], and these cells persist and remain functional at this location throughout the life of the animal [198].

Therefore, the splenic red pulp of healthy mice contains a population of cells with the same surface phenotype as BM HSCs (i.e. LSK, $CD150^+$, $CD48^-$. $CD34^-$), which are similarly capable of long-term haematopoietic reconstitution when single cells are transplanted into lethally irradiated recipients [199]. Studies of parabiotic mice indicate there is little of exchange of HSCs between BM and spleen, though mature cells do reach equilibrium [199]. Interestingly, splenic HSCs were more proliferative than those in BM, even when they reached BM niches after transplantation [199]. In humans or mice, splenic haematopoiesis may be expanded as a compensatory response to BM failure or in situations of increased demand for erythrocytes or granulocytes [197]. Experimental studies of mice suggest splenic EMH is particularly sensitive to increased concentrations of numerous cytokines with haematopoietic activity, such as granulocyte macrophage colony stimulating factor (GM-CSF) [200], interleukin (IL)-5 [201], IL-6 [202], IL-13 [203], IL-27 [204], IL-33 [205], EPO [206], and tumour necrosis factor (TNF)-α [207], if they are injected or overproduced during disease. However, in most cases, it remains unclear whether this expansion of splenic EMH represents accumulation of resident splenic HSPCs, migration of HSPCs from BM to spleen, or a combination of these effects.

Recently, other forms of EMH have been described in healthy mice. Megakaryocytes have been observed in histological sections of the lungs for decades [208], and recent work shows that approximately half of circulating platelets in healthy mice are derived from such pulmonary cells [209]. In the gut-associated lymphoid tissue (GALT), a population of c-Kit^+, Sca-1^+ progenitors could generate cells with the appearance of monocytes and basophils/mast cells in liquid culture [210]. These cells, which were detectable in healthy mice but expanded by injection of either IL-25 or IL-33, have been named '$MPP^{type\ 2}$' owing to their ability

to generate myeloid cells associated with type 2 immune responses; they are different from the MPP2 subset described in **section 1.1.3**. The detection of these cells in GALT but not in the intestine itself recalls an interesting epiphenomenon of domestic animals, which also have embryonic migration of HSPCs to peripheral lymph nodes [198]. Thus, EMH in lymph nodes is observed clinically in animals during situations of increased demand, such as severe anaemia.

Whereas HSPCs are predominantly confined to the BM, small numbers of cells enter the circulation in a manner that varies in synchrony with the circadian clock [211]. These cells circulate in the blood and lymphatic system [212], forming a pool of cells capable of reconstituting vacant niches in BM under homeostatic conditions [213]. While circulating, HSCs may be arrested at sites of inflammation or tissue damage, where they are able to generate progenitors and mature cells to contribute to the local response [212], which is discussed further in **section 1.2.3.3**.

When considering EMH, an important question is whether extramedullary sites are making a functional contribution to production of mature haematopoietic cells when considered alongside the output of the BM under homeostatic or disease conditions. In mice, neonatal splenectomy does not impair the maintenance of normal concentrations of haematopoietic cells in blood [214, 215], suggesting loss of any contribution made by splenic HSCs can be compensated by the BM. Under disease conditions, mature myeloid cells generated in the spleen can be detected in tissues [216], indicating expanded EMH does produce cells with a functional role. However, it remains unclear whether equivalent cells made in either BM or spleen are qualitatively similar.

This consideration of EMH under homeostatic conditions illustrates some important principles for haematopoiesis: 1) HSPCs are not confined to the BM in

normal mice, 2) the complex BM niche is dispensable for maintenance of HSCs but is probably required for preservation of a quiescent state and may be necessary for efficient differentiation of HSPCs, and 3) the BM is the major supplier of haematopoietic cells under homeostatic conditions but may be assisted by EMH during periods of demand or if BM haematopoiesis is defective.

1.2 Demand-adapted haematopoiesis

Haematopoiesis is a highly adaptable process, having the ability to respond to increased demand for mature cells imposed by blood loss, wounds, infections, and other inflammation. Others have suggested haematopoiesis responds to 'push' and 'pull' factors, with 'pull' factors including depletion or consumption of haematopoietic cells in the blood, and 'push' factors equating with responses of HSPCs to cytokines or pathogen derivatives [48]. Examples of 'pull' factors include experimental depletion of neutrophils using anti-Ly6G antibodies [217] or of erythrocytes using the lytic agent phenylhydrazine [218]: these interventions cause marked expansion of myelopoiesis or erythropoiesis, respectively. Conversely, the importance of 'push' factors has been highlighted by growing recognition that HSPCs, including the earliest HSCs, express pathogen recognition receptors [40], such as toll-like receptor (TLR)2, TLR4, and receptors for inflammatory cytokines. The cognate ligands for these receptors may cause HSPCs to proliferate and differentiate towards particular cell fates, producing a feed-forward response that contributes to resolution of the initiating insult.

1.2.1 Emergency and reactive myelopoiesis

Emergency myelopoiesis or granulopoiesis refers to rapid and expanded production of mature myeloid cells in response to infection, whereas the term reactive myelopoiesis has been used to described expanded myeloid output in response to non-infectious insults, such as sterile inflammation or ablation of replicating HSPCs by the cytotoxic drug 5-fluorouracil (5-FU) [219]. The distinction between these processes would seem increasingly semantic because experimental evidence reveals considerable overlap between the cellular and molecular events occurring among myeloid progenitors with different initiating insults. Experimentally, emergency myelopoiesis may be observed with induction of sepsis by caecal ligation and puncture in mice, with injection of lipopolysaccharide (LPS) [220], or with depletion of neutrophils in blood [217]. Others have suggested this process may be considered in several stages, beginning with detection of infection or injury, followed by translation to provide cytokine signals that can affect HSPCs, resulting in expansion of myelopoiesis, and terminated by restoration of normal haematopoietic regulation when the insult is resolved [219].

Most insults or injuries are detected by pathogen recognition receptors (PRRs) expressed by tissue resident cells. However, in response to LPS injection in mice, TLR4 expression on haematopoietic cells is dispensable for generation of the emergency granulopoietic response [220], suggesting that 1) stromal cells, particularly $TLR4^{+}$ vascular endothelial cells [221], are the essential link between infection and HSPCs, and 2) that TLR4 expression on HSPCs is not essential for development of emergency myelopoiesis in response to bacterial infection, though it may contribute by mobilising HSCs to support the response of downstream progenitors [222, 223]. Cells expressing PRRs produce cytokines to signal to

HSPCs, including G-CSF, GM-CSF, IL-3, IL-6, IL-27, and IFN-γ (reviewed by [224]). Of these, G-CSF is essential for production of neutrophils under homeostatic conditions and in emergency responses [225], whereas GM-CSF is only required for emergency responses [226]. Interestingly, the relative importance of different cytokines probably varies according to the nature of the insult, with both GM-CSF and G-CSF being indispensable for emergency granulopoiesis occurring with infection by the Gram negative bacterium *Listeria monocytogenes* [227] but both being redundant for the same response to infection with the fungal organism *Candida albicans* [228], for which stromal-derived IL-6 seems to be more important [229]. This suggests phenotypically similar emergency myelopoiesis responses may be induced by different cytokines in a manner presumably determined by the types of cells and PRRs activated by the particular pathogen or insult.

At a cellular level, myelopoietic cytokines alter normal patterns of transcription factor usage in myeloid progenitors. Normally, myeloid progenitors express C/EBP-α, which is required for neutrophil production [150]. This factor regulates neutrophil production by inhibiting the cell cycle members CDK2 and 4 to prevent uncontrolled proliferation [230]. However, G-CSF-induced STAT3 activation causes increased expression of C/EBP-β at the expense of C/EBP-α [231]. While these factors share many functions in specification of neutrophils, C/EBP-β does not inhibit CDK2 and 4, leading to increased proliferation of myeloid progenitors to support emergency myelopoiesis [232, 233]. In the BM, changes in the proliferation of myeloid progenitors lead to the formation of expansile clusters of GMPs, as seen during recovery from 5-FU ablation [234].

1.2.2 Stress and EPO-accelerated erythropoiesis

Anaemia increases the serum concentration of EPO by as much as 1000 times its normal level [235]. As well as increasing survival of proerythroblasts and erythroblasts [164], this increased EPO also affects earlier progenitors, causing expansion of all stages in the erythroid pathway in the BM [17, 88], an effect that can be replicated by injection of human recombinant EPO in mice. This effect is similar but not identical to stress erythropoiesis, which refers to changes in BM and splenic erythropoiesis in response to anaemia. In stress erythropoiesis, increased concentrations of EPO, bone morphogenetic protein (BMP)4, and SCF in the presence of hypoxia induce the emergence of a population of 'stress BFU-Es' in the spleen [236]. These cells differ from their counterparts in healthy BM by forming larger colonies over a shorter period of 5-7 days, and by their insensitivity to cytokines, such as IL-1β, that may suppress BM erythropoiesis [237]. Conversely, stress BFU-Es are more sensitive than BM progenitors to the anti-apoptotic effects of EPO [164, 238]. Stress BFU-Es derive from MPPs that migrate from BM to spleen [239], where exposure to Hedgehog licenses them to respond to BMP4 [240]. Conversely, BM erythroid progenitors are not responsive to BMP4, though forced expression of Hedgehog in the BM niche can generate a population with similar characteristics to splenic stress BFU-Es [239]. Splenic stress erythropoiesis and stress BFU-Es are observed commonly in inflammatory diseases in mice [241, 242], which is partly related to increased concentrations of EPO produced in response to anaemia of inflammatory disease (discussed in **section 1.2.3.4**). However, inflammatory signals may induce stress erythropoiesis directly by altering the behaviour of splenic macrophages that co-ordinate the response [218].

In the context of inflammation, splenic stress erythropoiesis is often described as a ‘compensatory’ response for loss of BM erythroid output [218]. However, in these models, it usually coexists with non-resolving anaemia. This means that, although changes in splenic erythropoiesis may be attempting to compensate assiduously, they are unable to provide a sufficient red cell mass to compensate for loss of definitive erythropoiesis in the BM.

1.2.3 Haematopoiesis during chronic inflammation

Chronic inflammatory diseases also impose demands on the haematopoietic system, reproducing many features of emergency myelopoiesis and stress erythropoiesis occurring in response to acute injury or infection [243]. However, unlike those insults, most chronic inflammatory diseases do not resolve, meaning that patients may have long-term remodelling of the haematopoietic system. Others have speculated that this dysregulation of haematopoiesis may contribute to progression of the inflammatory disease by providing effector cells that accumulate in inflamed sites, or by causing comorbidities, such as anaemia of inflammatory disease and BM failure [48, 243, 244].

1.2.3.1 HSC proliferation

Cytokines such as G-CSF, IL-1β, and IFNs emanating from inflamed sites may cause HSCs to emerge from quiescence and proliferate [34, 36, 245-247], expanding the LSK compartment in the BM. This presumably increases the production of MPPs to support increased haematopoietic output but decreases the competitive fitness of HSCs in transplantation assays when compared to those from healthy mice [34, 36, 222, 247]. However, HSCs exposed to chronic inflammatory

signals may re-enter a quiescent state owing to the engagement of proposed cellular braking mechanisms, which limit proliferation and presumably protect their self-renewal capacity [248]. This principle is observed in the setting of collagen-induced arthritis (CIA) in mice, where induction of inflammation did not expand the HSC population but increased expression of cell cycle inhibitory genes [249]. Conversely, colitis [250] and chronic *Mycobacterium avium* infection in mice expanded the population of HSCs; cells from the latter mice were less effective in reconstituting irradiated recipients compared to HSCs from healthy mice [37].

1.2.3.2 Lineage bias

Depending on its nature and origins, chronic inflammation usually increases demand for mature myeloid cells because these are consumed rapidly at inflamed sites. In the BM, this causes marked changes in the relative abundance of lineage-committed progenitors, with increased numbers of myeloid but fewer erythroid and lymphoid progenitors [243]. The reasons underlying this major change in progenitor frequency are not fully understood and are probably attributable to events at multiple levels in the haematopoietic system. Among HSCs, TNF-α [251] and IL-1β [247] both induce transcriptional signatures associated with myeloid lineage priming; exposed cells preferentially produce myeloid progenitors. Similarly, macrophage colony stimulating factor (M-CSF) exerts a lineage instructive effect among HSCs to induce formation of monocytes [87]. Inflammation is associated with accumulation of myeloid-biased MPP3 cells [79], though it is unclear whether this is attributable to expansion of existing MPP3s or increased production from upstream HSCs [252]. Additionally, the output of MPP4s (LMPPs), which normally produce lymphoid cells preferentially, shifts to generate myeloid cells at the expense

of lymphocytes [253]. In CIA [249], chronic colitis [250], and lupus [254] in mice, these changes are reflected in increased numbers of GMPs and decreased numbers of common lymphoid progenitors (c-Kit^{int}, Sca-1^{int}, IL-7Rα^{+}) [16] and CFU-Es in BM.

1.2.3.3 EMH in the spleen and inflamed sites

Increased concentrations of haematopoietic cytokines cause expansion of splenic haematopoiesis during chronic inflammation. During atherosclerosis, expansion of GMPs in BM and spleen increases the total capacity for myelopoiesis, with monocytes derived from splenic progenitors accumulating in vascular plaques [216, 255]. Additionally, mice with chronic inflammation frequently develop stress erythropoiesis in the spleen in response to contraction of the population of erythroid progenitors in BM [256]. Collectively, these changes cause gross enlargement of the spleen in inflamed mice.

Haematopoietic stem and progenitor cells circulating in the blood may lodge in sites of local inflammation, differentiating *in situ* to produce effector cells that contribute to the response. This phenomenon has been observed with injection of LPS in the kidney, which produces a localised haematopoietic response with *in situ* production of neutrophils and dendritic cells [212]. In some models of inflammation, including colitis [250] and wounds infected with *Staphylococcus aureus* [257], GMPs are observed in inflamed tissues and local lymph nodes, leading to the presumption that these cells might also migrate from BM or spleen to inflamed sites. However, it remains unclear whether these forms of localised haematopoiesis are important for sustenance of the inflammatory response when compared to the output of the much more numerous BM progenitors.

1.2.3.4 Anaemia of inflammatory disease and EPO resistance

A striking feature of many chronic inflammatory diseases is anaemia, which refers to reduction of the red cell mass and/or circulating haemoglobin concentration [258]. Anaemia decreases oxygen delivery to tissues, limiting the ability to exercise and impairing quality of life. Anaemia of inflammatory disease (AID) occurs frequently in patients with inflammatory arthritides and bowel disease, with approximately 1 million adults affected in the USA [259].

The pathogenesis of AID is multifactorial, with important components including the inhibitory effect of inflammatory cytokines on erythroid progenitors in the BM, decreased absorption or availability of iron for haem synthesis, decreased secretion of or responsiveness to EPO, and increased fragility of RBCs, resulting in a shorter circulating time in the blood [259]. Among those cytokines known to cause suppression of erythropoiesis and anaemia are IL-6 [260], TNF-α [261], TGF-β [262, 263], and IFN-γ [264, 265]. The reported mechanisms underlying the suppressive effects of these cytokines are diverse, with IL-6 inhibiting production of haemoglobin in a human erythroid cell line [266] by repressing transcription at the globin loci [267]. Additionally, IL-6 contributes to AID by inducing the expression of hepcidin in the liver, which limits gastrointestinal iron absorption by inhibiting the ferroportin channel that normally transports absorbed iron from enterocytes into the circulation [268]. Two different mechanisms of IFN-γ-mediated erythroid suppression have been described: the first caused by upregulation of PU.1 [269] with its binding partner IRF1 [270], which is necessary for early erythroid development but must be downregulated for terminal differentiation [162], and the second related to upregulation of TNF superfamily members that cause apoptosis [271]. No mechanism was proposed to explain the observation that TNF-α could impair the

development of erythroid cells from human $CD34^+$ progenitors [272]. Paradoxically, TGF-β suppressed erythropoiesis by causing accelerated differentiation of erythroid progenitors, decreasing the pool of cells available to generate new erythrocytes [262]. Although injection of IL-1α [273] or IL-1β [247] in mice causes suppression of erythropoiesis, neither cytokine inhibited development of human BFU-E colonies *in vitro*, suggesting this may not be a direct effect *in vivo* [274]. Collectively, these studies suggest that, in the context of diseases associated with complex networks of inflammatory cytokines and perturbations in other physiological pathways, it is likely that multiple mechanisms contribute to the development of anaemia, with the relative importance of these mechanisms varying according to their particular immunophenotypes. As noted in **section 1.2.2**, although stress erythropoiesis frequently develops in the spleen of mice with suppressed BM erythropoiesis, this is usually insufficient to restore normal erythroid parameters.

Experimentally, suppression of erythropoiesis caused by injection of IL-1α or TNF-α in mice can be alleviated by injection of EPO [273, 275], suggesting EPO might be a useful treatment for patients with AID. However, in some chronic inflammatory settings, including chronic kidney disease, attempts to treat anaemic patients with EPO or its synthetic derivatives have been unsuccessful, creating the clinical phenotype of 'EPO resistance' [276]. Like AID, the pathophysiology of this phenomenon is probably multifactorial and may involve changes in iron metabolism and effects of inflammatory cytokines on erythroid progenitors to decrease their sensitivity to EPO [277].

1.3 Type 2 Immunity

1.3.1 Overview

In 1986, two forms of differentiation were described when $CD4^+$ T cells were activated by antigen-presenting cells with different combinations of cytokines: type 1 (Th1) and type 2 (Th2) [278]. Whereas Th1 T cells classically produce IFN-γ upon activation, Th2 T cells produce the cytokines IL-4, IL-5, and IL-13 [279]. Subsequently, the distinction between type 1 and 2 responses has been expanded to include elements of the innate immune system that produce or respond to the same cytokines and participate in responses to similar types of pathogen. Therefore, type 2 immune responses are now broadly defined as those associated with production of IL-4, IL-5, IL-9, IL-13, IL-25, IL-33, and thymic stromal lymphopoietin (TSLP), with important cells including Th2 T cells, type 2 innate lymphoid cells (ILCs), IgE^+ B cells, eosinophils, basophils, mast cells, and alternatively activated macrophages [280, 281]. The evolutionary pressure driving the development of type 2 responses probably derives from extracellular parasites, such as helminths. However, type 2 responses also have essential roles in tissue development and repair and in regulation of tissue metabolism [280]. Conversely, type 1 responses are associated with IFN-γ, IL-12, and IL-18 production and involve Th1 T cells, $CD8^+$ T cells, $IgG2^+$ B cells, NK cells, neutrophils, and classically activated macrophages. These responses have probably developed to clear intracellular pathogens. Finally, more recent work has unveiled other forms of $CD4^+$ T cell differentiation associated with distinct immune responses, particularly type 17 responses characterised by production of IL-6, IL-17, IL-21, IL-22, and IL-23 and involving type 3 ILCs, neutrophils and monocytes. The exact role of type 17

responses is disputed but probably centres on clearance of extracellular fungi and filamentous and encapsulated bacteria.

Type 1 and 2 responses are broadly antagonistic, with IFN-γ suppressing host resistance to helminth infestation [282]. In the context of inflammatory disease, regulation of pro-inflammatory and destructive type 1 responses was seen as a major function of supposedly anti-inflammatory and reparative type 2 responses. Whereas type 2 effector elements do have important roles in tissue repair, dysregulated type 2 responses may be pathogenic owing to unregulated tissue inflammation or frustrated repair, which may result in fibrosis [280]. Furthermore, spontaneous immune-mediated diseases rarely produce a single type of immune response, with many having simultaneous type 1, 2, and other responses. The relative importance of these different responses may vary with time and location in the body, with their net effects determining the extent and nature of the clinical phenotype. This notion has been extended by promulgation of 'immune modules', which term refers to any distinctive and relatively self-contained process, not limited to either innate or adaptive immunity, that may be active during disease [283]. Such immune modules incorporate traditional concepts in immunity, such as type 1 and 2 responses, with more recent additions, such as NOD-like receptor/inflammasome activity and autophagy/endoplasmic reticulum stress [284].

1.3.2 Interleukin-4

The gene encoding IL-4 is located on chromosome 11 in mice, in close proximately to those for IL-5 and IL-13; collectively these form the Th2 cytokine locus, which is expressed in activated Th2 T cells [285]. In addition to T cells, IL-4 is produced by eosinophils, basophils, mast cells [286, 287], and NKT cells [288].

In most cases, although these cells express mRNA encoding IL-4 constitutively, additional stimulation is required for secretion of the cytokine [289]. Although it has been disputed, ILC2s also produce IL-4 when cultured with IL-7 and IL-33 [290]. The dimeric receptor for IL-4 is composed of a specific receptor, IL-4Rα, in combination with either the common gamma chain (IL-2Rγc), mainly expressed in haematopoietic cells, or the IL-13Rα1 chain, which is expressed on non-haematopoietic and myeloid cells [285]. Therefore, the receptor transmitting IL-4 signals differs between lymphoid cells (IL-4Rα/IL-2Rγc, type I receptor) and non-haematopoietic cells (IL-4Rα/IL-13Rα1, type II receptor), with myeloid cells expressing both receptors. Both IL-4 receptor complexes phosphorylate STAT6 to affect transcription, but the type I receptor also activates insulin receptor substrate (IRS)1/2, which has non-genomic effects via the Akt and mTORC1 pathways.

Some features of IL-4 biology differ from that of other cytokines. IL-4 has an extremely high affinity for the IL-4Rα/γc [291], meaning only a low concentration is required to produce a maximal effect. Additionally, although IL-4 has been regarded as a classical lymphoid, immunoregulatory cytokine with effects on T and B cells, its receptor is expressed widely among haematopoietic cells [292], meaning many may be sensitive to its effects.

Several effects of IL-4 have been studied widely. These include its ability to cause Th2 T cell differentiation [293], proliferation and immunoglobulin class switching in B cells [294], and cause alternative activation of macrophages [295], all of which effects are dependent on IL-4Rα/γc ligation and STAT6 activation [296-298]. In haematopoiesis, the reported effects of IL-4 have been diverse and contradictory, often depending on the presence of other growth factors or on the types and levels of purity of the exposed cells [299]. Thus, using whole BM in

methylcellulose assays, investigators in the 1980s reported that IL-4 had a synergistic effect with G-CSF to promote granulocyte colony formation [300-303], and with EPO to promote BFU-E and CFU-E formation [301, 302, 304]. However, administered without these companion factors, IL-4 had no effect. This work was refined using cell populations enriched for progenitors, which formed CFU-GM (i.e. mixed granulocyte and macrophage) colonies in preference to CFU-G (i.e. granulocyte) when exposed to IL-4 with SCF [305]. A similar effect is observed in IL-4 deficient mice, from which the BM has a decreased ability to form CFU-GM and (mixed, multipotent) CFU-GEMM colonies [306]. A further pro-myelopoietic role for IL-4 is implied by the observation that culture of whole BM with IL-4 and GM-CSF causes the emergence of a population of $CD11c^+$, MHC class II^+, antigen presenting cells that share many functional features with DCs (BM-derived DCs, BMDCs) [307]. However, these cells are largely derived from $CD11b^+$, $Ly6C^+$ cells in BM, suggesting they represent a specialised differentiation state of cells already reaching maturity, rather than an effect on HSPCs [308]. Contradictory to these studies suggesting IL-4 might promote myelopoiesis was the observation that BM from mice lacking STAT6 formed increased numbers of BFU-Es and CFU-GMs [309], implying IL-4 might restrict expansion of these progenitors or an upstream MPP population. However, this effect is complicated by changes in Th1:Th2 balance in the T cell compartment. Specifically, expansion of Th1 T cells, which are no longer restrained by IL-4 in $STAT6^{-/-}$ mice, leads to increased IFN-γ production [310], which has a stimulatory effect on myeloid progenitors. This notion is confirmed by the finding that depletion of $CD4^+$ T cells restores the native phenotype in $STAT6^{-/-}$ mice [311]. In the context of *Plasmodium chabaudi* infection, $STAT6^{-/-}$ mice had enhanced reticulocyte production [312], suggesting IL-4 could suppress

erythropoiesis in this context. *In vivo*, excessive IL-4 production in transgenic mice causes anaemia owing to expansion of erythrophagocytic macrophages in the spleen, liver, and BM [313]; this phenomenon is probably related to the effect of IL-4 to promote G-CSF-independent proliferation of tissue resident macrophages [314]. Finally, when examining functional responses, previous studies indicated that healthy, IL-4-exposed [315], or $STAT6^{-/-}$ HSCs [309] had no differences in reconstitution of irradiated recipients, and that either IL-4 injection in mice over 10 days or STAT6 deficiency caused no changes in blood cells [309, 315].

Collectively, these studies suggest IL-4 could have some role in myelopoiesis, but the nature of any effect is complicated by 1) the requirement for additional trophic factors, 2) the ability of IL-4 to affect differentiation of mature myeloid cells, and 3) by confounding effects of IL-4 on the T cell compartment. Thus, the role of direct IL-4 signalling in the regulation of HSPCs, if any, remains largely unknown.

1.3.3 Interleukin-5

Interleukin-5 is expressed from a gene in the Th2 locus, meaning it is produced by similar cell types to IL-4: Th2 T cells, ILC2s, eosinophils, mast cells, and basophils. The receptor for IL-5 is composed of a specific chain, IL-5Rα, which associates with the common beta chain, βc (encoded by *Csf2rb*), which is shared with the receptors for IL-3 and GM-CSF [316]. The specificity of IL-5 is related to the expression of its receptor, which is confined to cells of the eosinophil lineage, $CD5^{+}$ B-1 B cells, basophils, and mast cells.

Interleukin-5 has a particular role in generation and persistence of eosinophils, such that IL-5 deficiency in mice causes eosinopenia [317] whereas

transgenic overexpression causes eosinophilia [201]. These effects occur at several levels, with IL-5 increasing generation of eosinophils in BM and inhibiting apoptosis of mature eosinophils in circulation [318]. Among mature eosinophils, IL-5 also activates effector functions, including CD11b expression, production of reactive oxygen species, phagocytosis [319], and chemotaxis [320]. Interleukin-5 also acts as an essential factor promoting development of innate B-1 B cells and increases their production of IgA [317, 321].

In the BM, type 2 cytokines act sequentially to specify eosinophils from MPPs [322], with IL-33 causing emergence of an early, IL-5Rα^{+} progenitor [323] (the eosinophil progenitor, EoP), which is dependent on IL-5 for its terminal differentiation [324].

1.3.4 Interleukin-33

The IL-1 family cytokine IL-33 is produced predominantly in stromal and epithelial cells, then stored in the nucleus and released in response to mechanical strain or if the cell undergoes necrosis or necroptosis [325, 326]. Although disputed [327], myeloid cells appear to be capable of producing IL-33 in response to some stimuli, such as ligation of the receptor dectin-1 by the β-glucan molecule curdlan on dendritic cells [328] and osteoclasts [329]. The receptor for IL-33 is composed of a specific receptor chain ‘suppressor of tumorgenicity’ (ST)2 (encoded by the gene *Il1rl1*) with adaptor protein IL-1 receptor accessory protein (IL1RAP) [205], which is shared with other members of the IL-1 cytokine family. The receptor is expressed principally on haematopoietic cells that participate in type 2 immune responses, including eosinophils, basophils, mast cells, ILC2s, and Th2 T cells [330]. However, a number of other cell types also express the IL-33 receptor at

varying levels according to their activation state; these include macrophages, neutrophils, dendritic cells, regulatory T cells (Tregs), Th9 T cells, NK cells, and even transiently on Th1 cells when activated [330, 331].

When first described, IL-33 was considered a type 2 cytokine owing to the pattern of expression of its receptor and biological effects [205]. Indeed, IL-33 has many effects that promote type 2 immune responses [332], including chemoattraction of Th2 T cells [333] and a propensity to cause Th2 T cells [205, 334, 335], ILC2s [290], mast cells [336], basophils [337], and eosinophils [338] to produce IL-5 and IL-13. Consequently, polymorphisms in the human *IL33* locus have been associated with risk of developing allergic diseases, including asthma [339] and atopic dermatitis [340], which is related to the ability of IL-33 to recruit and activate type 2 effector cells. Conversely, a loss of function mutation in the *IL33* locus protects people from asthma [341].

However, the manner of release of IL-33 from damaged barrier surfaces renders it an effective ‘alarmin’, alerting distant tissues to the occurrence of damage at another site [342]. Accordingly, IL-33 causes release of not only type 2 cytokines but also non-type 2 pro-inflammatory molecules, such as TNF-α, IL-6, and GM-CSF, which have wider roles in immunity and repair [343]. As a corollary, IL-33 contributes to repair and maintenance of tissues by increasing the regulatory activity of $ST2^+$ Tregs in, for example, the intestine [344], pancreas [345], and adipose tissue [346]. Owing to its nature as an alarmin and inducer of cytokines, IL-33 has been implicated as a factor promoting inflammatory responses during diseases that do not have a typical type 2 immune signature. For example, the serum concentration of IL-33 is increased in patient with ankylosing spondylitis [347, 348] and rheumatoid arthritis [349], and deficiency of IL-33 ameliorates disease in murine

CIA and antigen-induced arthritis (AIA) by preventing accumulation and activation of mast cells in the joints [350-352]. In IBD, the role of IL-33 is complex and dependent on clinical subtype and experimental model. Thus, in type 2 biased ulcerative colitis, IL-33 is overexpressed in the colon, and blockade or absence of ST2 ameliorates disease in the acute stages of the analogous dextran sodium sulphate (DSS) model of colitis in mice [353, 354]. Conversely, IL-33 itself ameliorated disease in mice treated with 2,4,6-trinitrobenzene sulphonic acid (TNBS) [355], which is considered a useful model of type 1 dominated Crohn's disease in people. This effect was attributed to increased activity of $ST2^+$ Tregs and counter regulation of Th1 T cells by a bolstered Th2 T cell response. Similarly, IL-33 expedited repair of the colon in mice that had received DSS chronically [356], indicating its role in colitis also varies with time and stage of disease. Collectively, this shows that the inflammatory actions of IL-33 may be mediated by several distinct mechanisms according to the disease context and kinetics.

Interleukin-33 has pleiotropic effects on haematopoiesis, commensurate with its dual roles as type 2 cytokine and alarmin. The gene encoding ST2 is expressed in GMPs [357] and $GATA1^+$ pre-GM progenitors [80], which generate mast cells, basophils, eosinophils, platelets, and erythrocytes. However, the protein receptor was detected by flow cytometry only on the surface of MEPs (with the potential to generate platelets and erythrocytes) and the late progenitors for mast cells, basophils, and eosinophils, and not on GMPs or pre-GMs [80, 358], regardless of GATA1 expression. Recently, mRNA encoding ST2 was also detected in the LSK fraction of murine BM [357], but protein expression has been disputed, with one study reporting it by flow cytometry [359] and others not detecting it [358, 360]. The

ST2 receptor is also expressed on the dedicated progenitor for ILC2s (ILC2Ps) in BM [361], which is derived from the CLP in a process also dependent on IL-33 [362].

Injection of IL-33 causes eosinophilia in the blood, spleen, and BM [205], with expansion of EoPs in BM and spleen [358]. The expansion of EoPs is an indirect effect caused by increased IL-5 concentrations [358, 363], but IL-33 also directly expands a progenitor population upstream of the EoP [323], before the IL-5Rα is expressed. Conversely, mice lacking IL-33 or ST2 have decreased blood eosinophil counts compared to wild type counterparts [323], as do people with a loss of function mutation in *IL33* [341]. Numbers of mature basophils but not mast cells were increased by IL-33 injection in mice [358, 364], but neither progenitor population was expanded [358]. In *ex vivo* culture of MEPs, IL-33 appeared to have no effect on proliferation or erythroid differentiation, but this effect was measured only by assessing expression of CD71 [358], which marker is not unique to the erythroid lineage. Finally, IL-33 is required for ILC2P formation [362] and promotes egress of ILC2s from the BM to peripheral tissues [365]. Thus, consistent with its role in regulating type 2 immunity, IL-33 is required for eosinopoiesis and generation of ILC2s but is apparently dispensable for formation of other type 2 effector cells.

Upstream of lineage-committed progenitors, a previous study suggested IL-33 injection did not affect numbers of GMPs in BM [366], but this was contradicted by others [367] and by analysis of IL-33 transgenic mice, which had increased numbers of GMPs [368]. Indeed, this transgenic overexpression caused such marked expansion of the myeloid compartment as to produce neutrophilia and eosinophilia in the blood and infiltration of neutrophils into the paws to cause mild arthritis [368]. Injection of IL-33 consistently expanded the whole LSK population enriched for reconstituting cells in BM [366, 367] but did not affect number of the

primitive HSCs [369], suggesting this effect was attributable to expansion of some or all MPP subsets. In spite of this, $ST2^{-/-}$ cells were outcompeted by WT cells in mixed BM chimeras when examined 4 months after reconstitution [357], suggesting IL-33 signalling may have some role in regulating the HSC population. Collectively, these data suggest IL-33 could have broader effects on haematopoiesis than merely to enhance production of type 2 effector cells, and this could be related to its role as an alarmin, possibly remodelling haematopoiesis to meet demand.

Consistent with this latter hypothesis, IL-33 also causes migration of several types of cell out of BM into the periphery, licensing them to engage in EMH in damaged or inflamed tissues. Specifically, IL-33 mobilised cells with the capacity to form myeloid colonies from BM to blood and spleen, and this effect was attributable to increased production of the emigrant chemokine CCL7 from BM vascular endothelial cells [370, 371]. As noted in **section 1.1.8**, IL-33 also causes emergence of a population of cells with properties of MPPs in the GALT of mice [210, 372], which might be attributable to mobilisation of BM HSPCs to this location.

1.3.5 Myeloid cells

Myeloid cells deliver many of the final effector functions of type 2 responses. Exposure of macrophages to IL-4 and/or IL-13 induces a programme of differentiation described as alternative activation, which is characterised by upregulation of arginase-1, FIZZ, and Ym1/2, and by expression of CD163 and the mannose receptor CD206 at the cell surface [295]. Alternative activation cannot be induced by IL-33 alone, but it reinforces this pattern of differentiation [373]. Although a strict dichotomy between classical and alternative macrophage activation is probably a feature of experiments conducted *in vitro* and not always

translatable to disease settings, IL-4/IL-13-exposed alternatively activated macrophages (AAMφ) are considered to have broadly homeostatic, anti-inflammatory, and reparative roles in inflamed tissues [374].

Others have proposed that neutrophils might undergo similar differentiation into so-called N(IL-33) polarised neutrophils when exposed to IL-33, but this effect could only be achieved *in vitro* with high concentrations of the cytokine, suggesting it may have little relevance *in vivo* [375]. More broadly, IL-33 appears to have a role in recruitment of neutrophils to inflamed tissues, which is partially attributable to a direct effect on $ST2^+$ neutrophils [376] but is also dependent on production of cytokines, including TNF-α, by other cells in response to IL-33 [376, 377].

Classically, eosinophils have been implicated in expulsion of helminth parasites, which they accomplish by releasing the contents of pre-formed granules. However, others have speculated that they play a more important role in tissue homeostasis, remodelling, and repair [378], largely owing to their ability to induce AAMφs by secretion of IL-4 and IL-13. This role of eosinophils is exemplified by sterile surgical injury: in response to such an insult in the peritoneal wall, reparative AAMφs were induced by IL-4 produced by local eosinophils [379].

1.3.6 Co-ordination of type 2 responses

The various responses and effector mechanisms of type 2 immunity are complex and highly co-ordinated [280]. Thus, an initial insult may cause release of IL-33 from damaged cells, which subsequently causes local production of IL-4, IL-5, and IL-13 from ILC2s and mast cells in tissue. These effects increase recruitment of type 2 effector cells, particularly eosinophils, and induce polarisation of macrophages to an alternative state. Additionally, increased concentrations of IL-4

favour differentiation of Th2 T cells when naïve T cells are activated, reinforcing the type 2 response as the adaptive immune system participates. Increased concentrations of IL-5 and IL-33 also modulate myelopoiesis in the BM, increasing production of eosinophils to sustain the local response. In the tissue, interactions among eosinophils, AAMφs, and ILC2s produce the final effects of pathogen clearance and repair.

1.4 Spondyloarthritis

1.4.1 Overview

Spondyloarthropathies are a complex of chronic inflammatory diseases that affect some combination of the axial spine (spondylitis) and peripheral joints (arthritis) and have shared pathogenic elements [380]. Unlike RA, spondyloarthritis (SpA) is not associated with production of the autoantibody rheumatoid factor, meaning it is often described as a seronegative rheumatological disease. Characteristic clinical features of SpA include spondylitis that progresses to cause deposition of bone between vertebrae (ankylosis), asymmetrical inflammation of peripheral joints (oligoarthritis), inflammation at the site of tendon, ligament, or joint capsule insertion into bone (enthesitis), and inflammation of the skin (psoriasis), and eyes (uveitis) [381]. Additionally, SpA patients are more likely to develop IBD than matched controls, and analysis of endoscopic biopsies from people with SpA reveals that 50-60% have subclinical inflammation of the small intestine (enteritis) [382, 383]. Thus, SpA is a systemic disease causing pathology in multiple locations. The most common forms of SpA are ankylosing spondylitis (AS), which is estimated to affect ~1% of the adult population of the USA [384], psoriatic arthritis (PsA), reactive arthritis, and spondylitis occurring with IBD.

1.4.2 SKG model

Development of SpA has been modelled in the SKG strain of mice. This strain arose from a spontaneous mutation in the gene encoding ZAP-70 in a colony of BALB/C mice in Japan, causing the founder to develop spontaneous inflammation of multiple joints [385]. In the homozygous strain that was subsequently established, mice developed symmetrical inflammatory arthritis, dermatitis resembling psoriasis, pneumonitis, and uveitis by the age of 2-4 months when kept in standard conditions [385].

ZAP-70 is an important component of the T cell receptor (TCR) signalling complex [386], and the W163C mutation of SKG mice increases the threshold for T cell activation [387]. Consequently, only those thymocytes with relatively high affinity for self-antigens are positively selected, creating a repertoire of TCR clones biased towards autoreactivity [385]. Similarly, the activity of thymic Tregs is decreased owing to the higher threshold for TCR activation, producing defects in dominant as well as recessive tolerance [388]. Owing to these features, SKG mice are predisposed to development of autoreactive T cell responses when exposed to innate immune stimuli [389]. Under specific pathogen free (SPF) conditions prevailing in most animal facilities, there is insufficient exposure to microbial antigens to stimulate these responses, allowing mice to remain healthy [389]. However, in non-SPF conditions that permit colonisation of the lungs with fungal species, or with injection of microbial derivatives, activation of innate cells primes autoreactive T cells to generate harmful responses, resulting in the observed phenotype [389]. Because this disease is driven by T cell responses to self-antigens, it does not resolve, with mice normally being culled after 4-8 weeks (**Fig. 1.4**).

Figure 1.4

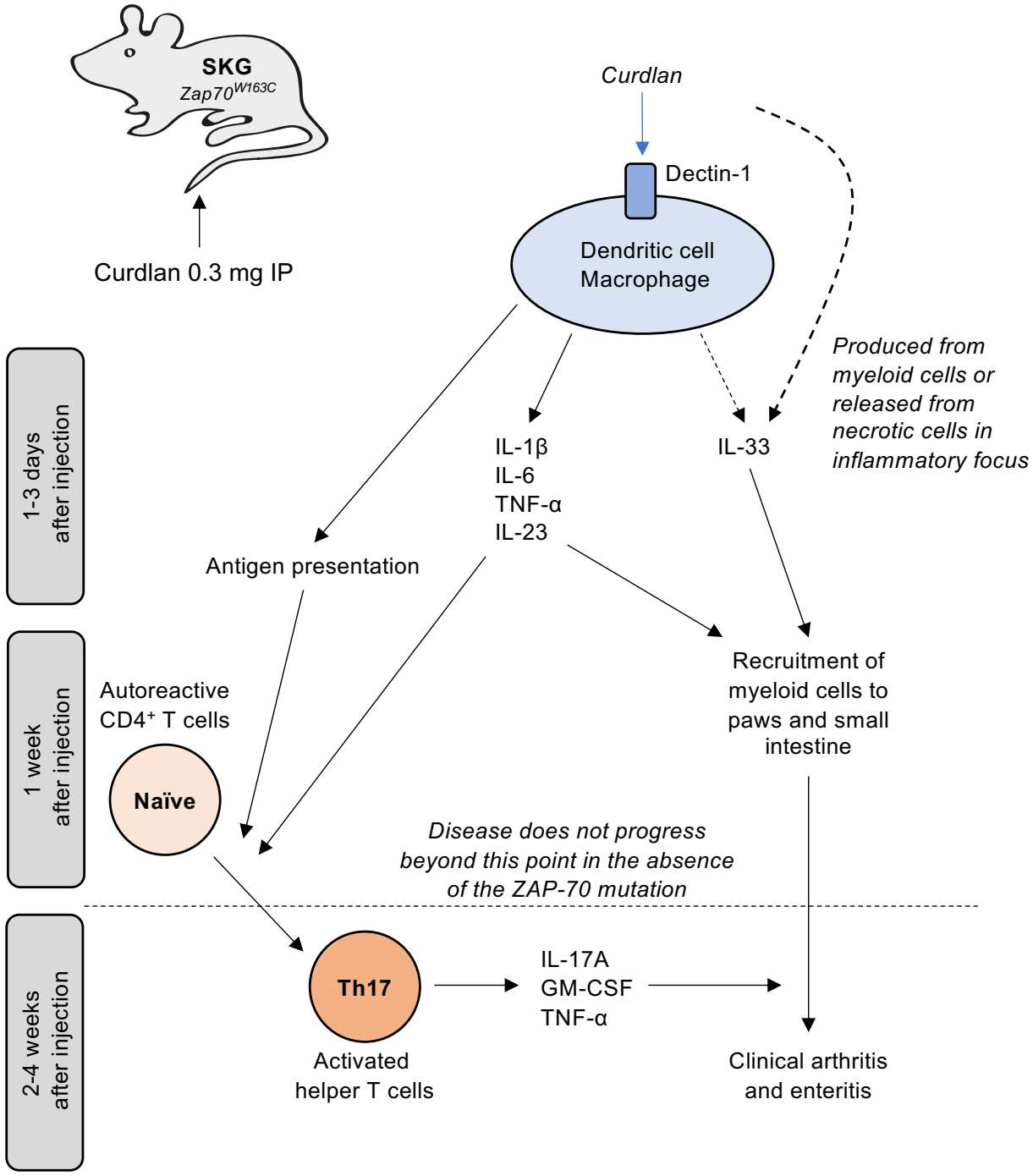

Figure 1.4: Outline of immunological events occurring after curdlan injection in SKG mice

Schematic diagram showing production of cytokines by innate immune cells after injection of curdlan, which causes initial recruitment of myeloid cells detectable in SKG or wild type mice. The background of innate immune activation is sufficient to activate autoreactive T cells in SKG mice, but not wild type mice, resulting in strong type 17 immune responses that sustain inflammation in the paws and small intestine to cause clinical disease detectable after 2-4 weeks. Timing of key events after curdlan injection is shown in grey boxes.

Not all microbial derivatives appear to cause the same response in SKG mice, with the TLR agonists LPS and poly(I:C) causing only mild and transient inflammation [389]. Conversely, compounds containing β-glucan molecules, which normally derive from fungi and are ligands for the receptor dectin-1 [390], generate strong T cell responses and severe disease [389]. Even among β-glucan compounds, different agents produce a variable phenotype, with zymosan and mannan causing principally arthritis and enthesitis [389], whereas curdlan, which is a β-1,3-glucan derived from the cell walls of fungi or the bacterium *Alcaligenes faecalis*, causes this and also spondylitis and new bone formation in the axial spine and ileitis in the small intestine [391]. Whereas arthritis and enthesitis are apparent from ~2 weeks after curdlan injection with almost complete penetrance, ileitis develops from 4-5 weeks with incomplete penetrance [391]. Consequently, curdlan injection in mice appears to produce the most faithful recapitulation of the clinical features of SpA, whereas zymosan- or mannan-injected mice are taken as models of RA [392]. However, in reality, there is considerable overlap in the pathogenic features and clinical manifestations of mice injected with any of these compounds [389]. With curdlan injection, there is an as-yet unexplained difference in disease phenotype in different sexes, with females developing more severe and progressive disease than males [391].

The importance of different elements of the immune system in development of SpA in SKG mice has been demonstrated experimentally. Thus, disease may be transferred to mice lacking lymphocytes by injection of $CD4^+$ T cells from SKG mice [385], indicating that T cells are essential for the clinical phenotype. Conversely, transfer of SKG BM to thymectomised mice does not produce disease, demonstrating that it is abnormal thymic selection that underlies the propensity for

autoimmunity [385]. Although T cells are essential for disease, SpA does not develop in mice injected with both curdlan and an antibody to block its receptor dectin-1 [389], indicating innate immune stimulation via this receptor is essential for initiation of disease. Breeding of SKG mice with various cytokine knockout strains reveals the dependence of disease on TNF-α, GM-CSF, IL-1β, IL-6, and IL-17 [393-395]. Conversely, IL-10 was protective, whereas IFN-γ and IL-4 appeared to have no effect on disease [393].

1.4.3 Pathogenesis and immune modules

The pathogenesis of human SpA is complex, involving aspects of innate and adaptive immunity. Indeed, others have proposed that SpA could arise from exuberant innate immune responses to damage- and pathogen-associated molecular patterns, which prime autoreactive T cells to become the major drivers of continued pathology [387]. Several immune modules appear to be important in progression of disease.

1.4.3.1: HLA-B27 and T cell reactivity

In people, possession of the HLA-B27 allele in the class I MHC complex is the single greatest risk factor for development of SpA, being present in 85-90% of patients [396]. Transgenic expression of HLA-B27 alleles in rodents is also sufficient to produce disease resembling SpA [397]. Because the major function of HLA-B alleles is to present peptides to the TCR of $CD8^+$ T cells, the characteristics of peptides presented by HLA-B27 have been compared to those of other alleles, with no difference detected in the features of peptides presented by these different alleles [398]. Despite this, clonal expansions of T cells with similar TCR

rearrangements are detected in patients with SpA [399, 400], which is presumably driven by antigen responsiveness. Thus, while it appears responses to peptide-HLA-B27 complexes might be an important determinant of antigen-specific T cell responses in SpA, the mechanistic basis for this process is currently lacking. However, in addition to its role in antigen presentation, HLA-B27 molecules may form 'open' homodimer complexes on the cell surface, which are not bound to peptide or associated with β2-microglobulin [401]. In this state, HLA-B27 homodimers act as ligands for the KIR3DL2 immunoreceptor expressed on $CD4^+$ and $CD8^+$ T cells, NK cells, and γδ T cells [402, 403], causing T cells to produce IL-17A and maintain Th17 differentiation (discussed in **section 1.4.3.2**) at the expense of IFN-γ production and Th1 differentiation [404].

1.4.3.2: IL-23/IL-17 axis

Patients with AS have increased serum and synovial fluid concentrations of IL-17A [405] and increased numbers of IL-17-producing Th17 T cells, γδ T cells, NKT cells, and group 3 ILCs in blood and inflamed joints [406-412]. Collectively, this indicates SpA is associated with prominent type 17 immune responses [413, 414], the importance of which is reinforced by association of polymorphisms in several loci, such as the defining Th17 transcription factor 'RAR related orphan receptor' (ROR)γt, and the receptors for IL-6, IL-17A, and IL-23, with risk of developing SpA in genome-wide studies [415, 416]. Mechanistically, it is likely IL-17A recruits neutrophils and other mature myeloid cells to inflamed sites by stimulating production of G-CSF from stromal cells, as it does in other settings [417, 418]; neutrophils are abundant in the inflamed joints and entheses of people with AS and implicated in the development of inflammation [419]. Although $IL\text{-}17A^+$

neutrophils [420] and mast cells [421] have been observed in the joints of SpA patients, current consensus suggests they sequester and release the cytokine rather than producing it themselves [422, 423].

Conventional understanding of type 17 responses states that naïve $CD4^+$ T cells may be induced to differentiate into Th17 T cells by exposure to some combination of IL-6, TGF-β, IL-1β, or IL-21 as they are activated by antigen-presenting cells [424-426]. Thereafter, the stability of Th17 differentiation is maintained by IL-23 [424, 427, 428], which is expressed by tissue-resident dendritic cells and macrophages [429]. Accordingly, the healthy synovium and enthesis of humans and mice contain populations of IL-23 $receptor^+$ cells [430, 431], which drive development of enthesitis in mice when exposed to IL-23 by producing IL-17A [432]. Although this might suggest IL-17A-producing cells could be activated directly in the joints and entheses as SpA develops [433, 434], a different thesis holds that Th17 T cells and IL-$17A^+$ γδ T cells could be induced in the gut and then home to the joints, following a chemotactic gradient of IL-23 and assisted by expression of homing integrins that are shared between joint and gut [435]. According to this notion, gastrointestinal barrier damage or microbiome perturbation would be initiating events in SpA, with activated IL-$17A^+$ cells distributing pathology to multiple sites.

As with human AS, development of SpA in SKG mice is associated with increased numbers of Th17 T cells in the joints, lymph nodes, and spleen [395, 436]. The importance of this response is demonstrated by the effects of injection of anti-IL-23 antibodies in curdlan-injected mice, which prevented development of SpA [391], and by crossing onto IL-$17^{-/-}$ mice, which ameliorated but did not abolish it [437]. Consistent with the hypothesis that priming of type 17 responses occurs in

the intestine, curdlan injection in SKG mice caused increased expression of *Il23* in the ileum, and IL-23 was necessary for increases in blood concentrations of IL-6 and IL-17A [437]. The increase in intestinal IL-23 in response to curdlan was dependent on the presence of microbiota because it was not observed in germ-free mice [438], suggesting interaction between the microbiome and intestinal immune system is responsible for IL-23 production when curdlan is injected.

1.4.3.3 Type 2 immunity in the intestine

Although the joints and circulation are dominated by IL-17A$^+$ cells, the immune signature obtaining in the small intestine of people with AS displays features of a type 2 immune response. This includes increased expression of the genes encoding IL-4 and IL-5 compared to healthy controls [439], and accumulation of macrophages with features of alternative activation, such as CD163 expression [440]. This suggests the possible existence of a concurrent type 2 immune module in the gut, though it remains unclear whether this is broadly anti-inflammatory and reparative or whether it contributes to development of enteritis or distant pathology, as occurs in ulcerative colitis. Consistent with its role as an alarmin released from cells experiencing damage or mechanical strain, the serum and synovial fluid concentrations of IL-33 are also increased in people with AS [347, 348], though the effects of this on immunity are unknown in this context.

1.4.3.4 GM-CSF

Production of GM-CSF by group 3 ILCs, CD4$^+$ T cells, synovial stromal cells, and mast cells has been implicated in development of inflammatory arthritis in SKG mice [394, 441], with administration of anti-GM-CSF antibodies preventing clinical

disease [441]. In people with SpA, GM-CSF is also produced by $CD4^+$ and $CD8^+$ T cells in blood and by ILCs in the synovium, often by cells also producing IL-17A [442]. Consistent with the widespread expression of its receptor among mature myeloid cells and HSPCs, GM-CSF caused increased infiltration of neutrophils into the paws and expansion of BM myelopoiesis in SKG mice [441], as well as increased TNF-α production in $CD14^+$ monocytes derived from the blood of people with SpA [443]. Collectively, this suggests GM-CSF production, which is associated with pathogenic type 17 responses, contributes to development of SpA in mice and people owing to its role in myelopoiesis and myeloid effector responses.

1.4.4 Haematopoietic changes

Several haematological abnormalities are observed in people when AS is diagnosed, suggesting haematopoiesis is affected by systemic inflammatory signals. These include increased neutrophil and decreased lymphocyte counts in blood, such that the neutrophil: lymphocyte ratio has been used as an indicator of disease activity [444]. Additionally, 15-20% of people have anaemia when AS is diagnosed [445-447]. Although this is partially responsive to administration of anti-IL-6 [445] and anti-TNF-α antibodies [446], it is unclear at what level these cytokines might be acting or whether they exert any important direct effect on erythroid progenitors during SpA. SKG mice are known to be lymphopenic [385], but this defect is related to abnormal selection of T cells in the thymus rather than to any abnormality in BM lymphopoiesis.

1.5 Aims of the thesis

Although SKG mice have been identified as useful models of RA and SpA, possible changes in haematopoiesis have not been investigated previously. Specifically, it is unknown if dysregulated haematopoiesis might contribute to progression of disease in this model. Similarly, previous investigations have not considered the possibility of different immune modules developing in SKG mice, including type 2 immune responses in the gut, as has been described in people with AS. Knowing that type 2 cytokines may modulate haematopoiesis through a number of different mechanisms, I sought to bring these unresolved areas together by asking whether a possible type 2 immune module in SpA might modulate haematopoiesis to contribute to progression of disease or cause important comorbidities. Therefore, the broad aims of the thesis were:

1. To produce a comprehensive description of haematopoietic changes in SKG mice developing SpA, assessing both phenotypic and functional features of the haematopoietic system (**Chapter 3**).
2. To determine whether SKG mice with SpA have evidence of a type 2 immune module in the intestine and to investigate whether this has any impact on haematopoiesis (**Chapter 4**).
3. To investigate causes of anaemia of inflammatory disease in SKG mice developing SpA, focussing on the role of IL-33 (**Chapter 5**).
4. To investigate the role of IL-33 in progression of disease and in wider regulation of haematopoiesis during disease (**Chapter 6**).

2 Materials and Methods

2.1 Materials

2.1.1 Mice

All mice were maintained in specific pathogen free (SPF) conditions in individually ventilated cages at the University of Oxford. All procedures were performed with appropriate licences issued under the Animals (Scientific Procedures) Act 1986 and with approval from the University of Oxford animal welfare and ethical review board (project licences 30/3218 and P508FFA1F).

Wild type C57BL/6 mice, CByJ.SJL-*Ptprc*^{a}, C57BL/6-*Ubc*^{GFP}, and C57BL/6-*Il6*$^{-/-}$ mice were purchased originally from the Jackson Laboratory but were bred at the University of Oxford. B6.SJL-*Ptprc*^{a} mice were bred at the University of Oxford and purchased from another facility for use in our laboratory. C57BL/6-*Il1rl1*$^{-/-}$ (ST2 knockout) mice were obtained from Professor Padraic Fallon (Trinity College Dublin, Ireland) and BALB/C-*Zap70*^{W163C} (SKG) mice were obtained from Professor Shimon Sakaguchi (Osaka University, Japan) then maintained at the University of Oxford. BALB/C-*Il33*$^{+/cit}$ mice were obtained originally from Professor Andrew McKenzie (University of Cambridge, UK) and then backcrossed with wild type C57BL/6 mice until the base genotype was 99.9% pure based on single nucleotide polymorphism (SNP) genotyping. The mice were also intercrossed to generate C57BL/6-*IL33*$^{cit/cit}$ mice, expressing citrine genes in both *Il33* loci instead of the functional genes.

Mice were used when aged 8-16 weeks and were ear-notched for identification during experiments. Mice of a single sex were used for experiments, or males and females were distributed equally among experimental groups.

Treatments were randomised by consecutive allocation but not blinded. An outline of the use of different animal models is shown in **Fig. 2.1**.

2.1.2 Antibodies

Antibodies used for flow cytometry or *in vivo* treatment are listed in **Tables 2.1-2.3**. Purchased antibodies for use *in vivo* were certified as low endotoxin and azide-free.

Table 2.1: Antibodies used for *in vivo* treatment

Specificity	**Clone**	**Source**
Interleukin-4	11B11	Bio X Cell
	11B11	BioLegend
	11B11	Hydridoma – Powrie laboratory
Isotype (rat IgG1)	HPRN	Bio X Cell
Interleukin-5	TRFK5	Bio X Cell
Isotype (rat IgG1)	HPRN	Bio X Cell
Interleukin-33	Polyclonal	R&D Systems
Polyclonal goat IgG	Polyclonal	R&D Systems
GM-CSF	MP1-22E9	Bio X Cell
Isotype (rat IgG2a)	2A3	Bio X Cell
CD4	YTS191	Bio X Cell
Isotype (rat IgG2b)	LTF-2	Bio X Cell

Figure 2.1

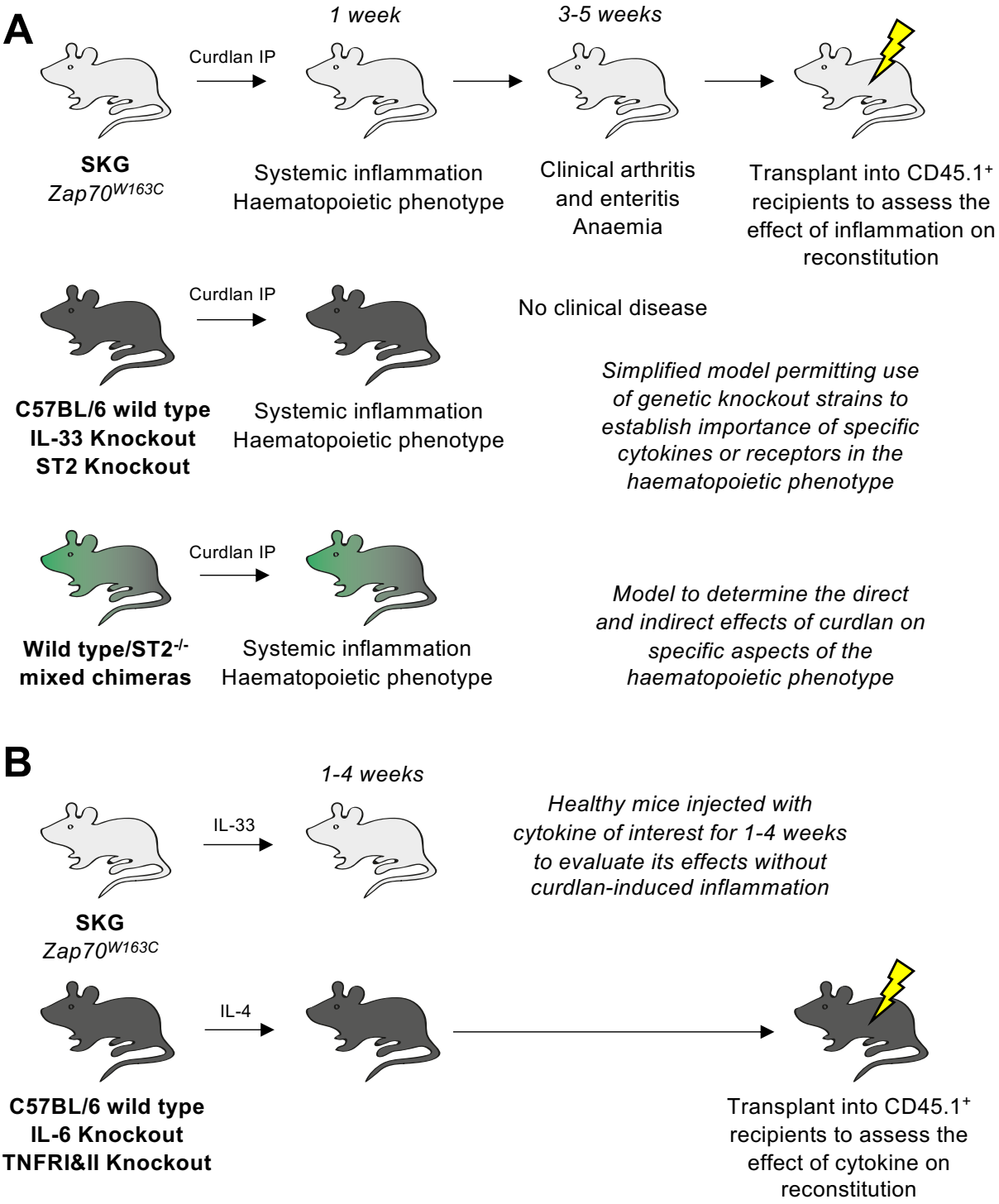

Figure 2.1: Outline of animal models used in this thesis
(**A**) Schematic diagram showing models of systemic inflammation induced with curdlan. In SKG mice, curdlan injection causes systemic inflammation followed by clinical disease, producing a useful model of human SpA. A simplified model recapitulating features of systemic inflammation and haematopoietic derangement may be created by injecting curdlan in wild type mice that lack the ZAP-70 mutation, and curdlan may then be injected into various C57BL/6 strains with specific knockouts to assess the importance of those molecules in development of the observed phenotype. This investigation may be extended by further by creating mixed bone marrow chimeras to determine which of the effects of curdlan are direct or indirect.
(**B**) Schematic diagram showing models for assessing effects of cytokines in vivo by injecting into healthy wild type or knockout mice, sometimes followed by transplantation of bone marrow to determine their effects on reconstitution potential.

Table 2.2: Anti-mouse antibody clones used for flow cytometry and sorting

Specificity	Clone	Source	Fluorochrome	Concentration
CD3ε	145-2C11	BioLegend	PerCP/Cy5.5	1:200
CD4	GK1.5	BioLegend	PerCP/Cy5.5	1:200
CD11b	M1/70	Biolegend	PerCP/Cy5.5, AF700, BV510, PE Dazzle	1:250
CD16/32	2.4G2	BD	APC/Cy7, PE/Cy7	1:100
CD16/32 (FC block)	93	BioLegend	None	1:200
CD31	390	BioLegend	APC Dragon	1:200
CD34	Ram34	BD	FITC	1:50
CD41	MWReg30	BioLegend	FITC, PerCP/Cy5.5, PE/Cy7	1:200
CD44	IM7	BioLegend	FITC	1:200
CD45 (pan-specific)	30-F11	BioLegend	AF700	1:200
CD45.1	A20	BioLegend	PE	1:200
CD45.2	104	BioLegend	APC	1:200
CD48	HM48-1	BioLegend	PE Dazzle	1:200
CD49b	DX5	BioLegend	PE Dazzle	1:200
CD51	RMV-7	BioLegend	PE	1:200
CD55	RIKO-3	BioLegend	PE, AF647	1:200
CD64	X54-517.1	BioLegend	PE	1:300
CD71	R17217	BioLegend	FITC, PE, PE/Cy7	1:500
CD105	MJ7/18	BioLegend	Pacific blue, APC	1:200
CD115	AFS98	BioLegend	PE/Cy7	1:200
CD117 (c-Kit)	2B8	BD	BV786	1:100
CD124 (IL-4Rα)	IO15F8	BioLegend	PE	1:100
CD140a (PDGFRα)	APA5	BioLegend	APC	1:200
CD150	TC15-12F12.2	BioLegend	BV605	1:200
CD169	3D6.112	BioLegend	APC	1:100
B220	RA3-6B2	BioLegend	FITC, PerCP/Cy5.5, AF700	1:200
Flt3	A2F10	Biolegend	APC	1:200
F4/80	BM8	BioLegend	PE, BV605	1:200
Ly6G	1A8	BioLegend	FITC, APC, PerCP/Cy5.5	1:200
Ly6C	HK1.4	BioLegend	BV711	1:400

Gr1	RB6-8C5	BioLegend	PerCP/Cy5.5, BV711	1:200
SiglecF	E50-2440	BD	BV421, PE	1:100
FcεRI	MAR-1	BioLegend	PerCP/Cy5.5, PE/Cy7	1:100
Ter119	TER119	BioLegend	APC, PerCP/Cy5.5	1:200
ST2	DIH9	BioLegend	PE, APC	1:100
ESAM	1G8/ESAM	BioLegend	PE/Cy7	1:200
EPCR	RCR-16	BioLegend	PE	1:200
Sca-1	D7	BioLegend	Pacific blue, BV605, BV711	1:100
TNFRI (p55)	55R-179	BioLegend	PE	1:100
TNFRII (p75)	MCA351A648T	AbD Serotec	AF647	1:100
GM-CSFRα	698423	R&D Systems	APC	1:100
IFNγR	2E2	BioLegend	Biotin	1:200
IL6R	D7715A7	BioLegend	PE/Cy7	1:100
IL-4	11B11	BD	AF488, APC	1:200
IL-5	TRFK	BioLegend	BV421	1:100
IL-17A	eBio17B7	eBioscience	APC	1:100
GM-CSF	MP1-22E9	BioLegend	PE	1:100
IgG1 isotype	RTK1071	BioLegend	PE	1:200
IgG2a isotype	RTK2758	BioLegend	PE	1:50
TNF	MP6-XT22	BioLegend	BV711	1:100
Ki67	16A8	BioLegend	PE	1:50
BrdU	Bu20a	BioLegend	PE	1:100
NF-kB p65	F-6	Santa Cruz Biotechnology	PE	1:100
STAT5 pY694	47/Stat5	BD	PE	5 µl per 10^6 cells
Akt pS473	M89-61	BD	AF647	
Akt pT308	J1-223.371	BD	PE	
ERK1/2 pT02/pY204	20A	BD	AF647	
P38 MAPK pT180/pY182	36/p38	BD	PE	
mTOR pS2448	MRRBY	BD	PE	
S6 pS235/pS236	N7-548	BD	PE	

Table 2.3: Anti-human antibodies used for flow cytometry and sorting

Specificity	Clone	Source	Fluorochrome	Concentration
CD3	DKT3	BioLegend	Biotin	1:200
CD19	HIB19	BioLegend	Biotin	1:200
CD14	63D3	Biolegend	Biotin	1:200
CD71	CY1G4	BioLegend	PE/Cy7	1:200
Flt3	6H6	BioLegend	APC	1:200
CD235a	HI264	BioLegend	APC	1:200
CD34	561	BioLegend	FITC	1:200

2.1.3 Recombinant cytokines

Recombinant murine cytokines used for *in vivo* treatment are listed in **Table 2.4**. For IL-4 injections, recombinant IL-4 was mixed with anti-IL-4 antibodies for 10 minutes at room temperature before injection, as described previously [448] These complexes prolong the half-life of IL-4 when injected but do not cause activation of Fcγ receptors, which is demonstrated by the lack of effect of complexes in IL-4Rα$^{-/-}$ mice [448].

Table 2.4: Recombinant cytokines used for *in vivo* treatment.

Cytokine	Dose	Frequency	Duration	Route	Source
Interleukin-4	5 µg IL-4 mixed with 25 µg 11B11 clone anti-IL-4 antibody per injection	One injection every 48 hours	Three injections	IP	Cytokine and antibody from BioLegend
Interleukin-33	0.5 or 1 µg per injection	Schedule 1: One injection every 48 hours for four injections, culling the day after the final injection. Schedule 2: One injection three times weekly for 4 weeks, with or without prior administration of curdlan.		IP	BioLegend

Erythropoietin	1875 IU per injection	One injection every 48 hours	Five injections	IP	BioLegend

IP: intra-peritoneal

2.2 SKG model of spondyloarthritis

2.2.1 Induction and monitoring of disease

Mice were induced to develop clinical disease by intra-peritoneal (IP) injection of 0.3 mg curdlan derived from *Alcaligenes faecalis* (Wako Chemicals) prepared in a total volume of 300 µl sterile PBS per mouse, as described previously [391]. For most experiments comparing healthy and inflamed mice and for experiments evaluating possible treatments, female mice were used because they develop more severe disease than males [391]. Conversely, for administration of substances that might aggravate disease, male mice were used so that the effect would be detectable. Mice were weighed weekly and the following measurements were made using callipers (Diatest Ltd): 1) dorso-ventral thickness of the carpus and manus, 2) dorso-ventral thickness of the pes distal to the tarsus, and 3) medio-lateral thickness of the tarsus. Measurements 1) and 2) for each paw were summated to generate a composite measure of 'paw swelling', whereas measurement 3) was summated from the two limbs to produce a measure of 'tarsal swelling'. Changes in paw and tarsal swelling were expressed as a percentage increase from the measurement on the day of injection of curdlan. Mice were culled if they lost more than 20% of their bodyweight compared to baseline, or if they developed marked abdominal distension or other complications affecting welfare. Most mice were culled 3-6 weeks after injection of curdlan after they had developed overt SpA.

Additionally, a clinical score was assigned for the limb of each mouse using the following scheme shown in **Table 2.5** [441]:

Table 2.5: Clinical arthritis score used in SKG mice

Score	Definition
0	No swelling or redness
0.5	Swelling or redness of digits and mild swelling and/or redness of carpi or tarsi
1	Mild swelling of the carpal or tarsal joints
2	Moderate swelling of carpal or tarsal joints
3	Substantial swelling of carpal or tarsal joints not inhibiting normal mobility, feeding, or drinking

Scores for all 4 limbs were summated to produce a total score for each mouse at each time point.

2.2.2 Dissection and preparation of cell suspensions

One pes was dissected from culled mice by cutting distal to the tarsus, and the skin was removed. The tissue was then cut into 3 pieces and incubated in 1 ml of RPMI 1640 medium (Gibco) supplemented with DNAse I (0.1 mg/ml, Sigma Aldrich) and liberase (0.3 mg/ml, Roche) for 105 minutes at 37^{o}C. After this time, the fragments of tissue were placed into a 70 μm filter inside a 50 ml tube containing 5 ml of RPMI 1640 medium with 5% fetal calf serum (FCS, Sigma Aldrich, heat-sterilised and non-US origin) and 0.5 mM EDTA (Invitrogen). The tissue was crushed using the plunger of a 5 ml syringe and then washed through the filter using 30 ml PBS with 0.1% bovine serum albumin (BSA, Sigma Aldrich). The solution was centrifuged, supernatant discarded, and cell pellet re-suspended in 0.5 ml PBS/0.1% BSA.

Mesenteric and popliteal lymph nodes were crushed and washed through a 70 μm filter using 10 ml of PBS/0.1% BSA. The solution was centrifuged and re-suspended in 0.5 ml (mesenteric) or 0.25 ml (popliteal) PBS/0.1% BSA.

Femurs, tibiae, and sometimes humeri were dissected, and extraneous muscle and fat were removed by sharp dissection. The epiphyses were removed, and the marrow cavities flushed with 5 ml PBS/0.1% BSA using a 1 ml syringe with 25G needle. The clumps of tissue were disrupted by pipetting approximately 10 times with a P1000 pipette before passing the suspension through a 70 μm filter. The suspension was centrifuged and re-suspended in 1 ml PBS/0.1% BSA. For some experiments, the centrifuged cell pellet was mixed with 1 ml red blood cell lysis solution (Sigma Aldrich) for 2 minutes before diluting with 10 ml PBS/0.1% BSA, centrifuging, and re-suspending as described above.

The spleen was removed then crushed and washed through a 70 μm filter using the plunger of a 5 ml syringe and 10 ml PBS/0.1% BSA. Clumps of tissue were disrupted by pipetting with a 10 ml pipette (StarLab) before transferring to a 15 ml tube. The suspension was centrifuged, supernatant discarded, and cell pellet re-suspended in 1-2 ml PBS/0.1% BSA. In some experiments, the cell pellet was mixed with 2 ml red blood cell lysis buffer for 2 minutes before handling as described above.

The small intestine was removed and washed in sterile PBS/0.1% BSA. The intestine was then opened longitudinally and cut into ~1-2 cm pieces. Excess mucus was removed by wiping on tissue paper. Tissue was incubated in RPMI 1640 supplemented with 5% FCS and 2 mM EDTA on a shaking incubator (150 rpm) heated to 37°C for 20 minutes. This EDTA incubation was repeated for 20 min, after which, pieces of tissue were incubated in RPMI 1640 supplemented with 5% FCS at room temperature for 10 minutes without shaking. Pieces of tissue were then transferred to new tubes and digested in RPMI 1640 supplemented with 10% FCS, DNase I (40 U/ml, Sigma-Aldrich) and collagenase VIII (0.25 mg/ml, Sigma-Aldrich)

for 30 minutes at 37°C on a shaking incubator. Tissue was filtered through a 70 µm strainer and centrifuged. Digested tissue was separated by centrifugation on a 30%/40%/70% Percoll gradient (GE Healthcare), centrifuging at 1800 rpm for 20 minutes with no brake. Cells at the 40%/70% interface were collected as the leukocyte-enriched fraction.

2.2.3 Cytokine blocking experiments

Concurrent with injection of curdlan, groups of mice were injected with antibodies specific for cytokines according to the schedules indicated in **Table 2.6**. Except where stated, a control group of mice were injected with a comparable dose of a matched antibody isotype.

Table 2.6: Schedules for administration of cytokine blocking or cell depleting antibodies *in vivo*

Antibody	**Antibody clone**	**Dose (per injection)**	**Frequency**	**Duration**	**Reference for dose**
Anti-IL-4	11B11	0.33 mg	Three times weekly	3-4 weeks	[449-451]
Isotype	HPRN	0.33 mg	Three times weekly	3-4 weeks	
Anti-IL-5	TRFK5	0.3 mg	Three times weekly	4-5 weeks	[452]
Isotype	HPRN	0.3 mg	Three times weekly	4-5 weeks	
Anti-IL-33	Polyclonal	2.5 µg	Every 48 hours	10 days	[453-455]
Control	Polyclonal goat IgG	2.5 µg	Every 48 hours	10 days	
Anti-GM-CSF	MP1-22E9	0.25 mg	Twice weekly	4 weeks	[250, 441, 452]
Isotype	2A3	0.25 mg	Twice weekly	4 weeks	
Anti-CD4	YTS191	0.1 mg	Twice weekly	4 weeks	[441]
Isotype	LTF-2	0.1 mg	Twice weekly	4 weeks	

2.2.4 Tissue explants

Three pieces of small intestine, each of ~0.5 cm length, were dissected: one each from the duodenum, jejunum, and ileum. These were placed in wells of a 24 well plate with 1 ml of RPMI 1640 medium supplemented with 10% FCS and penicillin/streptomycin (100 U/ml and 100 µg/ml). The plate was incubated overnight at 37^{o}C and 5% CO_2, after which the tissue pieces were weighed and the supernatants removed and centrifuged at 13,000*g* for 10 minutes. The supernatant was removed into 1.5 ml tubes and frozen at -80^{o}C until assayed. Similarly, the manus was dissected and cut into three pieces, then incubated and processed as described above. Measured concentrations of analytes in supernatant were expressed per weight of tissue.

2.2.5 Histology[1]

Dissected paws or pieces of small intestine were placed in 4% formalin for at least 24 hours. Paws were decalcified in a solution of 10% EDTA for 4 weeks. Tissue was mounted in paraffin, cut into 7 µm sections, and stained with haematoxylin and eosin. Images were obtained by light microscopy with an Olympus BX51 microscope.

2.3 Bone marrow lineage depletion

For some experiments, lineage^{+} BM cells were depleted using a commercial kit (ThermoFisher Scientific). To achieve this, flushed BM from the femurs and tibiae of 3 mice was mixed with a solution of biotinylated antibodies (shown in **Table**

[1] Processing was completed by the Kennedy Histology Core Facility, Kennedy Institute of Rheumatology, University of Oxford

2.7). This was incubated for 10 minutes at 4°C then washed and re-suspended in a solution of streptavidin conjugated to magnetic beads (ThermoFisher Scientific) for 10 minutes at 4°C. The solution was transferred to a 5 ml FACS tube, diluted to a total volume of 4 ml, and placed inside a magnet for 10 minutes at room temperature. The supernatant was poured into a 15 ml tube, washed, and the resulting BM suspension, enriched for HSPCs, was used for further analysis.

Table 2.7: Biotinylated antibody solutions used for lineage depletion, all from the eBioscience Mouse Haematopoietic Lineage Biotin Panel (ThermoFisher Scientific)

Specificity	Clone	Concentration	Volume used per 3 mice
CD3	145-2C11	0.125 mg/ml	50 µl
CD11b	M1/70	0.03 mg/ml	50 µl
B220	RA3-6B2	0.03 mg/ml	50 µl
Gr1	RB6-8C5	0.015 mg/ml	50 µl
Ter119	TER-119	0.03 mg/ml	50 µl

2.4 Blood, bone marrow plasma, and bone marrow stroma

2.4.1 Complete blood cell counts

Blood was collected by cardiac puncture after death was confirmed by aspirating 450 µl blood into a 1 ml syringe with 25G needle containing 50 µl 4% sodium citrate (Sigma Aldrich) anticoagulant. The blood was transferred to a plain 1.5 ml tube and kept at 4°C before analysis using a PX21 analyser (Sysmex). Cell count values were corrected for the dilution effect of the citrate anticoagulant using the following formula: actual count = (measured count / 9) x 10.

2.4.2 Serum

Blood was collected using the same technique as above but transferred to serum gel tubes (BD). Samples were allowed to coagulate on ice for at least 30

minutes before centrifugation at 13,000*g* for 10 minutes. The serum was transferred into plain 1.5 ml tubes and frozen at -80°C until assayed.

2.4.3 Bone marrow plasma

The BM of single femurs was flushed into 1.5 ml tubes using 250 µl of PBS/0.1% BSA, 1 ml syringes, and 25G needles. The suspension was vortexed briefly then centrifuged at 13,000*g* for 10 minutes. The supernatant was removed into a new tube and frozen at -80°C until assayed.

2.4.4 Bone marrow stroma

For analysis of stromal populations, femurs and tibiae were dissected, cleaned and then crushed in a Petri dish. The bone fragments were transferred to wells of a 48 well plate with 1 ml of Hanks buffered saline solution (Gibco) with DNAse I (15 µg/ml, Sigma Aldrich) and collagenase I (300 U/ml, Sigma Aldrich). The plate was incubated at 37°C with shaking at 100 rpm for 1 hour. After this, bone fragments were washed and, with the digestion solution, transferred to a new tube through a 70 µm filter. Cell preparations were then used for flow cytometry or sorted into RLT buffer (QIAGEN) for extraction of RNA. Populations sorted from digested BM are shown in **Table 2.8**.

Table 2.8: Populations sorted by FACS from digested BM for flow cytometry or RT-qPCR

Cell type	**Definition**
Mesenchymal stromal/stem cell (MSC)	$CD45^-$, $Ter119^-$, $CD31^-$, $CD51^+$, $PDGFR\alpha^+$, $Sca\text{-}1^-$
Endothelium (ENDO)	$CD45^-$, $Ter119^-$, $CD31^+$
Osteoblastic lineage cells (OBC)	$CD45^-$, $Ter119^-$, $CD31^-$, $CD51^+$
Erythroblastic island macrophages ($CD169^+$ MP)	$CD45^+$, $Gr1^-$, $F4/80^+$, SSC^{lo}, $CD169^+$
Neutrophils (NEUT)	$CD45^+$, $CD11b^+$, $Ly6G^+$
Monocytes ($Ly6C^+$ MONO)	$CD45^+$, $CD11b^+$, $Ly6G^-$, $Ly6C^+$

2.5 Flow cytometry

2.5.1 Instruments

LSRII or LSR-Fortessa cytometers (BD) were used interchangeably for acquisition of all flow cytometric data. Both instruments were calibrated monthly using cytometer setup and tracking (CST) calibration beads. Diva software (BD) was used for acquisition of data.

2.5.2 Staining

After preparation described in **section 2.2.2**, 1-2x10^6 cells per sample were added to 96 well plates and centrifuged. The pellet was mixed with a solution of fluorophore-conjugated antibodies and a fixable live/dead dye in a total volume of 40 µl PBS/0.1% BSA and incubated at 4^{o}C for 30-60 minutes. In some experiments, fixable live/dead dyes were added to cells first and incubated for 15 minutes before washing and adding the conjugated antibodies. If it was not included in the staining panel, purified anti-mouse CD16/32 was added to the solution to prevent non-specific binding to FcγR receptors. After this, 100 µl PBS/0.1% BSA was added to each well, the plate centrifuged, and the supernatant discarded. The cell pellets were then mixed with 100 µl of Cytofix/Cytoperm solution (BD) and incubated for 15 minutes at 4^{o}C. After this, cells were washed, re-suspended in PBS/0.1% BSA, and transferred to 5 ml FACS tubes for data acquisition. Cells were acquired in a volume of at least 300 µl.

Compensation was performed immediately before data acquisition using compensation beads (BD) with the same fluorophore-conjugated antibodies used to stain cells. Where indicated, additional samples were stained with isotypes of antibodies or with fluorescence minus one (FMO) controls to aid gating and evaluate

non-specific staining. Additionally, some results were confirmed by staining samples derived from mice lacking pertinent markers (e.g. $ST2^{-/-}$ mice).

2.5.3 Intracellular staining for cytokines and Ki67

Cells were stimulated with phorbol 12-myristate 13-acetate (PMA, 5 ng/ml, Cayman Chemical) and ionomycin (500 ng/ml, Sigma Aldrich) for 3-4 hours in a solution of RPMI 1640 with 10% FCS at 37°C and 5% CO_2 before staining for surface antigens and fixation. After this, cells were incubated in 100 µl 1X Perm/Wash solution (BD) for 15 minutes at 4°C. Cells were washed and then mixed with fluorophore-conjugated antibodies specific for intracellular antigens suspended in 50 µl Perm/Wash buffer before incubating at 4°C for 1 hour in the dark. After this, cells were washed with Perm/Wash buffer and re-suspended in PBS/0.1% BSA for acquisition. For Ki67 staining, cells were stained for surface antigens and fixed with Cytofix/Cytoperm solution (BD), washed with Perm/Wash solution, then incubated with 100 µl Permeabilisation Buffer Plus (BD) for 10 minutes at 4°C in the dark. After washing with Perm/Wash buffer, cells were re-fixed with 100 µl Cytofix/Cytoperm buffer for 5 minutes, then stained with an anti-Ki67 antibody or isotype diluted in 50 µl Perm/Wash buffer for 1 hour at room temperature. After washing with Perm/Wash buffer, cells were sometimes re-suspended in a solution of 4',6-diamidino-2-phenylindole (DAPI, 2 µg/ml, BioLegend) for 15 minutes at room temperature. Cells were then washed and re-suspended in PBS/0.1% BSA for acquisition.

2.5.4 Staining for annexin V expression

After staining for surface antigens, cells were washed and re-suspended in 100 µl annexin V staining buffer (BioLegend) at 4°C for 15 minutes. After this, cells were washed and mixed with annexin V conjugated to PE (BioLegend) suspended in staining buffer, then incubated for 45 minutes at 4°C. Cells were washed and re-suspended in staining buffer for acquisition.

2.5.5 Fluorescence-activated cell sorting[2]

Cells were prepared as described above or after depletion of lineage$^+$ cells (**section 2.3**). Cell populations were sorted using a FACSAria III (BD). Depending on the intended use, cells were sorted into 5 ml FACS tubes containing culture medium or 1.5 ml tubes containing RLT buffer (QIAGEN) with 2-mercaptoethanol.

2.5.6 Cell counts

Cell numbers in suspensions were determined by dilution in Trypan blue and counting manually with a haemocytometer or by adding counting beads (BioLegend) to cell suspensions before flow cytometry. Where counting beads were used, the following equation was used to calculate the total cell count of the suspension: (number of cell events / number of bead events) x (bead count of the lot / volume of the sample) x dilution factor.

[2] Sorting was undertaken by Mr Jonathan Webber of the Kennedy Flow Cytometry Core Facility, Kennedy Institute of Rheumatology, University of Oxford.

2.5.7 Analysis

Data were analysed using FlowJo software (version 10.0.8, FlowJo LLC). Gating strategies varied by experiment but always began with selection of a cell population based on forward and side scatter properties, exclusion of doublet events by plotting height and width forward scatter, and exclusion of dead cells using the channel of the viability dye.

2.6 Imaging flow cytometry

2.6.1 Preparation and staining of cells

The method was adapted from a previous study [456]. After lineage depletion, BM cells were re-suspended in serum-free expansion medium (SFEM, Stem Cell Technologies) at $1x10^6$ cells per well of a 96 well plate in a total volume of 100 µl and rested at 37°C and 5% CO_2 for 15-30 minutes. After this, cells were stimulated by adding IL-33 (final concentration 50 ng/ml) or medium to make a final volume of 200 µl, and also stained for surface markers at the same time (CD105 – pacific blue, Gr1 – FITC, CD16/32 – APC, cKit – PE/Cy7) and incubated in the same conditions for a further 30 minutes. After this, cells were centrifuged and re-suspended in 100 µl warmed 4% formalin for 15 minutes at 37°C. Cells were washed with PBS with 0.1% Triton X-100 and 3% FCS, then stained with NF-kB p65 – PE (5 µl per sample in the same buffer) for 1 hour at room temperature in the dark. Cells were washed and then stained with 7-aminoactinomycin D (7-AAD, 15 µg/ml in the same buffer, BioLegend) for 1 hour at room temperature in the dark. Cells were washed, re-suspended in PBS/0.1% BSA in a total volume of 40 µl, and transferred to 1.5 ml tubes for acquisition.

2.6.2 Acquisition

Samples were acquired using an Amnis Imagestream XMarkII cytometer with the following settings: magnification 60 µm, flow rate slow, side scatter laser off. Compensation was performed immediately before acquisition using the compensation wizard and compensation beads. Translocation of the p65 probe compared to the nuclear stain 7-AAD was assessed in erythroid progenitors ($Gr1^-$, $cKit^+$, $CD16/32^-$, $CD105^+$) using the nuclear translocation wizard in IDEAS6.2 software (Amnis).

2.7 Phosphoflow cytometry

Single cell suspensions of BM were obtained and $lineage^+$ cells were depleted as described above. The resulting suspensions of lineage-depleted BM cells were plated at 0.5-1x10^6 cells/well, re-suspended in SFEM, with or without IL-33 (10 ng/ml) and incubated for 6 hours at 37°C and 5% CO_2. After this, cells were stained with surface antibodies and viability dye (CD105-Pacific blue, FITC-CD71, PE/Cy7-CD16/32, AF700-CD11b, BV786-CD117) and simultaneously stimulated with EPO (4 U/ml) or PBS for 20 minutes, then fixed with warmed Cytofix/Cytoperm solution for 12 minutes in the same conditions. Cells were then centrifuged, washed with PBS/0.1%BSA and permeabilized with Fixation buffer III (BD, cooled to -20°C) on ice for 30 minutes. Cells were then washed with PBS/0.1% BSA and stained with phospho-antibodies (5 µl/sample) for 1 hour at room temperature in the dark. Cells were then washed and acquired as described above. Erythroid progenitors were gated as $CD11b^-$, $cKit^+$, $CD16/32^-$, $CD105^+$. Where indicated, the same procedure was used for stimulation and staining of sorted erythroid progenitors.

2.8 BrdU incorporation

Mice were injected IP with 1 mg BrdU (BioLegend) in a total volume of 100-200 µl PBS. For assessment of all BM HSPCs, mice were injected 6 hours before culling. For assessment of HSCs, mice were injected 12, 24, and 36 hours before culling. These timings were based on previously published results [23].

After preparation of cell suspensions and staining for surface antigens, cells (1-2x10^6/well) were fixed by mixing with 100 µl Cytofix/Cytoperm solution and incubating for 15 minutes at 4^{o}C in the dark. Cells were then washed with Perm/Wash buffer (BD) and mixed with 100 µl Permeabilization Buffer Plus (BD) for 15 minutes on ice in the dark. After washing with Perm/Wash solution, the cells were fixed again by mixing with 100 µl Cytofix/Cytoperm solution for 5 minutes on ice, then washed with Perm/Wash buffer. The cells were then incubated with DNAse I (100 µl of a 300 µg/ml solution, Sigma Aldrich) for 1 hour at 37^{o}C. After centrifugation, the BrdU was stained with PE-conjugated anti-BrdU antibody (BioLegend) suspended in 50 µl Perm/Wash solution for 20 minutes at room temperature. Finally, cells were washed with Perm/Wash buffer and re-suspended in PBS/0.1% BSA for acquisition.

2.9 Culture of primary HSPCs

2.9.1 Sorting populations of interest

Bone marrow suspensions were depleted of lineage$^+$ cells as described above and stained with fluorophore-conjugated antibodies for FACS. Progenitor cells were sorted according to the definitions shown in **Table 2.9,** based on previous publications [79, 159]. Cells were sorted into 5 ml FACS tubes containing 0.5 ml of

the definitive culture medium. All cells were cultured in a regulated incubator at 37°C and 5% CO_2.

Table 2.9: Definitions used for sorting indicated cell populations by FACS

Cell type	Definition (all lineage^{neg}, c-Kit^{+})
Colony forming unit – erythroid (CFU-E)	Sca-1^{-}, CD41^{-}, CD16/32^{-}, CD105^{+}, CD150^{-}
Pre-colony forming unit – erythroid (pre-CFU-E_	Sca-1^{-}, CD41^{-}, CD16/32^{-}, CD105^{+}, CD150^{hi}
Pre-megakaryocyte erythroid (pre-MegE)	Sca-1^{-}, CD41^{-}, CD16/32^{-}, CD105^{-}, CD150^{+}
Pre-Granulocyte macrophage progenitor (pre_GM)	Sca-1^{-}, CD41^{-}, CD16/32^{-}, CD105^{-}, CD150^{-}
Granulocyte macrophage progenitor (GMP)	Sca-1^{-}, CD41^{-}, CD16/32^{+}
Haematopoietic stem cell (HSC)	Sca-1^{+}, Flt3^{-}, CD150^{+}, CD48^{-}, (CD34^{-})*
Multi-potent progenitor (MPP) 2/3	Sca-1^{+}, Flt3^{-}, CD150$^{+/-}$, CD48^{+}, (CD34^{+})*
Multi-potent progenitor (MPP) 4	Sca-1^{+}, Flt3^{+}

* Gating with CD34 was used in some but not all experiments.

2.9.2 Culture of erythroid progenitors

Methods for the culture of pre-CFU-Es and CFU-Es were adapted from previous studies [457-459]. However, unlike commonly reported methods for erythroid cultures that use fetal liver cells [460], I opted to obtain cells from the BM to produce a representative model of definitive erythropoiesis. Sorted pre-CFU-Es and CFU-Es were cultured in SFEM medium supplemented with recombinant human EPO (2 U/ml, BioLegend) and murine stem cell factor (100 ng/ml, BioLegend) by plating 1000-2000 cells per well in a 96 well plate, in a volume of 200 µl per well, for 4 days. After 2 days, 60 µl of medium was removed and replaced with fresh medium. Where indicated, IL-33, TNF-α, IL-1β, or GM-CSF were added to the culture medium, all at 10 ng/ml. After 4 days, cells were stained with

antibodies to surface markers and fixable viability dye as described above. Cells were counted by adding counting beads at acquisition.

For assessment of morphology, some cells were incubated for 4 days, washed twice with plain PBS then spun onto plain glass slides (VWR) using a Shandon Cytospin centrifuge with the following settings: medium acceleration, 800 rpm, 5 minutes. The slides were stained with Shandon Kwik Diff (ThermoFisher Scientific) solutions according to the manufacturer's instructions; images were obtained using an Olympus BX51 microscope at X40 magnification.

For assessment of enucleation by flow cytometry [461], some cells were cultured for 4 days and then incubated with Hoescht 33342 (20 µg/ml) in SFEM for 30 minutes at 37°C and 5% CO_2. The cells were centrifuged and stained with Ter119-APC and CD71-PE before acquisition as described above.

For assessment of the direct/indirect effects of IL-33, pre-CFU-Es were sorted as above from C57BL/6-*Il1rl1*$^{-/-}$ (ST2 knockout) and C57BL/6-*Ubc*^{GFP} mice ('wild type', expressing GFP under the control of the ubiquitin c gene). These cells were plated individually (2000 cells per well) or mixed (1000 cells of each type per well) and incubated and assessed as described above.

In some cultures, small molecule inhibitors or an activator were added to determine the effects of key signalling pathways; these are listed in **Table 2.10**. In all cases, the inhibitor was left in the culture medium for 4 days until the final readout. For assessment of the effect of a higher dose of EPO, EPO was added to the culture at a final concentration of 20 U/ml for 4 days.

Table 2.10: Small molecule inhibitors and activators used in culture of erythroid progenitors

Molecule	Target	Source	Concentration	References
NEMO domain binding (NBD) peptide	IκB kinase (IKK)γ; inhibits	R&D Systems	10 μM	[88, 251, 462]
DB2313	PU.1; inhibits	Glixx Labs	440 nM	[463]
SC-79	Akt; activates	R&D Systems	10-100 μM	[464]

2.9.3 Single cell culture of pre-CFU-Es

Bone marrow suspensions were prepared as described above. Single pre-CFU-Es were sorted by FACS directly into wells of a 96 well plate, each containing 80 μl of SFEM medium supplemented with SCF (100 ng/ml), EPO (2 U/ml), and dexamethasone (10 μM, Sigma Aldrich), with or without IL-33 (10 ng/ml). Dexamethasone was added for single cell cultures to increase proliferation to obtain a reliable readout [465, 466]. The outside row/column of the plate was filled with 200 μl sterile water. Plates were incubated for 10 days. At this time, 50 μl of medium was removed and replaced with 50 μl of PBS/0.1%BSA with viability dye (Zombie Aqua, BioLegend) and surface antibodies (CD71-PE, Ter119-APC). The plate was incubated at 4^{o}C in the dark for 1 hour, then 50 μl was aspirated from each well and replaced with 150 μl PBS/0.1%BSA for acquisition by flow cytometry. The number of cells in each well was quantified using counting beads.

2.9.4 Culture of human erythroid progenitors

Anonymised human leukoreduction cones were obtained from the NHS Blood and Transfusion Service, University of Oxford. Blood donors had given consent for use of the samples for research purposes. The cones were drained into 50 ml tubes and diluted with PBS to a final volume of 50 ml. From this, 25 ml was layered onto 15 ml of Lymphoprep solution (Stem Cell Technologies) and

centrifuged as follows: 600*g*, 20 minutes, room temperature, acceleration 7, deceleration 0. The leukocyte layer was harvested with a P1000 pipette and washed three times with PBS.

From this suspension enriched for human peripheral blood mononuclear cells, $5x10^7$ cells were removed and mixed with 3 µg of biotinylated antibodies against CD3, CD19, and CD14 in 1 ml of PBS/0.1%BSA for 10 minutes at 4°C. Cells were washed and mixed with 0.4 ml streptavidin conjugated with magnetic beads in a final volume of 2 ml in a FACS tube and incubated at room temperature for 10 minutes. The volume was then adjusted to 4 ml and the FACS tube was placed inside a magnet for 10 minutes. After this, the supernatant was poured into a fresh tube and stained with the following panel: FITC-CD34, APC-CD123, PE/Cy7-CD71, PerCP/Cy5.5-Streptavidin and 7-AAD. Progenitors were sorted as Live, lineage^{neg} (i.e. PerCP/Cy5.5^{neg}), CD34$^+$, CD123$^-$, CD71$^+$ by FACS, as described in a previous report [467].

Sorted cells were re-suspended in SFEM with recombinant human SCF (100 ng/ml, Peprotech), recombinant human EPO (2 U/ml, Peprotech), with or without recombinant human IL-33 (10 ng/ml, Peprotech). Cultures were performed in triplicate, with 2000 cells in 200 µl volume per well in a 96 well tissue culture plate. Every 2 days, 60 µl of medium was removed and replaced with fresh medium. After 8-9 days, plates were centrifuged and cells were prepared for flow cytometry as described above. CD235a (glycophorin A) was used as a marker of mature erythroid cells in human cultures.

2.9.5 Culture of stem cells and myeloid progenitors

Sorted cells were plated as described above, with 400-600 cells per well (HSC), 1000-3000 cells per well (MPP, pre-GM), or 1000-5000 cells per well (GMP). The medium was composed of Iscove's modified Dulbecco medium (IMDM, Gibco) containing L-glutamine and HEPES and supplemented with 5% FCS, 2-mercaptoethanol (100 µM, Sigma Aldrich), penicillin/streptomycin (100 U/ml and 100 µg/ml, Gibco), non-essential amino acids (1X, Invitrogen), sodium pyruvate (1 mM, Invitrogen), murine stem cell factor (20 ng/ml), murine IL-6 (10 ng/ml), murine IL-11 (10 ng/ml), murine IL-3 (10 ng/ml), murine thrombopoietin (10 ng/ml), and human erythropoietin (10 ng/ml). This method was adapted from a previous study [247]. All cytokines were from BioLegend. Cells were cultured for 3-4 days (GMP) or 6-7 days (all others).

2.9.6 Single cell culture of HSCs

Single HSCs were sorted by indexed FACS directly into wells of a 96 well plate containing 100 µl of the culture medium described in **section 2.9.5** and cultured for 10 days. After this, cells were prepared for flow cytometry as described in **section 2.9.3**.

2.10 MEL585 Cell line

An aliquot of MEL585 immortalised erythroid progenitor cells was obtained from the core cell culture facility of the Weatherall Institute of Molecular Medicine, University of Oxford, courtesy of Jackie Sloane-Stanley. For maintenance of the cell line, 10^6 cells were seeded into 75 cm^2 flasks (Corning, treated with plug seal cap) containing 20 ml of culture medium. The culture medium was composed of

RPMI 1640 medium with 20% FCS. Cell aliquots were seeded into new flasks twice weekly to maintain the line. To induce erythroid differentiation, the culture medium was supplemented with 5 mM hexamethylene bisacetamide (HMBA, Sigma Aldrich). Over the following 2-3 days, cells progressively became smaller, expressed haemoglobin, and downregulated the surface marker CD44 [468, 469]. Cells were stained for flow cytometry as described in **section 2.5.2** or transferred into RLT buffer for RT-qPCR.

2.11 Colony forming assays

2.11.1 Whole bone marrow assays

Bone marrow was prepared as described above, with red blood lysis. The cell suspensions were counted and $5x10^4$ cells were re-suspended in IMDM medium with 10% FCS and penicillin/streptomycin (100 U/ml and 100 µg/ml) in a 1.5 ml tube. To this was added 1 ml M3434 methylcellulose medium (Stem Cell Technologies), and the tubes were shaken by hand and vortexed to mix the cells evenly. Additionally, before mixing with cells, the M3434 medium was supplemented with penicillin/streptomycin and placed on a rocker for 2 hours at room temperature to ensure complete mixing and even viscosity of the thawed suspension. The 1.1 ml cell/M3434 suspension was transferred to a 3 cm Petri dish and sealed with micropore tape. Two 3 cm dishes were placed inside a 10 cm Petri dish with a third, open 3 cm Petri dish containing 4 ml of autoclaved distilled and deionised water. The dishes were incubated at 37°C and 5% CO_2 for 8-10 days, when colonies were counted and identified manually using an inverted microscope (Wilovert). In particular, blast forming units – erythroid (BFU-E) were identified on the basis of their size (0.5-1 mm diameter), concentric growth, appearance of

staphyloform clusters of small cells around the periphery, and red colouration of mature colonies [160].

Where indicated, cells were re-suspended in IMDM with 10% FCS and either IL-33 (10 ng/ml) or IL-4 (10 ng/ml) and incubated in liquid cultures in 96 well plates for 6 hours at 37^{o}C and 5% CO_2 before mixing with M3434. For these assays, the M3434 was also mixed with the relevant cytokine and placed on a rocker for at least 2 hours at room temperature before mixing with cells. Cytokines were not supplemented during the subsequent incubation period.

2.11.2 Assays with sorted LSK cells

Bone marrow suspensions were prepared as for **section 2.3** before 10^3 LSK cells were sorted into 1.5 ml tubes containing 100 µl of IMDM with 10% FCS, penicillin/streptomycin (10,000 U/ml), with or without IL-4 (10 ng/ml). Culture dishes were then prepared as described in **section 2.11.1**, using plain M3434 or medium supplemented with IL-4 as appropriate.

2.11.3 Erythroid assays with whole bone marrow

Whole BM cells ($5x10^4$) were re-suspended in 0.3 ml SFEM with SCF (100 ng/ml) and EPO (2 U/ml). To this was added 0.8 ml M3236 methylcellulose medium (Stem Cell Technologies) that had been supplemented with the same cytokines. Where indicated, cells were pre-incubated with IL-33 (10 ng/ml) for 6 hours in liquid culture before mixing with M3236, and the M3236 was also pre-mixed with IL-33. Dishes were examined after 2-3 days for identification of CFU-E colonies and after 8-10 days for identification of BFU-E colonies. CFU-E colonies were identified as

small, loosely aggregated colonies of 8-32 cells, sometimes acquiring red colouration [163].

2.11.4 Assays with sorted pre-CFU-E cells

Bone marrow was prepared as described in **section 2.3** before 10^3 pre-CFU-E cells were sorted by FACS into 1.5 ml tubes containing 0.3 ml SFEM with SCF, EPO, and penicillin/streptomycin. Culture dishes were then prepared as described in **section 2.11.1**.

2.12 RT-qPCR

RNA was extracted from cell suspensions using RNEasy Mini or Micro kits (QIAGEN) depending on the number of cells per sample, using on-column DNAse treatment. Complementary (c)DNA (50 ng) was synthesised using the High-Capacity Reverse Transcription kit (Affymetrix eBioscicence). Quantitative RT−qPCR was performed using Taqman primers/FAM probes (ThermoFisher Scientific) listed in **Table 2.11** and PrecisionFast Mastermix (PrimerDesign) on a ViiA7 384-well real-time PCR system (ThermoFisher Scientific). All expression levels were normalized to an internal reference gene (*Hprt*) and calculated as $2^{-(CT\ gene - CT\ Hprt)}$. Real-time qPCR reactions were performed in duplicate.

Table 2.11: Primers and probes used for RT-qPCR assays

Gene	Protein product	Taqman primer
Hba-a1	Haemoglobin α chain	Mm02580841_g1
Hbb-b1	Haemoglobin β chain	Mm01611268_g1
Alas2	Aminolevulinic acid synthase	Mm00802083_m1
Epb41	Erythroid band protein 4.1	Mm01187466_m1
Gypa	Glycophorin A	Mm00494848_m1
Epor	Erythropoietin receptor	Mm00833882_m1
Aqp1	Aquaporin 1	Mm01326466_m1

Il33	IL-33	Mm00505403_m1
Il1b	IL-1β	Mm00434228_m1
Car1	Carbonic anhydrase	Mm00486717_m1
Gata1	GATA1	Mm01352636_m1
Gata2	GATA2	Mm00492301_m1
Spi1	PU.1	Mm00488140_m1
Klf1	KLF1	Mm00516096_m1
Cxcl12	CXCL12	Mm00445553_m1
Kitl	Stem cell factor, Kit ligand	Mm00442972_m1
Ang1	Angiopoietin 1	Mm00833184_s1
Runx2	Runx2	Mm00501584_m1
Hprt	Hypoxanthine phosphoribosyltransferase	Mm03024075_m1

2.13 RNA sequencing

2.13.1 Sample preparation

Pre-CFU-Es were sorted by FACS and re-suspended in SFEM with SCF and EPO as described in **section 2.9.1**. Cells were incubated with or without IL-33 (10 ng/ml) for 6 hours at 37°C and 5% CO_2. Plates were then centrifuged, supernatants discarded, and cells transferred to 1.5 ml tubes with 350 µl RLT buffer with β-mercaptoethanol. RNA was extracted using the RNEasy Micro kit, according to the manufacturer's instructions and re-suspended in ultrapure nuclease free water (ThermoFisher Scientific).

2.13.2 Sequencing[3]

The mRNA fraction was selected from the total RNA by binding of polyadenylated transcripts to oligoT beads before conversion to cDNA. The cDNA was end-repaired, A-tailed and adapter-ligated. The prepared libraries were size selected, multiplexed and assessed for quality using a TapeStation (Agilent) before

[3] Completed by the High-Throughput Genomics Group at the Wellcome Trust Centre for Human Genetics, University of Oxford.

sequencing with a HiSeq 4000 platform (Illumina) with paired end 75 base pair reads.

2.13.3 Data analysis[4]

RNA sequencing data were analysed using pipeline_scrnaseq.py (https://github.com/sansomlab/scseq/blob/master/pipelines/). Data quality was assessed using pipeline_readqc.py (https://github.com/cgat-developers/cgat-flow/). Sequence reads were aligned to the mouse genome with Hisat2 (version 2.1.0)[470] using a “genome” index built from the GRCm38 release of the mouse genome and known splice sites extracted from Ensembl version 91 annotations (using the hisat2_extract_splice_sites.py tool). A two-pass mapping strategy was used to discover novel splice sites (with the additional parameters: --dta and --score-min L,0.0,-0.2). The average alignment rate was 95.2% (as assessed with picard tools v2.10.9, https://github.com/broadinstitute/picard). Mapped reads were counted using featureCounts (Subread version 1.6.3; Ensembl version 91 annotations; with default parameters)[471]. Salmon v0.9.1 was used to calculate TPM values[472] using a quasi-index (built with Ensembl version 91 annotations and k=31) and gc bias correction (parameter “--gcBias”). Differential expression analysis of IL-33-exposed pre-CFU-E versus control samples was performed using DESeq2 (v1.24.0)[473].

Gene set enrichment analysis (GSEA) was performed using fgsea R-package (version 1.10.1) for KEGG pathways (using for ranking the Wald statistic from DESeq2) [474]. Enrichment of members of the NF-kB pathways and genes

[4] Completed by Dr Lada Koneva, Kennedy Institute of Rheumatology, University of Oxford, and included in this thesis with her permission.

upregulated by EPO in CEPs were assessed in RNAseq results using GSEA software, version 4.0.2. Genes upregulated in CEP by EPO were extracted from Supplementary Table 5 of [17]. NF-kB pathway genesets were obtained from the Pathway Interaction Database available through the GSEA software.

2.14 Immunofluorescence

Bone marrow was prepared as described in **section 2.3** and CFU-Es were sorted by FACS. Cells were incubated in SFEM supplemented with EPO and SCF as described in **section 2.9.2** at $9x10^4$ cells per well in a 96 well plate, with or without IL-33 (10 ng/ml) for 24 hours. The plate was centrifuged, and cells were fixed in 4% formalin for 20 minutes at room temperature. Cells were washed once with PBS/0.1% BSA then stained with polyclonal goat anti-mouse EPO receptor antibody (15 µg/ml, R&D Systems) for 2 hours at room temperature. Cells were then washed once and blocked with rabbit serum before staining with rabbit anti-goat IgG secondary AF555 antibody (1:500, Invitrogen) for 45 minutes at room temperature. Cells were washed once and then stained with Hoechst 33342 for 20 minutes. Cells were re-suspended in 30 µl of PBS/0.1% BSA, of which 10 µl was transferred to plain glass slide and covered with a 1 cm diameter glass coverslip. After 10 minutes to allow cells to rest on the slide, cells were imaged using an Olympus BX51 microscope.

2.15 Bone marrow chimeras and progenitor transfer experiments

2.15.1 Donors

Depending on the experiment, donor mice were used without treatment or injected with cytokines of interest for one week before culling. After culling, the BM

was prepared as described in **section 2.2.2**. In some experiments, whole BM was used without further treatment; in others, HSPCs were sorted for transplantation by FACS and injected with HSC-depleted (i.e. Sca-1$^-$) support cells (**Table 2.12**). The BM was re-suspended in plain PBS for injection.

Table 2.12: Experiments involving bone marrow chimeras; each row represents a separate experiment in this thesis

Recipient	Donor	Cells	Irradiation	Blood samples	Cull
Ub-GFP	1:1 mixture of Ub-GFP and ST2$^{-/-}$	Whole BM ($2.5x10^6$ cells of each genotype)	Lethal (4.5 Gy x2)	6 weeks	10 weeks, 1 week after curdlan injection
CD45.1 (B6.SJL-*Ptprc*^{a})	1:1 mixture of CD45.1 and CD45.2 ST2$^{-/-}$	Whole BM ($2.5x10^6$ cells of each genotype)	Lethal (4.5 Gy x2)	4 weeks	7 weeks, 1 week after curdlan or IL-33 injection
CD45.1 (B6.SJL-*Ptprc*^{a})	CD45.2, naïve or injected with IL-4 for 1 week	HSCs sorted by FACS (400 cells per mouse) with $5x10^5$ Sca-1$^-$ CD45.1$^+$ BM support cells	Lethal (4.5 Gy x 2)	2, 4, and 8 weeks	22 weeks
CD45.1 (CByJ.SJL-*Ptprc*^{a}) (BALB/C CD45.1)	SKG (CD45.2), healthy or with SpA	HSCs sorted by FACS (3000 cells per mouse) with $5x10^5$ whole BM CD45.1$^+$ support cells	Sublethal (1.25 Gy x 2)	4, 8, 12, and 16 weeks	28 weeks

Ub-GFP: ubiquitin GFP.

2.15.2 Recipients

For lethal irradiation, C57BL/6 mice received 9 Gy split into 2 doses given at least 4 hours apart, whereas BALB/C mice received 2.5 Gy at the same intervals because they are reported to be more radiosensitive than C57BL/6 mice [475]. After

irradiation, donor cells were injected into the tail vein within 3 hours. Donor cells were injected in a volume of 200 µl of plain sterile saline using a 27G insulin syringe. Mice were warmed at 38^{o}C for 5-10 minutes before injection. Recipient mice received drinking water supplemented with enrofloxacin ('Baytril', Bayer, 0.4 mg/ml) for 14 days after irradiation and were weighed daily.

Depending on the experiment, blood samples were obtained from the tail vein using a 25G needle, starting 2-4 weeks after injection of donor cells. Depending on the experiment, chimeric mice were injected with curdlan or recombinant cytokines 6-8 weeks after irradiation and after adequate chimerism was confirmed in blood samples. At the end of the experiment, mice were culled to evaluate chimerism in the BM, spleen, and sometimes blood by flow cytometry, as described in **section 2.5**.

Depending on the experiment, donor and recipient cells were distinguished by the expression of congenic markers (CD45.1 and CD45.2) or by expression of a fluorescent marker (green fluorescent protein, GFP, under the control of the ubiquitin c promoter, Ub-GFP). Fluorescent recipients were used when cells of interest did not express CD45, as is the case for erythroid progenitors and mature erythroid cells.

2.15.3 Tail vein blood samples

Blood samples were collected into 0.25 ml EDTA coated tubes (Sarstedt). From these, 5 µl of whole blood from each mouse was mixed with 150 µl PBS/0.1% BSA in wells of a 96 well plate. These were centrifuged, and the pellet was re-suspended in a suspension of fluorophore-conjugated antibodies in a total volume of 40 µl PBS/0.1% BSA for 30-60 minutes at 4^{o}C. After this, the plate was

centrifuged and pellets were re-suspended in 100 µl Cytofix/Cytoperm solution (BD) for 15 minutes at 4^{o}C. Samples were centrifuged and re-suspended in PBS/0.1% BSA for acquisition by flow cytometry, as described in **section 2.5**.

2.15.4 Progenitor transfer

Pre-CFU-E progenitors were sorted from suspensions of lineage-depleted BM from Ub-GFP mice, as described in **sections 2.3** and **2.9.1**. These cells were then maintained in culture medium overnight, as described in **section 2.9.2**, with or without IL-33 (10 ng/ml). The next day, cells were washed and re-suspended in sterile PBS for injection. Wild type C57BL/6 recipient mice were sublethally irradiated (2.25 Gy twice, 4 hours apart) before cells were injected into the tail vein. Mice were culled after 4 days, at the expected emergence of mature erythroid cells [104]. At this time, the blood, BM, and spleen were harvested for analysis by flow cytometry.

2.16 ELISAs and multiplex assays

Serum and supernatants were stored at -80^{o}C until assayed. The commercial ELISA kits listed in **Table 2.13** were used according to the manufacturers' instructions, unless otherwise stated. Additionally, a multiplex, bead-based kit was used for measurement of haematopoietic factors, according to the manufacturer's instructions.

Table 2.13: Details of ELISA kits used for measurement of cytokines

Cytokine	Manufacturer	Samples measured	Dilution	Changes to manufacturer protocol
IL-4	BioLegend – uncoated sandwich ELISA	Serum, BM plasma, supernatants from paw and small intestine explants	1:2	None
IL-33	R&D Systems – uncoated sandwich ELISA	Serum, BM plasma	1:2	Incubated samples and standards for 6 hours
TNF-α	BioLegend – pre-coated sandwich ELISA	BM plasma	1:2	None
EPO, IL-6	BioLegend (Legendplex)	Serum	1:2	Used half quantities of detection beads and antibodies

2.17 Statistical analysis

2.17.1 Handling of experimental data

Data from *in vivo* experiments were compared using Mann-Whitney U tests, Student's t tests, one-way or two-way analysis of variance (ANOVA), according to the number of groups and nature of the comparison. If ANOVA revealed significant associations, *post hoc* Tukey tests (one-way) or Sidak's multiple comparison tests (two-way) were conducted to evaluate differences between groups. Data from mouse experiments are presented as individual values with the mean and standard deviation (SD) for each group. Correlations between variables were assessed by linear regression. P values <0.05 were considered statistically significant.

For data from *in vitro* and *ex vivo* experiments, these are presented as mean and SD for single experiments representative of others, or as mean with standard error (SEM) where the results of multiple replicates are combined.

2.17.2 Haemosphere data analysis

Results of RNA sequencing from murine haematopoietic progenitors were obtained from the online Haemosphere database, reporting the results of the Haemopedia sequencing project [476]. Specifically, gene counts (expressed as transcripts per million, TPM) were downloaded for pre-CFU-Es, CFU-Es, and GMPs. Differential expression of genes between these cell types was evaluated using DEseq2 (v1.24.0) and EnchancedVolcano packages in R, version 3.6.1.

3 Haematopoiesis is perturbed in a mouse model of spondyloarthritis

3.1 Introduction

Chronic inflammatory diseases cause local tissue damage but also have distant effects owing to circulation of cytokines and other soluble mediators in blood and extracellular fluid. Previous studies have reported perturbed haematopoiesis in murine models of IBD [250, 452], atherosclerosis [216, 255], lupus [254], and bacterial wound infection [257], often causing expansion of HSPC populations and lineage bias, favouring myelopoiesis at the expense of erythropoiesis and/or lymphopoiesis. Many of these effects are attributable to inflammatory cytokines, which are produced in inflamed tissues but circulate to the BM to affect HSPCs.

Cytokines appear to regulate haematopoiesis through diverse mechanisms, with many having effects on mature cells as well as HSPCs. In previous models, much attention has focused on the effect of inflammation on primitive HSCs, with both IL-1β and TNF-α causing them to emerge from quiescence, proliferate, and adopt precocious myeloid transcriptional signatures [247, 251]. However, under homeostatic conditions, most of the daily output of the haematopoietic system is derived from highly proliferative MPPs and lineage-committed progenitors [13, 477]. These cells do not have the capacity for prolonged self-renewal but are much more abundant than HSCs. This creates a relatively large population of progenitors that are actively cycling and capable of producing mature cells in mice within 5-7 days, whereas formation of mature cells from HSCs requires approximately 14 days [23]. Therefore, an unresolved question is whether it is HSCs or their downstream progenitors that are chiefly responsible for remodelling of haematopoiesis in the face of demand.

In other murine models, inflammation also promotes EMH, with accumulation of HSPCs in the spleen and inflamed tissues, where local production of leukocytes may sustain or exacerbate the inflammatory response [216, 257]. This phenomenon is probably related to the known ability of HSPCs to recirculate through the blood and lymph, lodging in inflamed or infected sites to generate mature haematopoietic cells locally [212]. In many cases, this local production contributes to the inflammatory process, with neutrophils generated in wounds assisting in clearance of bacteria [257], whereas monocytes generated in the spleen contributed to progression of intimal plaque lesions in a model of atherosclerosis [216].

The aims of this chapter were:

1. To evaluate how medullary and extramedullary haematopoiesis were affected by the development of SpA in SKG mice.
2. To determine how the population characteristics and activity of HSCs, MPPs, and lineage-committed progenitors were altered during SpA.
3. To determine whether the changes occurring in haematopoiesis were attributable to the *Zap70* mutation of SKG mice, which predisposes to autoimmune responses.

3.2 Results

3.2.1 SKG mice develop spondyloarthritis when injected with curdlan

The SKG strain possesses a point mutation in the gene encoding ZAP-70, which is a tyrosine kinase that forms part of the T cell receptor signalling complex [386]. Owing to the *Zap70*^{W163C} mutation, T cells are less responsive to signals activating the T cell receptor [385]. Consequently, the repertoire of T cells is skewed

by positive selection of cells with relatively high affinities for self-antigens in the thymus, allowing self-reactive clones to emigrate into the circulation [387]. For the same reason, the activity of thymus-derived regulatory T cells is decreased [388]. Together, these defects in T cell function render SKG mice prone to autoimmune reactions when exposed to microbial-derived β-glucan molecules, which cause innate immune stimulation of sufficient intensity to activate autoreactive T cells [389].

In the SPF conditions of our colony, SKG mice were not exposed to this innate immune stimulation and remained healthy, with no measurable swelling of joints and progressive weight gain when fed *ad libitum* up to the age of 4 months. However, when injected with curdlan (**Fig. 3.1A**), mice developed a syndrome that closely resembles human SpA over the following 4-5 weeks, characterised by swelling of the fore- and hindpaws and tarsal joints (**Fig. 3.1B**), as reported previously [391]. This was monitored by measuring the joints with callipers (**Fig. 3.1C**) and assigning a clinical score based on the appearance of the joints (**Fig. 3.1D**). Development of inflammation in the hindpaws and tarsi was associated with enlargement of the draining popliteal lymph nodes, which was attributable to an increased total cell count (**Fig. 3.1E**).

Figure 3.1

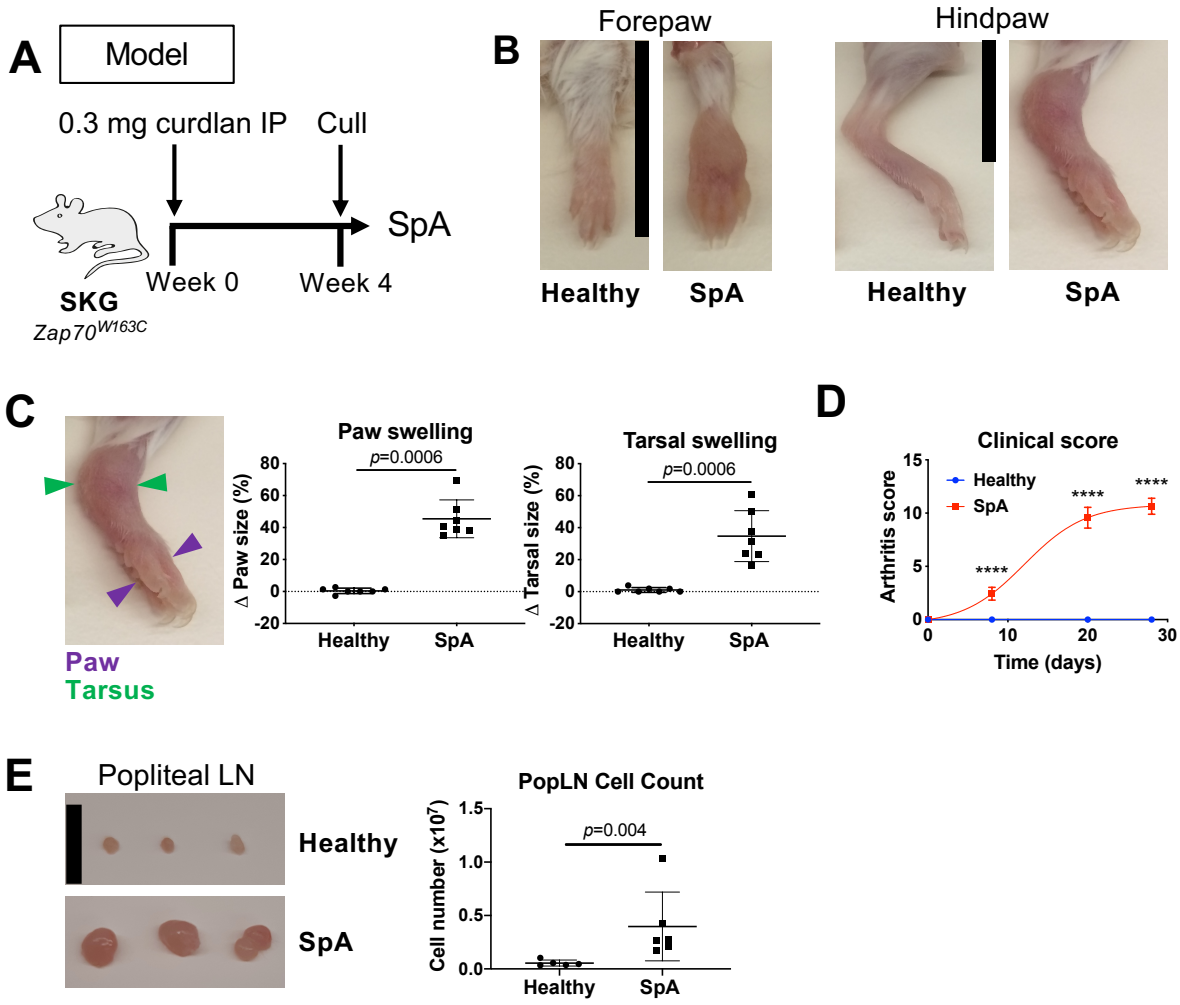

Figure 3.1: Curdlan causes inflammatory arthritis in SKG mice
(**A**) Female SKG mice aged 8-12 weeks were injected with 0.3 mg curdlan IP to induce spondyloarthritis (SpA), then culled after 4 weeks with littermate control mice injected with PBS to obtain data in (**B**)-(**E**).
(**B**) Representative images of fore and hindpaws. Scale bars indicate 1 cm.
(**C**) (Left) Image showing point of measurement of paws and tarsal region using dial callipers in mice developing SpA; (Right) Change in paw and tarsal size over 4 weeks after injection of curdlan.
(**D**) Clinical arthritis score. Points represent mean and SD values for n=7 mice per group, two-way ANOVA with Sidak's test. Lines show LOWESS splines.
(**E**) (Left) Representative images of popliteal lymph nodes. Scale bar indicates 1 cm. (Right) Total cell count from popliteal lymph nodes (PopLN)
For (**C**) and (**E**), points represent individual mice with mean and SD, Mann-Whitney U test.

Data representative of 5 independent experiments.

Using flow cytometric analysis of enzymatically digested paw tissue, I found swelling of the paws was associated with accumulation of $CD11b^+$, $Ly6G^+$ neutrophils (**Fig. 3.2A-B**). These represented a small proportion of the total population of $CD45^+$ leukocytes in tissue from healthy mice but constituted ~50% of $CD45^+$ cells in mice with SpA (**Fig. 3.2B**). The extent of this neutrophil infiltration was correlated with the arthritis score and changes in swelling of the paws and tarsi (**Fig. 3.2C**). Conversely, $CD11b^+$, $F4/80^+$ resident synovial macrophages were the most abundant myeloid cells in paws of healthy mice, as described previously [478], but constituted a lesser proportion of $CD45^+$ cells in inflamed mice (**Fig. 3.2A** and **Fig. 3.3A**). Development of SpA was also associated with accumulation of eosinophils and $Ly6C^+$ classical monocytes/macrophages (**Fig 3.3B**). These $Ly6C^+$ monocytes are likely to have entered the joints from the blood [479], where they were also present in increased numbers in mice with SpA (**Fig. 3.3C**), and have been implicated in the pathogenesis of K/BxN serum transfer arthritis [480, 481]. Histologically, gross swelling of the paws was associated with infiltration of leukocytes into perisynovial regions, producing inflammatory arthritis (**Fig. 3.3D**). Infiltration of neutrophils was also observed dramatically at the enthesis of the Achilles tendon in the tarsus, recapitulating the enthesitis that is an important feature of SpA in humans [433] (**Fig. 3.3D**). To assess the temporal dynamics of leukocyte infiltration in the paws, I performed a timecourse experiment, culling mice 1, 2, or 4 weeks after curdlan injections. Doing so, I found that infiltration of leukocytes was detectable by 1 week after curdlan injection but progressed with time; the accumulation of myeloid cells closely paralleled changes in the observed clinical score (**Fig. 3.4**).

Figure 3.2

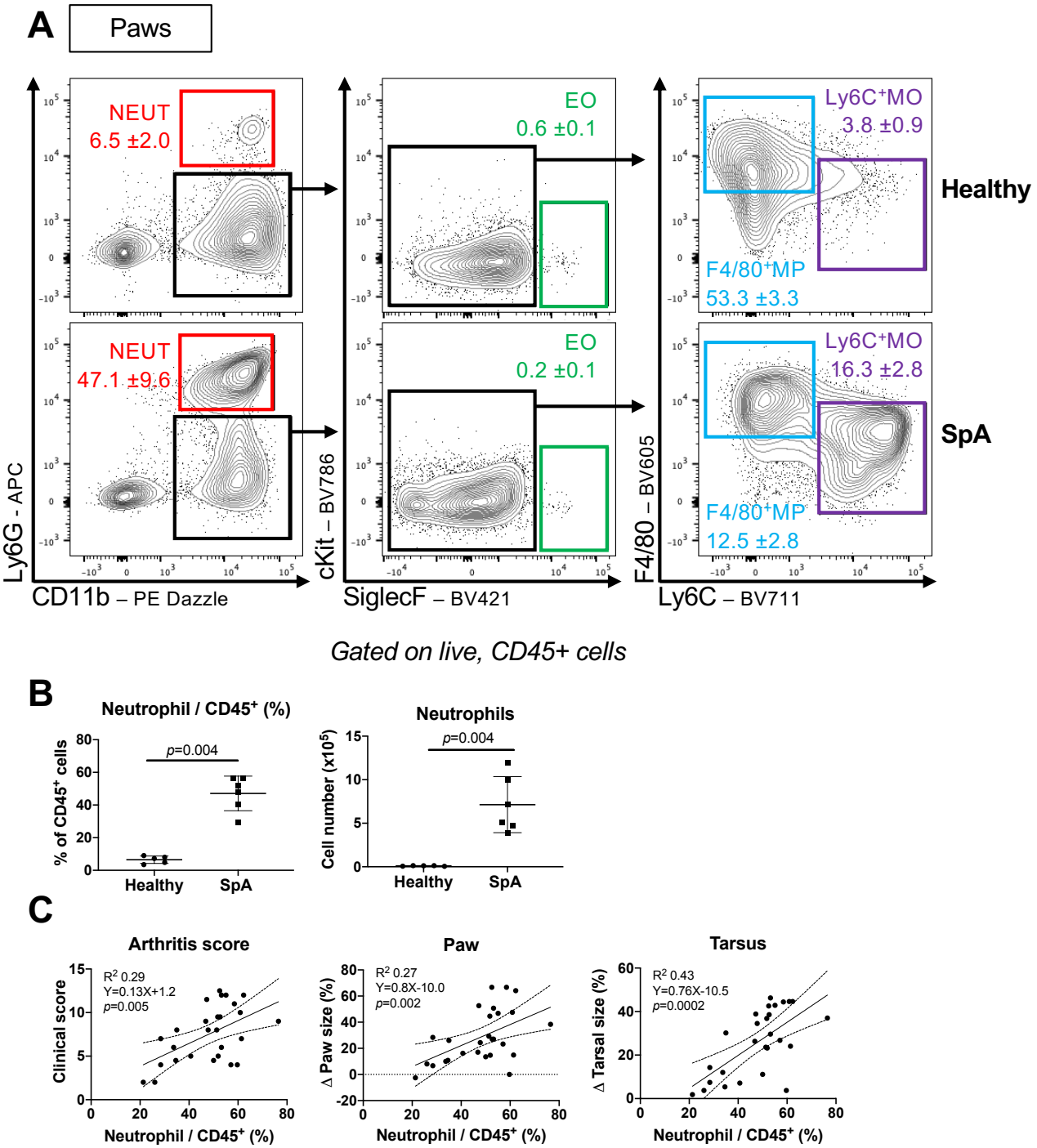

Figure 3.2: SpA is associated with accumulation of neutrophils in paws
(**A**) Representative flow cytometric images of enzymatically digested paws from healthy SKG mice and mice with SpA, 4 weeks after curdlan injection. Figures indicate frequencies among CD45$^+$ cells; mean and SD of n=5-6 mice per group. NEUT: neutrophil, EO: eosinophil, MP: macrophage, MO: monocyte.
(**B**) Frequency and absolute number of neutrophils in paws. Points represent individual mice with mean and SD, Mann-Whitney U test.
(**C**) Correlations between neutrophil infiltration of paws and indicated clinical parameters. Points represent individual mice with linear regression lines, dotted lines indicate 95% confidence interval.

Data representative of 5 independent experiments (**A**)-(**B**) or pooled from 3 independent experiments (**C**).

Figure 3.3

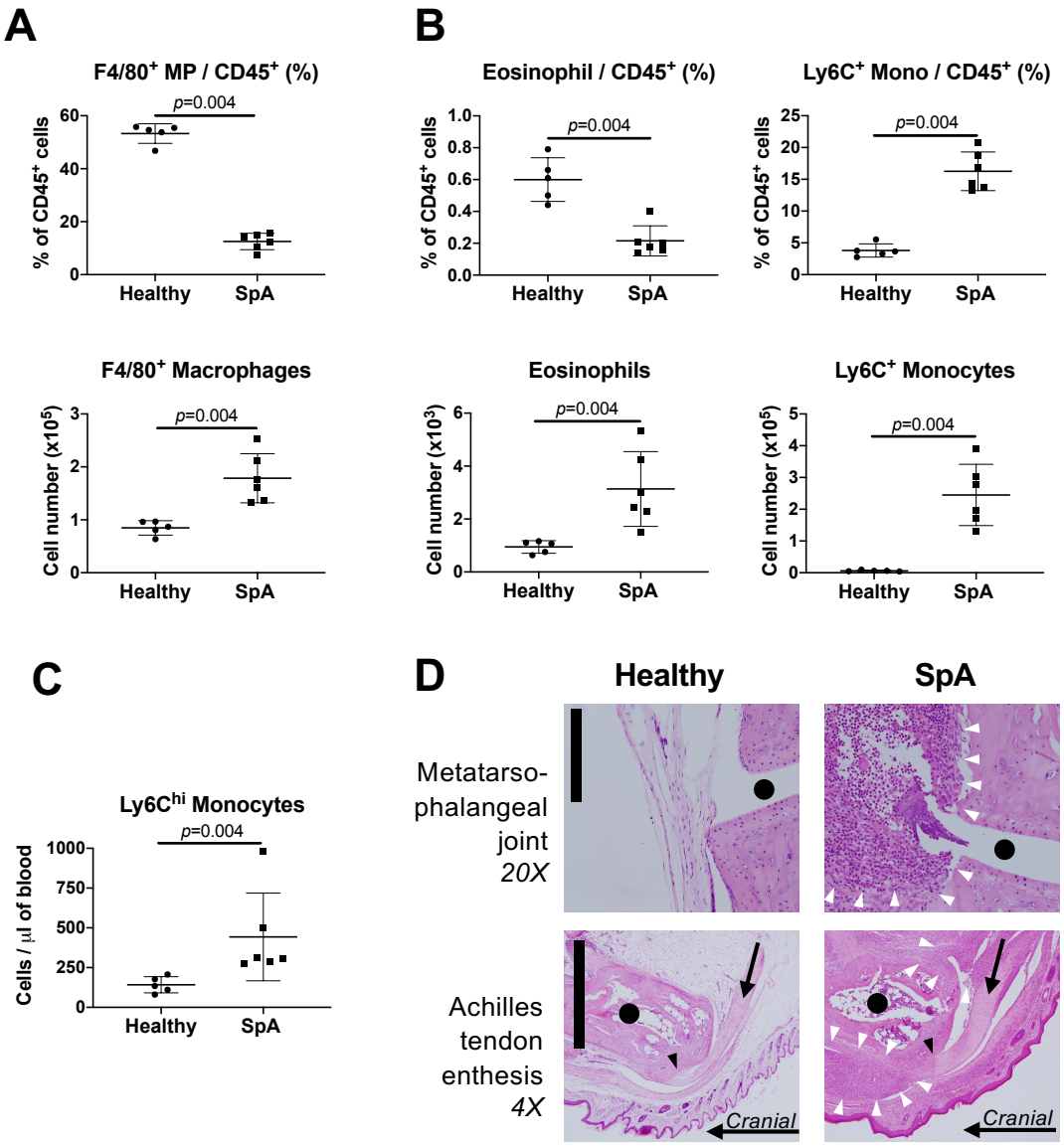

Figure 3.3: Diverse myeloid cells infiltrate the paws in SpA
(**A**) Frequency and absolute number of F4/80$^+$ resident synovial macrophages in paws from healthy mice and mice with SpA 4 weeks after curdlan injection.
(**B**) Frequency and absolute number of eosinophils and Ly6C$^+$ monocytes in paws.
(**C**) Number of Ly6C^{hi} monocytes in blood.
(**D**) Representative photomicrographs of sagittal sections through the metatarsophalangeal joints and tarsus (Top) Black circles show the joint space; white arrowheads show the perisynovial inflammatory infiltrate. Scale bar = 200 µm. (Bottom) Black arrows show the Achilles tendon; black circles show the calcaneus or 'heel bone'; black arrowheads show the Achilles tendon enthesis; white arrowheads show the entheseal inflammatory infiltrate. Note also the inflammatory infiltrate in the dermis and thickening of the epidermis, which are features of psoriasis. Scale bar = 1 mm. Sections stained with haematoxylin and eosin.
For (**A**)-(**C**), points indicate individual mice with mean and SD, Mann-Whitney U test.

Data representative of 5 independent experiments.

Figure 3.4

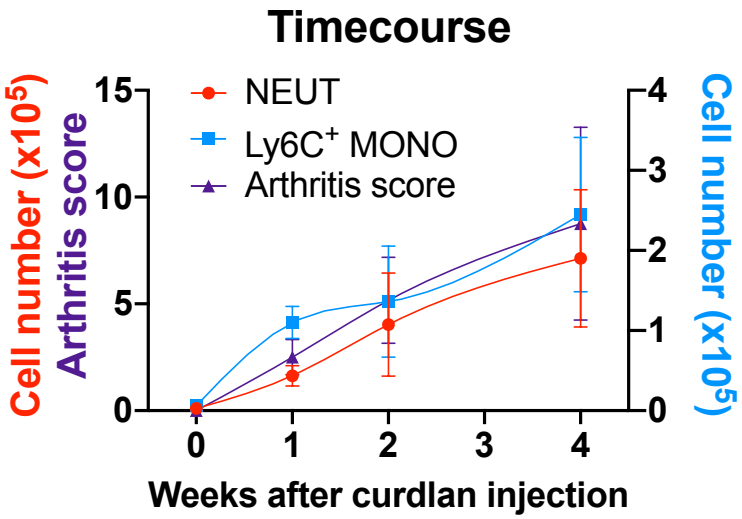

Figure 3.4: Clinical disease tracks accumulation of myeloid cells in paws
Changes in the absolute numbers of neutrophils (red) and Ly6C⁺ monocytes (blue) and in the clinical arthritis score (purple) over time in mice developing SpA. Points represent mean and SD for n=5-6 mice per group.

Data from a single experiment.

In addition to inflammatory arthritis and enthesitis, mice with SpA had inflammation of the small intestine (enteritis), which caused gross thickening of the intestinal wall in the most severe cases (**Fig. 3.5A**). However, the severity of enteritis was variable among individual mice, which was reflected in the variable appearance of the intestine and associated mesenteric lymph nodes, and in the wide range of total cell counts in the nodes (**Fig. 3.5B**). Using flow cytometric analysis of lamina propria leukocyte preparations, I found enteritis was also associated with variable infiltration of neutrophils, eosinophils, and Ly6C⁺ inflammatory monocytes (**Fig. 3.6A-B**), and I confirmed these findings using

histological sections of the small intestine, where granulocytic infiltrates were observed in the lamina propria (**Fig. 3.6C**).

Figure 3.5

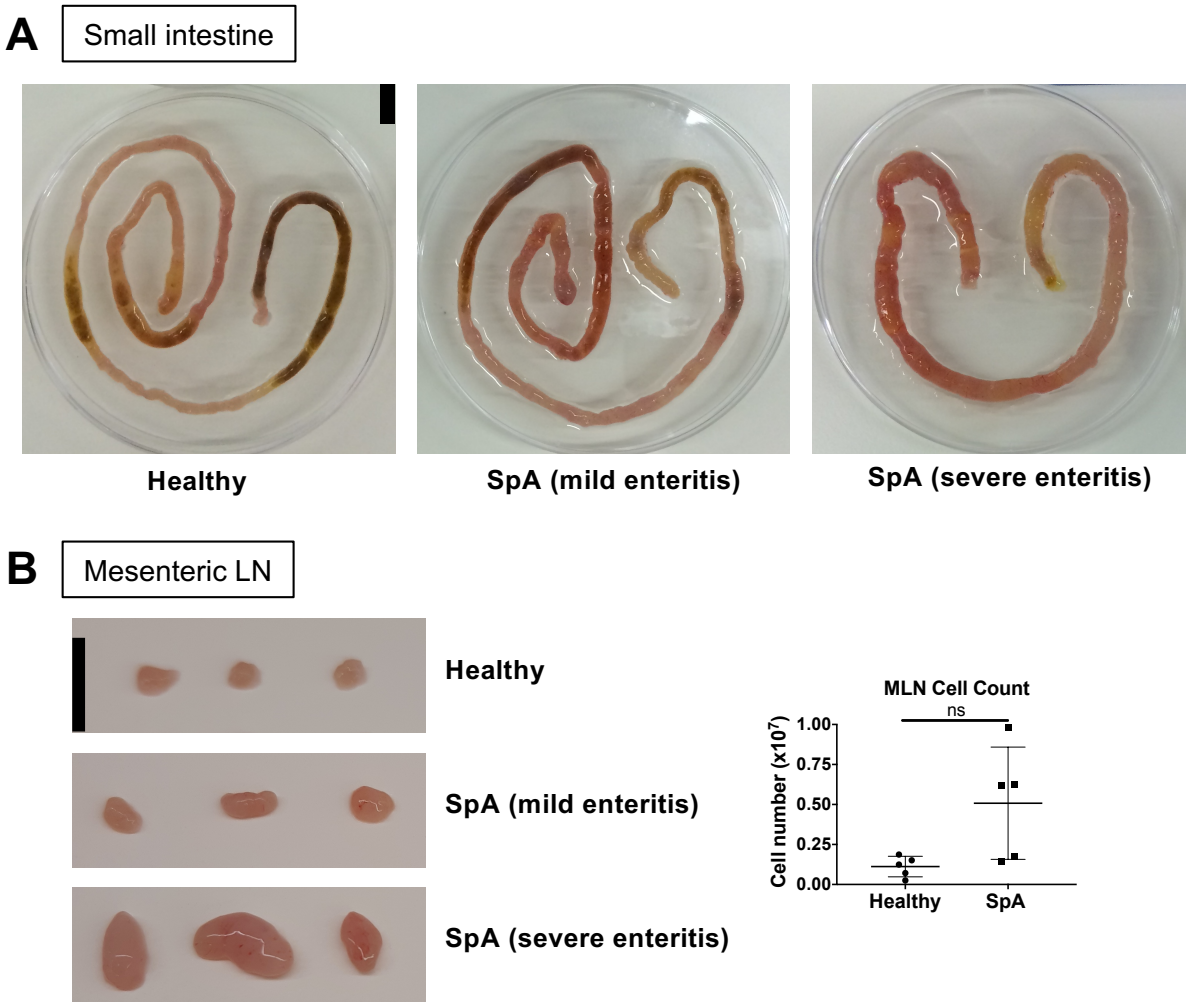

Figure 3.5: Mice with SpA develop enteritis
(**A**) Representative images of the small intestine removed from a healthy mouse and a mouse with SpA, 4 weeks after curdlan injection. Scale bar = 1 cm.
(**B**) (Left) representative images of mesenteric lymph nodes from healthy mice and mice with SpA. Scale bar = 1 cm. (Right) Absolute number of cells from mesenteric lymph nodes. Points indicate individual mice with mean and SD, Mann-Whitney U test.

Data representative of 5 independent experiments.

Figure 3.6

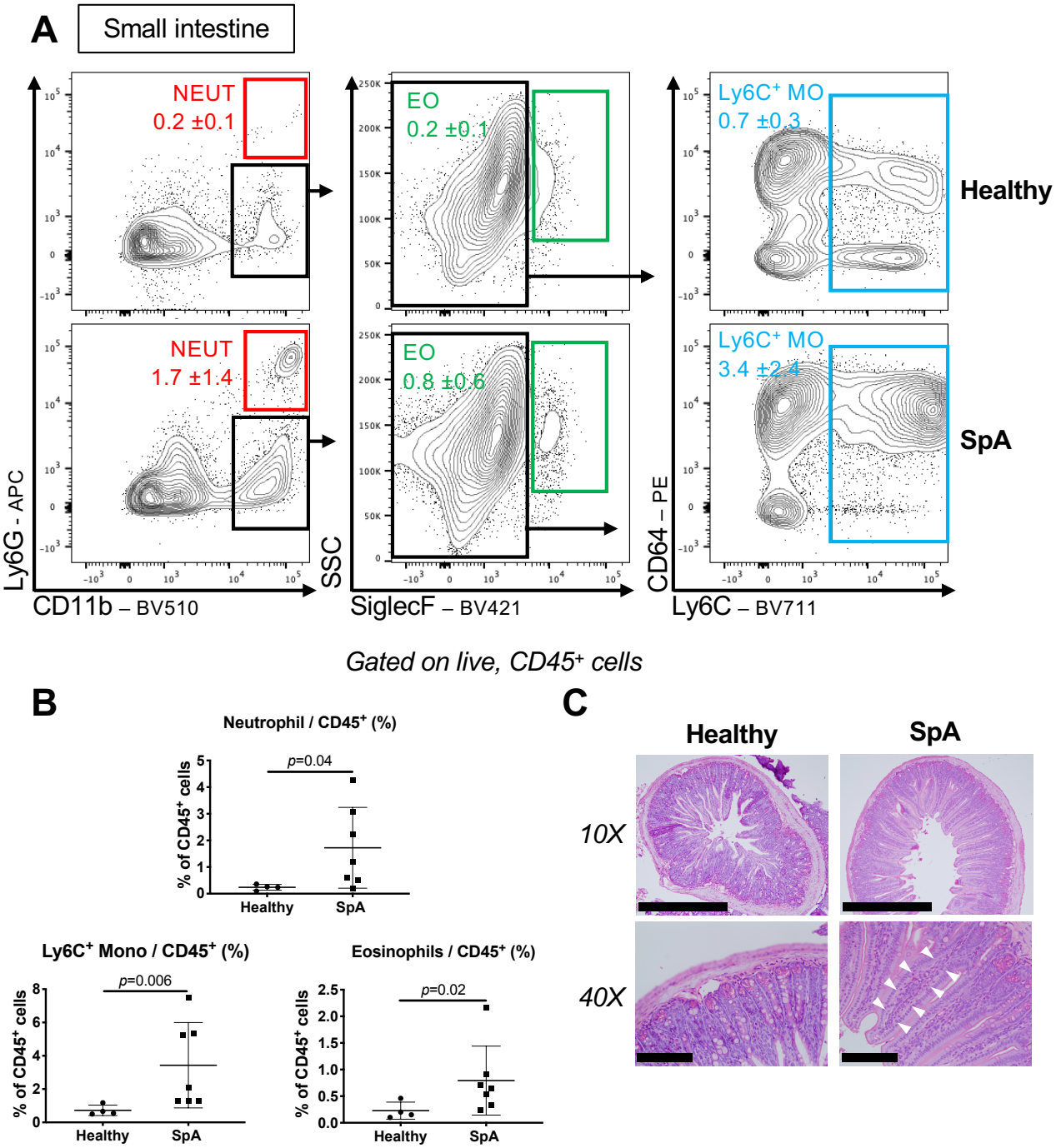

Figure 3.6: Myeloid cells infiltrate the small intestine of mice with SpA
(**A**) Representative flow cytometric images of lamina propria leukocytes after enzymatic digestion of the small intestine and density centrifugation in healthy mice and mice with SpA, 4 weeks after curdlan injection. Figures indicate frequencies among CD45⁺ cells; mean and SD of n=4-7 mice per group. NEUT: neutrophil, EO: eosinophil, MO: monocyte.
(**B**) Frequency of indicated myeloid populations in small intestine. Points represent individual mice with mean and SD, Mann-Whitney U test,
(**C**) Representative photomicrographs of transverse sections of the ileum. White arrowheads show inflammatory infiltrate expanding the lamina propria of the villus. (Top) Scale bar = 500 µm, (Bottom) Scale bar = 100 µm. Stained with haematoxylin and eosin.

Data representative of 5 independent experiments.

Systemically, mice with SpA lost weight (**Fig. 3.7A**) and had marked splenomegaly (**Fig. 3.7B**) when culled after 4-5 weeks, confirming that inflammation caused systemic sequelae. Accordingly, the severity of weight loss was positively correlated with the extent of neutrophil infiltration in the paws (**Fig. 3.7C**). In the peripheral blood, mice with SpA were anaemic, with decreased haemoglobin concentrations and RBC counts compared to healthy mice (**Fig. 3.7E**). Conversely, the number of neutrophils was increased in mice with SpA, reconciling with the marked myeloid infiltrates in inflamed sites, whereas the B cell count was decreased (**Fig. 3.7E**).

Collectively, this description of the clinical phenotype of mice with SpA revealed 1) that mice developed similar clinical features to those observed in human SpA, 2) that disease was associated with marked infiltrates of mature, blood-derived myeloid cells at inflamed sites, including cell types associated with tissue damage in other models of murine inflammatory arthritis, and 3) that consequences of disease were not limited to the inflamed sites but produced systemic abnormalities.

Figure 3.7

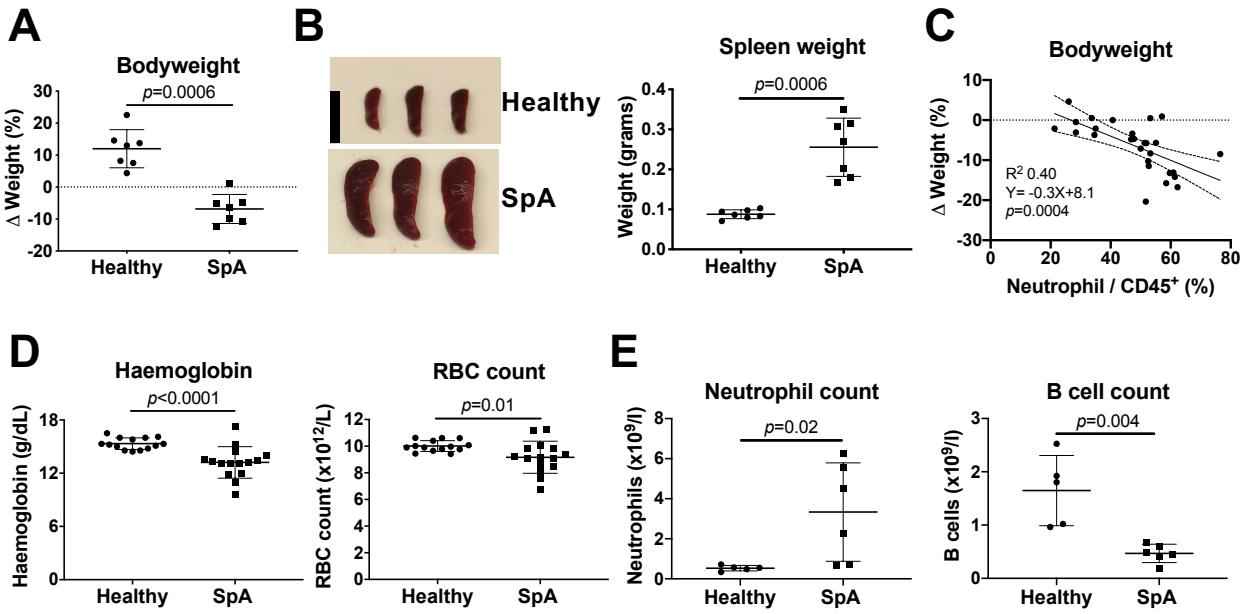

Figure 3.7: Mice with SpA have signs of systemic illness
(**A**) Changes in bodyweight in healthy mice and mice with SpA 4 weeks after curdlan injection compared to baseline.
(**B**) (Left) representative images of the spleen from healthy mice and mice with SpA. Scale bar = 1 cm. (Right) Weight of the spleen.
(**C**) Scatter plot of bodyweight against frequency of neutrophils in the paws in mice with SpA. Points represent individual mice with linear regression lines, dotted lines show 95% confidence intervals.
(**D**) Blood haemoglobin and red blood cell (RBC) concentrations.
(**E**) Blood neutrophil and B cell concentrations.
In (**A**)-(**B**), (**D**), and (**E**), points represent individual mice with mean and SD, Mann-Whitney U test.

Data representative of 5 independent experiments (**A**), (**B**), (**E**) or pooled from 3 independent experiments (**C**).

3.2.2 Expansion of the HSPC pool in mice with SpA occurs at the expense of reconstitution potential among HSCs

The accumulation of plentiful, blood-derived, mature myeloid cells at inflamed sites and development of anaemia in SKG mice with SpA suggested haematopoiesis could be perturbed, as described in other chronic inflammatory settings [243]. To investigate this, I determined the frequency and absolute number

of HSPC populations in BM by flow cytometry using previously-published definitions [79, 159] (**Fig. 3.8A**). Doing so, I found the number of primitive HSCs was not significantly increased with SpA, but all MPP subsets were expanded (**Fig. 3.8B**), particularly the myeloid-biased MPP3s [79]. These changes occurred even though the total cellularity of the BM was unchanged with SpA (**Fig. 3.8C**).

Further investigation of the population of Lineage^{neg}, c-Kit^{+}, Sca-1^{+} (LSK) cells enriched for HSCs and MPPs revealed no difference in the proportion of cells expressing Ki67, which identifies those cells in any stage of the cell cycle except G_0, between healthy and inflamed mice either 1 week or 4 weeks after curdlan injection (**Fig. 3.9A**). Using BrdU, which is incorporated into DNA by cells in S phase of the cell cycle, I found a lesser proportion of LSK cells were synthesising DNA in mice 1 week after curdlan injection compared to cells from healthy mice (**Fig. 3.9B**). However, it seemed paradoxical that Ki67 expression and BrdU incorporation would be similar or decreased among LSK cells when the size of the population was increased. To resolve this, I analysed the constituent MPP and HSC subsets using Ki67 and the DNA dye DAPI to identify separate cell cycle stages (**Fig. 3.9C**). Doing so, I confirmed that the proportion of HSCs, MPP2s, and MPP3s outside the cell cycle (in G_0) was increased with SpA, whereas there was no difference in the proportion of MPP4s that were cycling between healthy and inflamed mice (**Fig. 3.9C**). However, when taking into account changes in cell numbers, there was a reduction in the number of cycling HSCs but a significant increase in the number of all types of MPP that were cycling during SpA (**Fig. 3.9D**). This suggested that LSK populations expand with development of SpA but that, when analysed at a single time point, only a small proportion of cells are actively cycling, with the majority residing in G_0. In addition to changes in proliferation, I also

found that the expression of annexin V (**Fig. 3.10A**), a marker of the early phase of apoptosis, and of Fas (**Fig. 3.10B**), a receptor that induces apoptosis, were decreased among LSK cells from mice one week or 4-5 weeks after injection of curdlan. This suggested the accumulation of LSK cells might also be supported by a decreased rate of apoptosis.

Figure 3.8

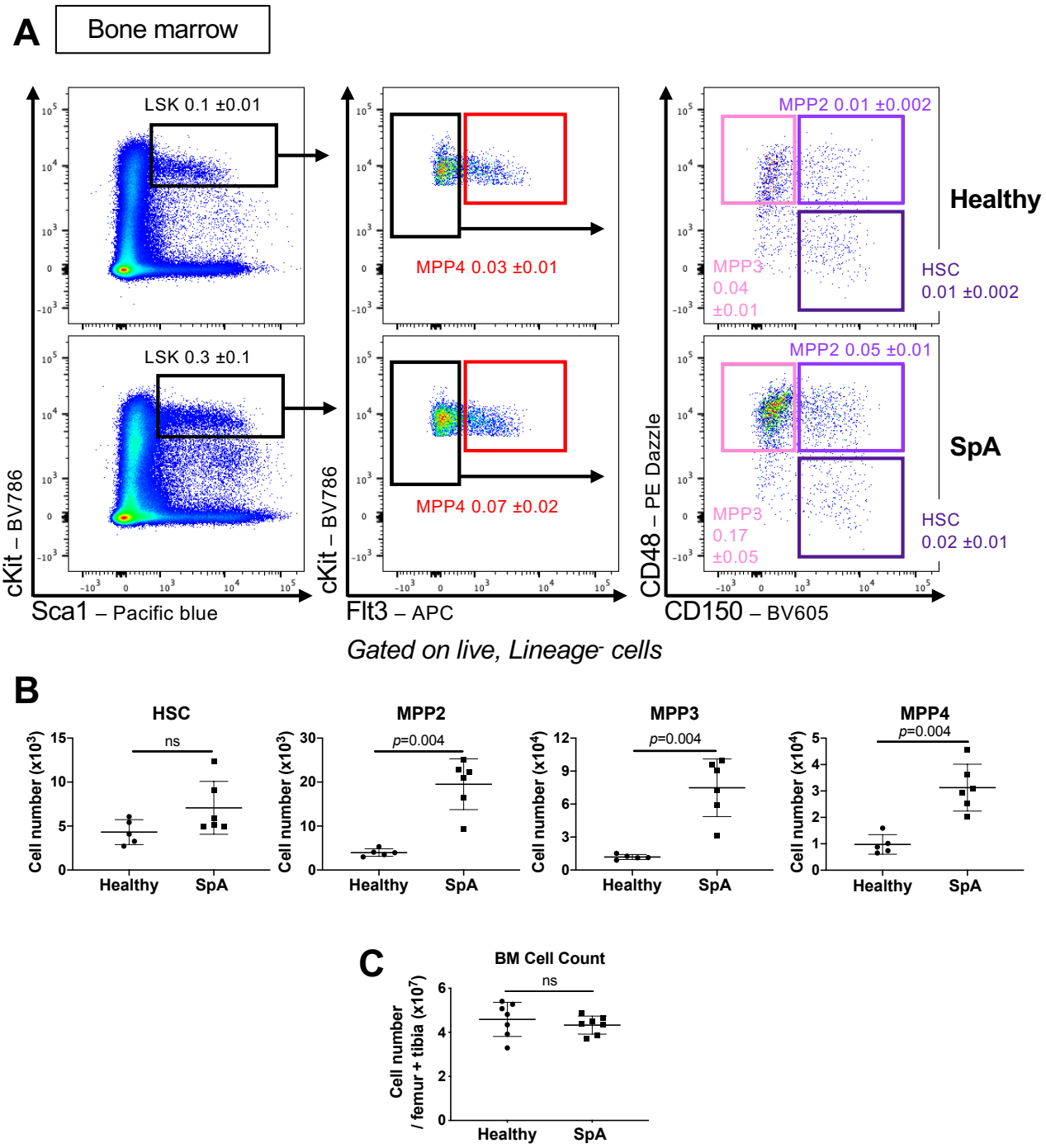

Figure 3.8: SpA expands the LSK compartment
(**A**) Representative flow cytometric images of HSPC populations in the lineage$^-$, Sca-1$^+$, c-Kit$^+$ (i.e. LSK) compartment of the BM. HSC: haematopoietic stem cell; MPP: multipotent progenitor. Figures show mean and SD for n=5-6 mice per group for frequency of indicated populations among live BM cells.
(**B**) Absolute numbers of indicated HSPC populations in BM from 1 femur and 1 tibia. Points represent individual mice with mean and SD, Mann-Whitney U test.
(**C**) Total number of live cells in BM of 1 femur and 1 tibia. Points represent individual mice with mean and SD, Mann-Whitney U test.

Data representative of 4 independent experiments.

Figure 3.9

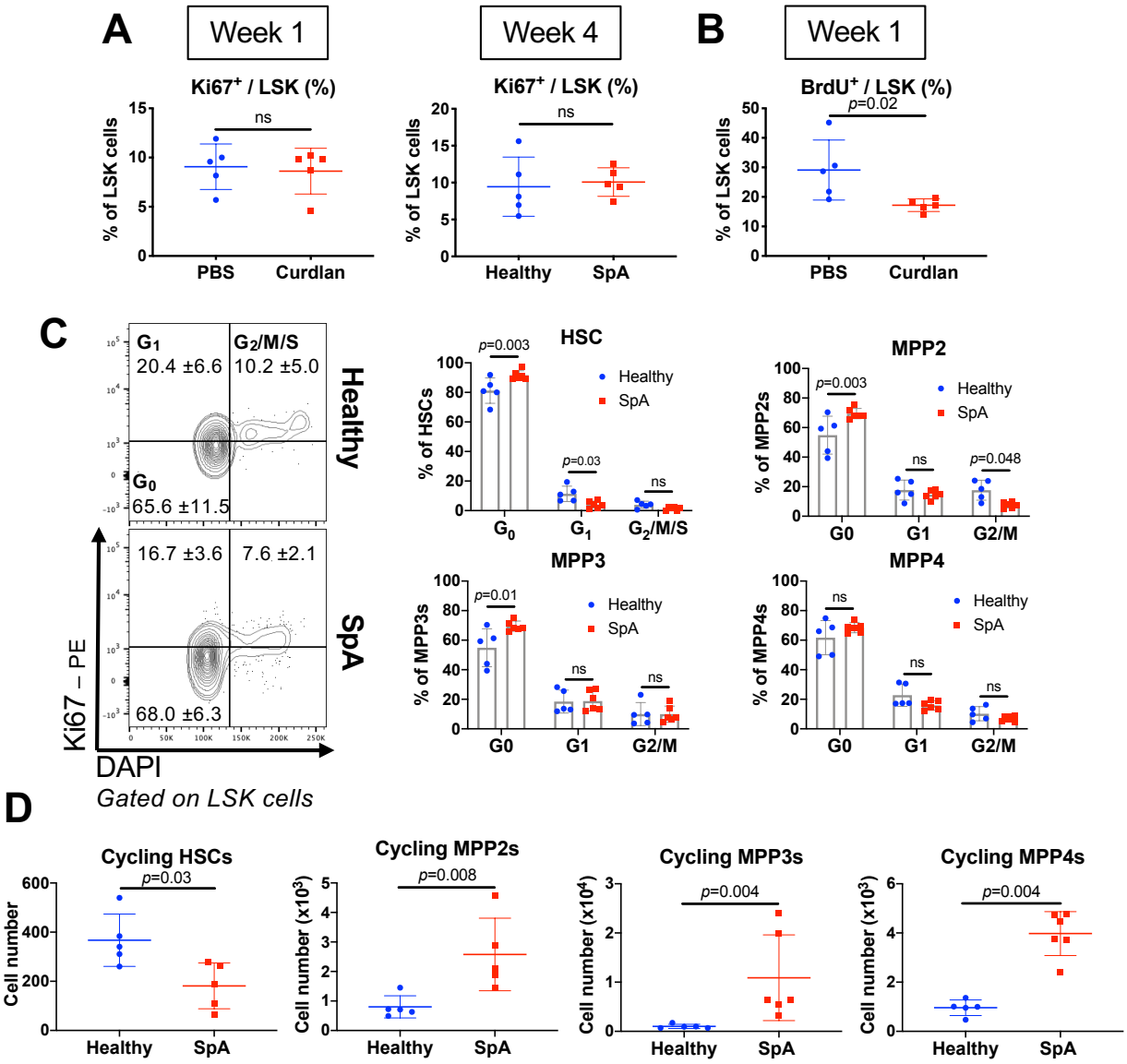

Figure 3.9: SpA causes changes in cell cycling of LSK cells

(**A**) Frequency of LSK cells expressing Ki67 1 week (left) or 4-5 weeks (right) after curdlan or PBS injection in SKG mice.

(**B**) Frequency of LSK cells incorporating BrdU in mice 1 week after curdlan or PBS injection. BrdU was injected 6 hours before mice were culled.

(**C**) (Left) Representative flow cytometric images of Ki67 expression and DNA staining with DAPI in LSK cells of mice 4 weeks after curdlan or PBS injection. Figures represent frequencies among LSK cells for n=5-6 per group. (Right) Frequency of indicated LSK constituent populations in indicated stages of the cell cycle. Points represent individual mice, bars show mean with SD. Two-way ANOVA with Sidak's test.

(**D**) Number of cells of indicated LSK constituent populations in G_1/G_2/M/S phase of the cell cycle ('cycling') in mice 4 weeks after curdlan or PBS injection.

For (**A**), (**B**), and (**D**), points represent individual mice with mean and SD, Mann-Whitney U test.

Data representative of 2 independent experiments.

I found it remarkable that the number of cycling HSCs was decreased in mice with SpA, recalling a hypothesis advanced by others that HSCs might become more quiescent in the face of chronic inflammation by applying cellular braking mechanisms as a strategy to protect their self-renewal capacity [56, 243, 249]. To examine this notion further, I investigated expression of the markers CD34 and EPCR, which have been used to distinguish 4 different subsets of HSCs with different biological properties [56] (**Fig. 3.10C**). Importantly, $CD34^-$, $EPCR^+$ cells had the greatest activity in haematopoietic reconstitution when transplanted into irradiated recipients and were more likely to be outside the cell cycle, in G_0. Using these markers, I found the proportion of HSCs with the surface phenotype of quiescent, self-renewing cells ($CD34^-$, $EPCR^+$) was increased with SpA, with a reciprocal decrease in $CD34^+$, $EPCR^-$ cells (**Fig. 3.10D**), indicating that HSCs from mice with SpA were more likely to have a surface phenotype associated with quiescence than those from healthy mice.

Figure 3.10

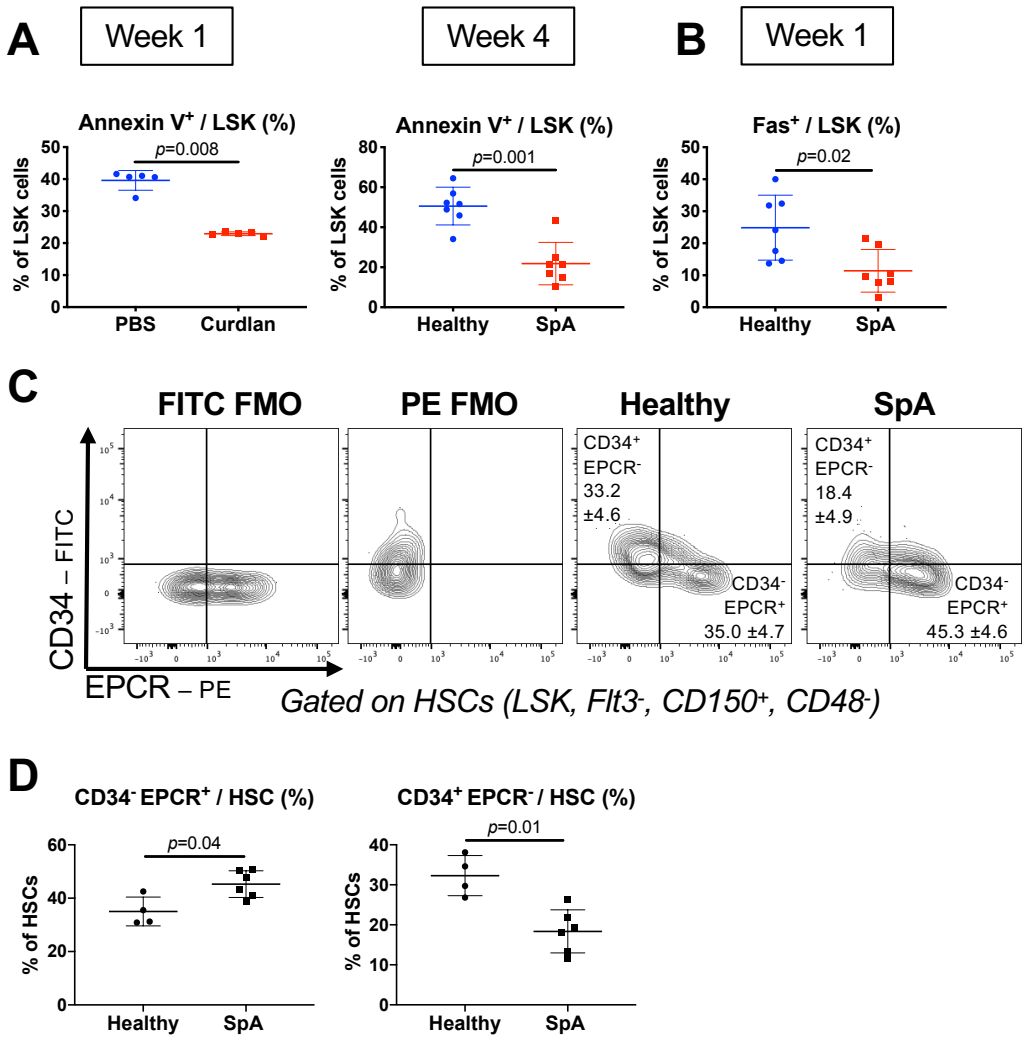

Figure 3.10: SpA causes changes in apoptosis of LSK cells
(**A**) Frequency of LSK cells expressing annexin V 1 week (left) or 4-5 weeks (right) after curdlan or PBS injection in SKG mice.
(**B**) Frequency of LSK cells expressing Fas in mice 1 week after curdlan or PBS injection.
(**C**) Representative flow cytometric images of CD34 and EPCR expression on haematopoietic stem cells (HSCs). Figures indicate mean and SD of n=5-6 mice per group, expressed as proportion of HSCs. FMO: fluorescence minus one control.
(**D**) Frequency of HSCs expressing CD34 and EPCR in mice 4 weeks after injection of curdlan or PBS.
For (**A**), (**B**), and (**D**), points represent individual mice with mean and SD, Mann-Whitney U test.

Data representative of 2 independent experiments (**A**)-(**B**) or from a single experiment (**C**)-(**D**).

To explore whether these changes in LSK population behaviour were reflected in functional differences in the number of cells that could be produced from HSPCs, I sorted HSCs and MPP3/4 cells from healthy SKG mice and from inflamed mice, 4 weeks after injection of curdlan. When these cells were cultured in medium containing a cocktail of cytokines intended to support haematopoiesis (SCF, IL-3, IL-11, Flt3 ligand, EPO, and thrombopoietin, TPO), there was no difference in the total number of cells derived from either setting after 7 days (**Fig. 3.11A**). This suggested HSPCs from mice with SpA were not proliferating at a different rate compared to those from healthy mice when grown *ex vivo*, but any difference might have been lost in this setting if it was dependent on continuous exposure to inflammatory signals.

In other models, changes in cellular behaviour caused by inflammation decreased the ability of HSCs to reconstitute lethally irradiated recipients in transplantation assays when forced to compete against cells from healthy mice. In the context of SpA, I wished to determine whether exposure to the inflammatory milieu would affect the reconstitution abilities of HSCs, despite their phenotype of apparent quiescence. Therefore, I isolated HSCs from mice with SpA or healthy mice and transplanted them into different irradiated congenic ($CD45.1^+$) mice (**Fig. 3.11B**). Owing to the radiosensitivity of BALB/C mice, recipient mice were treated cautiously with only 2.5 Gy of ionising radiation; this was a sublethal dose, meaning that transplanted HSCs would have competed against native $CD45.1^+$ HSCs. Over the ensuing 4 months, the extent of blood chimerism was similar in mice receiving HSCs from either healthy or inflamed mice (**Fig. 3.11C**) but, when mice were culled after 8 months, the BM chimerism was significantly lower in mice that received HSCs from inflamed mice (**Fig. 3.11D**). Importantly, at this stage after

transplantation, all of the CD45.2^{+} haematopoietic cells in the chimeras should have been derived exclusively from HSCs because other HSPC subsets are unable to self-renew beyond ~4 months [9]. This effect was apparent in both myeloid (CD11b^{+}) and B cell (B220^{+}) lineages (**Fig. 3.11E**). Collectively, this indicated that HSCs deriving from mice with SpA had decreased reconstitution potential compared to cells from healthy mice, suggesting exposure to the inflammatory milieu compromised their self-renewal capacity.

Taken together, results in this section show that SpA causes expansion of LSK populations, with decreased apoptosis and increased numbers of MPPs actively involved in the cell cycle. The frequency and number of cycling HSCs are decreased with SpA when analysed cross-sectionally, and these cells may be adopting a cellular phenotype associated with greater quiescence. However, when transplanted, HSCs from mice with SpA do not compete against healthy HSCs as effectively as do those from uninflamed control mice, suggesting their capacity for self-renewal is impaired by the prevailing conditions of SpA.

Figure 3.11

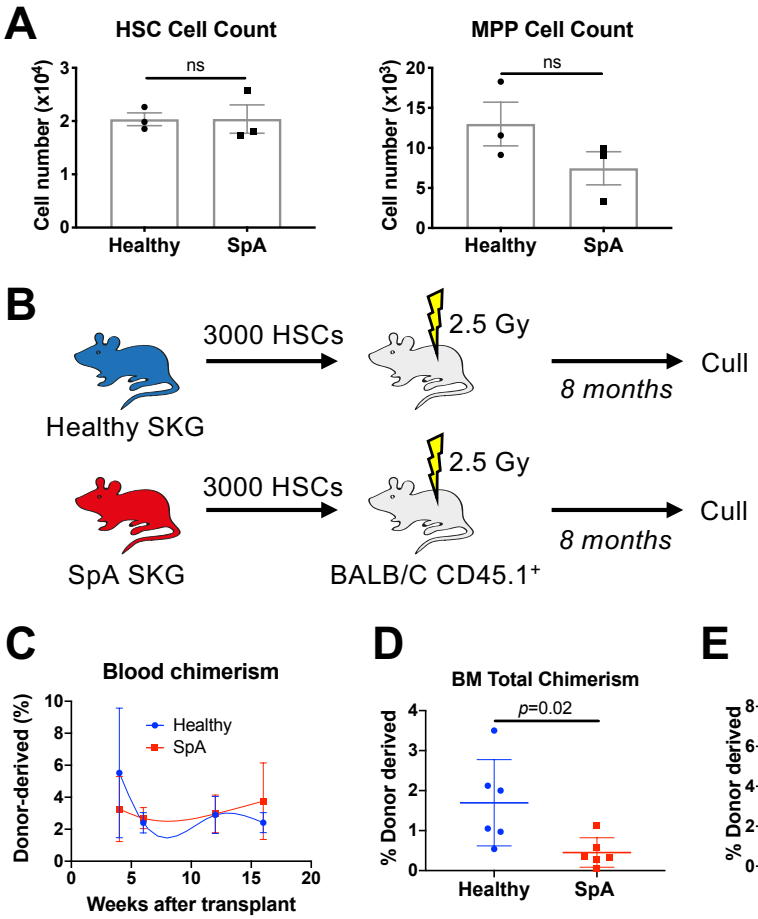

Figure 3.11: HSCs from mice with SpA have decreased reconstitution potential
(**A**) Total number of cells recovered from culture of 500 HSCs (left) or 2000 MPP3/4 cells (right) for 7 days in medium with haematopoietic cytokines. Cells sorted by FACS from healthy mice or mice with SpA. Points represent mean of individual experiments; bars show mean with standard error, Mann-Whitney U test.
(**B**) Schematic diagram, showing isolation of HSCs from healthy SKG mice and mice with SpA by FACS, followed by injection into irradiated CD45.1⁺ recipients. Serial blood samples were obtained by tail bleeding, before the mice were culled after 8 months to assess the BM to generate data for (**C**)-(**D**).
(**C**) Total blood chimerism among CD45⁺ cells over time. Points represent mean with SD for n=6 per group, connecting line is LOWESS spline.
(**D**) Total chimerism among CD45⁺ BM at 8 months. Points represent individual mice with mean and SD, Mann-Whitney U test.
(**E**) Chimerism of indicated lineages of cells in the BM at 8 months. Points represent individual mice; bars show mean with SD. Two way ANOVA with Sidak's test.

Data from a single experiment (**B**)-(**E**) or 3 independent experiments (**A**).

3.2.3 SpA promotes myelopoiesis at the expense of erythropoiesis and lymphopoiesis in the bone marrow

Examining BM progenitors downstream of the HSCs and MPPs (**Fig. 3.12A**), I found a marked difference in the frequency and absolute number of different lineage-committed progenitors 4-5 weeks after curdlan injection. Specifically, I noted expansion of myeloid progenitors (granulocyte macrophage progenitors, GMPs), with reductions in erythroid progenitors ([pre-]colony forming units – erythroid, [pre-]CFU-Es), whether expressed as frequencies among total live BM cells (**Fig. 3.12A**) or as absolute numbers (**Fig. 3.12B**). Overall, this produced a marked imbalance in the ratio of myeloid: erythroid progenitors normally observed in the BM (**Fig. 3.12C**). I also noted a reduction in the number and frequency of CLPs (**Fig. 3.12D**), indicating that lymphopoiesis was also suppressed. Temporally, changes in the frequency of CFU-Es, GMPs, and LSK cells in BM were apparent from 1 week after curdlan injection, before the onset of clinical disease, and were maintained throughout the remainder of the disease course (**Fig. 3.13**).

Functionally, these changes were reflected in the formation of colonies by BM cells plated in methylcellulose medium, with a lesser number of erythroid colonies (blast-forming units erythroid, BFU-E) derived from the BM of SpA mice compared to healthy littermates (**Fig. 3.14A**). Downstream of BM HSPCs, I found similar changes in populations of mature cells in the BM, with decreased numbers of erythroid cells ($Ter119^+$) and B cells ($B220^+$) (**Fig. 3.14B**) but an increased number of mature neutrophils ($CD11b^+$, $Ly6G^+$) (**Fig. 3.14C**). These changes were sufficient to cause a difference in the gross appearance of the femur, which was noticeably paler in mice with SpA (**Fig. 3.14D**).

Figure 3.12

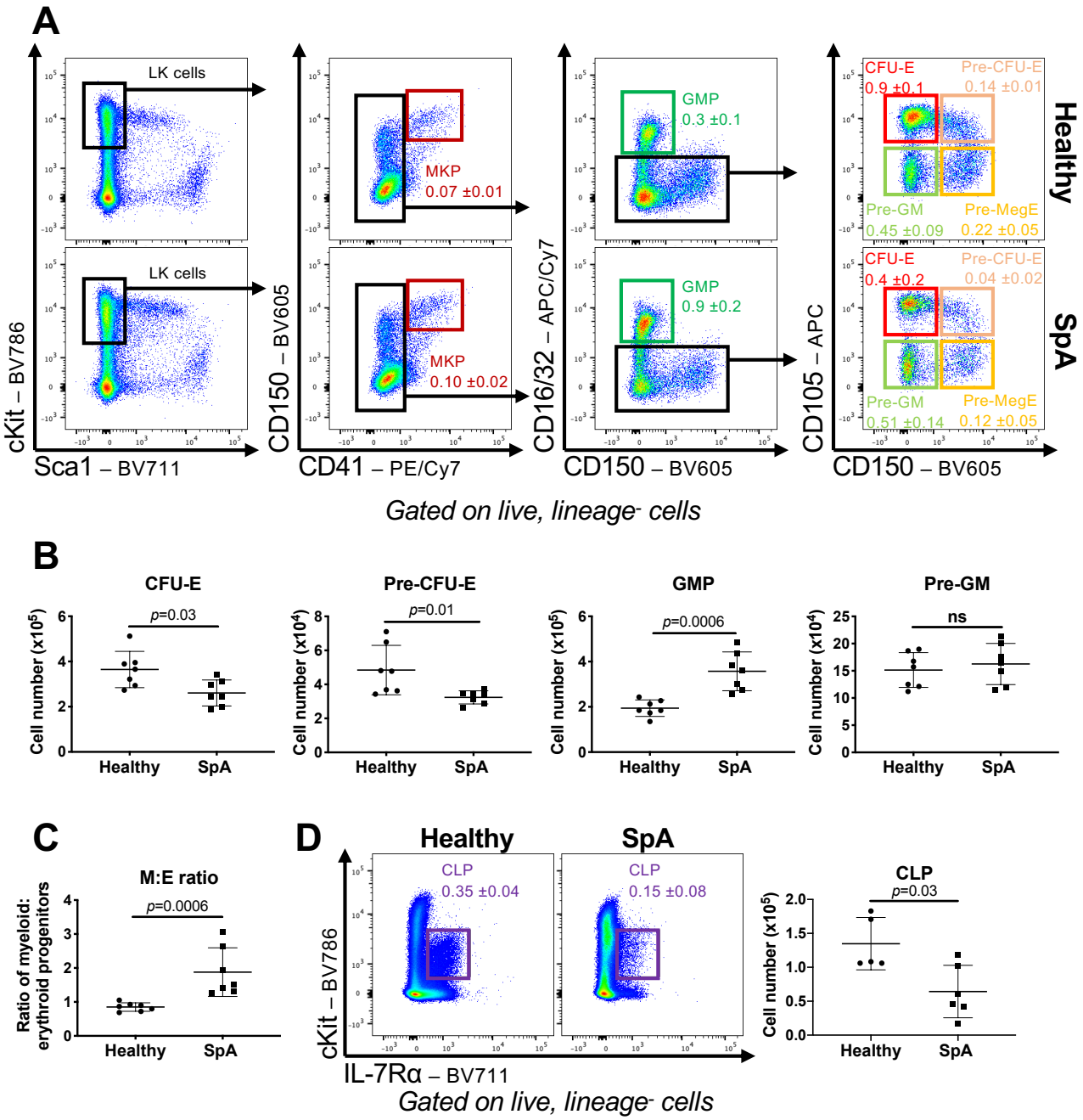

Figure 3.12: SpA causes lineage bias among HSPCs in bone marrow

(**A**) Representative flow cytometric images of indicated HSPC populations among the population of lineage$^-$, c-Kit$^+$ (LK) progenitors in BM. Figures show mean and SD for frequency of indicated populations among live BM cells for n=6 mice per group. MKP: megakaryocyte progenitors, GMP: granulocyte macrophage progenitor, CFU-E: colony forming unit – erythroid, pre-MegE: pre-megakaryocyte erythroid progenitor, pre-GM: pre-granulocyte macrophage progenitor.

(**B**) Number of indicated HSPC cells in BM from 1 femur and 1 tibia in mice 4 weeks after curdlan or PBS injection.

(**C**) Ratio of myeloid (M, GMP and pre-GM) to erythroid (E, CFU-E and pre-CFU-E) in BM.

(**D**) (Left) representative flow cytometric images of common lymphoid progenitors (CLP) in BM of healthy mice and mice with SpA. Figures show mean and SD frequency of CLPs among total live BM cells for n=5-6 mice per group. (Right) Number of CLPs in 1 femur and 1 tibia from the same mice.

For (**B**), (**C**),and (**D**), points indicate individual mice with mean and SD, Mann-Whitney U test.

Data representative of 5 independent experiments.

Figure 3.13

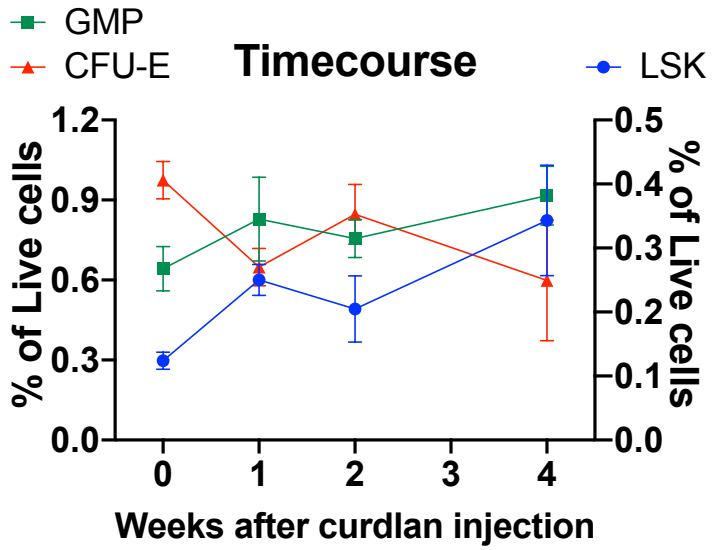

Figure 3.13: Haematopoietic remodelling begins in the first week after curdlan injection
Changes in the frequency of indicated HSPC populations as a proportion of total live BM cells over time in mice developing SpA.
Points represent mean and SD for n=5-6 mice per group.

Data from a single experiment.

Figure 3.14

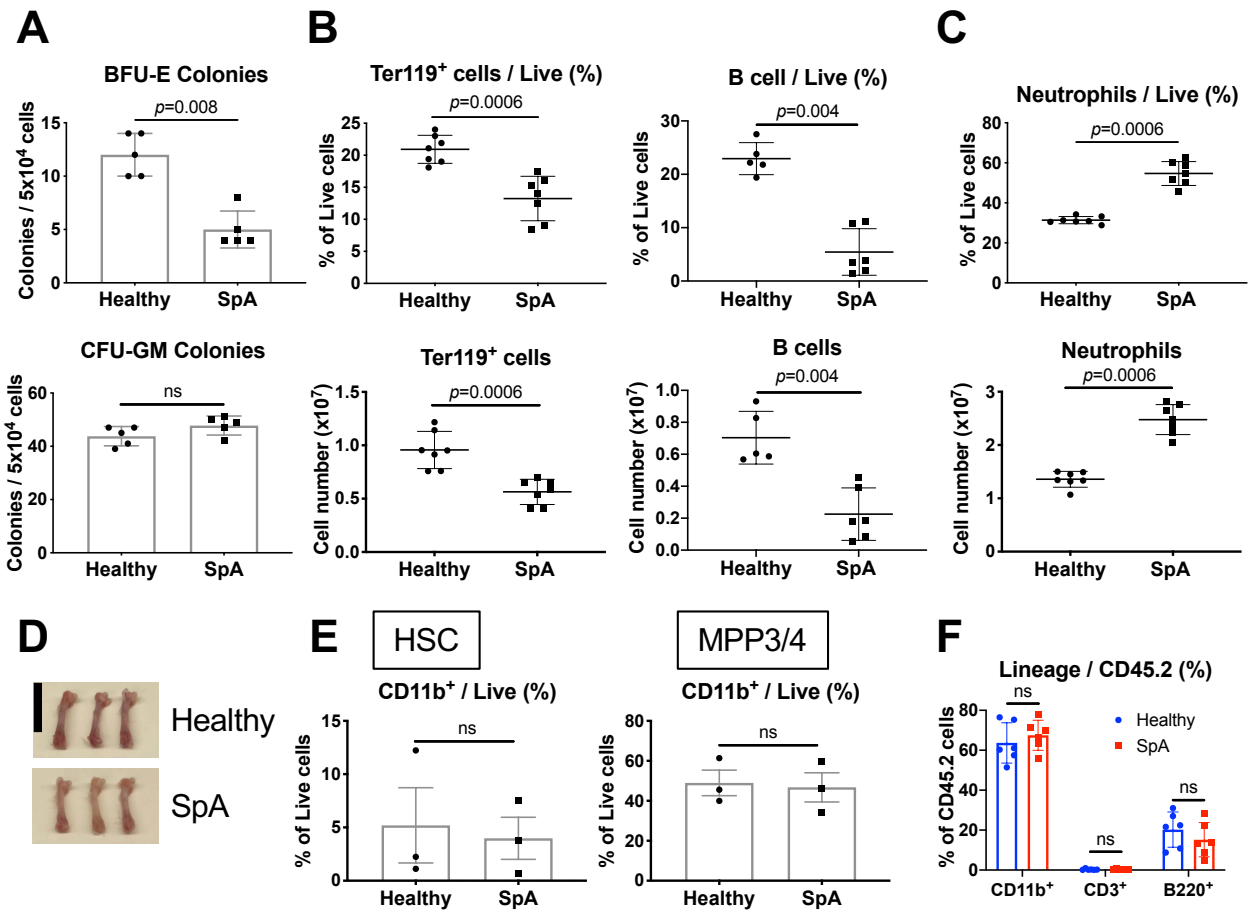

Figure 3.14: LSK populations show no evidence of functional lineage bias
(**A**) Number of colonies of indicated types derived from 5x10^4 whole BM cells taken from healthy mice or mice with SpA after 10 days in methylcellulose medium. CFU-GM: colony forming unit – granulocyte macrophage; BFU-E: blast forming unit – erythroid.
(**B**) Frequency and absolute number of mature erythroid cells (Ter119$^+$) and B cells (B220$^+$) in BM of healthy mice and mice with SpA.
(**C**) Frequency and absolute number of mature neutrophils (CD11b$^+$, Ly6G$^+$) in BM.
(**D**) Representative images of femurs dissected from healthy mice and mice with SpA. Scale bar = 1 cm.
(**E**) Frequency of cells expressing CD11b in cultures of FACS-sorted HSCs (left) or MPP3/4 (right) after liquid culture for 7 days. Points represent mean of individual experiments, bars show mean with standard error, Mann-Whitney U test.
(**F**) Frequency of cells expressing indicated lineage markers among CD45.2$^+$ cells, which derive from HSCs sorted by FACS from either healthy mice or mice with SpA, 4 weeks after curdlan injection, and transplanted into irradiated CD45.1$^+$ recipients for 8 months. Points represent individual mice, bars show mean and SD. Two-way ANOVA with Sidak's test.
For (**A**)-(**C**), points represent individual mice with mean and SD, Mann-Whitney U test.

Data representative of a single experiment (**F**) or 2 (**A**), or 5 (**B**)-(**D**) independent experiments. For (**E**), graphs show data from 3 independent experiments.

I asked whether the marked bias in lineage-committed progenitors in SpA could be related to differences in the output of multipotent HSC and MPP populations as inflammation develops. To investigate this, I cultured HSCs and MPP3/4s sorted by FACS from healthy mice and mice with SpA in medium supplemented with haematopoietic cytokines. However, I observed no difference in the proportion of cells recovered from these cultures after 7 days that were expressing the myeloid marker CD11b (**Fig. 3.14E**). Similarly, when I examined the relative frequency of different lineages among cells deriving from transplanted HSCs, as outlined in **Fig. 3.11B**, I found no difference between mice that received HSCs from healthy mice and those receiving HSCs from mice with SpA (**Fig. 3.14F**). Collectively, these data were consistent with one or more of the following interpretations, which are not mutually exclusive: 1) continued exposure to inflammatory signals is required to induce any lineage bias among LSK cells that might contribute to the observed phenotype in SpA, 2) change in lineage bias among LSK cells is enshrined in differences in MPP subset frequency rather than changes in cellular output on a per cell basis, or 3) most of the observed lineage bias in mice with SpA is attributable to changes in frequency and/or behaviour of lineage-committed progenitors downstream of LSK cells.

To explore this latter notion in more detail, I examined the expression of proliferation and apoptosis markers among lineage-committed progenitors, noting a striking difference in pattern between erythroid and myeloid progenitors. In erythroid progenitors (CFU-Es and pre-CFU-Es), the normally very high proportion of cells expressing Ki67 was decreased (**Fig. 3.15A**), suggesting fewer cells were actively participating in the cell cycle. Similarly, the incorporation of BrdU was decreased in erythroid progenitors one week after curdlan injection (**Fig. 3.15B**),

and these changes were confirmed by analysis of cell cycle stages using Ki67 and DAPI (**Fig. 3.15C**). This suggested the contraction of the population of erythroid progenitors and mature erythroid cells during inflammation could be attributable to decreased proliferation. I also found the expression of annexin V (**Fig. 3.15D**) and Fas (**Fig. 3.15E**) were decreased in the same cells, which could have been a compensatory response to the suppression of erythropoiesis, possibly mediated by increased production of EPO, which exerts an anti-apoptotic effect on erythroid progenitors [164, 177]. I confirmed the functional importance of these findings by sorting erythroid progenitors (CFU-Es and pre-CFU-Es) by FACS from healthy mice and mice with SpA and culturing them in serum-free medium supplemented with SCF and EPO. Doing so, I found progenitors from mice with SpA generated fewer cells in total and a smaller number of cells expressing the erythroid maturity marker Ter119 (**Fig. 3.15F**), indicating that inflammation causes durable changes in committed erythroid progenitors that limit their functional output.

Among myeloid progenitors (GMPs), curdlan injection caused a slight reduction in Ki67 expression after one week (**Fig. 3.16A**), no difference in BrdU incorporation (**Fig. 3.16B**), and a slight increase in the proportion of cells in G_1 phase of the cell cycle (**Fig. 3.16C**), suggesting expansion of GMPs observed in SpA was not attributable to increased recruitment of cells into the cell cycle. Consistent with this, there was no difference in the number of cells derived from GMPs that were sorted by FACS from either healthy mice or mice with SpA (**Fig. 3.16D**). As with erythroid progenitors, there was a reduction in expression of annexin V (**Fig. 3.16E**) and Fas (**Fig. 3.15F**) in primary GMPs, suggesting the expansion of the GMP pool could be related to decreased apoptosis, as also suggested for LSK cells.

Collectively, these findings suggested lineage bias observed in the BM and blood of mice with SpA could be attributable, at least in part, to differences in proliferation and cell survival among lineage committed progenitors.

Figure 3.15

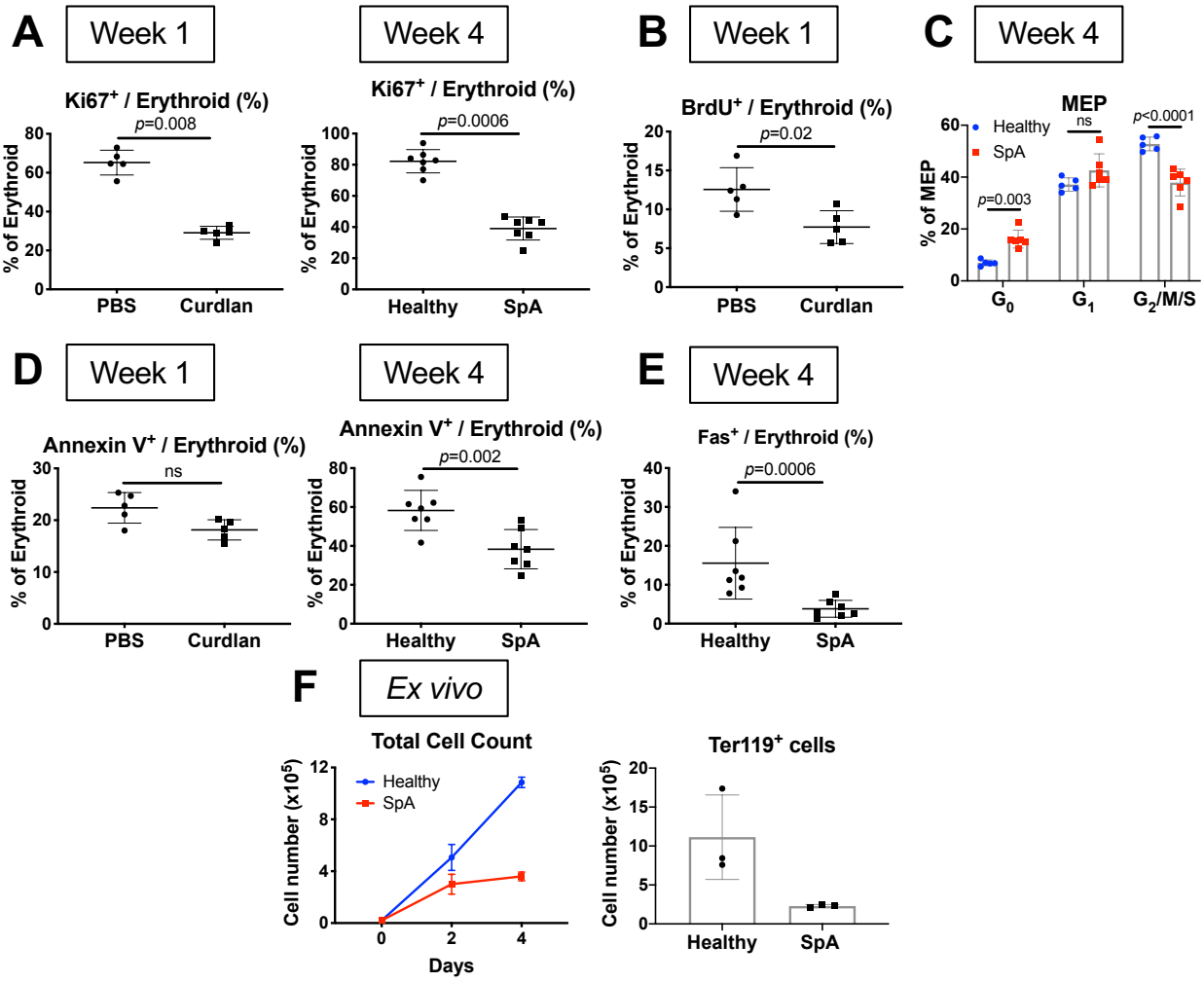

Figure 3.15: Proliferation of erythroid progenitors is suppressed in SpA
(**A-B**) Frequency of BM erythroid progenitors (i.e. CFU-E and pre-CFU-E) expressing (**A**) Ki67 in healthy mice and mice 1 week (Left) or 4 weeks (Right) after curdlan injection, or (**B**) BrdU in healthy mice and mice 1 week after curdlan injection.
(**C**) Frequency of megakaryoid/erythroid progenitors (MEPs, predominantly CFU-Es) in different stages of the cell cycle, as determined by staining for Ki67 and with DAPI. Points represent individual mice, bars show mean and SD, two-way ANOVA with Sidak's test.
(**D-E**) Frequency of BM erythroid progenitors expressing (**D**) annexin V in healthy mice and mice 1 week (Left) or 4 weeks (Right) after curdlan injection, or (**E**) Fas in healthy mice and mice 4 weeks after curdlan injection.
(**F**) (Left) Total number of cells derived from 2000 erythroid progenitors (CFU-E and pre-CFU-E) sorted by FACS from healthy mice or mice with SpA and cultured in serum-free medium with cytokines for 4 days. Points represent mean and SD of technical triplicates. (Right) Number of Ter119+ cells obtained from the same cultures at day 4. Points show technical replicates, bars indicate mean with SD.
For (**A**)-(**B**) and (**D**)-(**E**), points represent individual mice with mean and SD, Mann-Whitney U test.

Data representative of 2 (**B**), (**E**), (**F**), or 4 (**A**), (**D**) independent experiments.

Figure 3.16

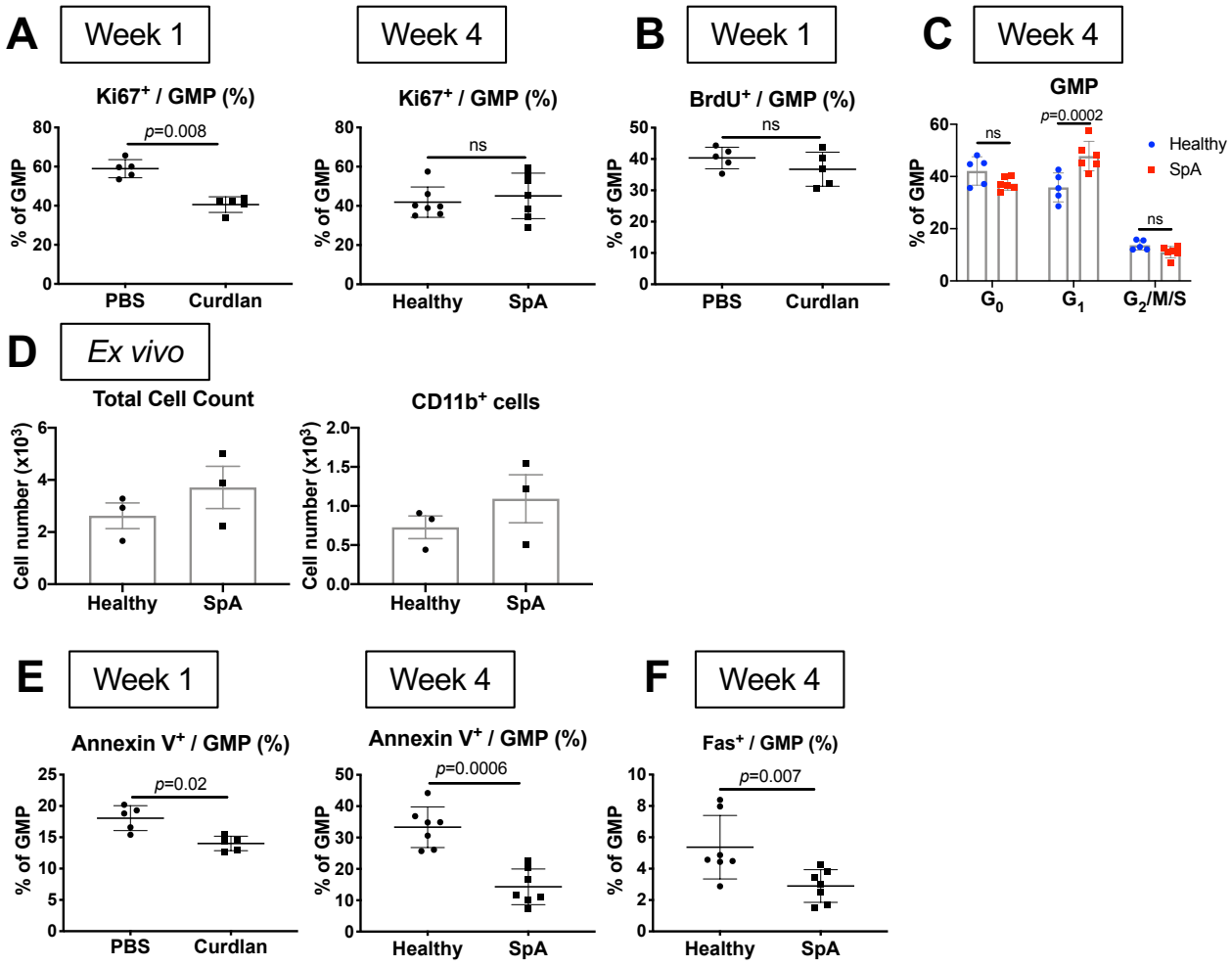

Figure 3.16: Proliferation of myeloid progenitors is unaltered in SpA
(**A-B**) Frequency of GMPs expressing (**A**) Ki67 in healthy mice and mice (Left) 1 week or (Right) 4 weeks after curdlan injection, or (**B**) BrdU incorporation in healthy mice and mice 1 week after curdlan injection.
(**C**) Frequency of GMPs in different stages of the cell cycle, as determined by staining for Ki67 and with DAPI. Points represent individual mice, bars show mean and SD, two-way ANOVA with Sidak's test.
(**D**) (Left) Total number of cells derived from 10^3 GMPs sorted by FACS from healthy mice or mice with SpA and cultured for 4 days. (Right) Number of CD11b$^+$ cells obtained from the same cultures at day 4. Points show technical replicates, bars indicate mean with SD.
(**E-F**) Frequency of GMPs expressing (**E**) annexin V in healthy mice and mice 1 week (Left) or 4 weeks (Right) after curdlan injection, or (**F**) Fas in healthy mice and mice 4 weeks after curdlan injection.
For (**A**)-(**B**) and (**E**)-(**F**), points represent individual mice with mean and SD, Mann-Whitney U test.

Data representative of 2 (**B**), (**C**), (**F**), or 4 (**A**), (**E**) independent experiments.
For (**D**), graphs show results from 3 independent experiments.

3.2.4 Extramedullary haematopoiesis contributes to accumulation of myeloid cells in the paws of mice with SpA

Noting the marked enlargement of the spleen in mice with SpA (**Fig. 3.7B**) and knowing that the spleen is an important location for haematopoiesis in mice under homeostatic conditions and in the face of demand [197, 198], I asked whether there were also changes in extramedullary haematopoiesis (EMH) during inflammation. Accordingly, I found the frequency and number of LSK and lineage-committed progenitors (erythroid, GMP, and MKP) was increased in the spleens of mice with SpA compared to those of healthy mice (**Fig. 3.17A-B**). However, in contrast to the lineage bias observed in the BM, the ratio of myeloid to erythroid progenitors in the spleen was unchanged with inflammation (**Fig. 3.18A**). This suggested expansion of splenic EMH occurs without regard to haematopoietic lineage during inflammation, whereas adaptation of BM haematopoiesis was accompanied by dramatic changes in the nature of lineage output. This dichotomy could be a function of differences in the composition or maximal size of the niche, or to differences in the cell-intrinsic responses of progenitors in different locations. In support of the latter notion, I found the proportions of GMPs and erythroid progenitors expressing Ki67 were slightly increased in the spleen (when they were similar or decreased in BM, respectively) after mice were injected with curdlan (**Fig. 3.18B**), suggesting expansion of both progenitor populations could be caused by increased proliferation *in situ*. However, I could not discount other possibilities, including migration of progenitors from the BM to spleen.

Figure 3.17

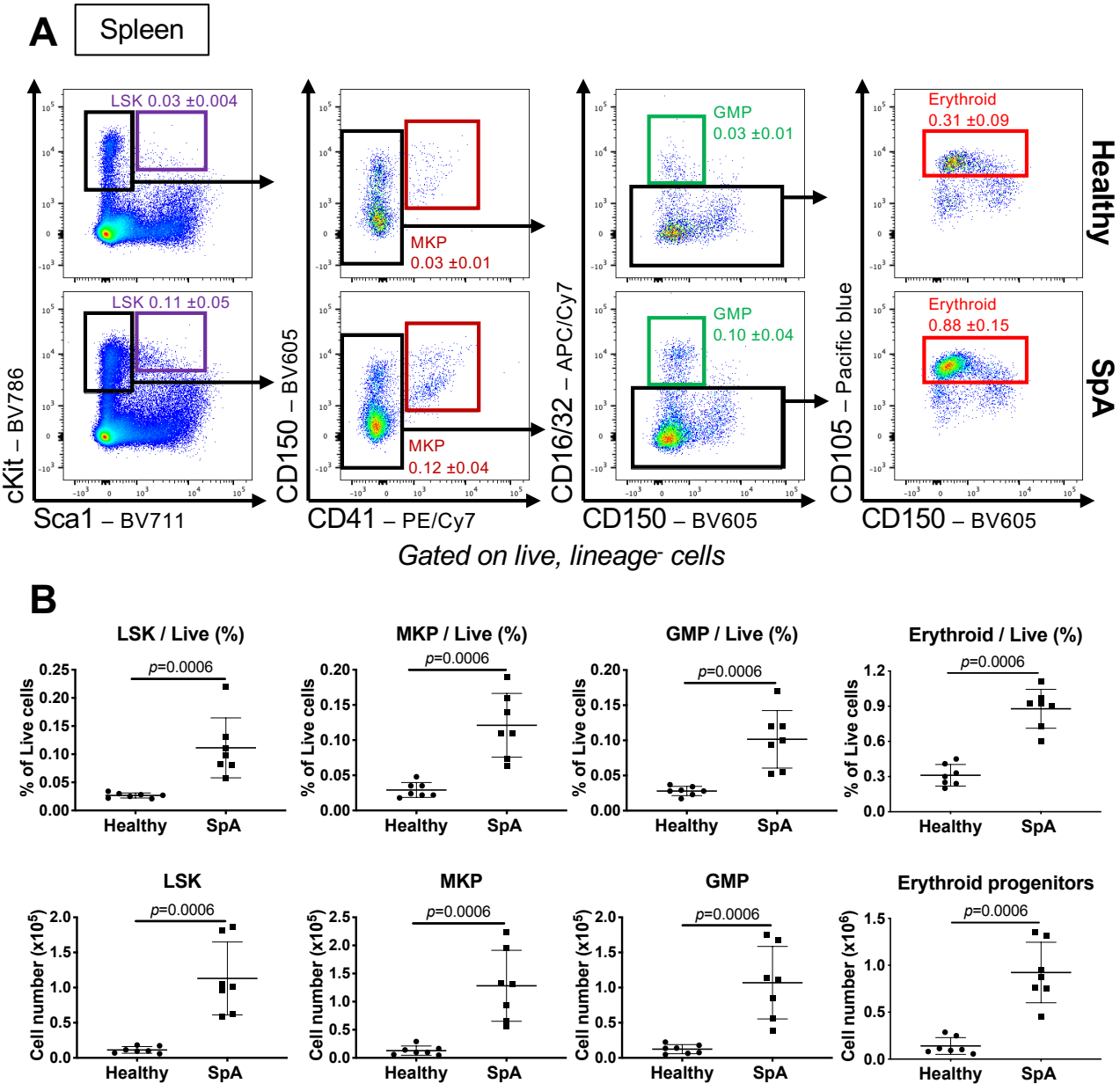

Figure 3.17: HSPCs accumulate in the spleen during SpA
(**A**) Representative flow cytometric images of indicated HSPC populations in the spleen of mice 4 weeks after injection of curdlan or PBS. Figures show mean and SD among total spleen live cells for n=7 mice per group.
(**B**) Frequency and absolute numbers of indicated HSPC populations in the spleen of healthy mice and mice with SpA. Points show individual mice with mean and SD, Mann-Whitney U test.

Data representative of 5 independent experiments.

Figure 3.18

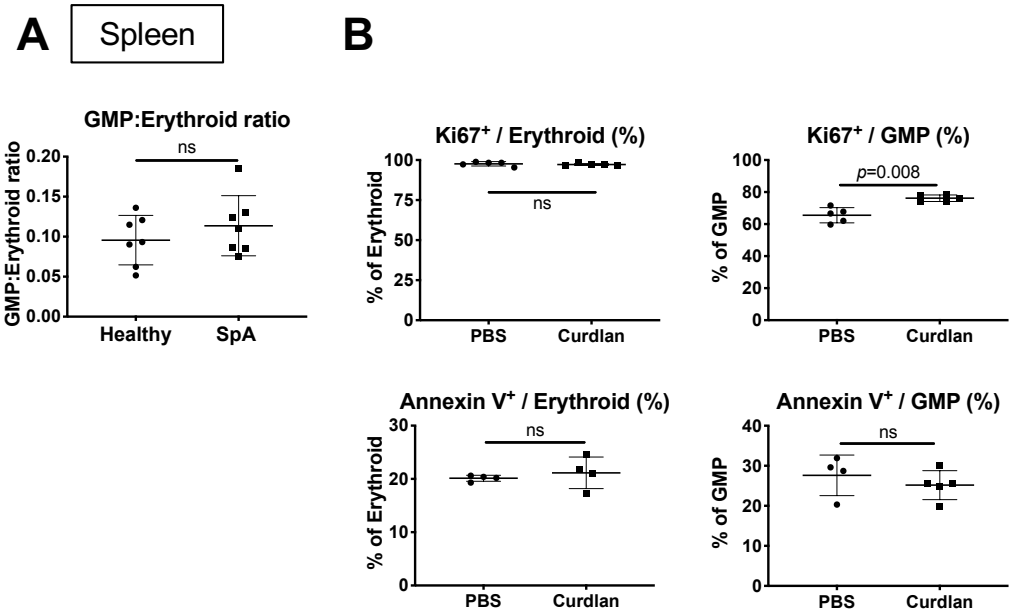

Figure 3.18: Splenic progenitors have different cellular behaviour to those in BM
(**A**) Ratio of GMPs to erythroid progenitors in the spleen of mice 4 weeks after injection of curdlan or PBS.
(**B**) Frequency of erythroid progenitors (Left) and GMPs (Right) expressing Ki67 and annexin V in healthy mice and 1 week after curdlan injection.
For (**A**)-(**B**), points represent individual mice with mean and SD, Mann-Whitney U test.

Data representative of 2 (**B**) or 5 (**A**) independent experiments.

In addition to subsisting in BM and spleen, HSPCs circulate through the blood and lymphatic systems and may lodge in inflamed tissues to produce mature cells locally according to demand [482]. Similarly, in SpA, I found populations of cells with the surface phenotype of GMPs (i.e. lineage^{neg}, c-Kit^{+}, Sca-1^{-}, CD34^{+}, CD16/32^{+}) and LSK cells in the paws, which were absent or present at very low numbers in healthy mice (**Fig. 3.19A-B**). I sorted these cells by FACS from mice with SpA and cultured them *ex vivo*, finding they gave rise to cells with the flow cytometric phenotype of mature neutrophils (CD11b^{+}, Ly6G^{+}), albeit with a lower number of total cells than comparable cells obtained from the BM (**Fig. 3.19C**). This

progenitor activity was not observed in a control population of lineage^{neg}, c-Kit^{neg}, Sca-1^{neg} ('double negative', DN) cells that were also sorted from the paws. Previous work in our laboratory has shown that GMPs from the paws are highly proliferative (based on expression of Ki67) and have the ability to form colonies of mature granulocytes (colony forming units – granulocyte macrophage, CFU-GM) in methylcellulose medium [441]. The same work also demonstrated that GMPs injected intravenously into SKG mice developing SpA can home to the joints and produce mature granulocytes [441]. Collectively, this confirms the presence of a population of myeloid progenitors accumulating in inflamed joints of mice with SpA, where they are able to produce granulocytes that contribute to the inflammatory response.

Taken together, this description of SKG mice shows that curdlan injection causes changes at multiple levels of the haematopoietic system, expanding populations of early LSK cells and causing marked bias in the relative proportions of erythroid and myeloid progenitors and their progeny in BM. Indeed, the suppression of erythropoiesis is sufficient to cause anaemia in mice with SpA, which is not compensated by accumulation of erythroid progenitors in the enlarged spleen. In the joints, there is accumulation of myeloid progenitors that produce granulocytes locally, contributing to the inflammatory response. The demands of SpA therefore cause cellular, temporal, and spatial remodelling of haematopoiesis in this system.

Figure 3.19

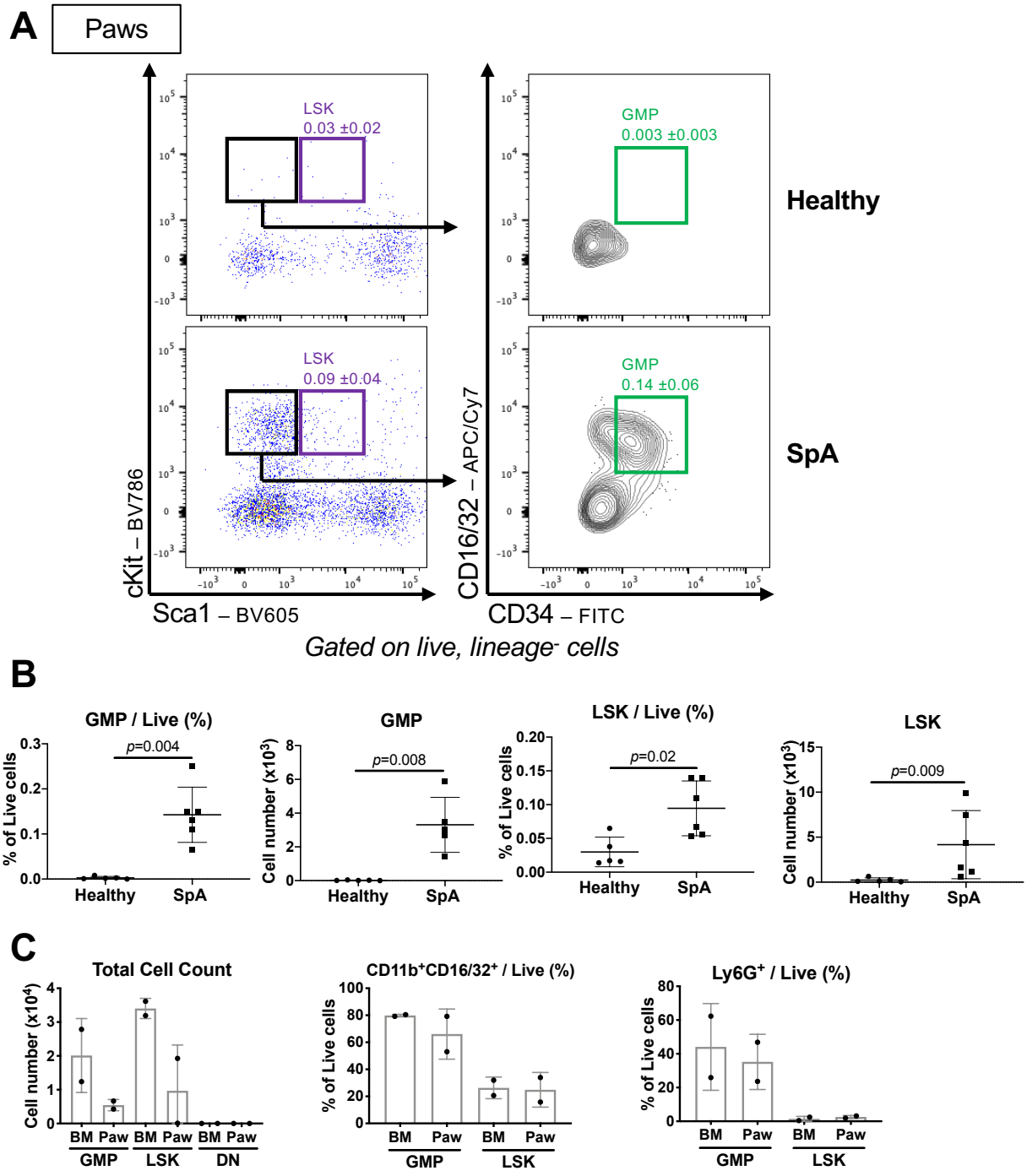

Figure 3.19: Myeloid progenitors accumulate in inflamed joints
(**A**) Representative flow cytometric images of LSK cells and GMPs in enzymatically digested paw suspensions from SKG mice 4 weeks after injection of PBS or curdlan. Figures show mean and SD frequency of indicated cells among live paw cells for n=5-6 mice per group.
(**B**) Frequency and absolute number of indicated populations in paws. Points show individual mice with mean and SD, Mann-Whitney U test.
(**C**) Total cell number (Left), frequency of $CD11b^+$, $CD16/32^+$ (Middle), and frequency of cells with the surface phenotype of mature neutrophils ($CD11b^+$, $Ly6G^+$, Right) derived from culture of GMPs and LSKs from BM and paws of mice with SpA. Points show mean of triplicates for independent experiments, bars show mean and standard error.

Data representative of 3 independent experiments (**A**)-(**B**). For (**C**), graphs show data from 2 independent experiments.

3.2.5 The mutation in *Zap70* in SKG mice is not responsible for haematopoietic changes observed in response to curdlan injection

I wished to confirm that the haematopoietic changes observed in SKG mice were not attributable to the mutation in *Zap70*, which predisposes to autoimmune responses [385]. Using previously-published RNA sequencing data from a range of haematopoietic cells [476], I found *Zap70* was not expressed in primitive HSCs but was expressed in MPPs, albeit to a much lower level than observed in CLPs or mature lymphoid cells that depend on ZAP-70 signalling for activation [386] (**Fig. 3.20A**). Among MPPs, expression was similar between myeloerythroid MPP2, myeloid-biased MPP3, and $Flt3^+$ cells that may differentiate into myeloid or lymphoid pathways according to demand (i.e. MPP4 or LMPP) [79], suggesting this was not necessarily a marker of lymphoid potential (**Fig. 3.20B**). Downstream of LSK cells, *Zap70* was not expressed in committed myeloid (GMP) or erythroid (CFU-E) progenitors (**Fig. 3.20A**).

To demonstrate that the *Zap70* mutation was not the proximate cause of the haematopoietic phenotype in SKG mice, I also injected curdlan in wild type C57BL/6 mice (**Fig. 3.20C**). I hypothesised that these mice would mount a similar inflammatory response to curdlan, mediated by binding to dectin-1, but would not generate an autoreactive T cell response that would cause arthritis, enthesitis, and enteritis. Accordingly, I culled these mice one week after curdlan injection, when I expected the innate response to be maximal [385]. Unlike SKG mice, which had abnormal neutrophil infiltration of the paws one week after curdlan injection, C57BL/6 mice had no leukocyte infiltration of the paws at the same time point (**Fig. 3.20D**). However, C57BL/6 mice did develop the same haematopoietic perturbations in response to curdlan, with increased frequencies and absolute

numbers of GMPs and neutrophils in BM, and decreased numbers of erythroid progenitors and Ter119^{+} cells (**Fig. 3.20E-F**). This showed that curdlan-induced activation of the innate immune system was sufficient to produce a comparable inflammatory milieu without a requirement for autoreactive T cell responses. To confirm that T cell responses were dispensable for the haematopoietic phenotype of mice with SpA, I injected SKG mice repeatedly with anti-CD4 antibodies or an isotype control after triggering inflammation with curdlan. This treatment effectively depleted CD4^{+} T cells in the blood and mesenteric lymph nodes (**Fig. 3.21A**) but did not cause any difference in the frequency or absolute number of BM HSPCs, neutrophils, or erythroid cells compared to the isotype (**Fig. 3.21B**). Collectively, these observations showed that the *Zap70* mutation, and ZAP-70^{+}, CD4^{+} T cells, were not required for the haematopoietic derangements that developed in SpA.

Figure 3.20

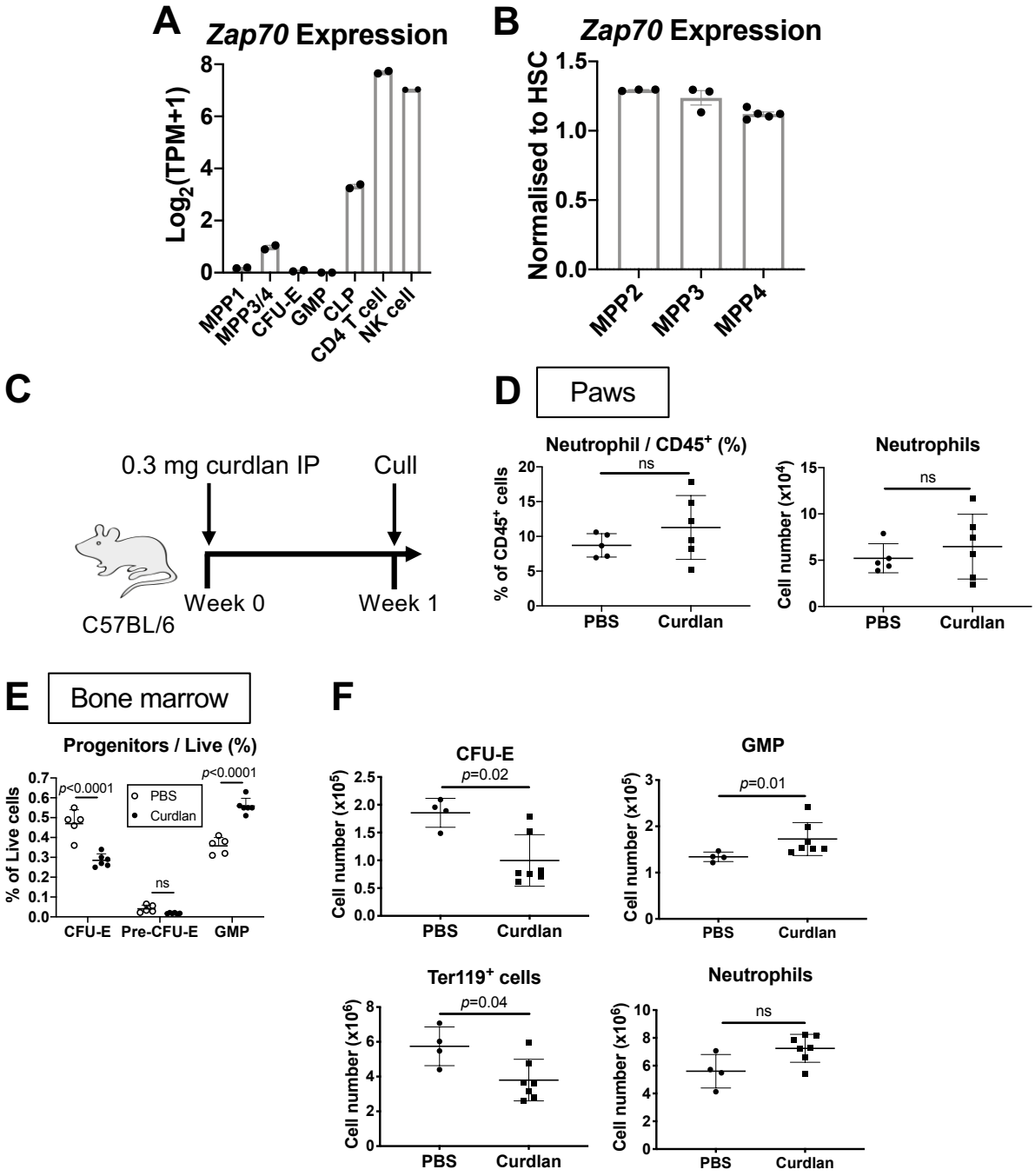

Figure 3.20: Curdlan-induced haematopoietic changes are not dependent on the *Zap70* mutation in SKG mice

(**A**) Expression of *Zap70* in indicated cell populations by RNA sequencing in transcripts per million (TPM). Points represent biological replicates in previously published data, bars show mean and standard error. Data from [473].

(**B**) Expression of *Zap70* in indicated MPP populations by RNA sequencing, normalised to expression in haematopoietic stem cells (HSCs). Points represent biological replicates in previously published data, bars show mean and standard error. Data from [79].

(**C**) Schematic showing injection of curdlan in wild type C57BL/6 mice before culling after 1 week to obtain data shown in (**D**)-(**F**).

(**D**) Frequency and absolute number of neutrophils in enzymatic paw digests.

(**E**) Frequency of indicated HSPC populations among total BM live cells.

(**F**) Absolute number of indicated HSPC and mature populations in BM.

For (**D**)-(**F**), points represent individual mice with mean and SD, Mann-Whitney U test except for (**E**), where two-way ANOVA with Sidak's test was used.

Data representative of 4 independent experiments (**C**)-(**F**).

Figure 3.21

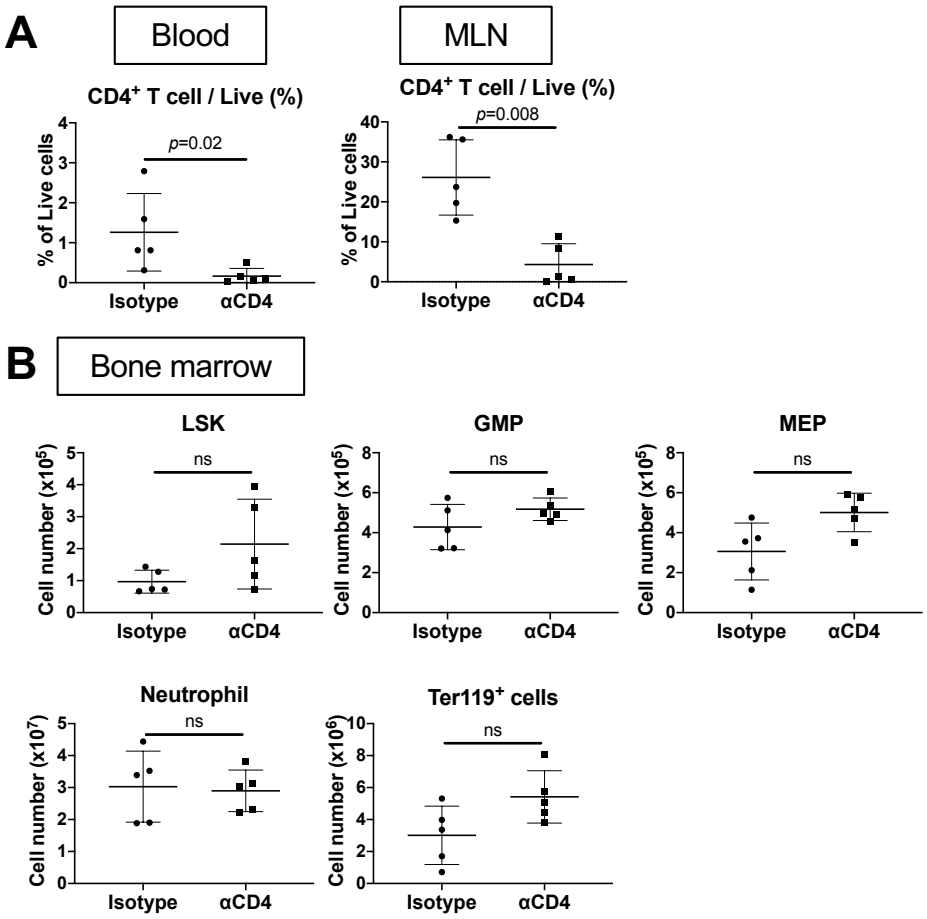

Figure 3.21: Curdlan-induced haematopoietic changes are not dependent on CD4⁺ T cells
(**A**) Frequency of CD4⁺ T cells in blood (Left) and mesenteric lymph node (MLN, Right) in mice with SpA injected with anti-CD4 antibodies or isotype for 4 weeks after injection of curdlan.
(**B**) Absolute number of indicated HSPCs and mature cells in 1 tibia and 1 femur. MEP: megakaryocyte/erythroid progenitor.
For (**A**)-(**B**), points represent individual mice with mean and SD, Mann-Whitney U test.

Data from a single experiment.

3.3 Discussion

In this chapter, I confirmed that curdlan injection in SKG mice replicates clinical features of human SpA, causing inflammatory arthritis of peripheral joints, enthesitis, and enteritis. Curdlan injection causes chronic, non-resolving inflammation with high consistency among individual mice, making it an amenable

model to study interactions between chronic inflammation and haematopoiesis. I add to the idoneous features of this model by showing that the *Zap70* mutation is not necessary for curdlan to cause derangement of haematopoiesis and that mutation-bearing $CD4^+$ T cells do not affect the haematopoietic phenotype after SpA has been induced.

Development of SpA was associated with accumulation of large numbers of mature myeloid cells in blood and inflamed sites, and progression of clinical arthritis closely tracked the accumulation of paw neutrophils and monocytes. Because these cells have a short circulating half time in the blood, this suggested the rate of production of new cells could be increased, implying some perturbation of haematopoiesis. Further evidence for this notion was provided by the observation of anaemia and decreased blood B cell count in mice with SpA. Accordingly, I found haematopoiesis was remodelled on multiple levels, with changes in LSK cell numbers and cellular activity, overall lineage bias towards myelopoiesis at the expense of lymphopoiesis and erythropoiesis, and functional EMH in the spleen and inflamed joints (**Fig. 3.22**).

Figure 3.22

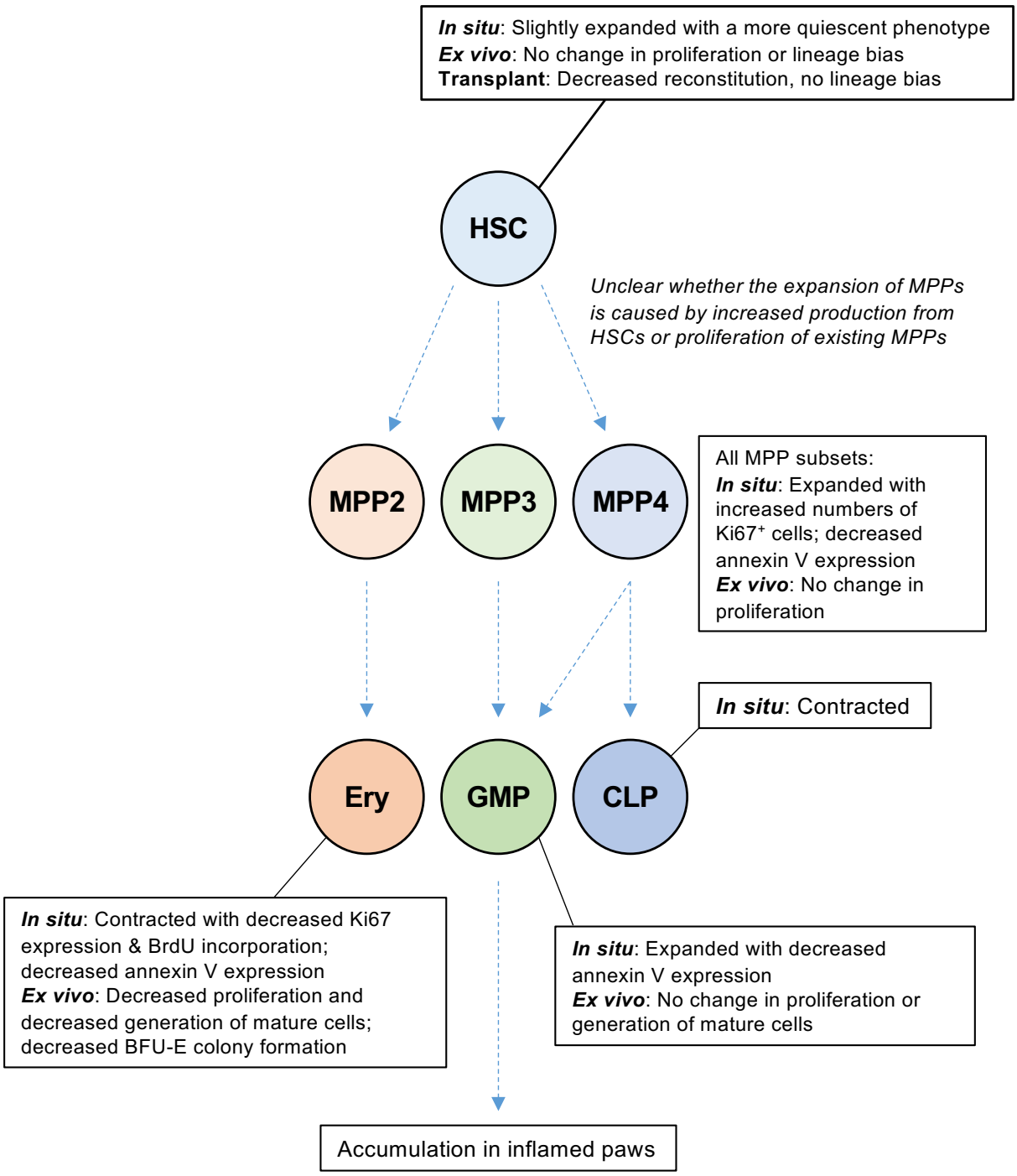

Figure 3.22: Summary of haematopoietic changes in BM in murine SpA
Text in boxes summarises findings in this chapter, separated by observations of BM from mice with SpA compared to healthy mice ('*in situ*'), observations from culture of FACS-sorted cells ('*ex vivo*'), or from transplantation assay. Ery: erythroid progenitors.

3.3.1 LSK compartment

In murine SpA, I found evidence that HSCs were remaining quiescent, with little increase in cell number and decreased expression of the proliferation marker Ki67. These analyses do not permit a comprehensive evaluation of proliferation because they do not show how often cells were entering and exiting the cell cycle, which could have been assessed using a combination of two different decoy nucleotides injected at different times, or by injecting a cellular dye such as carboxyfluorescein succinimidyl ester (CFSE). For example, although the proportion of HSCs expressing Ki67 at any moment might be decreased with SpA, individual cells might be transiently entering the cell cycle more often than in healthy mice to produce a fast division rate. However, my findings are similar to those from the K/BxN serum transfer model, which causes inflammatory arthritis in mice and is taken as a model of RA: in this setting, the number of HSCs was not increased with inflammation and Ki67 expression among HSCs was unchanged [249]. This suggests either that HSCs might be relatively insensitive to the effects of inflammatory stimuli when located in the BM niche, or that HSCs might proliferate transiently but then re-enter a quiescent state owing to proposed 'braking mechanisms' that limit uncontrolled proliferation [243]. Such a mechanism has been demonstrated for HSCs exposed to type I IFNs [248], G-CSF [245], or IL-1β [247], which proliferate initially but then regain a quiescent state that is postulated to protect their self-renewal capacity by limiting the cellular damage imposed by repeated division. At a cellular level, these braking mechanisms are associated with increased expression of transcription factors, such as Myc, Foxo3a, and Rb1 [56, 247], that inhibit progression in the cell cycle. My data suggest but do not prove that a similar mechanism could be operating in SpA. However, unlike HSCs from

mice with K/BxN arthritis, those from mice with SpA had a competitive disadvantage against healthy cells when transplanted, suggesting the inflammatory milieu eroded their competence for haematopoietic reconstitution. In support of this, previous analysis of the bulk transcriptome of HSCs from mice with SpA in our laboratory revealed increased expression of CDK6 [441], which is an early marker of emergence from quiescence [63] that is probably more reliable than surface expression of CD34 and EPCR. Interpretation of these findings is complicated by the known heterogeneity of the HSC population with respect to its quiescence status [21], meaning that overall changes in behaviour of the whole population could reflect divergent behaviours of different subgroups of HSCs rather than uniform changes in all cells. For example, although the majority of HSCs could be quiescent during SpA, a small number of cells might be proliferating at a faster rate.

Downstream of HSCs, I observed marked expansion of all MPP subsets, with a particular increase in MPP3s, which have been described as 'myeloid-biased' in previous reports [79, 95]. It was unclear whether increased numbers of MPPs were attributable to increased generation of these cells from HSCs or to increased proliferation of existing MPPs. In support of the latter notion, others have shown that, in conditions of increased demand, MPP3s divide more frequently *in vivo* than in healthy mice [252]. Because MPPs derive from HSCs, a further possibility is that changes in the transcriptome of HSCs could lead to the production of MPPs that have a greater propensity to proliferate and preferentially produce some lineages at the expense of others, even if the quantitative output of HSCs is unchanged.

In SpA, the proportion of actively cycling MPP2s and MPP3s was decreased at a single timepoint but, unlike HSCs, the number of cycling cells was increased

owing to population expansions. One hypothesis deriving from these changes is that MPPs could be contributing more to the remodelling of haematopoiesis in SpA than HSCs, which would be consistent with their role as the major HSPC stage supporting haematopoietic output under homeostatic conditions [13]. This discussion overlaps with debate about the exact role of HSCs in haematopoiesis, which is disputed [483]: because HSCs are essential for reconstitution of animals that receive cytotoxic drugs such as 5-FU or undergo lethal irradiation, there has been an assumption that they also respond to extraordinary demands imposed on the haematopoietic system during inflammation by increasing their output. However, reconstitution of myeloablated animals requires regeneration of the entire haematopoietic compartment, which must all be derived from HSCs. In contrast, during situations like SpA, my data suggest the total output of the BM may be quantitatively similar to homeostatic conditions, with no change in total BM cellularity and with expansion of some HSPC populations offset by contractions of others. Similarly, in the blood, an increased neutrophil count is offset by decreased RBC and B cell counts, suggesting total output is broadly unchanged. I therefore speculate that, during inflammation, the major response of the haematopoietic system in BM is redistribution of the proportions of different HSPCs to meet the demand for mature myeloid cells, without increases in total output that would necessitate widespread HSC recruitment. In agreement with this notion, selective depletion of HSCs but not MPPs or later progenitors by expression of diphtheria toxin under the control of the stem cell leukaemia (*Scl)3'* enhancer [484] did not impair the haematopoietic response to the inflammatory cytokine G-CSF, but did hamper reconstitution after 5-FU injection, which depletes the progenitor compartment [12]. A similar approach could be adopted in SpA or other models of

chronic inflammation to determine whether HSCs are required for the haematopoietic phenotype I describe.

As a further possible contributor to population expansion, I show that expression of annexin V and Fas was decreased among LSK cells, suggesting the rate of apoptosis may be decreased. Various knockout models reveal that regulation of apoptosis is important for maintenance of the LSK compartment under homeostatic conditions [485-487], and a recent study revealed that TNF-α prevents necroptosis in HSCs [488]. It is therefore possible that an important effect of inflammation is to prevent cell death in the LSK compartment, permitting the observed population expansions. This hypothesis could be investigated further using small molecule caspase inhibitors or activators in murine SpA, or with mice lacking key members of cell death pathways.

3.3.2 Lineage bias

In other models, enhanced myelopoiesis during chronic inflammation is attributed to a number of effects, including 1) early adoption of myeloid transcriptional signatures in primitive HSCs, producing a lineage-instructive effect among their progeny [247, 251], 2) selective expansion of myeloid-biased MPP3 subsets [79, 252], 3) diversion of the output of bipotent lymphoid/myeloid progenitors, MPP4s or LMPPs, towards myeloid output at the expense of lymphoid [79, 253], and 4) increased proliferation or decreased apoptosis of GMPs [232-234, 489].

In SpA, I found that myeloid-biased MPP3s were expanded, which would presumably lead to an increased rate of formation of GMPs. However, others have reported that GMPs may also acquire the capacity to self-renew when exposed to

inflammatory signals like G-CSF and IL-1β, which cause aberrant expression of β-catenin to suppress further differentiation [234]. This raises the possibility that expansion of the GMP pool is not entirely dependent on increased input from MPPs but could also be attributable to direct expansion of the existing GMP pool. Additionally, I found that GMPs had a decreased rate of apoptosis in SpA while continuing to proliferate at a normal rate, which may contribute to population expansion. I suggest the decreased apoptosis of GMPs could be mediated by the same switch in transcription factor usage from C/EBP-α to C/EBP-β as is also described in emergency granulopoiesis (see **section 1.2.1**) because GM-CSF, which is known to cause this effect [489], is also increased in mice with SpA [441].

Contrary to GMPs, the number of erythroid progenitors was decreased in SpA, which was associated with decreased expression of proliferation markers *in vivo* and reduced capacity to generate cells when cultured *ex vivo*. Collectively, these data on lineage-committed progenitors reveal interesting differences in activity that probably contribute to the overall lineage bias in BM of mice with SpA, which is discussed further in **chapter 5**.

3.3.3 Extramedullary haematopoiesis

Development of SpA was associated with marked splenomegaly; the spleen contained increased numbers of both myeloid and erythroid progenitors. In murine models of atherosclerosis, monocytes generated in the spleen preferentially accumulate in inflamed plaque lesions [216]. I suggest myeloid cells produced in the spleen in SpA could also be entering the paws and small intestine, but I have not determined the relative importance of myeloid output from BM and spleen by performing splenectomies after SpA is induced. Additionally, I noted the

accumulation of erythroid progenitors in the spleen which, unlike their counterparts in the BM, had undimmed expression of Ki67 with SpA. The high proliferative rate undaunted by inflammation and the low rate of apoptosis are characteristic features of 'stress BFU-Es' (see **section 1.2.2**), which are derived from MPPs in the spleen under the influence of BMP4, EPO, and hypoxia [236]. However, in common with other models of chronic inflammation, emergence of stress erythropoiesis in the spleen was insufficient to compensate for loss of BM erythropoiesis, meaning that mice with SpA developed anaemia.

Finally, I observed a population of cells with the phenotypic and functional properties of GMPs in the inflamed joints of mice with SpA. The origin of these cells is not proven but we demonstrated previously that GMPs injected intravenously into mice developing SpA can home to the joints [441], suggesting GMPs may migrate from BM or spleen to this site. Importantly, we showed that these cells fulfil functional definitions of progenitors by observing colony formation and expansion in liquid culture, and, in previous work in our laboratory, we also confirmed considerable overlap in the transcriptome of GMPs from joints and BM by RNA sequencing (data not shown). As with other examples of *in situ* haematopoiesis, it is difficult to state whether local generation of mature cells makes an important contribution when compared to the output of the BM. In quantitative terms, the number of GMPs in BM far exceeds that in the joints, and I found that the total number of cells generated per BM GMP was greater in *ex vivo* liquid culture than per joint GMP. However, in murine atherosclerosis, monocytes generated outside the BM had a more inflammatory phenotype than those emanating from BM [216]. Therefore, although I have not investigated it to date, myeloid cells deriving from

GMPs in the joints could be qualitatively different from those delivered in the blood, possibly affecting the progression of disease.

3.4 Conclusions

- Curdlan injection in SKG mice produces a consistent phenotype of inflammatory arthritis that closely resembles human SpA.
- Arthritis is associated with accumulation of mature myeloid cells in inflamed joints, indicating demand for myeloid cells is increased.
- Haematopoietic stem cells from mice with SpA have a quiescent phenotype but have decreased reconstitution potential when transplanted.
- There is marked lineage bias in the BM of mice with SpA; contraction of the erythroid population is associated with decreased proliferation of committed erythroid progenitors.
- Extramedullary haematopoiesis is expanded with SpA but the importance of this phenomenon in disease progression is unclear.

4 Type 2 cytokines influence haematopoiesis in SpA

4.1 Introduction

Spondyloarthritis in humans is frequently described as an archetypal type 17 immune response [413, 414], which is associated with increased frequencies of IL-17A producing $CD4^+$ T cells and γδ T cells in blood [407, 408] and increased serum and synovial fluid concentrations of IL-17 and IL-22 [406]. In SKG mice, previous studies have also revealed that SpA is prevented by injection of anti-IL-23 antibodies [437] and ameliorated by crossing onto a strain deficient in IL-17 [395]. However, in the inflamed small intestine of people with AS, macrophages have an alternatively activated phenotype [440], and there was increased expression of the genes encoding IL-4 and IL-5 in mucosal biopsies [439]. This suggests multiple immune modules are active in SpA, but it remains unclear whether concurrent type 2 responses could be contributing to the development of disease or counteracting the inflammatory response by promoting repair or fibrosis, as described in other forms of chronic inflammation [280]. I therefore aimed to investigate whether concurrent immune modules were apparent in mice with SpA in different locations or at different stages of disease, and whether a type 2 immune module might have a broadly pro- or anti-inflammatory role.

In **chapter 3**, I observed that a major pathological feature of SpA was accumulation of mature myeloid cells in the inflamed sites, which was associated with expanded BM and extramedullary myelopoiesis. Previous studies have suggested type 2 cytokines may affect myelopoiesis, with IL-4 reported to increase formation of neutrophil colonies (CFU-G) when combined with G-CSF [299] but to promote macrophage colony formation (CFU-M and GM) when combined with SCF

[305]. Consistent with these *ex vivo* findings, mice deficient in IL-4 had decreased formation of CFU-GM and mixed CFU-GEMM colonies [306]. Additionally, IL-5 has a well-known role in promoting eosinopoiesis [490, 491] through its effects on dedicated IL-5Rα$^+$ eosinophil progenitors (EoPs).

In this section, I sought to bring these areas of investigation together by asking whether a putative type 2 immune module developing in SpA might modulate haematopoiesis to facilitate formation of the myeloid cells that infiltrate the inflamed sites. Therefore, the aims of this chapter were:

1. To investigate the nature of the immune modules occurring in mice with SpA in different locations.
2. To investigate how the type 2 cytokines IL-4 and IL-5 modulate haematopoiesis and disease progression during SpA.

4.2 Results

4.2.1 SpA in SKG mice is associated with different immune modules

First, I examined the cytokine production of CD4$^+$ T cells in the paw, small intestine, and their respective popliteal and mesenteric draining lymph nodes. In the paw, small intestine, and popliteal lymph nodes of mice with SpA, IL-17A-producing cells were more frequent than those producing other cytokines, expressed as a proportion of all CD4$^+$ T cells or as the absolute number of cells (**Fig. 4.1A-B**). The number of these Th17 T cells was increased in all three tissues with SpA compared to healthy mice. However, in the mesenteric lymph nodes, IL-4 producing T cells were more abundant than those producing other cytokines, and the numbers of cells producing IL-4, IL-5, or GM-CSF were increased with SpA (**Fig. 4.1A-B**). This increase in IL-4$^+$ T cells was detectable one week after curdlan

injection (**Fig. 4.1C**), before the onset of gross enteritis. Importantly, I found approximately one third of IL-4 producing T cells co-expressed GM-CSF (**Fig. 4.2A**), whereas approximately two thirds co-expressed TNF-α (**Fig. 4.2B**), suggesting these cells were still contributing to the inflammatory response. Finally, I found that IL-4 was detectable by ELISA in explants of small intestine derived from healthy mice or those with SpA (**Fig. 4.2C**) but could not be detected in explants of paw tissue or in serum (data not shown). Collectively, this suggested immune responses occurring simultaneously in different lymphoid tissues had different signatures, recapitulating the pattern observed in people with AS.

Figure 4.1

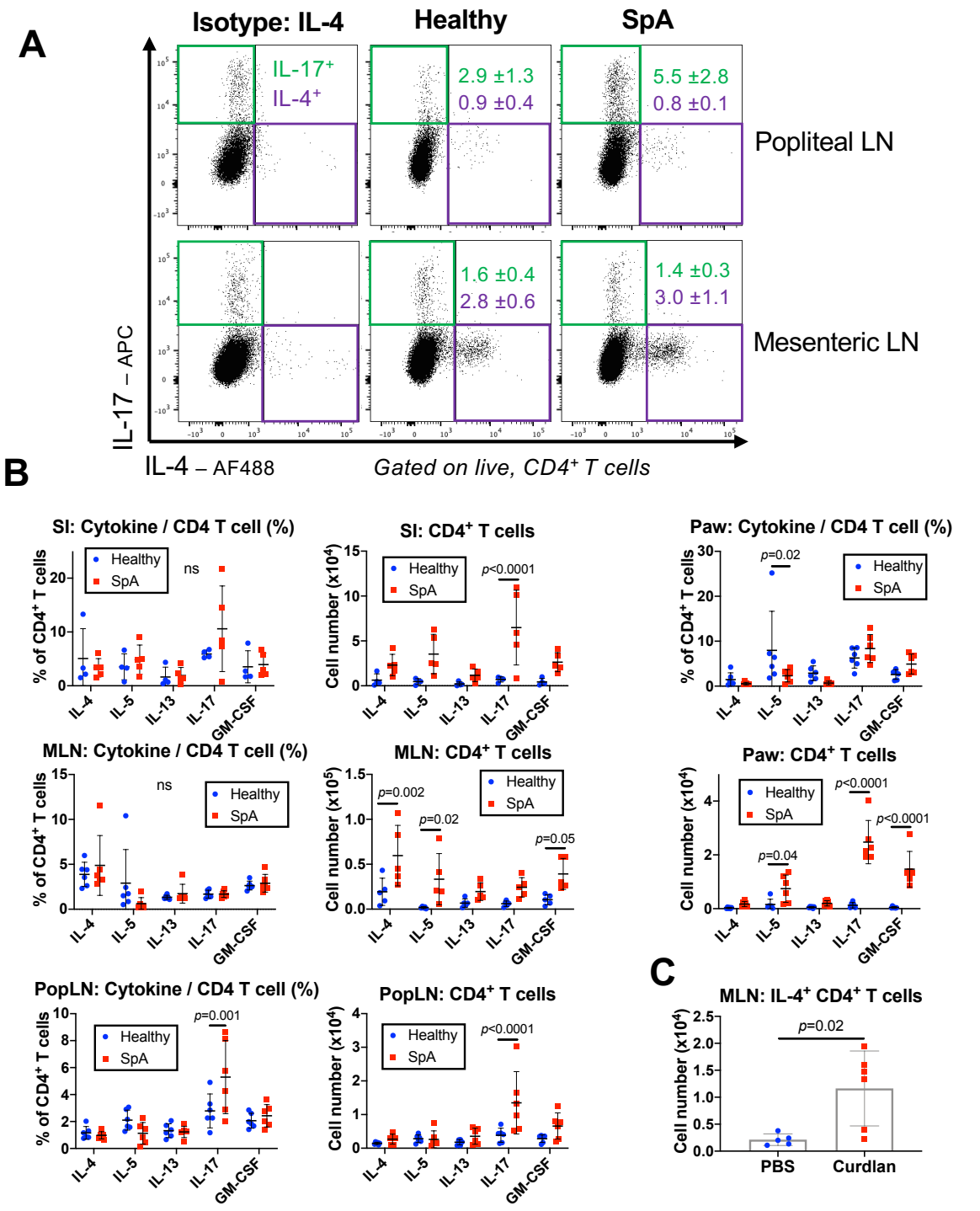

Figure 4.1: A type 2 immune module exists in the intestine of mice with SpA
(**A**) Representative flow cytometric images of expression of indicated cytokines among CD4+ T cells from the popliteal (Top) and mesenteric (Bottom) lymph nodes (LN). Figures show mean and SD frequency for n=6 mice per group among CD4+ T cells in healthy mice and mice with SpA.
(**B**) Frequency and absolute number of CD4+ T cells expressing indicated cytokines in indicated tissues. Points represent individual mice with mean and SD, two-way ANOVA with Sidak's test.
(**C**) Number of IL-4+ CD4+ T cells in mesenteric lymph nodes (MLN) of healthy mice and mice 1 week after curdlan injection. Points represent individual mice with mean and SD, Mann-Whitney U test.

Data representative of 2 (**C**) or 3 (**A**)-(**B**) independent experiments.

Figure 4.2

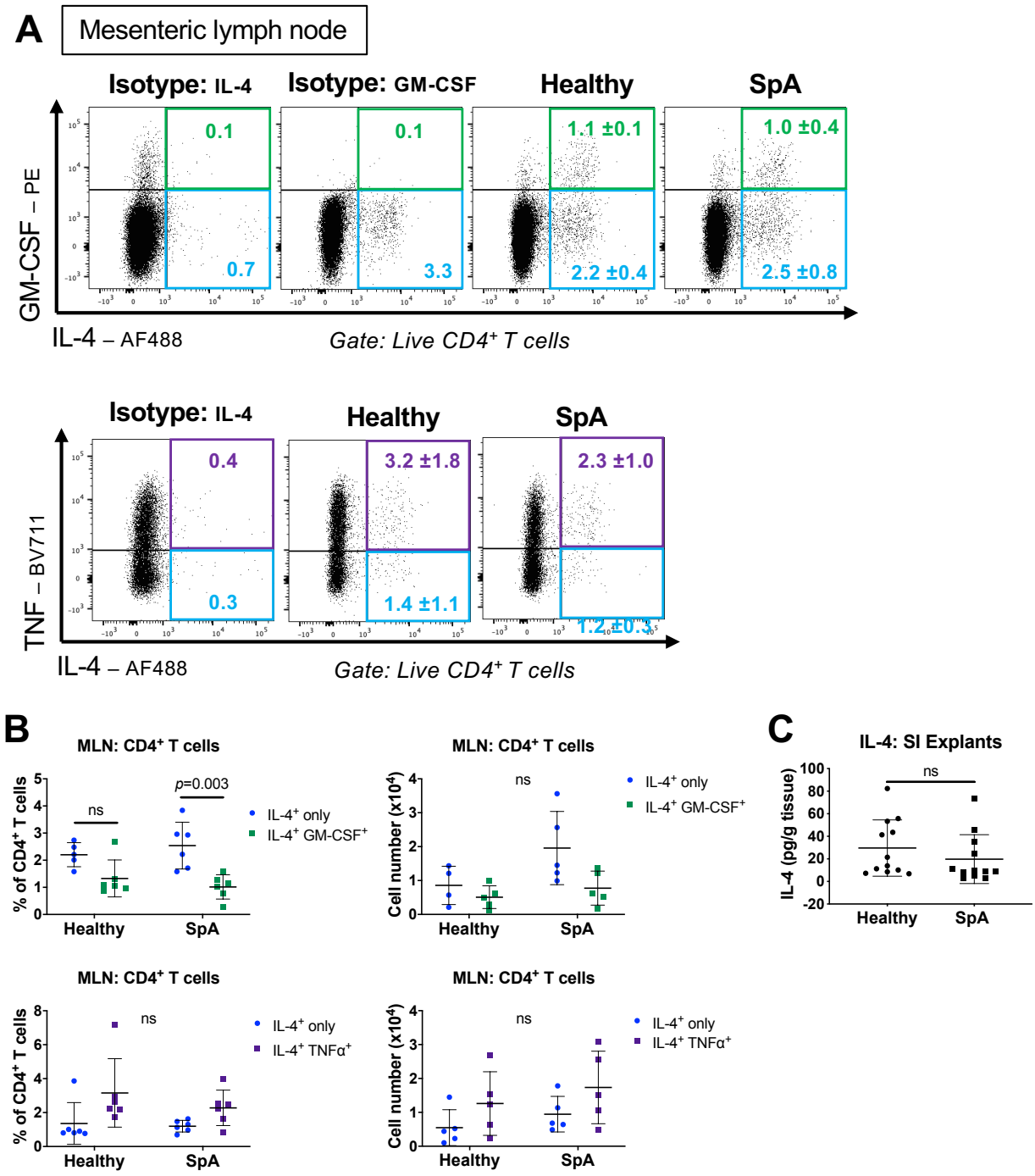

Figure 4.2: IL-4⁺ T cells also produce pro-inflammatory cytokines
(**A**) Representative flow cytometric images of expression of indicated cytokines among CD4⁺ T cells from the mesenteric lymph nodes. Figures show mean and SD frequency for n=6 mice per group among CD4⁺ T cells in healthy mice and mice with SpA, 4 weeks after curdlan injection.
(**B**) Frequency and absolute number of CD4⁺ T cells expressing indicated cytokines in mesenteric lymph nodes (MLN). Points represent individual mice with mean and SD, two-way ANOVA with Sidak's test.
(**C**) Concentration of IL-4 measured by ELISA in supernatants of small intestinal explants obtained from healthy mice and mice with SpA and cultured overnight. Concentration normalised to weight of tissue. Points represent individual mice with mean and SD, Mann-Whitney U test.

Data representative of 3 independent experiments (**A**)-(**B**) or pooled from 2 experiments (**C**).

4.2.2 HSPCs express receptors for type 2 cytokines

My description of SpA revealed a preponderance of mature myeloid cells infiltrating the inflamed tissues, with related expansion of myelopoiesis in the BM, spleen, and inflamed paws. Therefore, I asked whether a type 2 immune module in SpA, characterised by increased numbers of IL-4 and IL-5 producing cells in the mesenteric lymph nodes, could be contributing to disease progression through an effect on medullary and/or extramedullary haematopoiesis.

To investigate this, I first asked whether the receptors for these or other type 2 cytokines were expressed on HSPCs in BM. Using RNA sequencing data generated previously in our own laboratory or available from a previous publication [476], I found the genes encoding the specific alpha chain of the IL-4 receptor (*Il4ra*, CD124), as well as the shared common gamma chain (*Il2rg*) were both highly expressed on all LSK populations (i.e. primitive HSCs and MPPs), and on myeloid progenitors (GMPs) and mature myeloid cells (neutrophils and eosinophils) (**Fig. 4.3A-B**). Conversely, *Il4ra* was not expressed on erythroid progenitors (CFU-Es). In contrast, the genes encoding the specific receptors for IL-5 (*Il5ra*), IL-9 (*Il9r*), and IL-13 (*Il13ra1*) were expressed at very low levels by all HSPCs, although *Il5ra* expression increased progressively with commitment to the myeloid lineage, presumably because some cells destined to become eosinophil progenitors would have been included in this group. Among HSPCs, I found the IL-4 receptor (CD124) was most highly expressed on primitive HSCs by flow cytometry but was not detectable on most MPP subsets or on any lineage-committed progenitors using this technique (**Fig. 4.3C**).

In addition to the expression of cytokine receptors, I wished to know whether HSPCs from mice with SpA showed evidence of responsiveness to type 2 and other

cytokines. To investigate this, I took previously-generated RNA sequencing data from HSPC populations sorted from healthy SKG mice or mice with SpA [441] and used gene-set enrichment analysis (GSEA) to ask whether SpA produced transcriptomic signatures in these cells associated with particular cytokines. Using this approach, I found significant enrichment for gene sets associated with several cytokines of known importance in the SKG model in HSCs from mice with SpA (GM-CSF, IL-1β, and IL-6), but also found significant enrichment for a signature associated with IL-4 in the same cells (**Fig. 4.3D**).

Figure 4.3

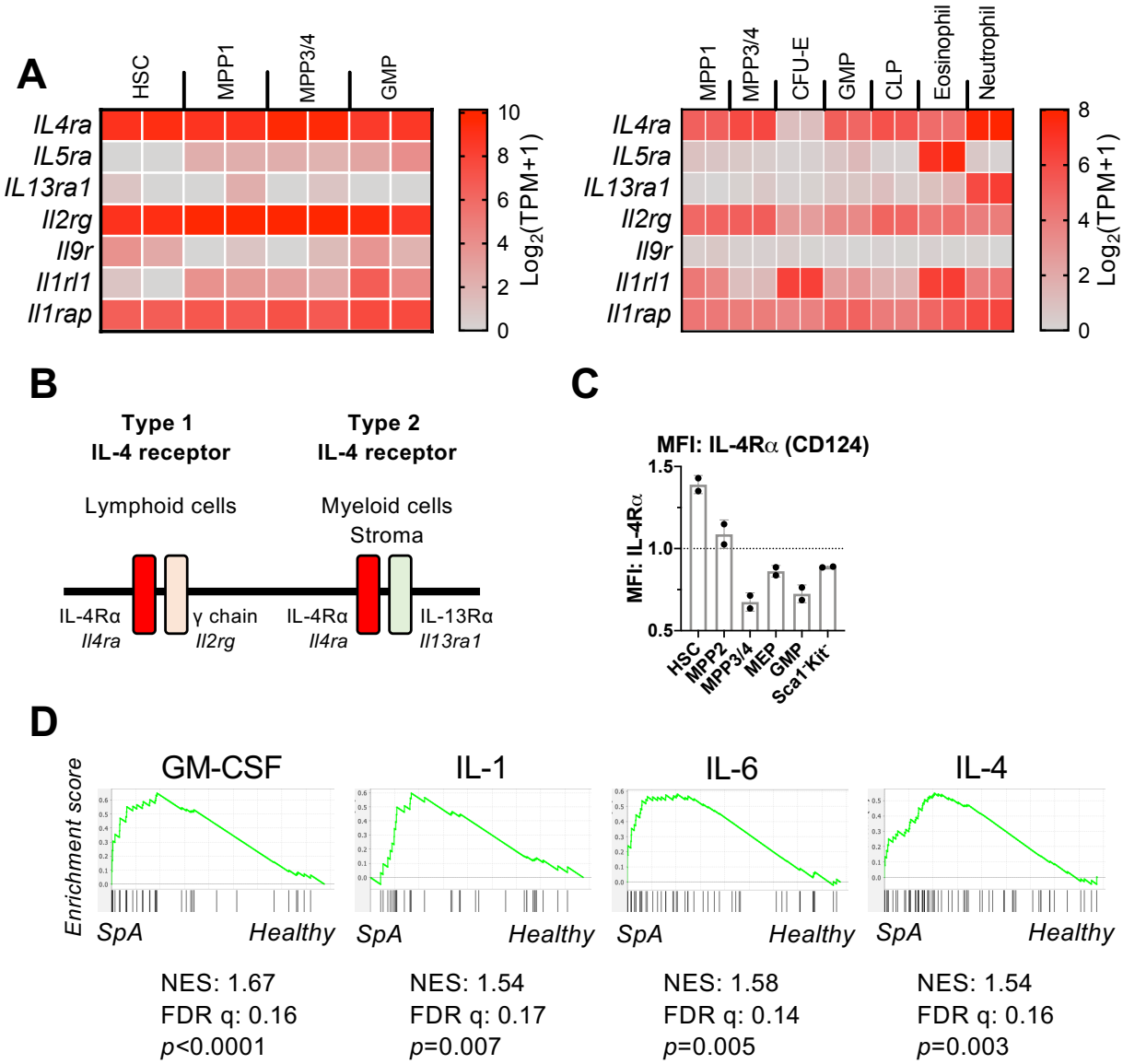

Figure 4.3: The IL-4 receptor is expressed on HSPCs
(**A**) Heatmap showing expression of mRNA encoding indicated genes in indicated HSPC populations by RNA sequencing, in transcripts per million (TPM). HSC: haematopoietic stem cell, MPP: multipotent progenitor, GMP: granulocyte macrophage progenitor, CFU-E: colony-forming unit erythroid, CLP: common lymphoid progenitor. Data derived from RNA sequencing of FACS-sorted populations from our laboratory (Left) or previously published data (Right). Columns represent biological replicates. Data from [473].
(**B**) Schematic diagram showing composition of the known receptors for IL-4, with their component protein genes and genes.
(**C**) Median fluorescence intensity (MFI) of expression of the IL-4Rα chain (CD124) on indicated HSPC populations by flow cytometry, normalised to fluorescence minus one control. Points represent individual mice with mean and SD. MEP: megakaryoid/erythroid progenitor.
(**D**) Enrichment plots showing significant enrichment of sets of genes upregulated by indicated cytokines among those genes also upregulated in RNA sequencing analysis of HSCs from mice with SpA compared to healthy mice. NES: normalised enrichment score; FDR: false discovery rate. Figures generated with Gene Set Enrichment Analysis (GSEA) software.

Data representative of 2 independent experiments (**C**).

4.2.3 Interleukin-5 is not required for development of SpA

The gene encoding the receptor for IL-5 was not expressed on LSK cells and was expressed at low levels on myeloid progenitors. To determine whether it played any role in the development of SpA and its associated haematopoietic changes, I injected mice with anti-IL-5 antibodies or isotype over 4-5 weeks after injecting curdlan. Despite effectively depleting eosinophils from the BM, paws, and small intestine (**Fig. 4.4A**), this treatment had no impact on the severity of clinical disease, as assessed by clinical score, changes in bodyweight, or changes in the size of the paws and tarsi (**Fig. 4.4B**). Similarly, anti-IL-5 treatment did not ameliorate neutrophil accumulation in the BM, paws, or small intestine compared to isotype-treated mice (**Fig. 4.4C**). In the BM however, anti-IL-5 treatment did partially alleviate the SpA-induced expansion of LSK and GMP cells, suggesting IL-5 could be a factor driving the observed accumulation of these cells during disease (**Fig. 4.4D-E**). Taken together, these data showed that eosinophils and IL-5, whether acting locally in the gut or distantly in the BM, were dispensable for development of all major clinical features of SpA, but IL-5 was implicated in the expansion of LSK and GMP cells. I suspect the latter changes could be attributable to an effect of IL-5 to increase formation of eosinophils during SpA, even though these cells appear to have little role in disease.

Figure 4.4

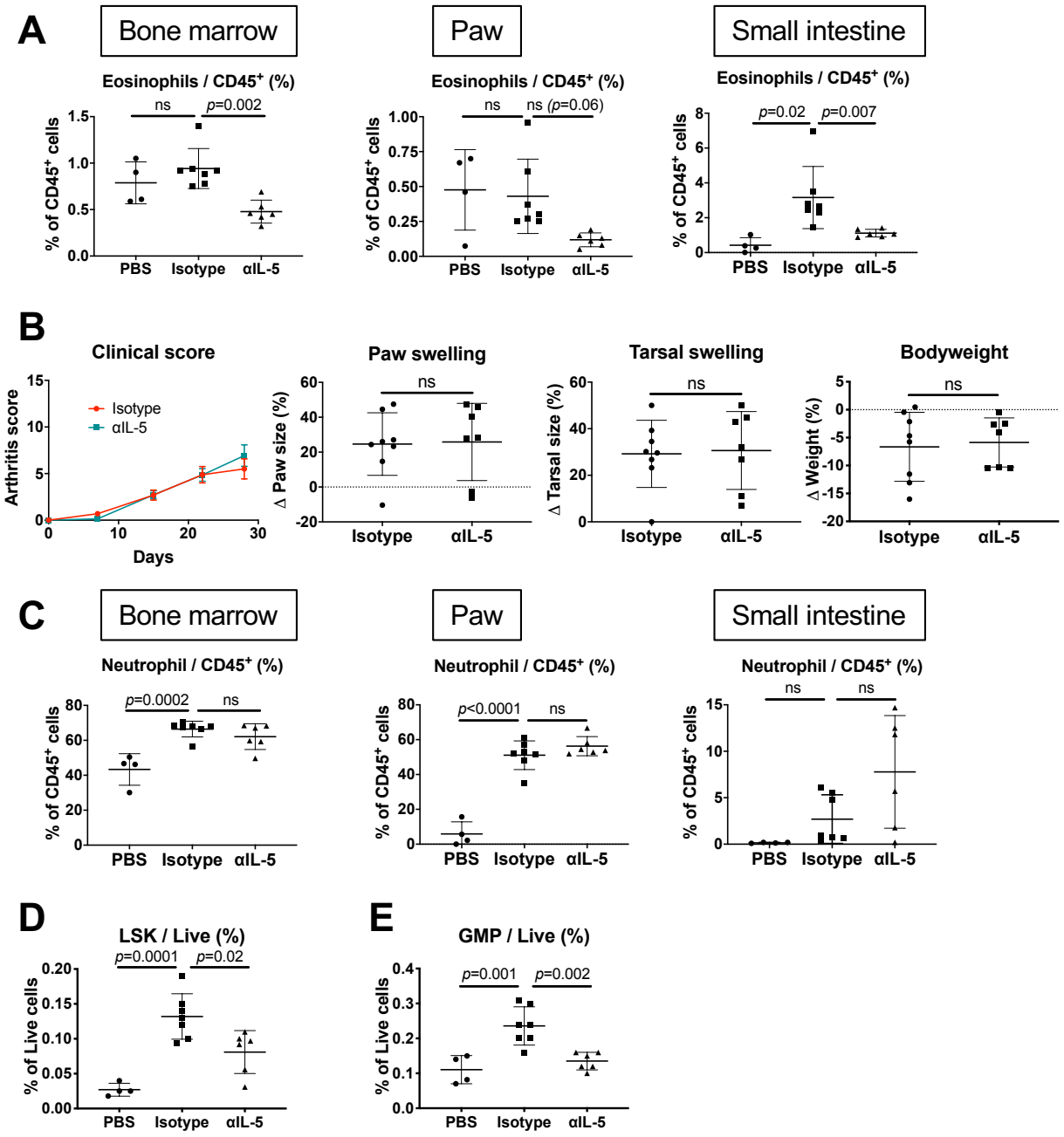

Figure 4.4: IL-5 is dispensable for development of murine SpA
(**A**) Frequency of eosinophils among CD45⁺ leukocytes in indicated tissues in PBS-injected mice and mice with SpA injected with either anti-IL-5 antibodies or isotype over 4 weeks. Points represent individual mice with mean and SD, one-way ANOVA with Tukey's test.
(**B**) Clinical arthritis score (Left) and changes in paw swelling, tarsal swelling, and bodyweight (Right). Left: Points represent mean with SD for n=7 mice per group, two-way ANOVA; Right: points represent individual mice with mean and SD, Mann-Whitney U test.
(**C**) Frequency of neutrophils among CD45⁺ leukocytes from indicated tissues.
(**D**) Frequency of LSK cells among total live BM cells.
(**E**) Frequency of GMPs among total live BM cells.
For (**C**)-(**E**), points represent individual mice with mean and SD, one-way ANOVA with Tukey's test.

Data from a single experiment.

4.2.4 Interleukin-4 promotes myelopoiesis

Having largely discounted IL-5 as an important cytokine promoting disease or haematopoietic changes in SpA, I focused on the role of IL-4. I had found that the IL-4 receptor was expressed on HSCs and I found HSCs from mice with SpA had a transcriptomic signature associated with response to IL-4. I also showed IL-4 was produced in the mesenteric lymph nodes and small intestine of mice with SpA and, even though any IL-4 in plasma was below the limit of detection of an ELISA assay, I hypothesised that it might still have a biological effect on haematopoiesis because the affinity of the IL-4 receptor for its ligand is high. I began by asking what effect IL-4 might have on HSPCs in an attempt to clarify previous reports that have described multiple, sometimes contradictory, roles for IL-4 in haematopoiesis. When I plated whole BM in methylcellulose medium supplemented with haematopoietic factors, addition of IL-4 decreased the total number of colonies formed compared to control conditions (**Fig. 4.5A**). Of these colonies, there was a lower number of CFU-G and CFU-GM colonies with IL-4 and a greater number of CFU-M colonies, indicating IL-4 favoured the formation of myeloid colonies with monocyte/dendritic cell potential at the expense of those forming granulocytes under these conditions (**Fig. 4.5A**). There was no significant difference in the formation of erythroid, megakaryoid, or mixed colonies. I obtained similar results when repeating these assays using LSK cells sorted from BM, indicating the effect was not dependent on the presence of mature BM cells, such as $CD4^+$ T cells, which have confounded previous investigations of this type (**Fig. 4.5B**).

Figure 4.5

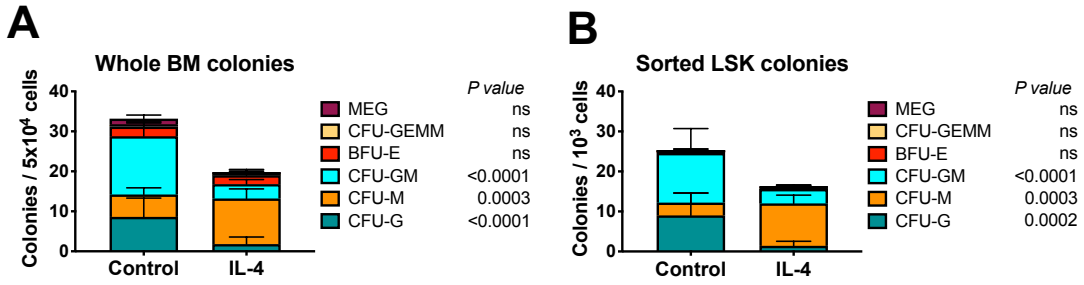

Figure 4.5: IL-4 decreases total colony formation but promotes monocytes
(**A**) Number of colonies derived from $5x10^4$ total BM cells plated in methylcellulose medium for 10 days, with or without IL-4. MEG: megakaryocyte colony, CFU-GEMM: colony forming unit – granulocyte erythroid myeloid megakaryocyte, BFU-E: blast-forming unit erythroid, CFU-GM: colony forming unit granulocyte macrophage, CFU-M: colony forming unit macrophage, CFU-G: colony forming unit granulocyte.
(**B**) Number of colonies derived from 10^3 LSK cells sorted by FACS then plated in methylcellulose medium with or without IL-4 for 10 days.
For (**A**)-(**B**), bars show mean and SD for 5 replicates, two-way ANOVA with Sidak's test.

Data representative of 2 independent experiments (**A**)-(**B**).

In liquid culture of sorted HSCs, addition of IL-4 had no effect on total cell number (**Fig. 4.6A**) but caused a striking increase in the proportion of live cells committed to the myeloid lineage (i.e. expressing CD11b) after 7 days, with particular increases in the frequencies of cells with the surface phenotype of monocytes ($CD11b^+$, $CD115^+$) (**Fig. 4.6B-C**). Prior to expression of CD11b, there was a considerable increase in expression of CD16/32 (FcγRII/III), which is chiefly expressed by myeloid cells, after 3 days (**Fig. 4.7A**), suggesting bias towards myeloid cell production was an early event in these cultures.

Figure 4.6

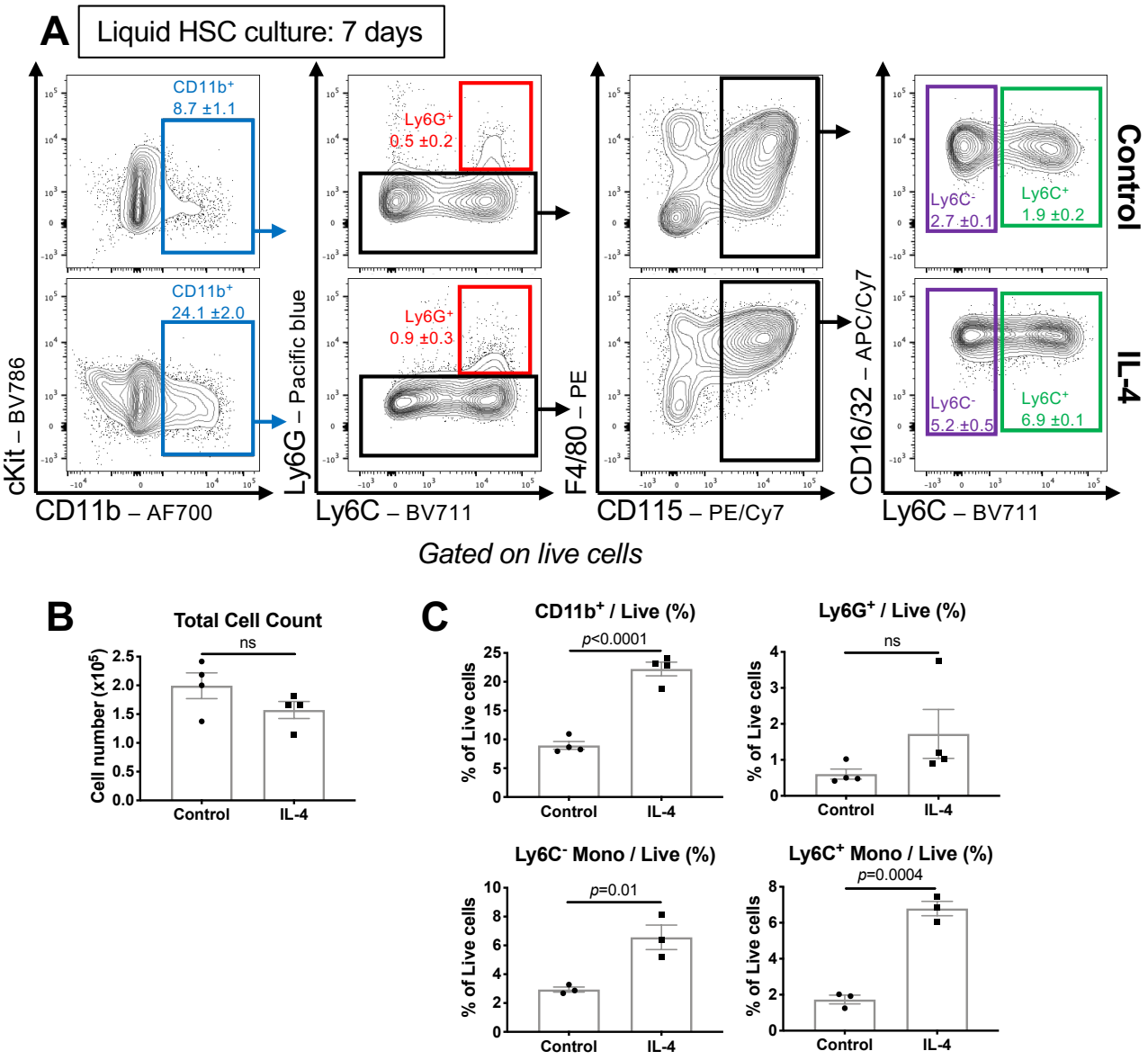

Figure 4.6: IL-4 promotes myelopoiesis *ex vivo* (I)
(**A**) Representative flow cytometric images of cells derived from culture of FACS-sorted HSCs after 7 days in medium with haematopoietic cytokines, with or without IL-4. Figures show mean frequencies of cells with SD among total live cells for technical triplicates of a single experiment.
(**B**) Total number of cells derived from culture described in (**A**).
(**C**) Frequency of indicated cell types illustrated in (**A**) among total live cells.
For (**B**) and (**C**), points represent mean of triplicates in independent experiments with mean and standard error, Mann-Whitney U test.

Data representative of (**A**) or show results of (**B**)-(**C**) 3 independent experiments.

To separate the possible effects of IL-4 on proliferation and differentiation, I performed similar assays with single sorted cells, finding that IL-4 decreased the total output derived from single cells, just as it had decreased the number of colonies derived from BM cells in methylcellulose medium (**Fig. 4.7B-C**). Among the cell output, there was again a significant increase in the frequency of monocyte cells, but, in contrast to bulk liquid cultures, this occurred at the expense of neutrophils ($CD11b^+$, $Ly6G^+$) (**Fig. 4.7C**). Taken together, these *ex vivo* assays showed that IL-4 decreased the proliferation and colony-forming efficiency of HSCs and caused a bias towards monocytic myeloid cells, at the expense of granulocytes. Because IL-4 could be acting at multiple points in the haematopoietic system, I completed similar assays for downstream MPP2/3s and GMPs that were also sorted by FACS from the BM. In bulk cultures of MPP2/3s, IL-4 did not affect the total cell yield (**Fig. 4.8A**) and produced only a slight increase in the proportion of cells expressing CD11b (**Fig. 4.8B**). With sorted GMPs, IL-4 decreased the cell yield (**Fig. 4.8C**) and also decreased the proportion of cells expressing CD11b and the proportion with phenotypes of monocytes or neutrophils (**Fig. 4.8D**). Collectively, this suggested the major actions of IL-4 among HSPCs were directed at HSCs, as might be expected from their greater expression of the receptor protein (**Fig. 4.3B**). Among these cells, IL-4 seemed to promote early myeloid differentiation at the expense of self-renewal.

Figure 4.7

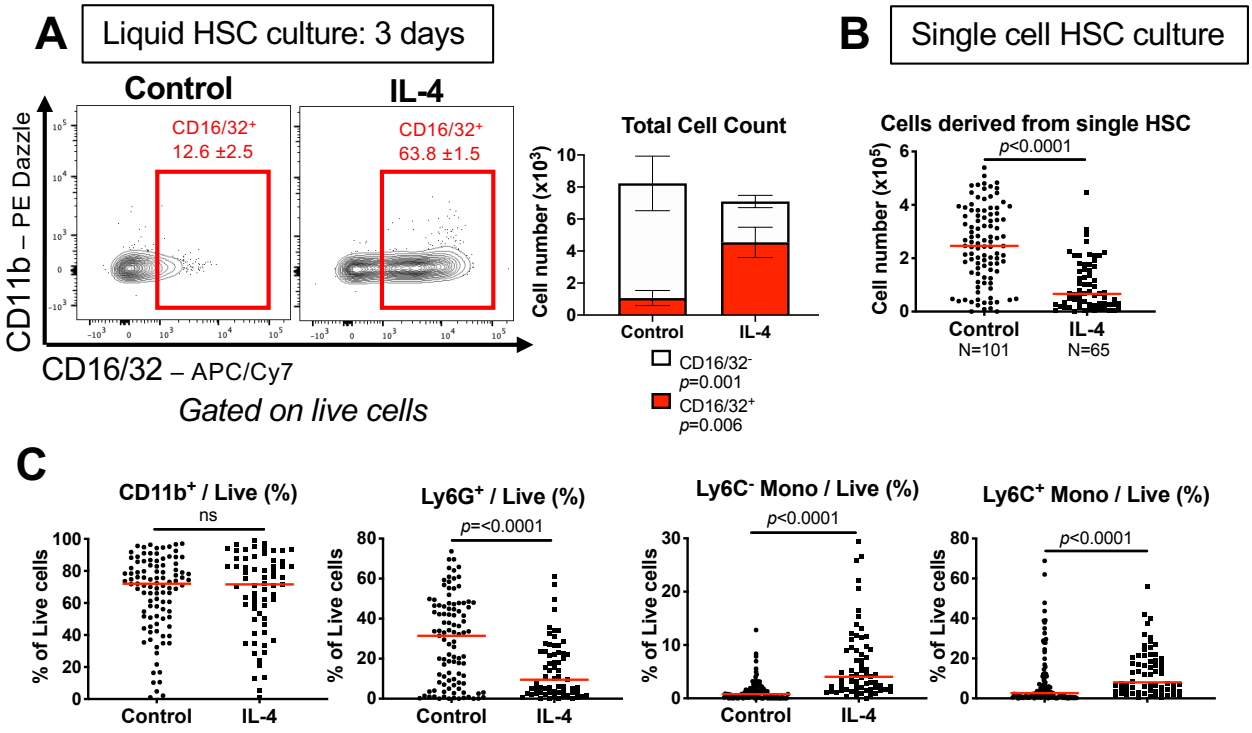

Figure 4.7: IL-4 promotes myelopoiesis *ex vivo* (II)
(**A**) (Left) Representative flow cytometric images of cells derived from HSCs cultured for 3 days with or without IL-4. Figures show mean frequencies with SD among total live cells for technical triplicates of a single experiment. (Right) Number of cells of types indicated. Mean and SD of technical triplicates, two-way ANOVA with Sidak's test.
(**B**) Number of cells derived from single HSCs sorted by FACS from BM and cultured for 10 days with haematopoietic cytokines, with or without IL-4. Points represent individual cells with median (red line), Mann-Whitney U test.
(**C**) Frequency of indicated cell types among total live cells derived from single HSCs. Points represent individual cells with median (red line), Mann-Whitney U test.

Data representative of 2 (**A**) or pooled from 4 (**B**)-(**C**) independent experiments.

Figure 4.8

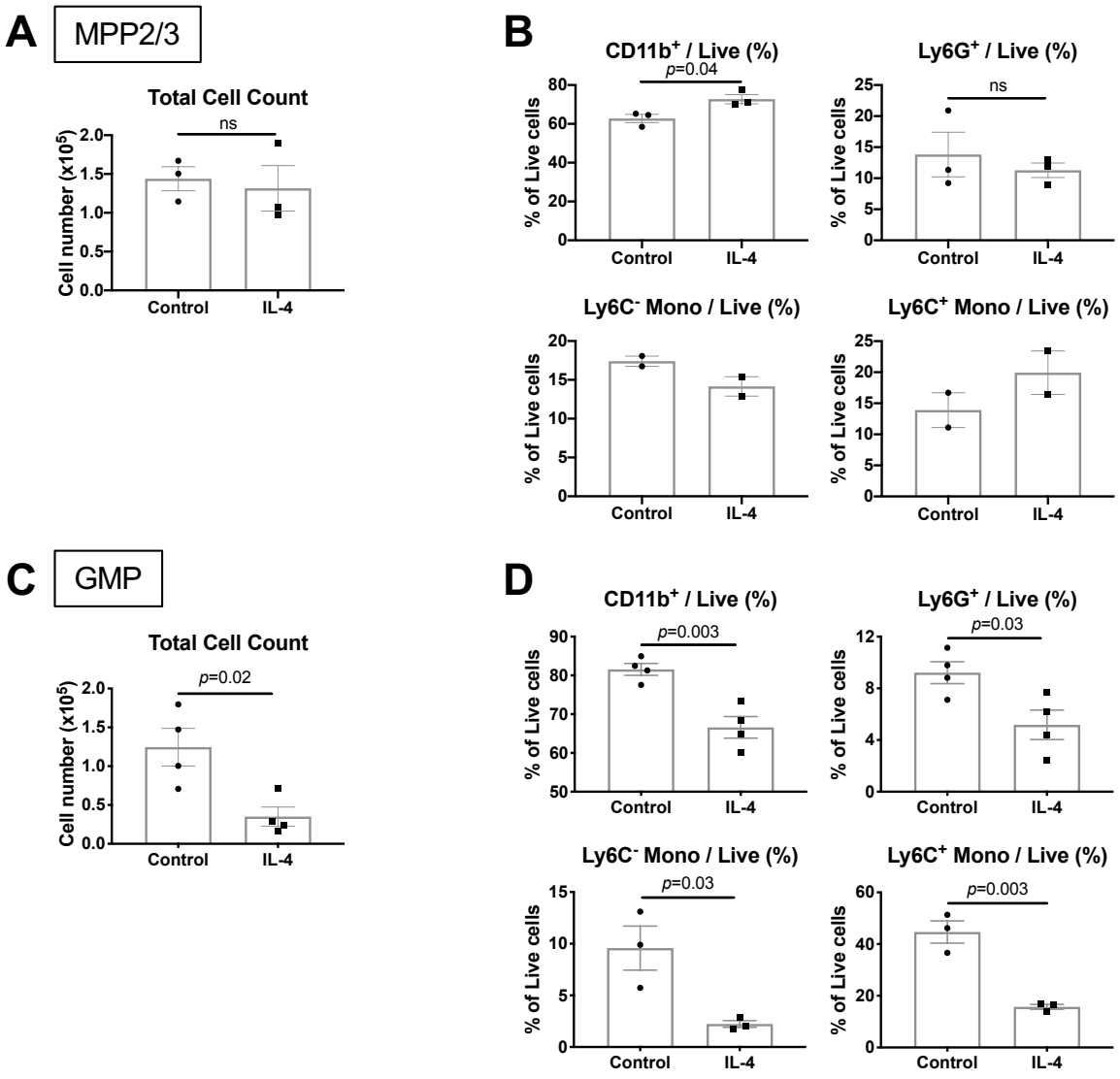

Figure 4.8: MPPs are insensitive to the effect of IL-4 *ex vivo*
(**A**) Total number of cells derived from culture of FACS-sorted MPP2/3 cells for 7 days in medium with haematopoietic cytokines, with or without IL-4.
(**B**) Frequency of indicated cell types among total live cells derived from culture of MPP2/3s.
(**C**) Total number of cells derived from culture of FACS-sorted GMP cells for 4 days in medium with haematopoietic cytokines, with or without IL-4.
(**D**) Frequency of indicated cell types among total live cells derived from culture of GMPs.
For (**A**)-(**D**), points represent mean of technical triplicates from independent experiments with mean and standard error, Mann-Whitney U test.

Graphs show results of 3 independent experiments.

To determine whether IL-4 would exert a similar effect on HSPCs *in vivo*, I injected a mixed IL-4 and anti-IL-4 antibody complex, intended to prolong the half-life of the cytokine [314, 448], into wild type C57BL/6 mice, before culling after one week. This treatment did not affect the total BM cellularity (**Fig. 4.9A**), nor the frequency or absolute number of the most primitive HSCs (**Fig. 4.9B**). However, treatment with IL-4 did cause expansion of the myeloerythroid MPP2 subset, and of the MPP4 (LMPP) subset that has the potential to produce lymphoid or myeloid cells according to demand (**Fig. 4.9C**). Strikingly, IL-4 caused the same upregulation of CD16/32 among HSCs as was observed in liquid culture (**Fig. 4.9D**), suggesting the lineage bias of HSCs was altered towards myelopoiesis. Assessing haematopoiesis downstream of the LSK cells, I found further evidence of myeloid bias caused by IL-4, with increased frequency and absolute number of GMPs (**Fig. 4.10A**) and of the common monocyte progenitor (cMoP, LK, CD16/32^{+}, Ly6C^{+}, CD115^{+}) (**Fig. 4.10B**). In line with this, when BM from control or IL-4 injected mice was plated in methylcellulose medium without any additional cytokines, I observed a similar bias in the type of myeloid colonies formed as had been seen with *ex vivo* exposure to IL-4: decreased frequency of CFU-G and -GM and increased frequency of CFU-M (**Fig. 4.10C**). In contrast to its effect on myelopoiesis, IL-4 caused a significant reduction in the number and frequency of erythroid pre-CFU-E progenitors but not of the more numerous CFU-Es (**Fig. 4.10D**).

Figure 4.9

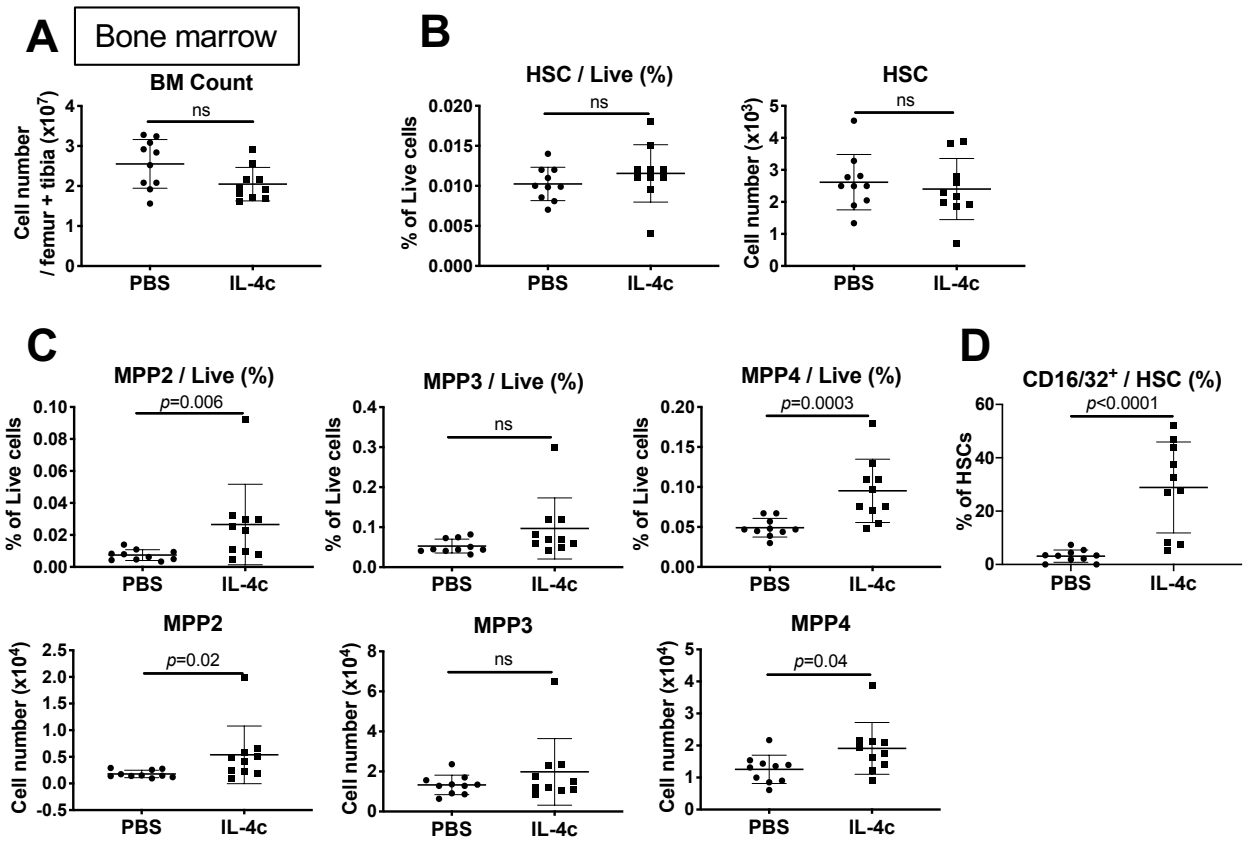

Figure 4.9: Injection of IL-4 affects the LSK compartment *in vivo*
(**A**) Total number of BM cells in 1 femur and 1 tibia from mice injected with PBS or IL-4 + anti-IL-4 complexes for 1 week.
(**B**) Frequency and absolute number of HSCs in BM.
(**C**) Frequency and absolute number of indicated cell populations in BM.
(**D**) Frequency of HSCs expressing CD16/32 in BM.
For (**A**)-(**D**), points represent individual mice with mean and SD, Mann-Whitney U test.

Data pooled from 2 independent experiments.

Figure 4.10

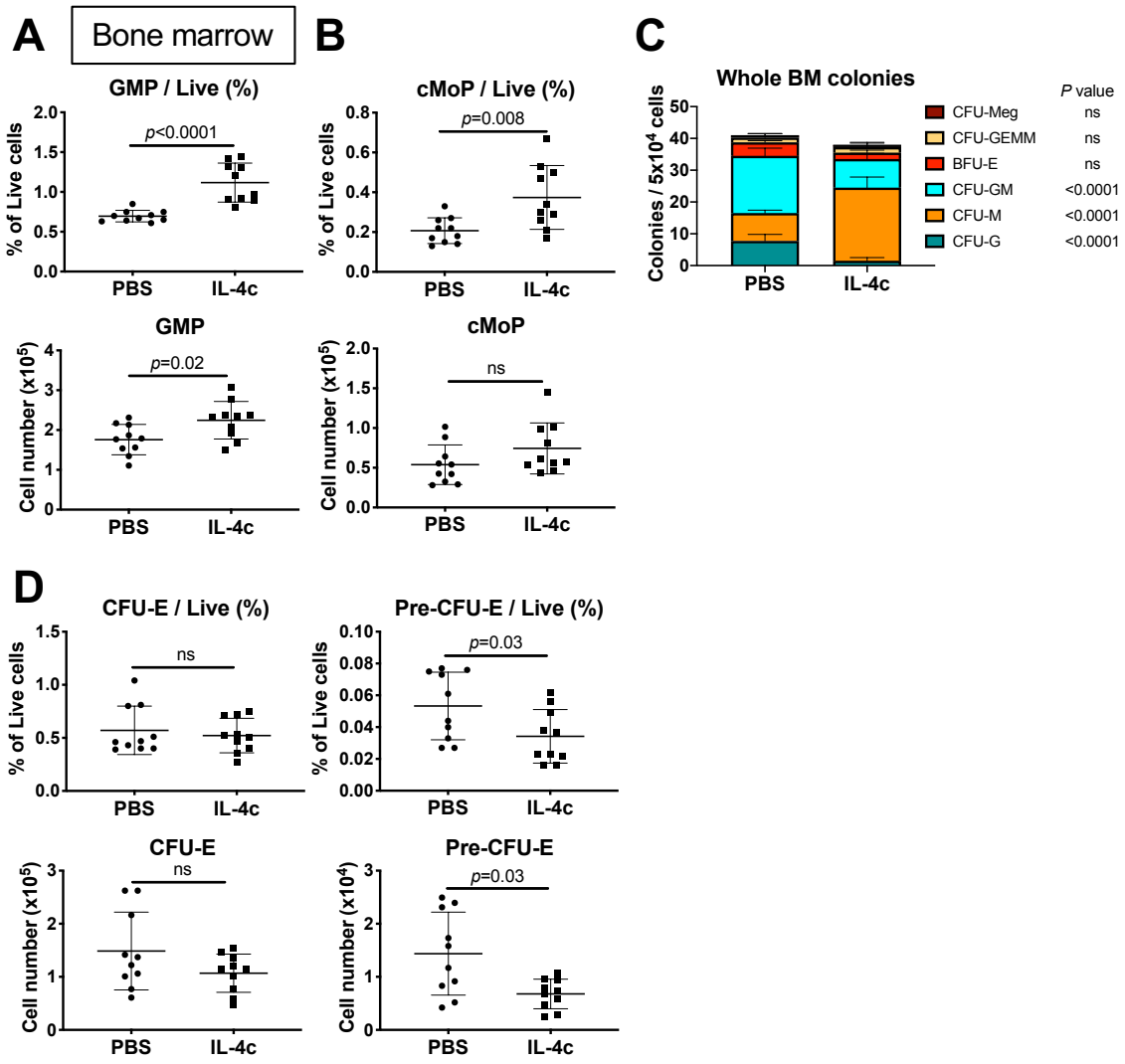

Figure 4.10: IL-4 promotes myelopoiesis *in vivo*

(**A**) Frequency and absolute number of GMPs in BM from mice injected with PBS of IL-4 + anti-IL-4 antibody complexes for 1 week.

(**B**) Frequency and absolute number of common monocyte progenitors (cMoPs).

(**C**) Number of colonies derived from $5x10^4$ total BM cells plated in methylcellulose medium for 10 days with or without IL-4. Bars show mean and SD, two-way ANOVA with Sidak's test. MEG: megakaryocyte colony, CFU-GEMM: colony forming unit – granulocyte erythroid myeloid megakaryocyte, BFU-E: blast-forming unit erythroid, CFU-GM: colony forming unit granulocyte macrophage, CFU-M: colony forming unit macrophage, CFU-G: colony forming unit granulocyte.

(**D**) Frequency and absolute number of erythroid progenitors (CFU-E and pre-CFU-E) in BM of mice injected with PBS or IL-4 for 1 week.

For (**A**), (**B**), and (**D**), points represent individual mice with mean and SD, Mann-Whitney U test.

Pooled pooled from (**A**)-(**B**), (**D**) or representative of (**C**) 2 independent experiments.

Among mature BM cells, the bias towards myelopoiesis was unexpectedly associated with an increased frequency of neutrophils but a similar frequency and decreased number of ($Ly6C^+$) monocytes (**Fig. 4.11A**), contradicting the results obtained from *ex vivo* assays. Administration of IL-4 caused splenomegaly (**Fig. 4.11B**), which was associated with increased numbers of neutrophils but no significant change in GMPs or monocytes (**Fig. 4.11C-D**).

Collectively, these results showed that exposure of HSPCs to IL-4 *in vivo*, in addition to any secondary mediators that it might induce, caused an overall bias towards myelopoiesis that might emanate from changes in lineage priming among the earliest HSCs. However, unlike the *ex vivo* assays, this did not favour the production of monocytes over other forms of myeloid cells; instead, there were increased numbers of neutrophils in BM and spleen.

Figure 4.11

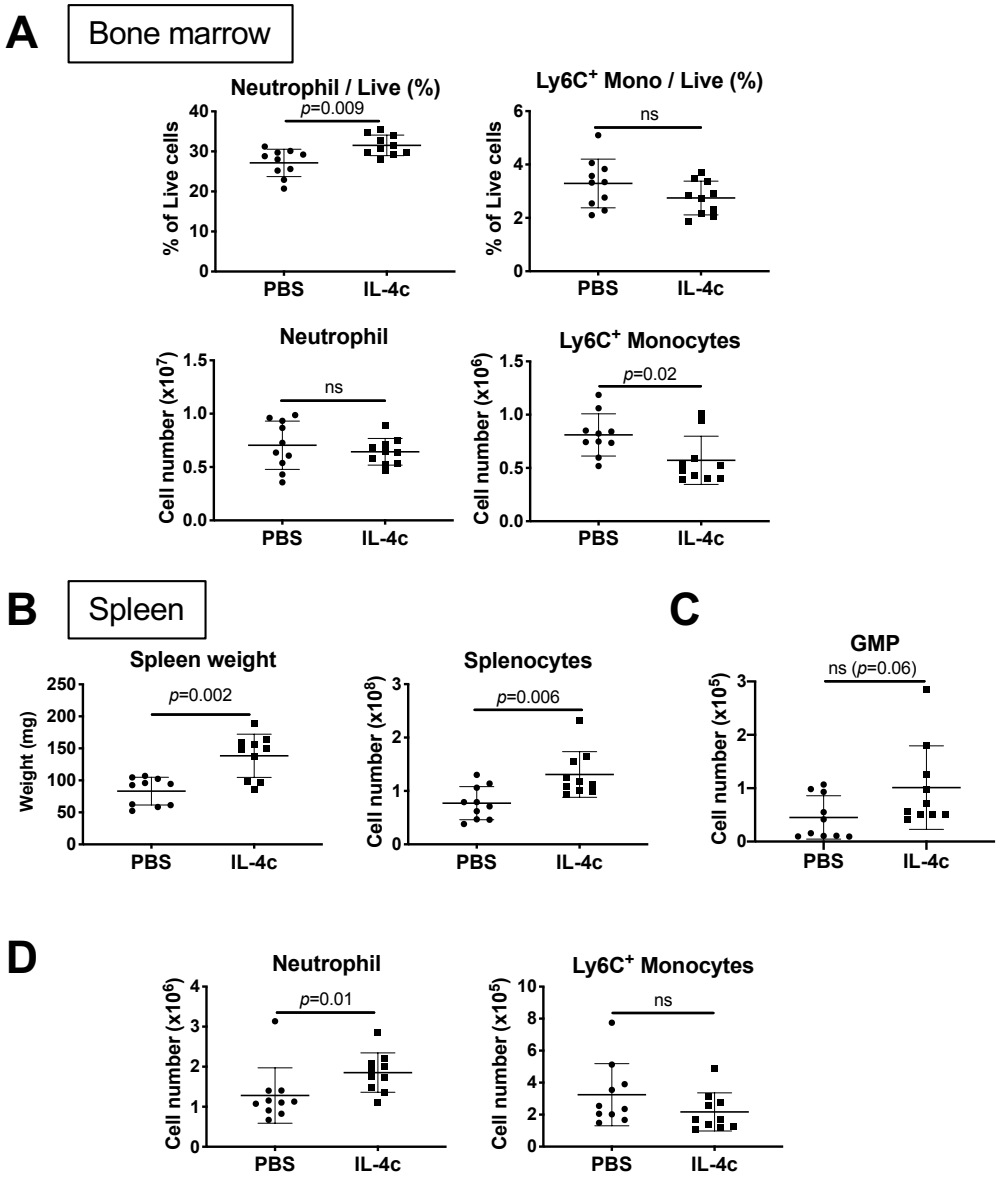

Figure 4.11: IL-4 causes accumulation of mature myeloid cells i*n vivo*
(**A**) Frequency and absolute number of indicated cell populations in BM from mice injected with PBS or IL-4 + anti-IL-4 antibody complexes for 1 week. Mono: monocyte.
(**B**) Weight of the spleen (Left) and total number of splenocytes (Right).
(**C**) Absolute number of GMPs in the spleen.
(**D**) Absolute number of indicated cell populations in the spleen.
For (**A**)-(**D**), points represent individual mice with mean and SD, Mann-Whitney U test.

Data pooled from 2 independent experiments.

4.2.5 Transient exposure to IL-4 decreases reconstitution potential of HSCs

Culture of single HSCs with IL-4 in liquid culture decreased the total cell yield, and addition of IL-4 to methylcellulose medium decreased the total colony forming efficiency of sorted LSK cells. Owing to these features, I hypothesised that IL-4 might promote precocious myeloid differentiation among HSCs at the expense of self-renewal potential. To determine whether this could produce functional differences in the reconstitution potential or lineage bias of HSCs, I injected wild type CD45.2^{+} mice with IL-4 complexes or PBS for one week, then harvested the BM, sorted HSCs, and injected these into separate, lethally irradiated CD45.1^{+} recipients with 5x10^{5} CD45.1^{+}, Sca1^{-} support cells (**Fig. 4.12A**). Comparing mice injected with IL-4 exposed or IL-4 naïve HSCs, there was no significant difference in overall chimerism of CD45^{+} blood cells over time (**Fig. 4.12B**), but total BM chimerism was significantly lower in mice that received IL-4 exposed HSCs when mice were culled after 22 weeks (**Fig. 4.12C**). Further analysis of HSPC populations and mature cells in BM revealed a significant effect of IL-4 treatment on chimerism, with IL-4 exposed HSCs contributing to MPP cell populations and the myeloid lineage to a lesser extent than IL-4 naïve (**Fig. 4.12D**). This suggested IL-4 exposure decreased the overall ability of HSCs to reconstitute the haematopoietic system after transplantation, recapitulating the effects of IL-4 to decrease the overall efficiency of colony formation in methylcellulose assays and to decrease total cell yield in single cell cultures.

Among CD45.2^{+} donor-derived cells, IL-4 had no significant effect on lineage bias, with similar frequencies of all major lineages observed in mice receiving IL-4-exposed or IL-4-naïve HSCs (**Fig. 4.12E**). This suggested the pro-myelopoietic effect of IL-4 observed after injection in WT mice might be dependent

on continuous exposure of HSCs to IL-4 and was lost after they were exposed to the additional stress of transplantation.

Figure 4.12

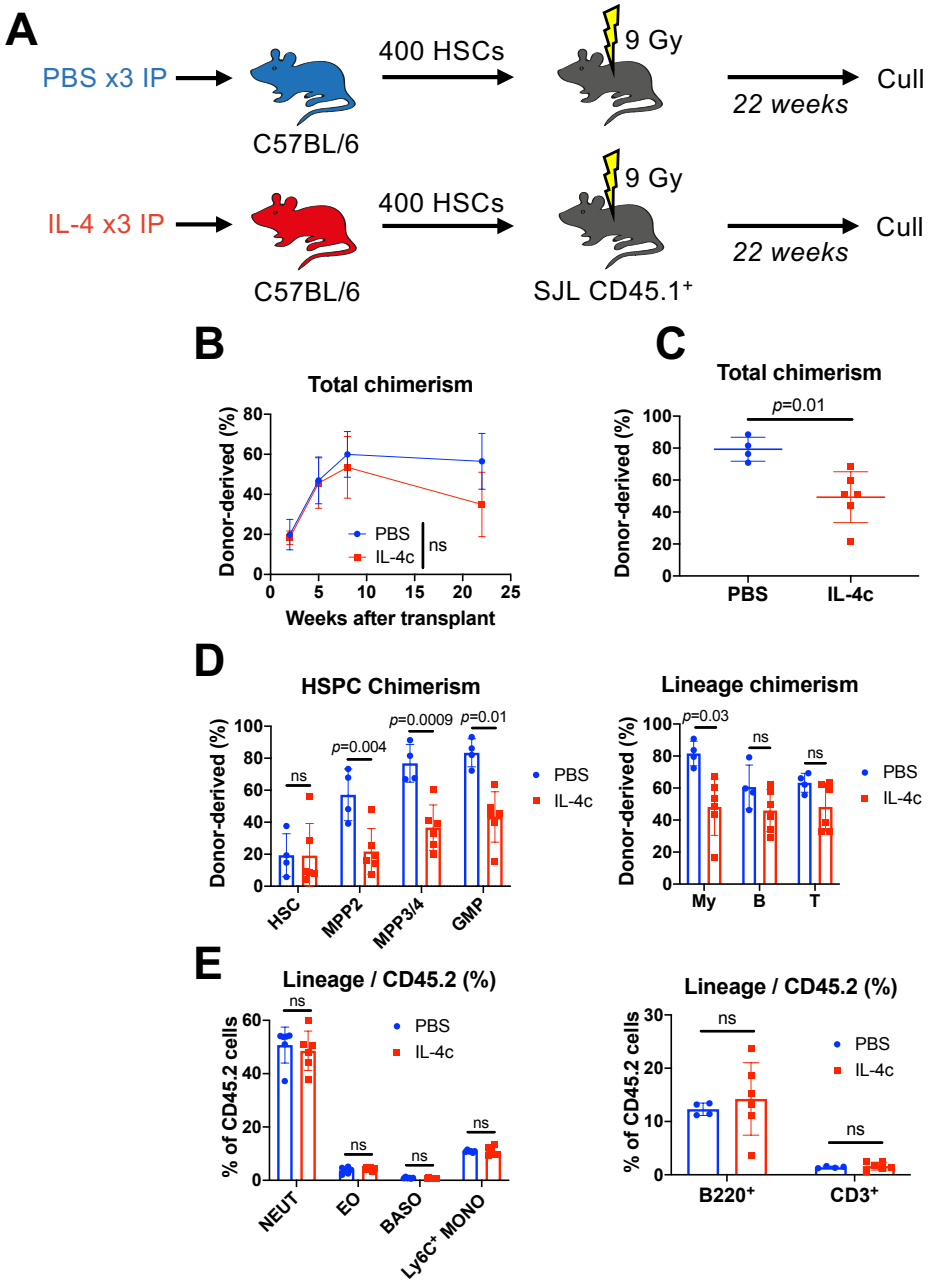

Figure 4.12: IL-4 decreases fitness of HSCs

(**A**) Schematic diagram showing transplantation of HSCs sorted by FACS from mice injected with either PBS or IL-4 for 1 week into lethally irradiated CD45.1+ recipients. Serial blood samples were obtained from the chimeras before they were culled after 22 weeks.

(**B**) Total chimerism among CD45+ cells in blood over time. Points represent mean with SD for n=4-6 mice per group, two-way ANOVA with Sidak's test.

(**C**) Total chimerism among CD45+ BM at 22 weeks. Points represent individual mice with mean and SD, Mann-Whitney U test.

(**D**) Chimerism among indicated HSPC (Left) and mature (Right) cells in BM at 22 weeks. Points represent individual mice, bars show mean with SD, two-way ANOVA with Sidak's test. My: myeloid, B: B cells, T: T cells.

(**E**) Frequency of indicated myeloid (Left) and non-myeloid (Right) cells among transplanted BM CD45.2+ cells at 22 weeks. Points show individual mice, bars show mean with SD, two-way ANOVA with Sidak's test. NEUT: neutrophil, EO: eosinophil, BASO: basophil, MONO: monocyte.

Data from a single experiment.

4.2.6 Blockade of IL-4 partially alleviates neutrophilia but does not ameliorate clinical disease in SpA

Having demonstrated that IL-4 can promote myelopoiesis, I wished to evaluate its possible role in remodelling of haematopoiesis during chronic inflammation by injecting SKG mice with anti-IL-4 antibodies as they developed SpA. This treatment caused variable effects across experiments, sometimes causing significant amelioration of clinical features of SpA and, on other occasions, having no impact on disease (**Fig. 4.13A**). This variability did not appear to be caused by variation in different batches of antibody (clone 11B11), which performed similarly in a competitive sandwich ELISA (**Fig. 4.13B**). Consequently, I repeated this experiment in a total of 6 replicates, each including n=4-8 mice per group, so that effects could be estimated more accurately. Comparing clinical parameters in this way across experiments, I found no overall difference in clinical arthritis score, paw and tarsal measurements, or changes in bodyweight (**Fig. 4.13C**).

For flow cytometric data from these experimental replicates, I normalised the results to the mean of values for the isotype control group to account for differences in disease severity across experiments. Therefore, in the paws, there was a minor reduction across experiments in neutrophil accumulation expressed as a proportion of $CD45^+$ cells, but not in the absolute number of neutrophils per paw, nor in the frequency and number of $Ly6C^+$ monocytes (**Fig. 4.14A**). Similarly, IL-4 blockade did not affect the frequency of myeloid cells in the small intestine in the single experiment where this was evaluated (**Fig. 4.14B**). Collectively, this showed that IL-4 blockade produced a modest reduction in neutrophil infiltration into the paws that was not sufficient to have a statistically significant impact on clinical disease.

Figure 4.13

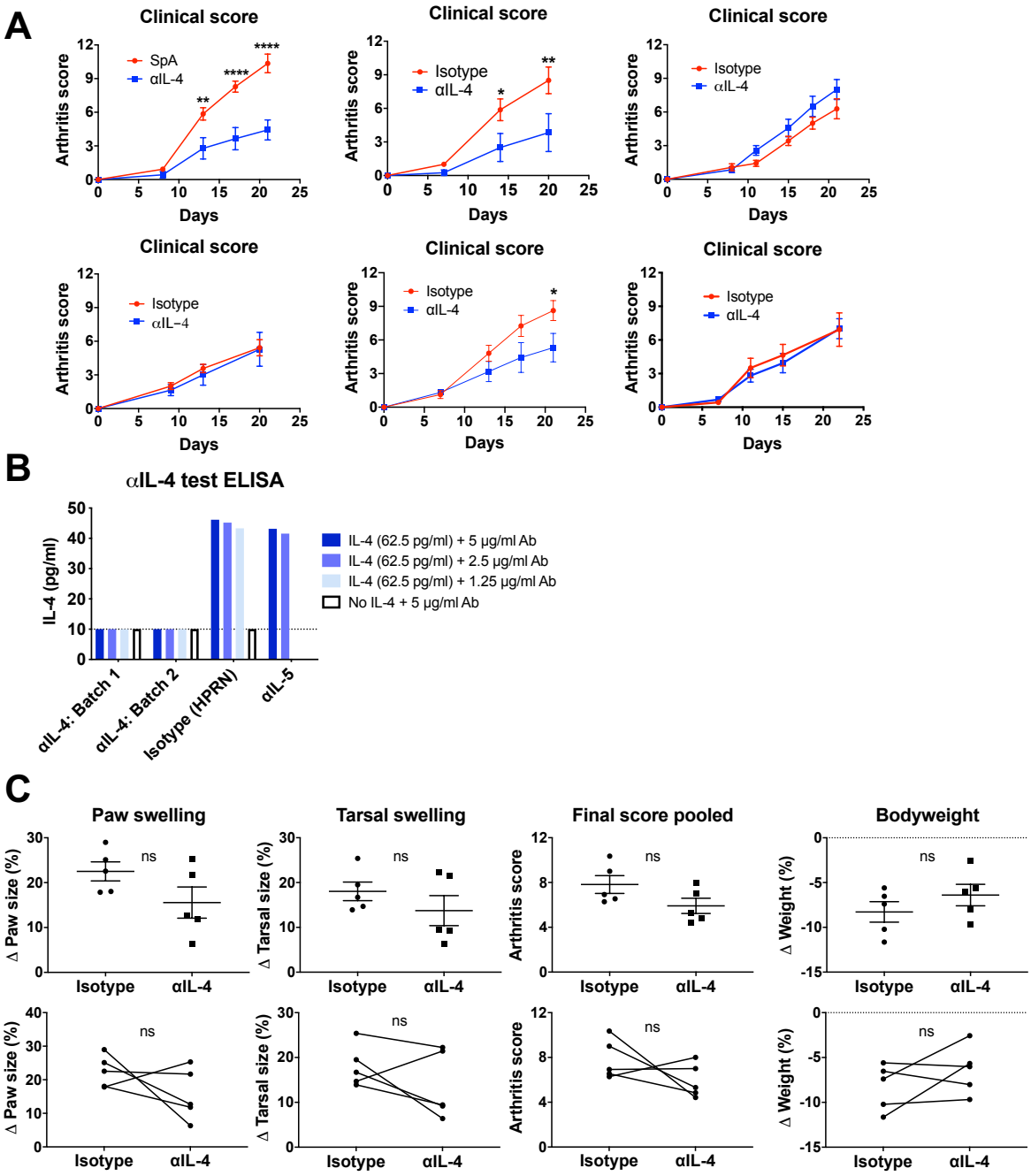

Figure 4.13: IL-4 has little effect on clinical disease in SpA

(**A**) Clinical arthritis score in 6 experimental replicates where mice were injected with curdlan then either anti-IL-4 antibodies or isotype as they developed SpA. Points represent mean of n=4-8 mice per group with SD, two-way ANOVA with Sidak's test. **p*<0.05, ***p*<0.01, *****p*<0.0001.
(**B**) Measurement of IL-4 by ELISA after wells were spiked with IL-4 at 62.5 pg/ml, then incubated with anti-IL-4 11B11 clones, isotype, or anti-IL-5 antibodies at indicated concentrations before completing the sandwich ELISA. Dotted line indicates lower limit of detection. Bars represent mean of technical replicates.
(**C**) (Top) Change in paw and tarsal swelling, arthritis score at the end of experiments, and change in bodyweight in mice injected with curdlan then injected with either anti-IL-4 antibodies or isotype as they developed SpA. Points represent mean of independent experimental replicates with mean and standard error, Mann-Whitney U test. (Bottom) Same data, with points representing individual experiments and connecting lines showing paired results. Paired t tests.

Data show results of (**A**) or are pooled from (**C**) 6 independent experiment. Data in (**B**) from single experiment

Figure 4.14

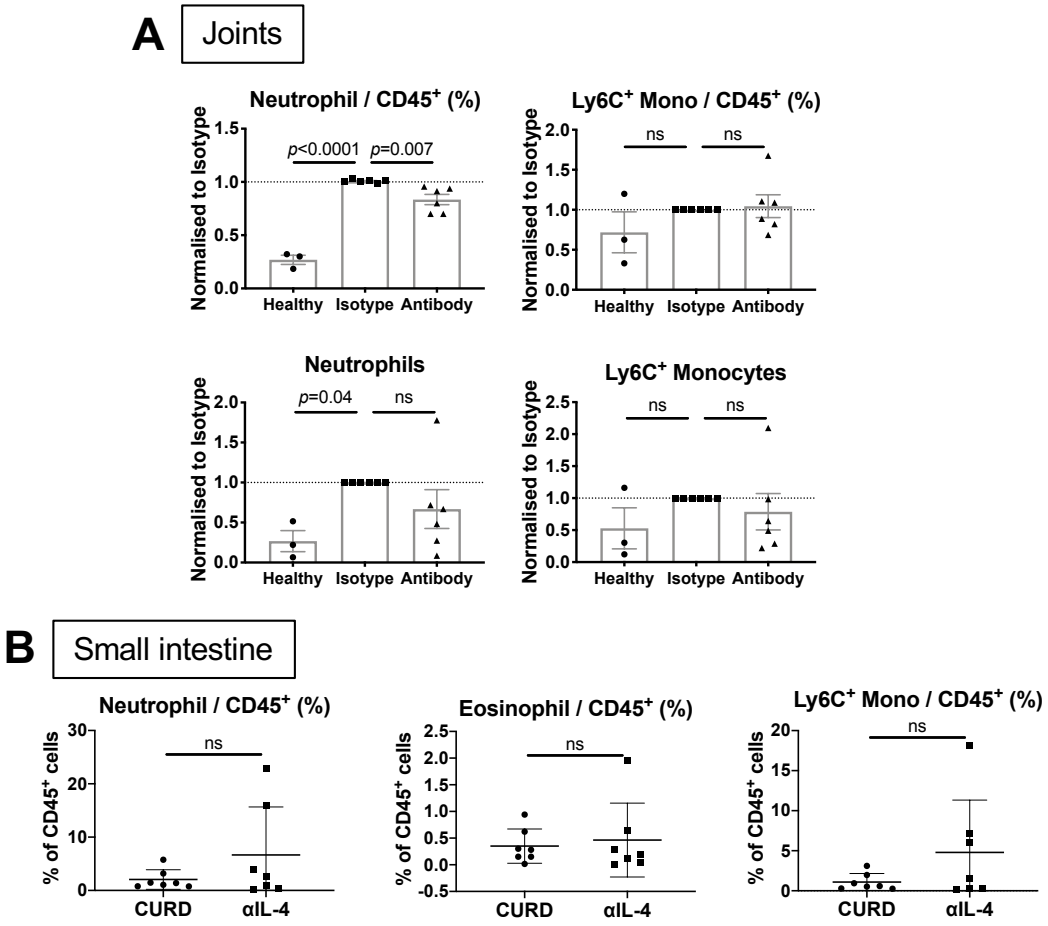

Figure 4.14: IL-4 promotes neutrophil accumulation in the joints in SpA
(**A**) Frequency and absolute number of neutrophils in the joints of healthy mice and mice injected with curdlan then injected with either anti-IL-4 antibodies or isotype for 3-4 weeks. Points represent mean of 6 experimental replicates, each with n=4-8 mice per group. Results are normalised to the mean of the isotype group for each replicate. One-way ANOVA with Tukey's test.
(**B**) Frequency of indicate leukocyte populations among total CD45+ leukocytes in the small intestine. Points represent individual mice with mean and SD, Mann-Whitney U test.

Data pooled from 6 independent experiments (**A**) or from single experiment (**B**).

In the BM, administration of anti-IL-4 antibodies caused no overall difference in the frequency or number of any group of LSK cells (**Fig. 4.15A**), though the gating strategy used in these experiments did not permit separation of the MPP3 and MPP4 groups. Similarly, there was no effect of anti-IL-4 treatment on annexin V or Ki67 expression in LSK cells in the single experiment where this was evaluated

(**Fig. 4.15B**), and no changes were observed in expression of CD16/32 among HSCs, as had been seen with IL-4 injection (**Fig. 4.15C**). Downstream of LSK cells, anti-IL-4 treatment did not prevent the expanded myelopoiesis caused by SpA but did ameliorate the suppression of erythropoiesis, with significantly increased frequencies and numbers of CFU-E progenitors in anti-IL-4-treated mice compared to those receiving the isotype (**Fig. 4.16A**). This corresponded with the observation that injection of recombinant IL-4 caused a reduction in erythroid progenitors, albeit at the earlier pre-CFU-E stage in WT mice. There was no difference in expression of Ki67 or annexin V in either erythroid progenitors or GMPs from anti-IL-4 or isotype treated mice in a single experiment (**Fig. 4.16B**). Although anti-IL-4 treatment did not prevent the expansion of the GMP pool from occurring in SpA, treated mice had significantly lower frequencies (though not absolute numbers) of mature neutrophils in the BM (**Fig. 4.17A**), as they did in the paws. Conversely, the increased frequency of CFU-E in BM was not reflected in the numbers of mature erythroid ($Ter119^+$) cells, which were similar in isotype and anti-IL-4 treated mice (**Fig. 4.17B**).

Taken together, these results indicated that IL-4 was largely dispensable for development of SpA in SKG mice, but blockade did produce modest reductions in the frequency of mature neutrophils in BM and paws. This effect did not appear to be dependent on major changes in BM myelopoiesis because numbers and proliferative capacity of GMPs in the BM were unchanged compared to isotype-treated mice, suggesting this could also have been an effect of IL-4 on mature neutrophils to alter survival or migration.

Figure 4.15

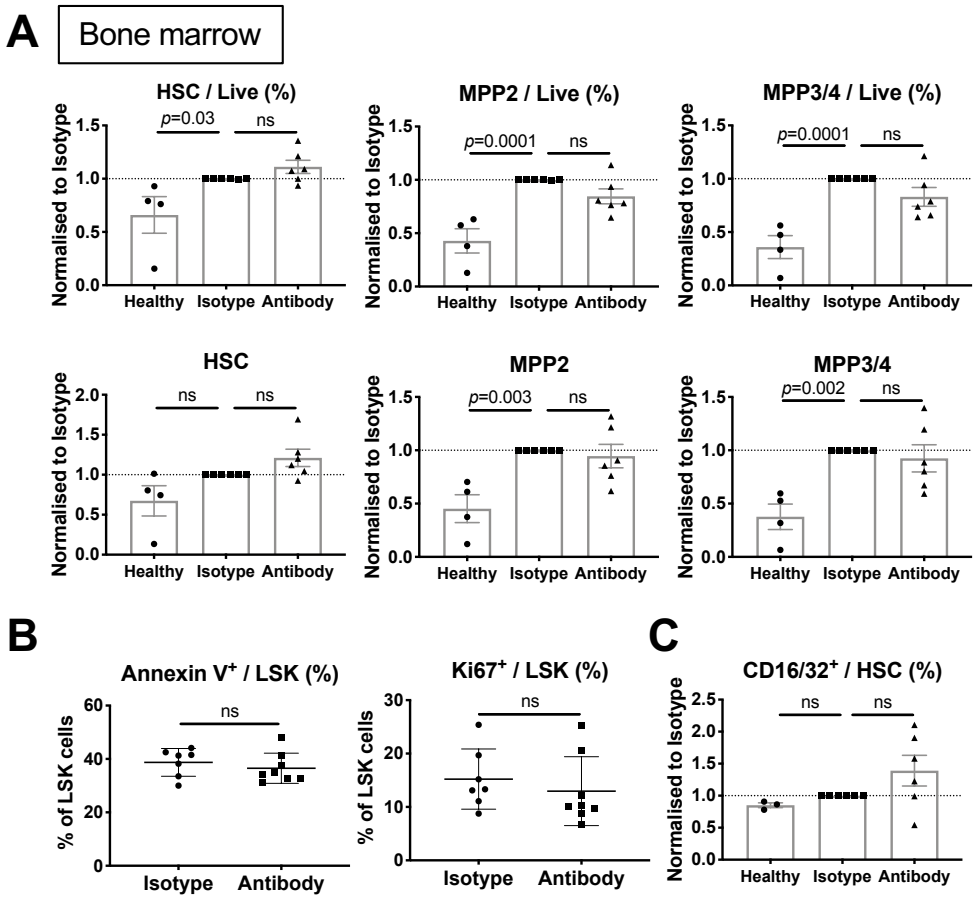

Figure 4.15: Anti-IL-4 treatment does not affect the LSK compartment in SpA
(**A**) Frequency and absolute number of indicated HSPC populations in the BM of healthy mice and mice injected with curdlan then injected with either anti-IL-4 antibodies or isotype for 3-4 weeks.
(**B**) Frequency of expression of annexin V and Ki67 among LSK cells in BM of mice injected with anti-IL-4 antibodies or isotype after being injected with curdlan to induce SpA. Points represent individual mice with mean with SD, Mann-Whitney U test.
(**C**) Frequency of HSCs expressing CD16/32 in mice injected with curdlan then injected with either anti-IL-4 antibodies or isotype for 3-4 weeks.
For (**A**) and (**C**), points represent mean of 6 experimental replicates, each with n=4-8 mice per group. Results are normalised to the mean of the isotype group for each replicate. One-way ANOVA with Tukey's test.

Data pooled from 6 independent experiments (**A**), (**C**) or from single experiment (**B**).

Figure 4.16

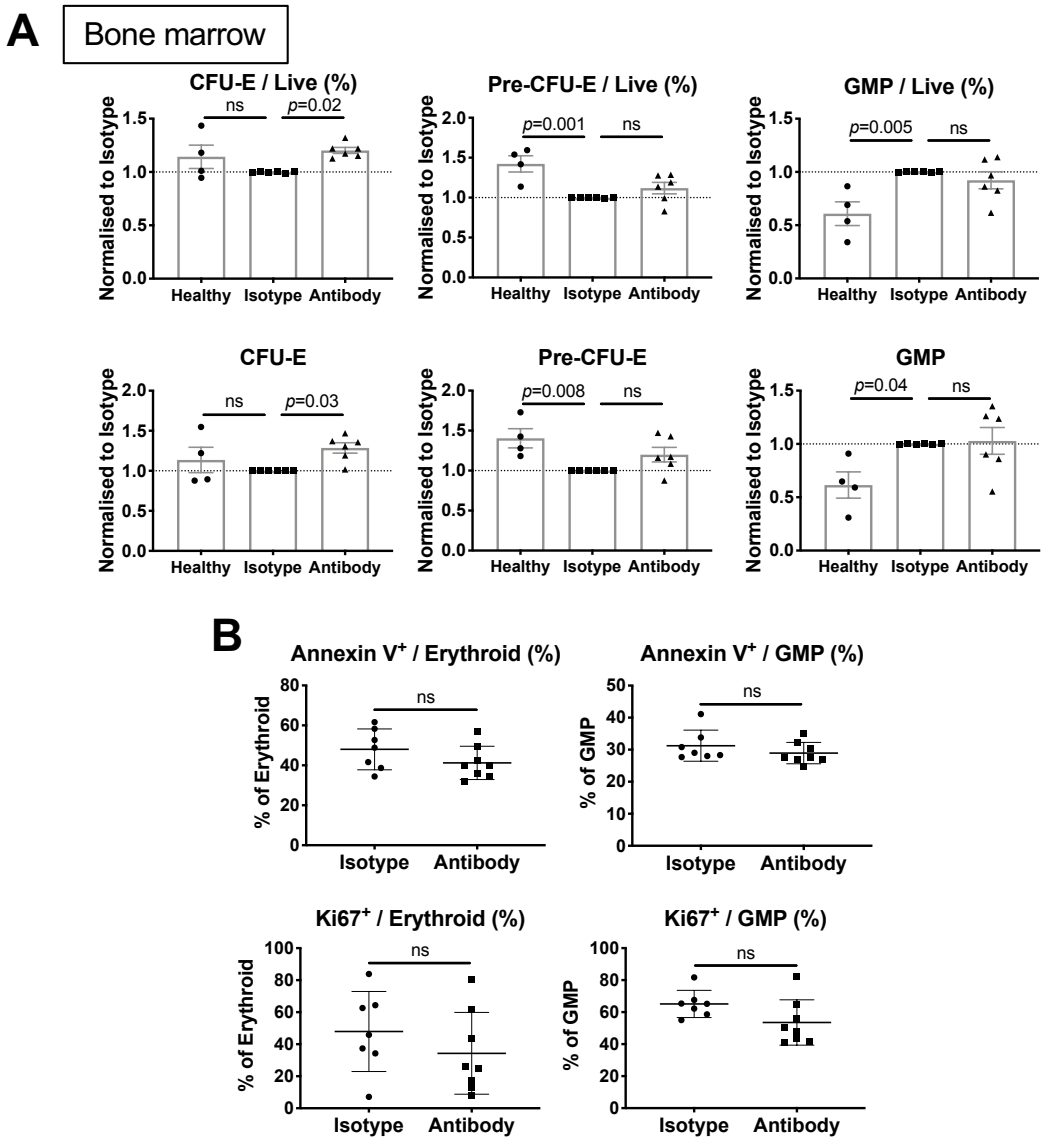

Figure 4.16: Anti-IL-4 prevents suppression of erythroid progenitors in SpA
(**A**) Frequency and absolute number of indicated HSPC populations in the BM of healthy mice and mice injected with curdlan then injected with either anti-IL-4 antibodies or isotype for 3-4 weeks. Points represent mean of 6 experimental replicates, each with n=4-8 mice per group. Results are normalised to the mean of the isotype group for each replicate. One-way ANOVA with Tukey's test.
(**B**) Frequency of expression of annexin V and Ki67 among indicated progenitor cells in BM of mice injected with anti-IL-4 antibodies or isotype after being injected with curdlan to induce SpA. Points represent individual mice with mean and SD, Mann-Whitney U test.

Data pooled from 6 independent experiments (**A**) or from single experiment (**B**).

Figure 4.17

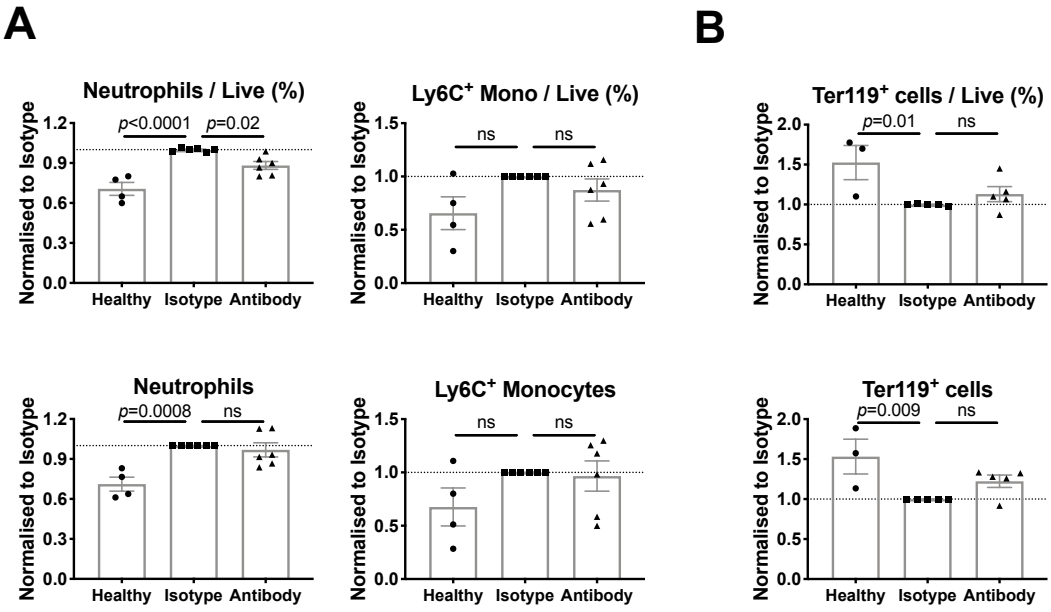

Figure 4.17: Anti-IL-4 treatment partially alleviates neutrophil accumulation in the BM in SpA
(**A**) Frequency and absolute number of indicated mature cell populations in the BM of healthy mice and mice injected with curdlan then injected with either anti-IL-4 antibodies or isotype for 3-4 weeks. Mono: monocyte.
(**B**) Frequency and absolute number of mature erythroid cells in BM.
For (**A**)-(**B**), points represent mean of 6 experimental replicates, each with n=4-8 mice per group. Results are normalised to the mean of the isotype group for each replicate. One-way ANOVA with Tukey's test.

Graphs show data from 6 independent experiments.

4.3 Discussion

4.3.1 A type 2 immune module in murine SpA

Previous reports have described human and murine SpA as a disease dominated by a type 17 immune response, and I also identified increased numbers of IL-17A producing cells in the paws, popliteal lymph nodes, and small intestine of inflamed mice. However, in common with human AS, I found evidence of a concurrent type 2 immune module in the small intestine and mesenteric lymph nodes, characterised by accumulation of IL-4 and IL-5 producing T cells. Mechanistically, it is possible this type 2 response in the intestine is induced by

release of the cytokines IL-33, IL-25, or TSLP from damaged epithelial cells. These factors may promote local production of IL-4 and IL-5 from tissue resident cells and reinforce a type 2 response by favouring the differentiation of Th2 T cells in the local mesenteric lymph nodes. In some forms of IBD, increased expression of IL-4, IL-5, and IL-33 might regulate or mitigate type 17 responses induced by local production of IL-23 [492]. However, in murine SpA, I suggest IL-4^{+} T cells are contributing to the inflammatory response because a large proportion co-produced GM-CSF or TNF-α, both of which are necessary for disease in this model [393, 441]. This assertion is supported by my observation that blockade of IL-4 did not worsen disease in the intestine. My investigation of a possible type 2 immune module in the intestine could be extended to consider the production and importance of IL-13. This could be important because IL-13-producing NKT cells have a critical role in the pathogenesis of type 2 biased ulcerative colitis [493], and IL-13 regulates HSPC activity *ex vivo* [305] and *in vivo* [203], even though I show the specific receptor chain is not expressed in HSPCs using RNA sequencing data.

4.3.2 Interleukin-4 as a regulator of haematopoiesis

Earlier reports suggested IL-4 had a role in regulation of HSPCs *ex vivo*, and I add to this field by confirming that mRNA encoding the IL-4Rα/γc complex is expressed in HSPCs. Although the *Il4ra* gene was expressed widely in the haematopoietic compartment, the protein was only detectable in HSCs by flow cytometry. This is consistent with the results of my culture of HSPCs sorted from BM, with IL-4 producing differences in output among HSCs but not MPP2/3s.

Summarising results from liquid bulk and single cell cultures and from methylcellulose assays, IL-4 decreased the total cell output from HSCs but caused

greater myeloid differentiation. Similarly, when IL-4 was injected *in vivo*, the frequency of GMPs was increased. These data are consistent with descriptions of IL-4$^{-/-}$ mice, which have striking deficiencies in BM CFU-GM but not BFU-E activity [306]. Collectively, this led me to speculate that IL-4 might cause more rapid myeloid differentiation of HSCs at the expense of self-renewal, decreasing the total number of cells that could be derived from each HSC. This was supported by the observation that IL-4 caused early upregulation of CD16/32 in HSCs *in vivo* and *ex vivo*, which is typically expressed on GMPs and mature myeloid cells, suggesting changes in lineage priming. Others have reported that HSCs may differentiate directly into lineage-committed progenitors, including GMPs, by omitting intermediate MPP stages [78, 494]; my data suggest that IL-4 might promote this process. Accordingly, HSCs from IL-4-exposed mice were less effective in reconstituting lethally irradiated mice than were HSCs from IL-4 naïve animals. These results contradict those of a similar experiment conducted previously [315], possibly owing to the duration of IL-4 exposure. In the previous experiment, HSCs were sorted by FACS then exposed to IL-4 *ex vivo* for 3 days before transplantation, whereas I injected IL-4 for 1 week before isolating HSCs. Alternatively, injection of IL-4 could induce production of other cytokines affecting HSC behaviour that would not be apparent with exposure *in vitro*, producing a combination of direct and indirect effects.

In *ex vivo* assays, IL-4 consistently promoted the formation of monocytes, sometimes at the expense of neutrophils, confirming results of similar assays conducted previously [305]. However, when IL-4 was injected *in vivo*, the major change observed was an increased neutrophil frequency in BM and spleen. The cause of this discrepancy is unclear but is probably related to the presence of other

factors *in vivo* that were absent *ex vivo*. For example, in previous studies, IL-4 co-operated with G-CSF to promote formation of neutrophil colonies [301, 303]. Therefore, if G-CSF is available *in vivo*, development of neutrophils may occur preferentially.

4.3.3 The role of type 2 cytokines in SpA

Despite demonstrating an effect of IL-4 on haematopoiesis in various assays, its blockade in SpA did not have a significant effect on development of disease when assessed across multiple experimental replicates, aligning with previous work showing that complete loss of IL-4 (by crossing SKG mice to an IL-$4^{-/-}$ strain) did not affect development of disease after zymosan injection [393], which produces a similar phenotype to curdlan in the joints. This could be attributable to a relatively low systemic level of IL-4 in SpA, which is probably lower than is achieved with injection of IL-4 complexes. Indeed, the concentration of IL-4 in plasma in healthy mice and mice with SpA was below the lower limit of detection by ELISA, though I cannot exclude the possibility that association of IL-4 with binding proteins in serum could have affected the results of this assay, as is described commonly for measurement of cytokines in serum and plasma [495].

Administration of anti-IL-4 antibodies caused a small reduction in the frequency of neutrophils in the joints and BM, which reconciles with the effect of IL-4 complex injection to increase neutrophil frequency in BM and spleen. However, this effect was not sufficient to consistently ameliorate clinical disease, suggesting any contribution of IL-4 to the accumulation of neutrophils in SpA is relatively minor or redundant when many other cytokines with pro-myeloid effects, such as GM-CSF and TNF-α, are also being produced. Similarly, although injection of anti-IL-4

antibodies decreased neutrophil frequency in the BM, there was no effect on the frequency of GMPs or LSK populations, suggesting this could have been an effect on mature neutrophils, possibly to decrease the rate of apoptosis as described in human neutrophils [496]. In further support of the notion that IL-4 might be targeting mature cells rather than myelopoiesis in this model, upregulation of CD16/32, which was notable in the HSCs of mice injected with IL-4, was not observed in SpA. Collectively, this suggests IL-4 might be capable of modulating myelopoiesis in some settings but, with the data I have collected so far, this does not seem to be an important pathway in SpA (**Fig. 4.18**).

Figure 4.18

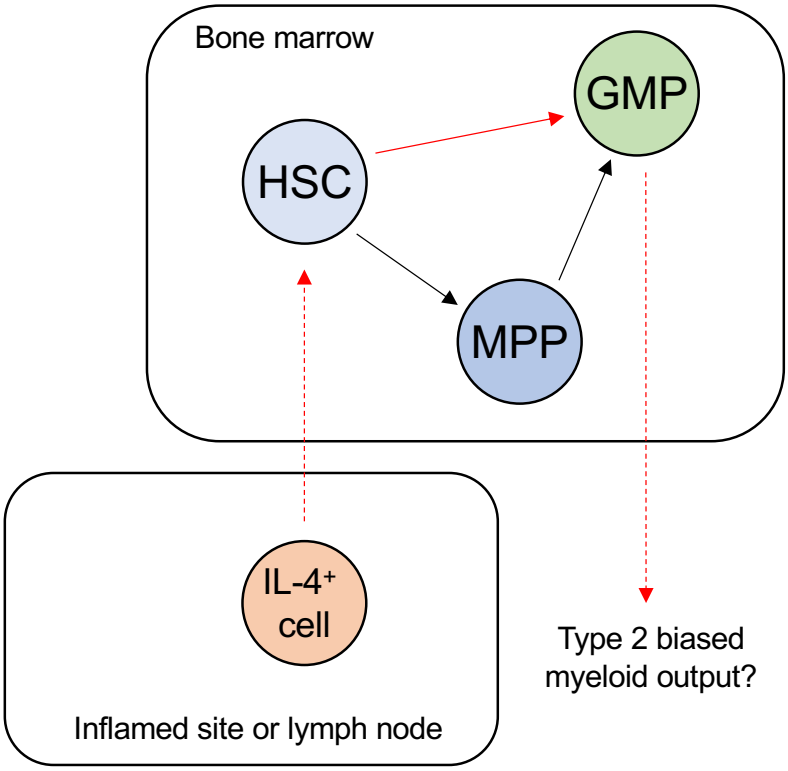

Figure 4.18: Working model for a possible role of IL-4 in regulation of haematopoiesis during inflammation
I hypothesise that IL-4 produced during some types of inflammatory response, such as parasite infestation or allergic disease, might affect HSCs in the BM, causing them to differentiate precociously into myeloid-committed progenitors by omitting MPP stages. Interleukin-4 could also exert epigenetic effects that alter the qualitative nature of the myeloid cells produced by IL-4 exposed HSCs. In SpA, this mechanism does not seem to be responsible for the marked myeloid bias in BM, though IL-4 might be having some effects on mature myeloid cells in the inflamed joints. Solid red line indicates inferences supported by data in this chapter, dashed red lines indicate hypotheses.

I observed variable results in independent experiments where I injected anti-IL-4 antibodies. Technically, this could have been related to differences in the biological activity of different batches of the 11B11 antibody clone, and I could have investigated this further by conducting bioassays of IL-4 activity. For example, I could have assessed the ability of antibody batches to inhibit the well-known phenomenon of IL-4-induced B cell proliferation [292]. Additionally, I could have administered anti-IL-4 antibodies at a higher dose or more frequently, though I used a dose that produced biological effects in a number of other model systems [449-451]. Perhaps more likely than a technical limitation is possible variation in the extent of IL-4 production in the intestine and mesenteric lymph nodes. I found the frequency and number of IL-4$^+$ T cells were variable among individual mice with SpA, and this could be related to the severity of intestinal damage. For example, in those mice with more severe enteritis, increased release of IL-33 from damaged epithelium could have promoted a stronger type 2 response in the mesenteric lymph nodes. Because the penetrance and extent of enteritis are more variable in SKG mice injected with curdlan than arthritis and enthesitis, this could have produced the variability I observed. This could have been compounded by the effect of the microbiome, which has an important role in development of enteritis in murine SpA owing to its tendency to promote intestinal IL-23 production [437]. Therefore, changes in the microbiome between different litters of mice or over time in our animal facility could have contributed to the variability I observed by modulating the severity of enteritis and the local immune response.

4.4 Conclusions

- Development of SpA is associated with accumulation of IL-4$^+$ and IL-5$^+$ CD4$^+$ T cells in small intestine and mesenteric lymph nodes but not popliteal lymph nodes, suggesting a type 2 immune module might exist in the intestine in murine SpA.
- IL-5 is dispensable for development of murine SpA but may have an impact on BM myelopoiesis.
- The receptor for IL-4 is expressed on HSPCs, and IL-4 promotes myelopoiesis *in vivo* and *ex vivo*, which is associated with early adoption of features of myeloid differentiation in HSCs.
- Injection of anti-IL-4 antibodies in mice developing SpA does not ameliorate disease or alter frequencies of myeloid progenitors, suggesting expansion of myelopoiesis in SpA is not dependent on IL-4.

5 Interleukin-33 specifically inhibits erythropoiesis

5.1 Introduction

Approximately 15-20% of people with AS have anaemia at diagnosis, and I showed in **chapter 3** that development of murine SpA suppressed BM erythropoiesis, resulting in anaemia. This anaemia of inflammatory disease (AID) is observed with other chronic inflammatory diseases, such as RA and IBD, such that an estimated 1 million people in the USA have this comorbidity [259]. Clinically, AID decreases the capacity to undertake normal activities and impairs quality of life.

The pathogenesis of AID is multifactorial (see **chapter 1.2.3.4**), with important elements including decreased absorption and increased sequestration of iron, altered RBC survival, and suppression of BM erythroid progenitors by inflammatory cytokines [258]. Accordingly, anaemia in AS and RA frequently responds to treatment with anti-TNF-α and anti-IL-6 monoclonal antibodies [445, 497-499] and, in RA patients, anti-TNF-α treatment alleviated suppression of BM erythropoiesis [500]. Therefore, in this section, I asked whether the highly regulated process of definitive BM erythropoiesis was perturbed by the inflammatory cytokine network of SpA to cause AID. My specific aims were:

1. To determine whether there was differential expression of receptors for inflammatory cytokines between committed erythroid and myeloid progenitors
2. To assess the effect of candidate cytokines on erythropoiesis, using *in vivo* models and *in vitro* techniques to define their cellular effect
3. To establish possible molecular mechanisms for any effect of inflammatory cytokines on the activity of erythroid progenitors.

5.2 Results

5.2.1 ST2 is preferentially expressed on erythroid progenitors in BM

Building on my observations in **chapter 3** that the lineage bias in BM of mice with SpA was associated with striking differences in the activity of lineage-committed progenitors (**chapter 3.2.3**), I began by comparing the expression of major cytokine receptor proteins on erythroid (CFU-E) and myeloid (GMP) progenitors in murine BM because I hypothesised that inflammatory cytokines might be having direct but differential effects on progenitors at this stage in haematopoiesis. Doing so, I confirmed expression of receptors on GMPs that have known roles in regulating myelopoiesis, including those for GM-CSF, TNF-α, and IFN-γ (**Fig. 5.1A**). However, I was surprised to observe the specific receptor for IL-33, ST2, was expressed at much higher levels on CFU-Es than GMPs (**Fig. 5.1A**). To explore this further, I evaluated the expression of a wider range of inflammatory cytokine receptors in the same progenitor stages using a publicly available RNA sequencing database [476] (**Fig. 5.1B**). Among these, only the gene encoding ST2 (*Il1rl1*) was expressed at higher levels in CFU-Es (**Fig. 5.1C**), and this was also among those genes significantly differentially regulated when comparing cell types (**Fig. 5.1D**). The gene encoding IL1RAP, which is shared with other IL-1 family members [501] and forms the complete receptor for IL-33 in combination with ST2, was also expressed in erythroid progenitors but was not differentially regulated when compared to GMPs (**Fig. 5.1B-C**).

Figure 5.1

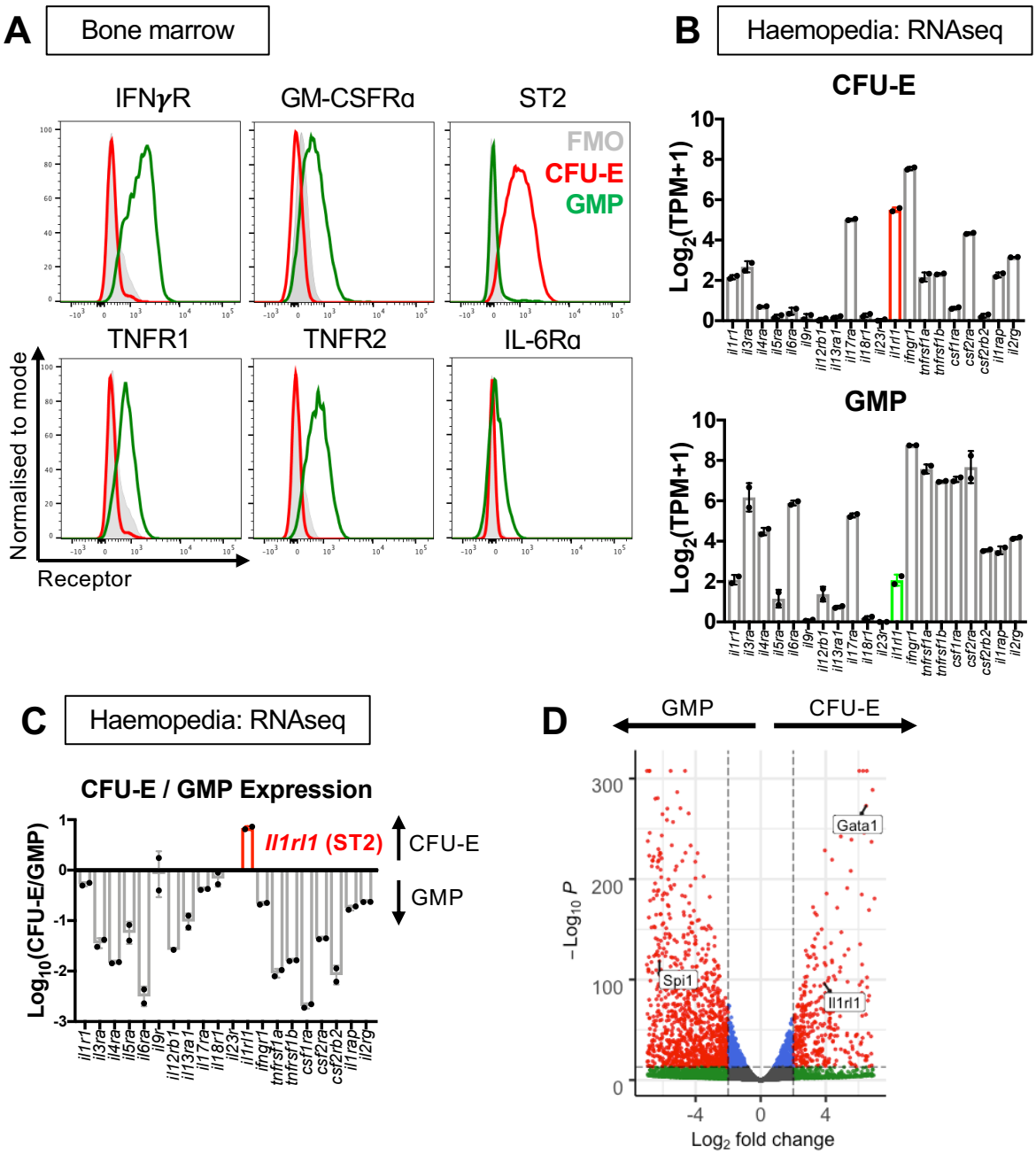

Figure 5.1: IL-33 receptor is expressed on erythroid progenitors
(**A**) Representative flow cytometric images of indicated cytokine receptors on colony forming units erythroid (CFU-Es, red) and granulocyte macrophage progenitors (GMPs, green) in BM. FMO: fluorescence minus one control.
(**B**) Expression of indicated cytokine receptor genes by RNA sequencing (in transcripts per million, TPM) in BM CFU-Es (Top) and GMPs (Bottom) sorted by FACS. The receptor for IL-33, ST2, is highlighted. Points represent biological replicates, bars show mean with standard error.
(**C**) Ratio of expression of indicated cytokine receptor genes by RNA sequencing between BM CFU-Es and GMPs. Points represent biological replicates, bars show mean with standard error. The receptor for IL-33, ST2, is highlighted
(**D**) Volcano plot showing genes differentially expressed by RNA sequencing between CFU-Es and GMPs sorted from BM. Genes highlighted in red were significant at $p<10^{-14}$ and differentially expressed at $Log_2(2)$. Selected genes encoding ST2 (*Il1rl1*), PU.1 (*Spi1*) and GATA1 (*Gata1*) are highlighted.
Data representative of 3 independent experiments (**A**).
Data for (**B**)-(**D**) were derived from [473], with 2 biological replicates.

Using flow cytometry, I confirmed that staining for ST2 on erythroid progenitors was specific by using $ST2^{-/-}$ mice as controls (**Fig. 5.2A**), and I found that expression of both mRNA and protein was highest in progenitors at the point of commitment to the erythroid lineage (pre-CFU-E and CFU-E) but declined with progressive maturity (**Fig. 5.2B-C**), suggesting any effect of IL-33 would occur in the early stages of differentiation. Importantly, the receptor was expressed at much lower levels on the upstream MPPs and HSCs, reducing the likelihood of a lineage-instructive effect (**Fig. 5.2D**). Collectively, this suggested IL-33 might exert a differential effect on erythroid progenitors compared to GMPs by virtue of the pattern of expression of its receptor, possibly contributing to the changes in CFU-E behaviour described in **chapter 3.2.3**.

Figure 5.2

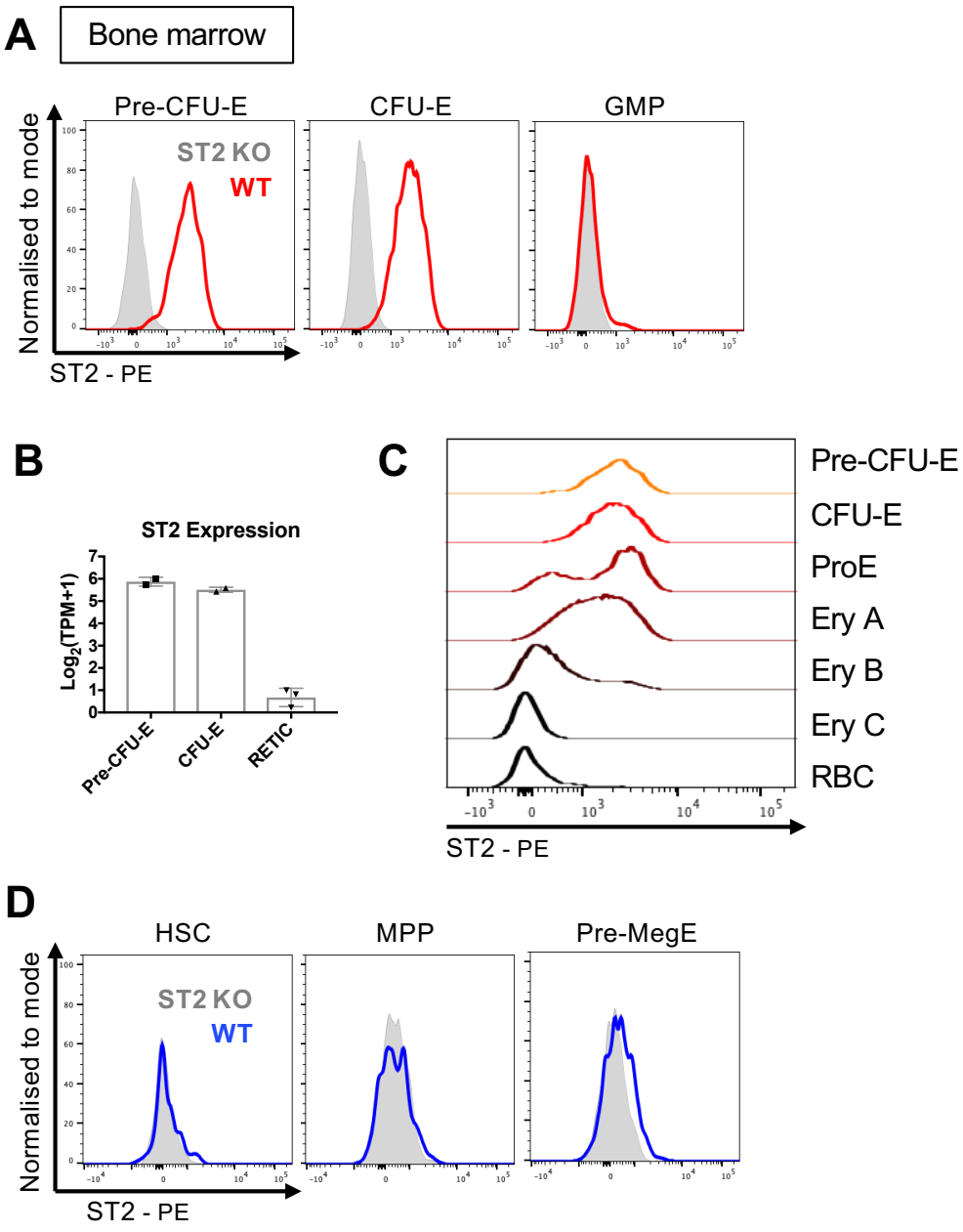

Figure 5.2: IL-33 receptor expression decreases with erythroid maturation
(**A**) Representative flow cytometric images of expression of ST2 in indicated progenitor populations in BM in wild type C57BL/6 (WT) and ST2$^{-/-}$ (ST2 KO) mice.
(**B**) Expression of the gene encoding ST2 (*Il1rl1*) in indicated progenitor populations by RNA sequencing. TPM: transcripts per million, RETIC: reticulocyte. Points represent biological replicates, bars show mean with standard error. Data derived from [473].
(**C**) Representative flow cytometric images of expression of ST2 in indicated erythroid populations, with least mature at the top and most mature at the bottom. ProE: proerythroblast, Ery: erythroblast, RBC: red blood cell.
(D) Representative flow cytometric images of expression of ST2 in indicated progenitor populations in healthy wild type (WT) and ST2$^{-/-}$ (ST2 KO) mice. HSC: haematopoietic stem cell, MPP: multipotent progenitor, pre-MegE: pre-megakaryoid/erythroid progenitor.

Data representative of 3 independent experiments (**A**), (**C**)-(**D**).

5.2.2 IL-33 inhibits differentiation of murine and human erythroid progenitors *ex vivo*

With the receptor ST2 expressed on erythroid progenitors, I hypothesised that IL-33 would exert a direct effect on these cells that might promote development of AID. To investigate this, I sorted progenitors at the earliest stage after commitment to the erythroid lineage (pre-CFU-E) by FACS from adult murine BM. I cultured these cells in pro-erythroid medium supplemented with SCF and EPO, with or without IL-33 or the SpA-promoting cytokine TNF-α [393], for 4 days before assessing cells according to their size and expression of Ter119. With progressive differentiation, primary pre-CFU-Es become smaller, upregulate then downregulate the transferrin receptor CD71, lose c-Kit and CD105, and express Ter119 [17, 161, 166] (**Fig. 5.3**). In control conditions and with TNF-α, the majority of cultured cells were small and had little granularity, but, in the presence of IL-33, a greater proportion of cells kept a larger, blast-like profile, as observed in primary BM pre-CFU-Es (**Fig. 5.3, 5.4A**). Similarly, IL-33 caused a striking reduction in the proportion of cells expressing Ter119 and, even among the less mature $CD71^+$, $Ter119^-$ cells, IL-33 also decreased the extent of downregulation of the surface receptor c-Kit, which is normally lost with maturation (**Fig. 5.4A-B**). As with TNF-α, I found inclusion of either IL-1β or GM-CSF, which promote arthritis in murine SpA [393, 441], in cultures of pre-CFU-Es did not inhibit the emergence of $Ter119^+$ cells in the same way as did IL-33 (**Fig. 5.4C**). In the terminal stages of erythroid maturation, the nucleus is extruded from progenitors to form reticulocytes. In my culture system, addition of IL-33 decreased the number of these enucleated cells observed cytologically (**Fig. 5.5A**) and by staining for nuclear material in $Ter119^+$ cells by flow cytometry (**Fig. 5.5B**).

Figure 5.3

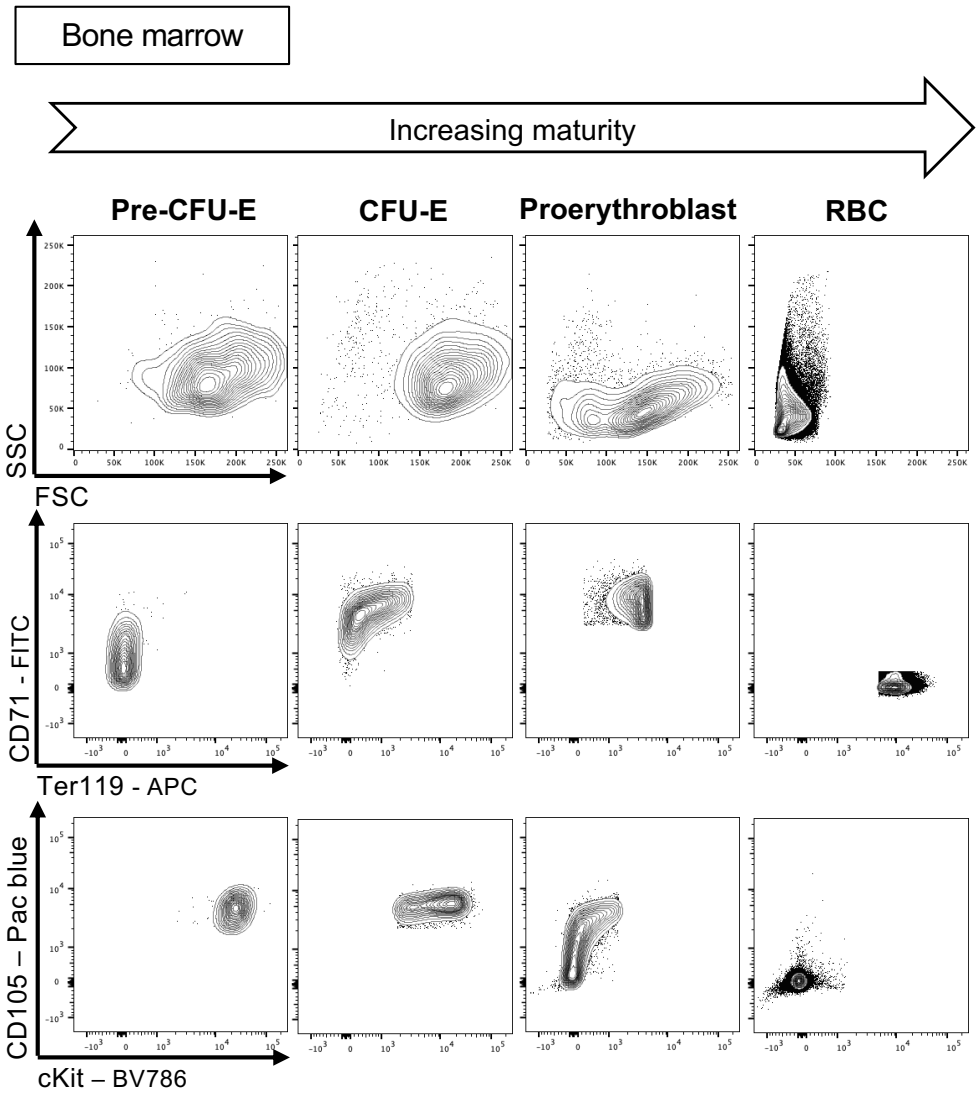

Figure 5.3: Surface marker expression in maturing erythroid cells
Representative flow cytometric images of indicated markers in indicated progenitor stages in the erythroid lineage. RBC: red blood cell.

Data representative of 5 independent experiments.

Figure 5.4

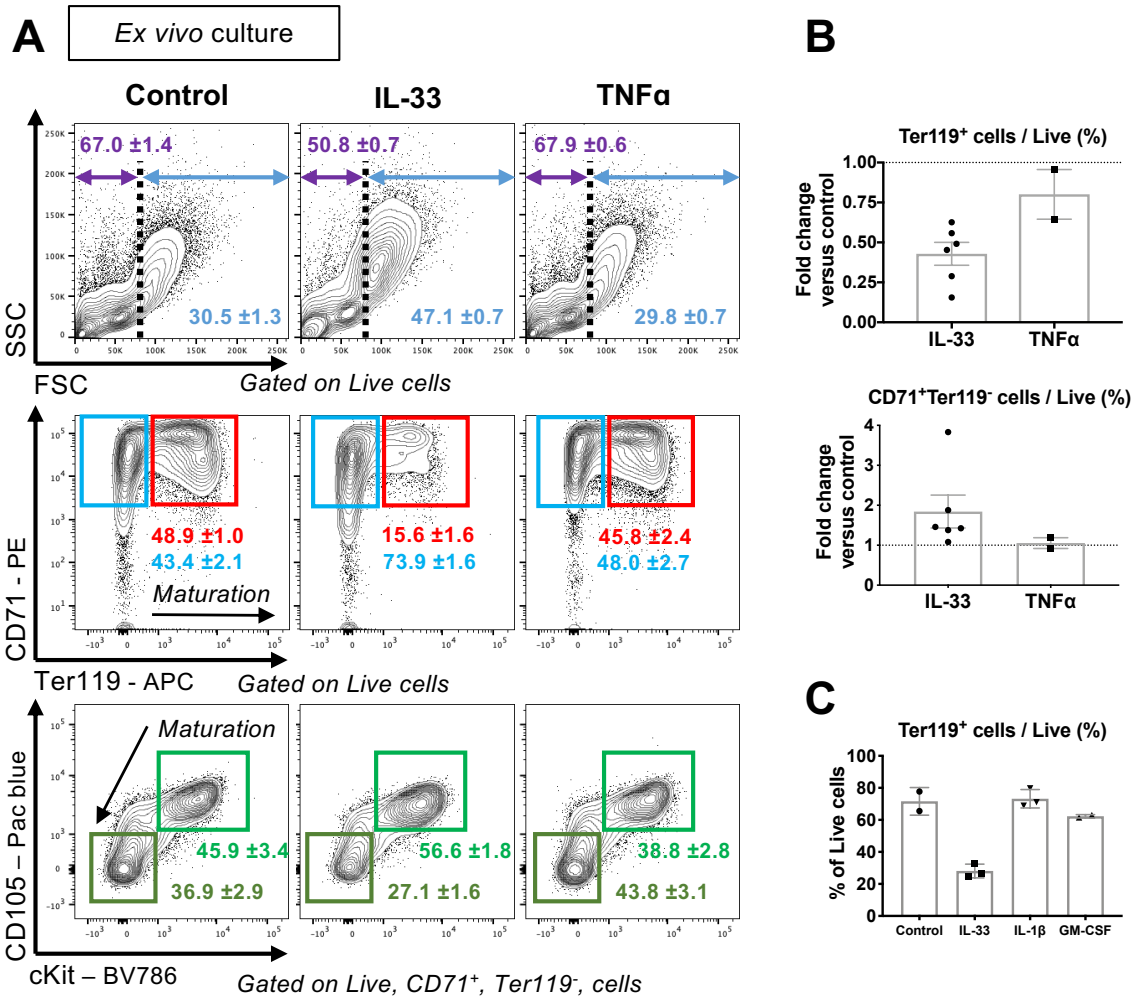

Figure 5.4: IL-33 inhibits erythroid differentiation *ex vivo*
(**A**) Representative flow cytometric images of cells derived from pre-CFU-Es sorted by FACS from murine BM and then cultured *ex vivo* in serum-free medium with erythropoietin and stem cell factor, with or without IL-33 or TNF-α, for 4 days. Figures show frequency of indicated populations among total live cells, mean and SD for technical triplicates of a single experiment.
(**B**) Frequency of indicated cell types derived from cultures described in (**A**) after 4 days. Points show mean of triplicates from independent experiments, bars show mean and standard error.
(**C**) Frequency of Ter119$^+$ cells derived from culture of pre-CFU-Es for 4 days with indicated cytokines. Points show technical triplicates from a single experiment, bars show mean with SD.

Data representative of 2 (**C**) or 2-6 independent experiments (**A**)-(**B**).

Figure 5.5

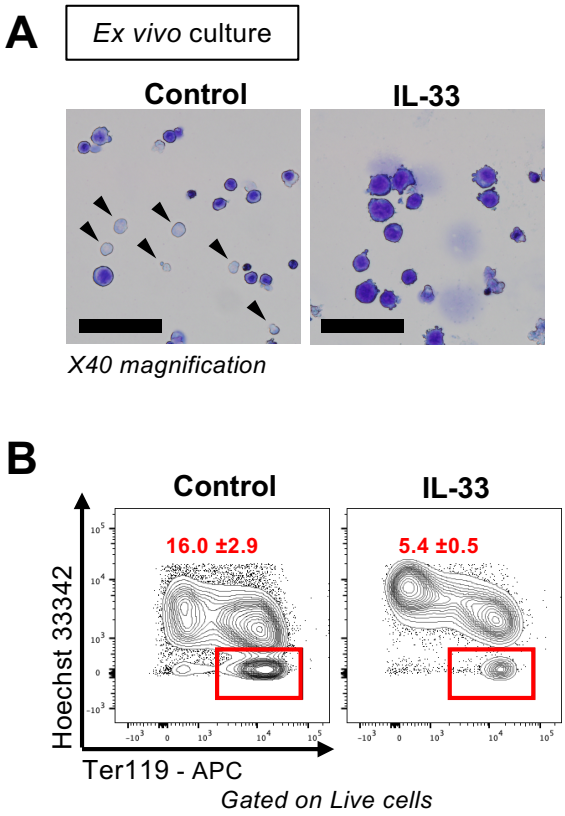

Figure 5.5: IL-33 inhibits terminal erythroid differentiation *ex vivo*
(**A**) Representative photomicrographs of cytospins of cells derived from culture of pre-CFU-Es sorted by FACS from murine BM then cultured, with or without IL-33 for 4 days. Stained with KwikDiff. Scale bar = 50 μm. Black arrowheads show more mature, enucleated red blood cells.
(**B**) Representative flow cytometric images of cells derived from cultures described in (**A**), showing cells that have undergone enucleation (Hoechst^{-}, Ter119^{+}). Figures show mean and SD frequency among total live cells for technical triplicates from a single experiment.

Data representative of 2 independent experiments.

Haematopoietic stem and progenitor cells can secrete cytokines themselves in response to pathogen derivatives and cytokines [502], possibly superseding the effects of the original stimulus by autocrine signalling. To evaluate whether the observed effects of IL-33 *ex vivo* were dependent on other factors, I cultured pre-CFU-Es from mice expressing GFP under control of the ubiquitin c promoter (Ub-GFP), which is still expressed in maturing RBCs, and from ST2$^{-/-}$ mice, alone or in

a 1:1 mixture. As expected, IL-33 had no effect on the proportion of Ter119^{+} cells derived from ST2$^{-/-}$ cells when cultured alone (**Fig. 5.6A**). Importantly however, the frequency of Ter119^{+} cells was also unchanged in ST2$^{-/-}$ cells in mixed cultures with Ub-GFP cells that were affected by IL-33 (**Fig. 5.6A**), indicating this inhibition of differentiation was a direct effect mediated through the ST2 receptor.

In bulk cultures of differentiating cells, it is difficult to determine whether experimental interventions are affecting primarily differentiation, blocking progression from one defined cell stage to the next, or affecting primarily proliferation, yielding fewer cells to progress along the differentiation pathway. To investigate this, I first evaluated the total yield of all types of cell in bulk cultures, finding no difference between cells cultured with IL-33 and those in control conditions (**Fig. 5.6B**). Further evaluation of markers of proliferation (Ki67, **Fig. 5.6C**) and apoptosis (annexin V, **Fig. 5.6D**) in bulk cultures of pre-CFU-Es showed no difference in the frequency of cells expressing either marker with addition of IL-33 compared to control conditions. This suggested the primary effect of IL-33 might be on differentiation rather than proliferation. To develop this, I separated the effects of IL-33 on proliferation and differentiation by sorting single pre-CFU-E cells and culturing them for 10 days before assessing the output by flow cytometry. I found the total cell yield was similar, but the proportion of Ter119^{+} cells was decreased by addition of IL-33, as it was in bulk cultures, confirming a primary effect on erythroid differentiation (**Fig. 5.6E**).

Figure 5.6

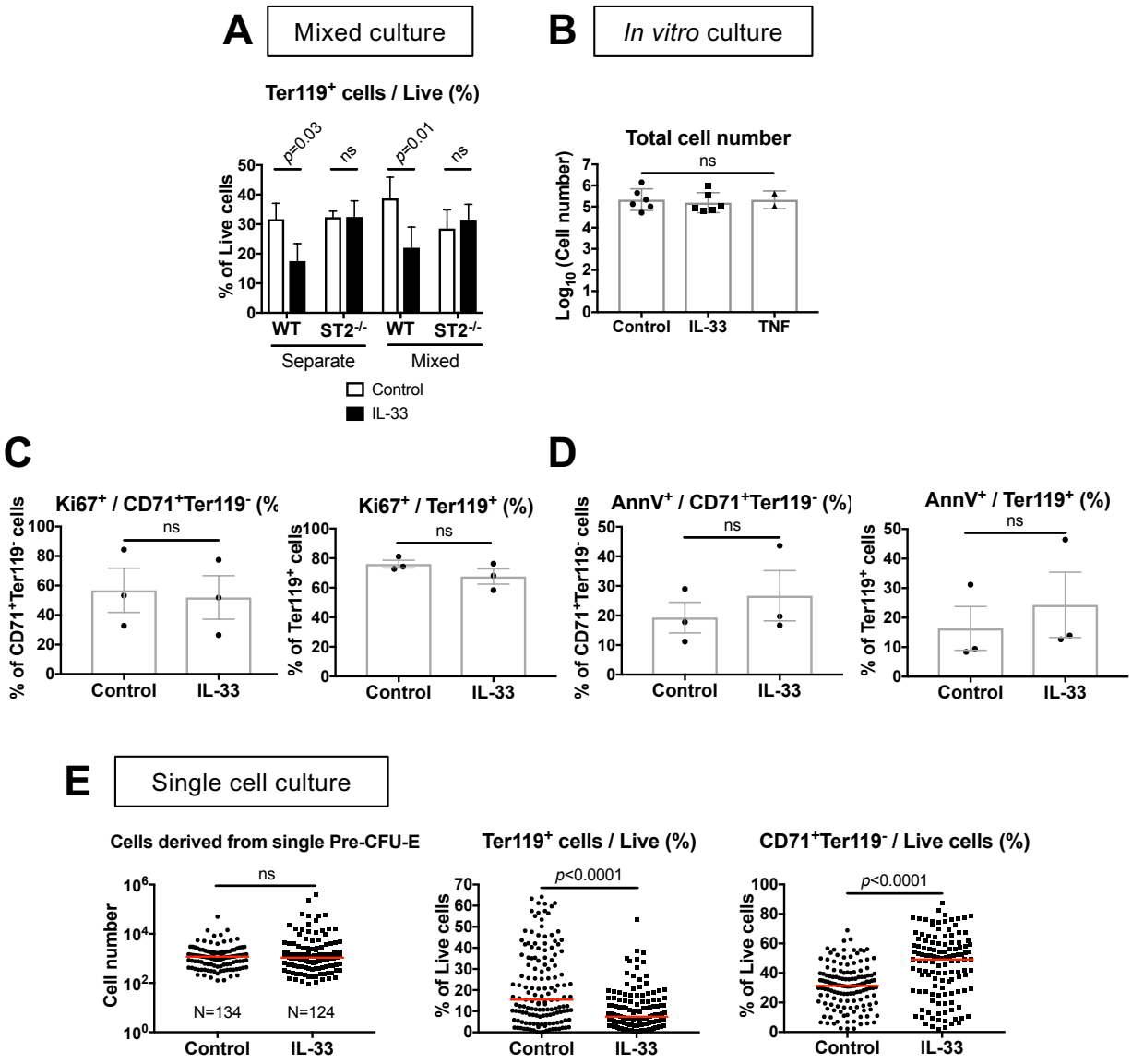

Figure 5.6: IL-33 inhibits erythroid differentiation directly *ex vivo*

(**A**) Frequency of Ter119$^+$ cells among total live cells derived from culture of pre-CFU-Es sorted by FACS from murine BM then cultured for 4 days. Cells were derived from wild type (WT) or ST2$^{-/-}$ mice and cultured alone ('Separate') or in a 1:1 mixture ('Mixed'). Bars show mean with SD for technical triplicates. Two-way ANOVA with Sidak's test.

(**B**) Total number of live cells derived from culture of pre-CFU-Es for 4 days. (**C**) Expression of Ki67 among indicated cell populations derived from culture of pre-CFU-Es for 4 days.

(**D**) Expression of annexin V among indicated cell populations derived from culture of pre-CFU-Es for 4 days.

(**E**) (Left) Total number of live cells derived from single sorted pre-CFU-Es cultured for 10 days. (Right) Frequencies of indicated cell types among live cells in the same cultures. Points represent cells from single cells with median (red line), Mann-Whitney U test.

For (**B**)-(**D**), Points show mean of triplicates from independent experiments, bars show mean and standard error. One-way ANOVA (**B**) or Mann-Whitney U test (**C**)-(**D**).

Data representative of 2 (**A**), 3 (**C**)-(**D**), or 2-6 (**B**) independent experiments, or pooled from 4 independent experiments (**E**).

Functionally, this effect was recapitulated by decreased formation of CFU-E colonies when FACS-sorted pre-CFU-Es were plated in methylcellulose medium with IL-33 (**Fig. 5.7A**). To try to establish whether this functional effect might also be apparent *in vivo* after IL-33 exposure, I sorted pre-CFU-Es by FACS from Ub-GFP mice, cultured them overnight with or without IL-33, then injected them into sublethally irradiated WT recipient mice. After 4 days, I could identify the progeny of these cells in the blood (**Fig. 5.7B**) and spleen (**Fig. 5.7C**) as $CD71^+$, $Ter119^-$ and $CD71^+Ter119^+$ erythroblasts, but the frequency of cells did not differ between mice receiving either IL-33-naïve or IL-33-exposed cells (**Fig. 5.7B-C**). This suggested continuous exposure to IL-33 might be necessary to produce the functional effects observed *ex vivo* in liquid culture and methylcellulose assays.

Finally, I asked whether this effect of IL-33 on erythroid progenitors was common to other species by isolating $CD34^+$, $CD71^+$ progenitors [467] from human blood leukoreduction cones. When culturing these cells for 8-9 days in similar conditions, inclusion of IL-33 decreased the frequency of mature erythroid cells expressing glycophorin A (CD235a, similar to murine Ter119 [165]) by approximately twofold (**Fig. 5.8**). Collectively, these observations show that IL-33 signalling through ST2 suppresses differentiation of erythroid progenitors directly, in a mechanism that appears to be common to mice and humans.

Figure 5.7

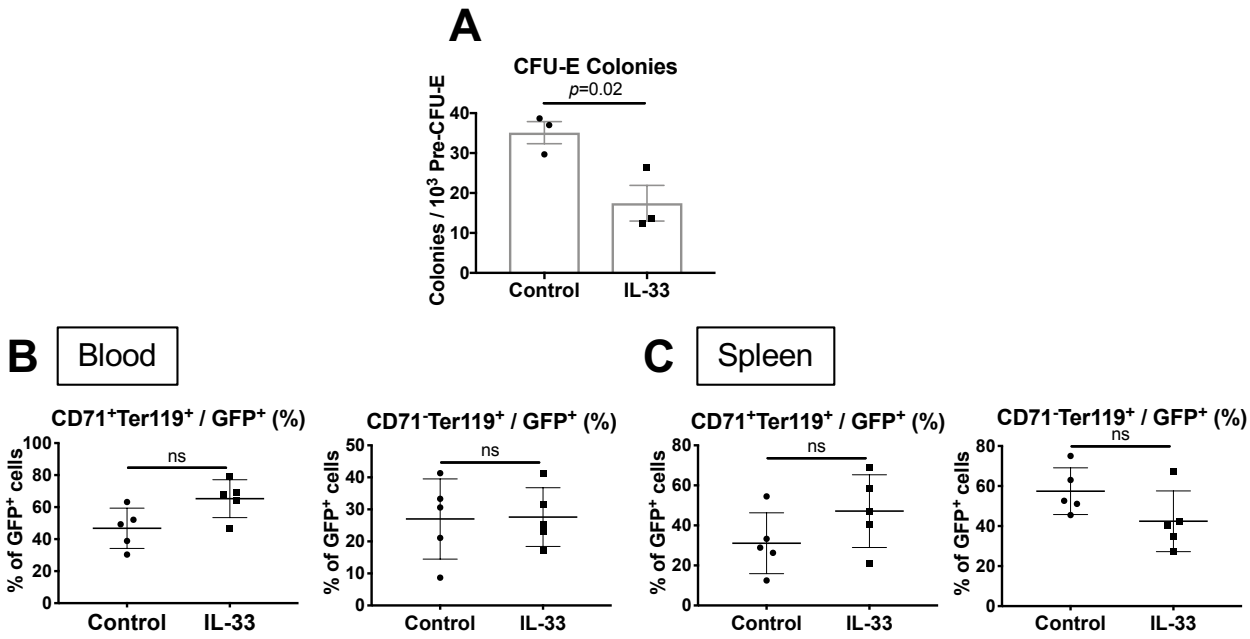

Figure 5.7: IL-33 does not inhibit erythroid differentiation of transplanted progenitors

(**A**) Number of CFU-E colonies derived from 10^3 pre-CFU-E cells sorted by FACS from healthy murine BM and plated in methylcellulose medium for 2 days. Points represent mean of independent experiments, each with n=4-6 replicates, with SEM, Student's t test.

(**B-C**) Frequency of indicated cell types in blood (**B**) and spleen (**C**) of sublethally irradiated mice injected with 10^5 GFP$^+$ pre-CFU-Es that were sorted from healthy murine BM then cultured overnight, with or without IL-33, before injection. Mice were culled after 4 days. Points represent individual mice with mean and SD, Mann-Whitney U test.

Data from single experiment (**B**)-(**C**) or 3 independent experiments (**A**).

Figure 5.8

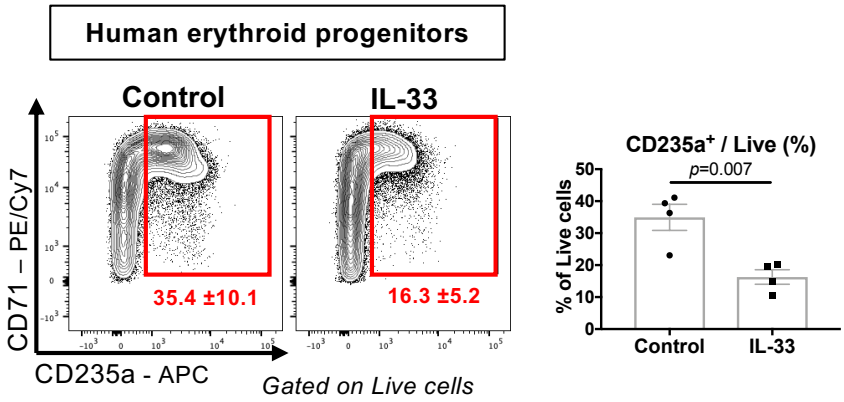

Figure 5.8: IL-33 inhibits differentiation of human erythroid progenitors
(Left) Representative flow cytometric images of cells derived from human CD34+ progenitors that were sorted by FACS from blood leukoreduction cones then cultured for 8-9 days *ex vivo*. Figures show mean and SD for technical triplicates for a single experiment. (Right) Frequency of CD235a+ cells among total live cells derived from the same cultures. Points represent individual cones with mean and SEM, Mann-Whitney U test.

Data representative of 4 independent experiments.

5.2.3 IL-33 has no effect on the MEL585 murine erythroid cell line

To facilitate further studies of the effect of IL-33 on erythroid cells, I evaluated the murine erythroid cell line MEL585, originally produced by infection of mice with Friend leukaemia virus. This produced stable clones of erythroid progenitors arrested at the pre-CFU-E stage of differentiation owing to constitutive, ligand-independent activation of the EPO receptor and to preferential insertion of the virus into the *Spi1* locus, causing increased expression of the transcription factor PU.1 [503]. This PU.1 is normally downregulated to permit terminal erythroid differentiation [504, 505], and MEL585 cells can be induced to undergo terminal differentiation by various stimuli that alter oxidation/reduction status and cause PU.1 downregulation, including hexamethylene bisacetamide (HMBA), in the presence of

the iron source provided by porcine haemin [468, 506]. Even though the regulation of differentiation in this cell line differs considerably from that occurring in primary cells, it has been used extensively to study the terminal cellular events in the formation of mature RBCs [507].

I confirmed that the MEL585 line expressed ST2 by flow cytometry, though to a lesser extent than in primary cells (**Fig. 5.9**), and addition of IL-33 to cultures of proliferating or differentiating cells had no effect on cell expansion (**Fig. 5.10A**). Because Ter119 is expressed at very low levels by MEL585 cells [165], I also assessed progression of differentiation induced with HMBA by evaluating the surface expression of CD44, which is normally downregulated with maturation [166]. However, expression of neither marker was altered by IL-33 at various concentrations as cells underwent HMBA-induced differentiation (**Fig. 5.10B-C**). Because the surface phenotype of MEL585 cells differs from that of primary cells, I also evaluated progression of differentiation by measuring expression of the genes encoding the major globin chains (*Hbb-b1* and *Hba-a1*), cellular enzymes (aminolevulinic acid synthase 2, *Alas2*, and carbonic anhydrase, *Car1*), surface proteins (glycophorin A, *Gypa*, and band protein 4.1, *Epb41*) (**Fig. 5.11**), and transcription factors (GATA1, GATA2, KLF1, PU.1) (**Fig. 5.12**) by RT-qPCR. However, expression of none of these markers was affected by IL-33 over a period of 72 hours as cells underwent HMBA-induced differentiation.

Figure 5.9

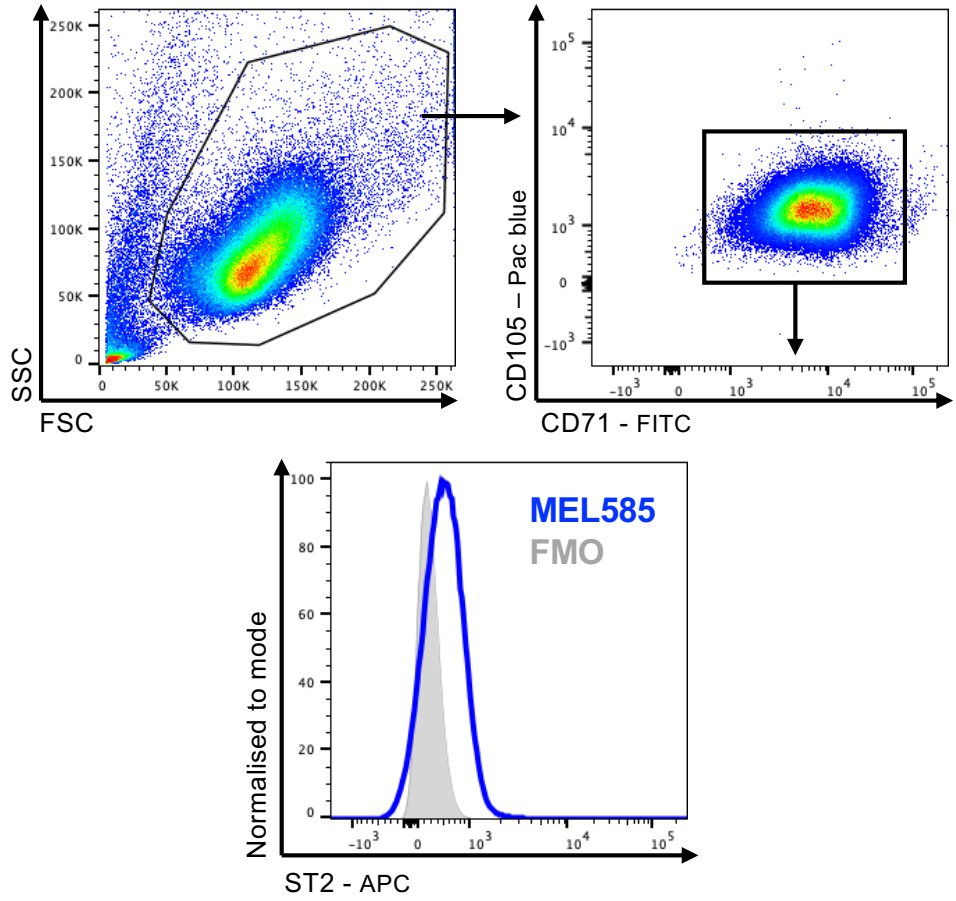

Figure 5.9: The MEL585 cell line expresses ST2
Representative flow cytometric images of MEL585 cells showing expression of the ST2 receptor. FMO: fluorescence minus one control.

Data representative of 2 independent experiments.

Figure 5.10

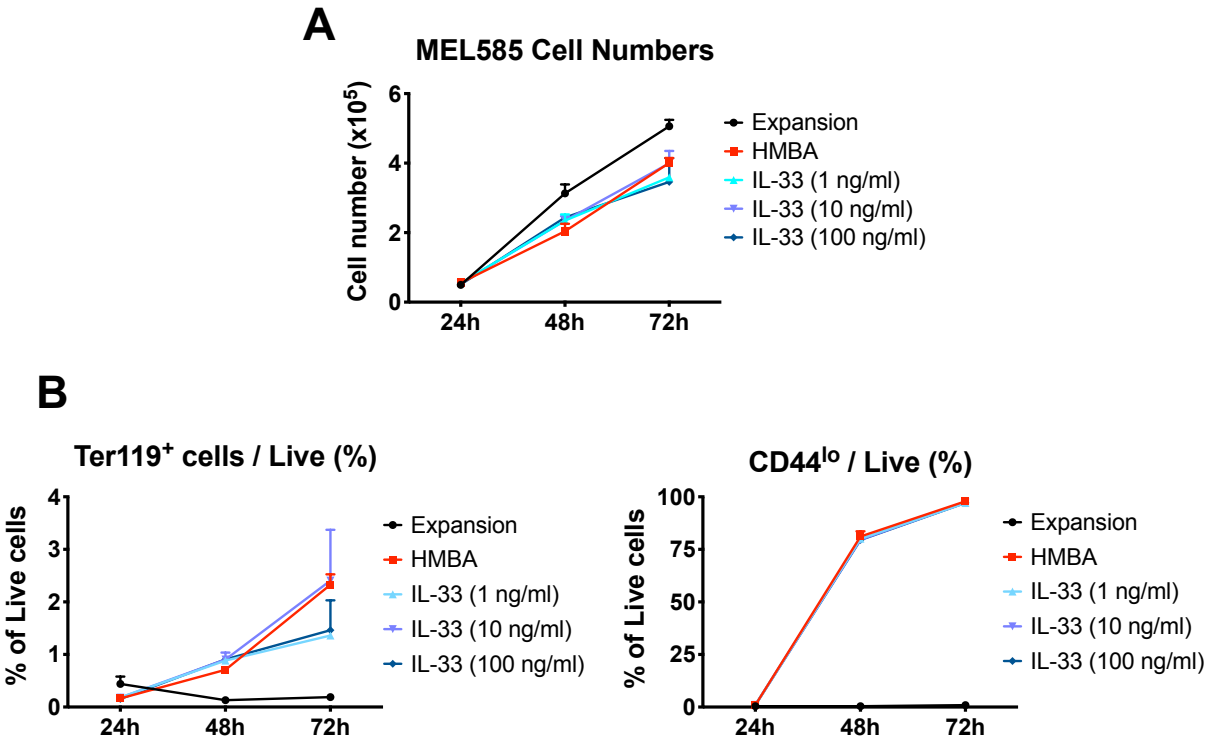

Figure 5.10: Proliferation and differentiation of MEL585 cells are unaffected by IL-33

(**A**) Number of MEL585 cells in culture over time under indicated conditions, with 10^4 starting cells per condition; IL-33 was added with HMBA. Points represent mean and SD of technical triplicates. HMBA: hexacetylene bisacetamide.

(**B**) Frequency of MEL585 cells expressing either Ter119 (Left) or losing expression of CD44 (Right) under indicated conditions in culture among total live cells. Points indicate mean and SD of technical triplicates.

Data representative of 2 independent experiments.

Figure 5.11

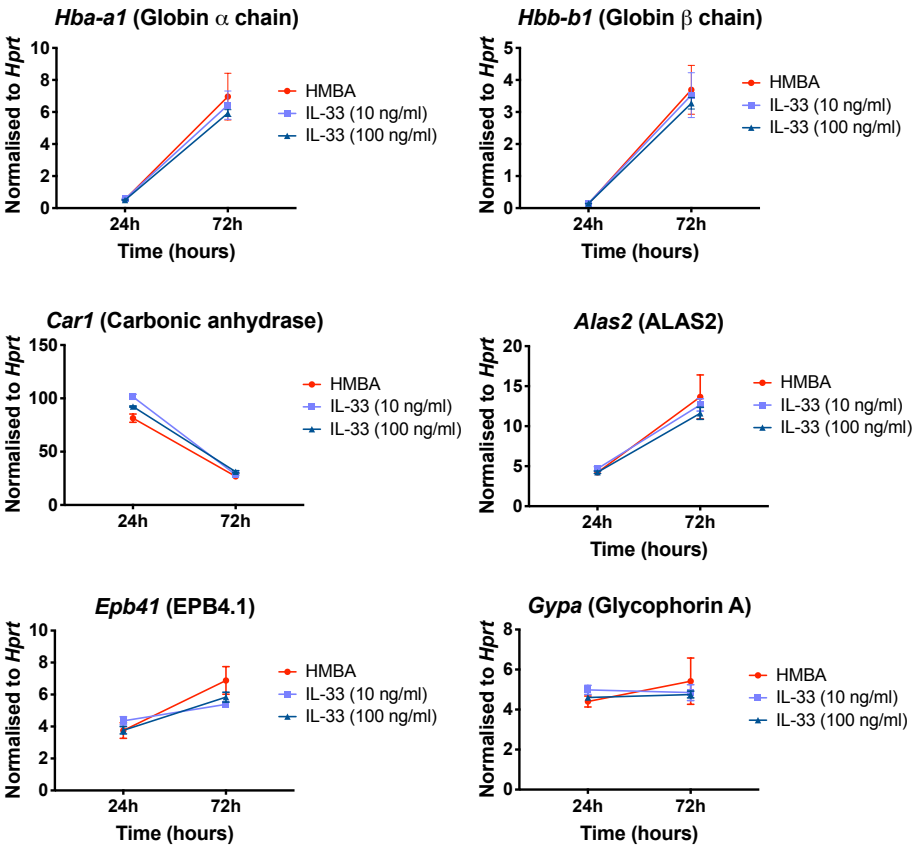

Figure 5.11: Gene expression in MEL585 cells is unaffected by IL-33 (I)
Expression of indicated genes by RT-qPCR in MEL585 cells in culture under indicated conditions over time; IL-33 was added with HMBA. Expression normalised to *Hprt*. Points represent mean and SD of technical triplicates for cultures.

Data from single experiment.

Figure 5.12

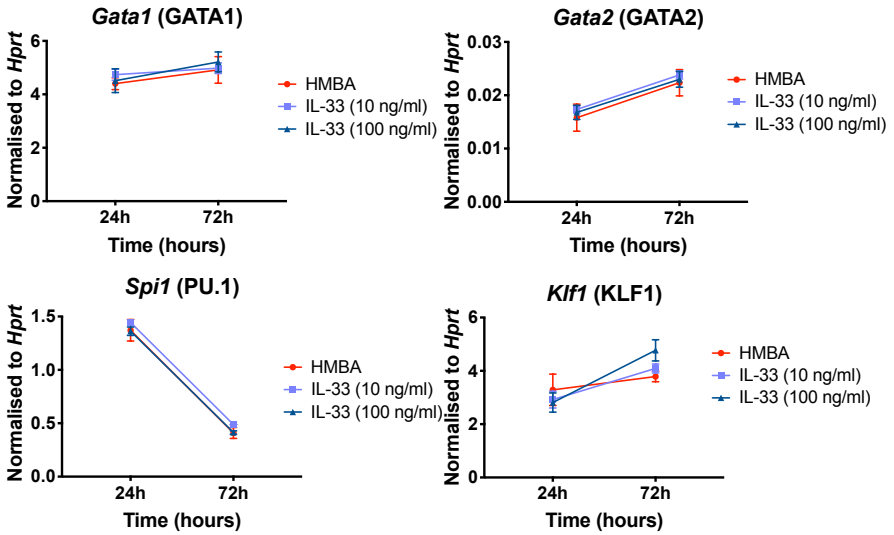

Figure 5.12: Gene expression in MEL585 cells is unaffected by IL-33 (II) Expression of indicated genes by RT-qPCR in MEL585 cells in culture under indicated conditions over time. Expression normalised to *Hprt*. Points represent mean and SD of technical triplicates for cultures.

Data from single experiment.

Collectively, this showed that although MEL585 cells expressed the ST2 receptor, IL-33 exerted no detectable effect on their proliferation or on their differentiation to mature RBCs when induced with HMBA. This could be related to aberrant signalling of the ST2 receptor or to the mutations causing transformation of the cell line, producing changes in cellular metabolism that negate the effects of IL-33. Specifically, MEL cells are EPO independent and may have increased Akt activity [508], which I identify later as a possible cellular pathway affected by IL-33 (**section 5.2.9**).

5.2.4 IL-33 is dispensable for erythropoiesis under homeostatic conditions

Having detected expression of its receptor at high levels on erythroid progenitors, I asked whether IL-33 had a role in erythropoiesis in healthy mice. However, mice lacking either the *Il33* (**Fig. 5.13A**) or *Il1rl1* (**Fig. 5.13B**) genes had normal Hgb concentrations and progenitor frequencies compared to WT counterparts, contrasting with a previous study that suggested BALB/C ST2$^{-/-}$ mice were anaemic compared to WT controls [509]. To determine whether IL-33$^{-/-}$ mice could have differences in erythropoiesis that were compensated owing to absence of IL-33 from birth, I measured serum EPO concentrations but found no difference between IL-33$^{-/-}$ and WT mice (**Fig. 5.13C**). Collectively, this suggested IL-33 was dispensable for maintenance of normal RBC mass and Hgb concentration under homeostatic conditions.

Figure 5.13

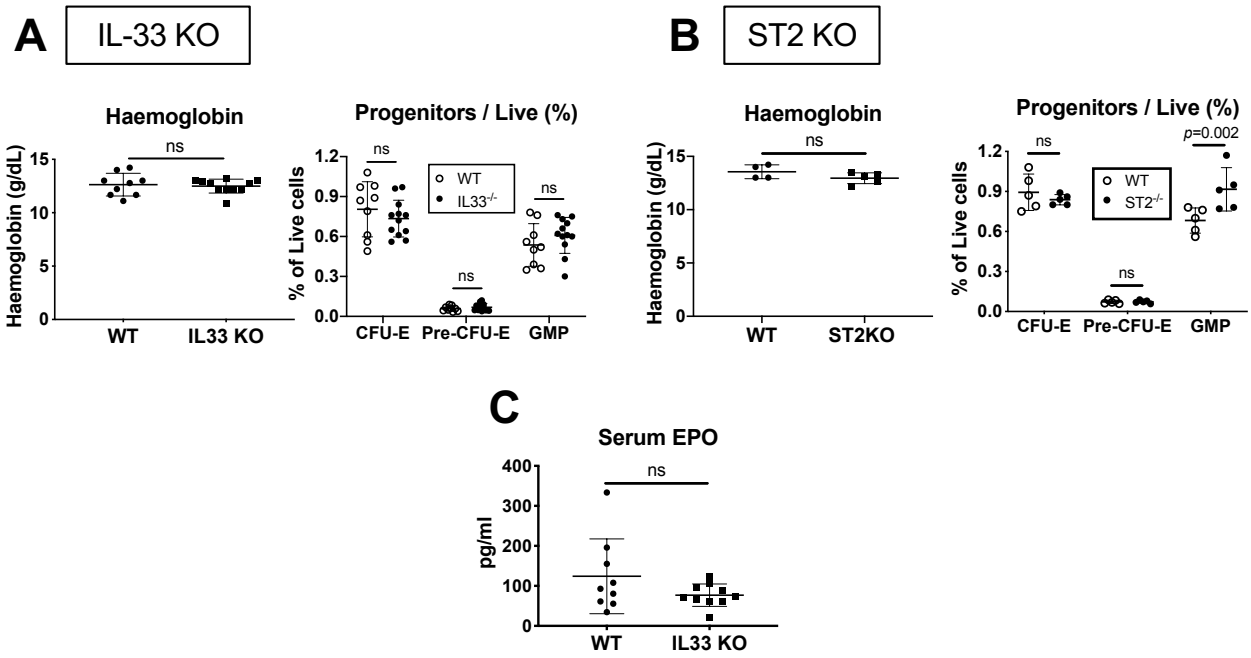

Figure 5.13: IL-33 is not required for erythropoiesis under homeostatic conditions

(**A**) (Left) Concentration of haemoglobin in blood of wild type C57BL/6 (WT) and IL-33$^{-/-}$ (IL33 KO) mice. Points represent individual mice with mean and SD, Mann-Whitney U test. (Right) Frequency of indicated progenitor populations among live BM cells of WT and IL33 KO mice. Points represent individual mice with mean, two-way ANOVA with Sidak's test.

(**B**) (Left) Concentration of haemoglobin in blood of wild type C57BL/6 (WT) and ST2$^{-/-}$ (ST2 KO) mice. Points represent individual mice with mean and SD, Mann-Whitney U test. (Right) Frequency of indicated progenitor populations among live BM cells of WT and ST2 KO mice. Points represent individual mice with mean, two-way ANOVA with Sidak's test.

(**C**) Concentration of erythropoietin (EPO) measured in serum using a bead-based multiplex assay in healthy WT and IL33 KO mice. Points represent individual mice with mean and SD, Mann-Whitney U test.

Data representative of 2 (**B**) or 5 (**A**) independent experiments or from a single experiment (**C**).

5.2.5 IL-33 is increased in the bone marrow niche with inflammation

To establish whether IL-33 is produced in the BM niche, I sorted major populations of haematopoietic and stromal cells by FACS using published definitions [113, 128, 136] and found the *Il33* gene, unlike the gene encoding the related cytokine IL-1β, was preferentially expressed in $CD169^+$, $F4/80^+$ macrophages (**Fig. 5.14A**), previously described as erythroblastic island macrophages that maintain close physical contact with erythroid progenitors in the BM and contribute to their retention and differentiation [136] (**see chapter 1.1.7**). Using mice expressing a citrine reporter in place of the *Il33* gene, I found these $CD169^+$ macrophages were abundant IL-33 producers in the BM, exceeding the numbers of $IL\text{-}33^+$ $Ter119^+$ and $CD45^-$ stromal cells described previously [369, 510] (**Fig. 5.14B**). After injecting curdlan to trigger SpA, the concentration of IL-33 measured in BM plasma increased rapidly (**Fig. 5.15A**) whereas its expression in $CD169^+$ macrophages decreased in mice with SpA (**Fig. 5.15B**). This suggests increased IL-33 production in inflamed tissues, which I describe further in **chapter 6** [441], may supersede local production in the BM niche, leading me to hypothesize that IL-33 could be a factor regulating erythropoiesis after curdlan injection. Importantly, the number of $CD169^+$ macrophages in the BM was not altered with SpA (**Fig. 5.15C**) or in IL-33-injected mice (**Fig. 5.15D**) compared to healthy controls. Therefore, the mechanism by which IL-33 perturbs erythropoiesis is distinct from that of G-CSF, which depletes $CD169^+$ macrophages in BM [511].

Figure 5.14

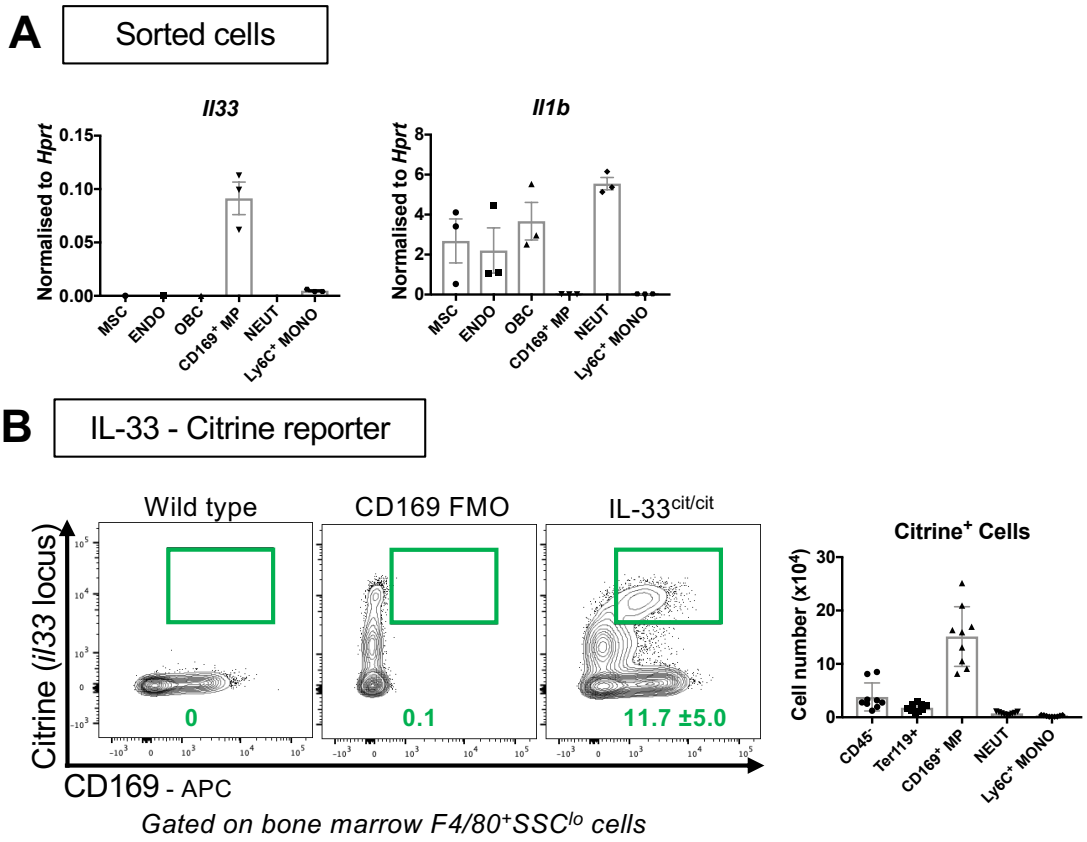

Figure 5.14: IL-33 is expressed in the bone marrow niche
(**A**) Expression of indicated genes in indicated cell populations sorted from BM of healthy SKG mice by RT-qPCR. Expression normalised to *Hprt*. Points show biological replicates, bars indicate mean and SEM. MSC: mesenchymal stem/stromal cell, ENDO: endothelium, OBC: osteoblastic lineage cell, MP: macrophage, NEUT: neutrophil, MONO: monocyte.
(**B**) (Left) Representative flow cytometric images of expression of citrine reporter in the *Il33* locus in C57BL/6 (wild type) and reporter (IL-33$^{cit/cit}$) mice. Figures show mean and SD for n=5 mice. FMO: fluorescence minus one control. (Right) Absolute number of indicated cells expressing citrine in the BM of one femur and one tibia. Points represent individual mice, bars show mean with SD.

Data from 3 independent experiments.

Figure 5.15

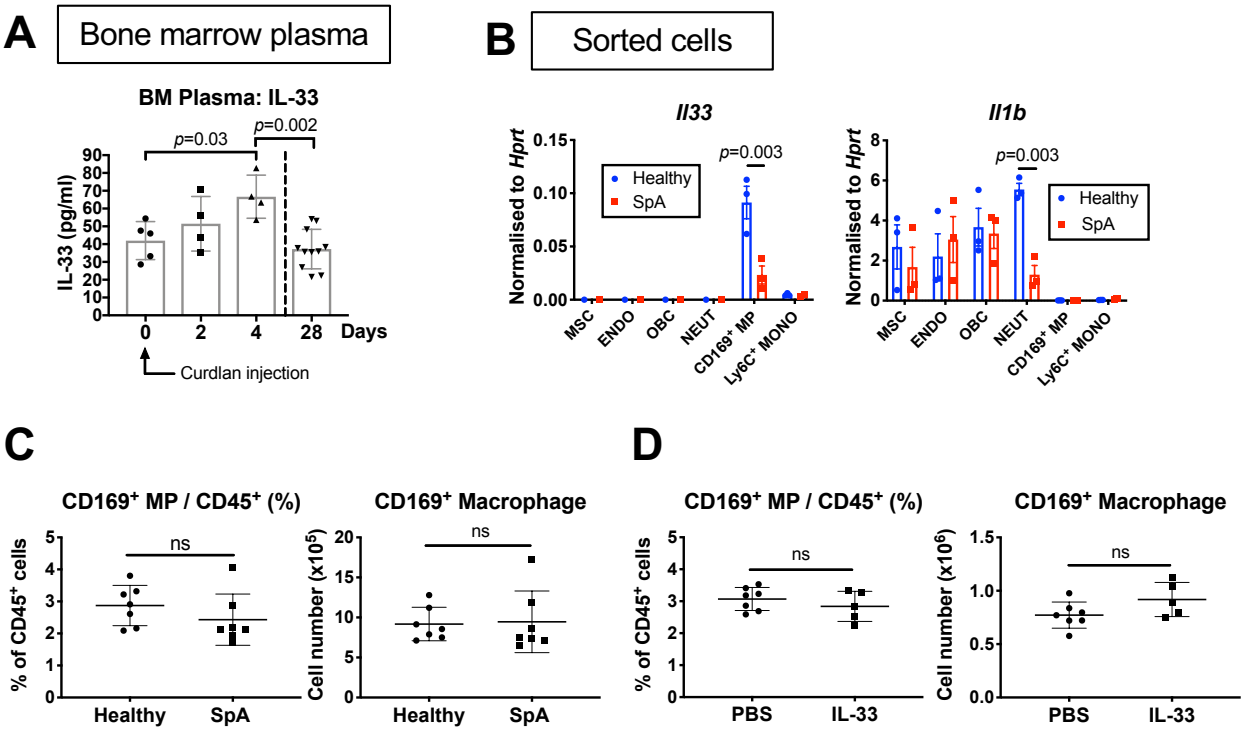

Figure 5.15: IL-33 is increased in the bone marrow with inflammation
(**A**) Concentration of IL-33 measured by ELISA in BM plasma of SKG mice injected with curdlan then culled at indicated times. Points represent individual mice, bars show mean with SD. One-way ANOVA with Tukey's test.
(**B**) Expression of indicated cytokine genes in indicated populations of BM cells sorted by FACS from SKG 4 weeks after curdlan or PBS injection. Expression normalised to *Hprt*. Points represent biological replicates, bars indicate mean and SEM, two-way ANOVA with Sidak's test. MSC: mesenchymal stem/stromal cell, ENDO: endothelium, OBC: osteoblastic lineage cell, MP: macrophage, NEUT: neutrophil, MONO: monocyte.
(**C**) Frequency and absolute number of CD169+, F4/80+ macrophages (MP) in BM of SKG 4 weeks after curdlan or PBS injection.
(**D**) Frequency and absolute number of CD169+, F4/80+ macrophages (MP) in BM of healthy SKG mice and mice injected with IL-33 or PBS for 4 weeks.
For (**C**)-(**D**), points represent individual mice with mean and SD, Mann-Whitney U test.

Data representative of 2 (**A**), (**C**), (**D**) or contain data from 3 (**B**) independent experiments.

5.2.6 IL-33 is required for curdlan-induced suppression of erythropoiesis

Interleukin-33 suppressed differentiation of erythroid progenitors *ex vivo* and was increased in BM after induction of inflammation. Against this backdrop, I investigated the functional role of IL-33 in AID by injecting SKG mice with curdlan to trigger SpA then injecting either polyclonal anti-IL-33 antibodies or a control preparation of goat IgG1 antibodies as disease developed. I opted to cull these mice after only 10 days because I noted that the concentration of IL-33 in BM plasma was increased 4 days after curdlan injection but had decreased by 4 weeks (**Fig. 5.15A**), suggesting it might have an early effect on BM erythropoiesis. Accordingly, I found those mice treated with anti-IL-33 antibodies had a higher blood Hgb concentration (**Fig. 5.16A**) and frequency of CFU-Es and mature $Ter119^{+}$ cells in BM compared to controls after 10 days (**Fig. 5.16B**). To confirm this, I also injected curdlan in mice lacking the *Il33* gene ($IL\text{-}33^{-/-}$) and matched WT C57BL/6 controls (**Fig. 5.17A**). Whereas the frequency of erythroid progenitors decreased significantly in WT mice with this treatment, there was no significant reduction in CFU-Es in $IL\text{-}33^{-/-}$ mice receiving either PBS or curdlan when results from individual mice were pooled or compared across independent experiments (**Fig. 5.17B**), with a less striking difference in the number of cells (**Fig. 5.17C**).

Figure 5.16

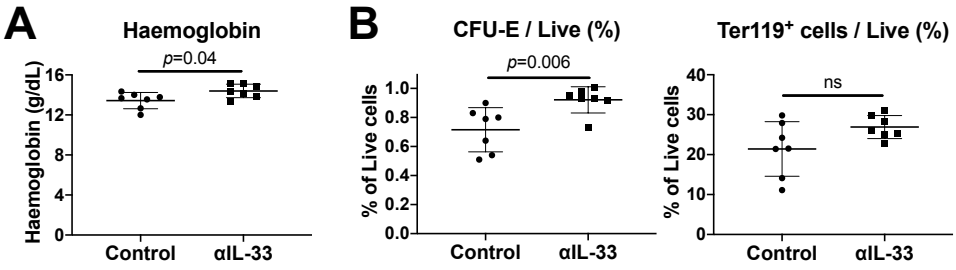

Figure 5.16: IL-33 is implicated in anaemia of inflammation in murine SpA
(**A**) Concentration of haemoglobin in blood of SKG mice injected with curdlan then either polyclonal anti-IL-33 antibodies (αIL-33) or control goat IgG1 antibodies (Control) for 10 days before culling.
(**B**) Frequency of CFU-Es (Left) and Ter119$^+$ cells (Right) in BM.
For (**A**)-(**B**), points represent individual mice with mean and SD, Mann-Whitney U test.

Data from a single experiment.

Figure 5.17

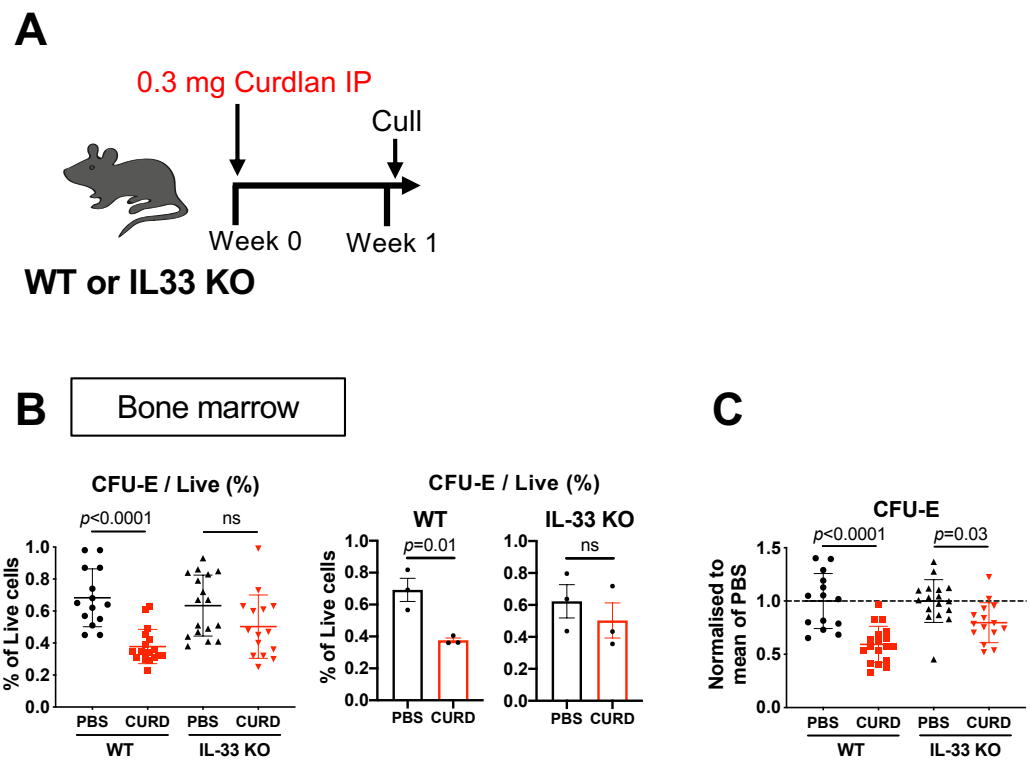

Figure 5.17: IL-33 is implicated in anaemia of inflammation in C57BL/6 mice
(**A**) Schematic diagram showing injection of curdlan IP in either C57BL/6 wild type (WT) mice or IL-33$^{-/-}$ (IL33 KO) mice before culling after 1 week to obtain data shown in (**B**)-(**C**).
(**B**) Frequency of CFU-Es among live BM cells; either as data pooled from 3 independent experiments (Left) or as mean of separate experiments, each with n=5-6 mice per group (Right). Left: points represent individual mice with mean, one-way ANOVA with Tukey's test. Right: Points represent mean of independent experiments, bars show mean with SEM, Student's t test.
(**C**) Number of CFU-Es in 1 femur and 1 tibia. Results are pooled from 3 independent experiments, with individual results normalised to the mean of the PBS control for that experiment. Points represent individual mice with mean and SD, one-way ANOVA with Tukey's test.

Data pooled from 3 independent experiments.

Having shown it was necessary for complete curdlan-induced suppression of BM erythropoiesis, I next asked whether administration of IL-33 alone would be sufficient to produce the same hematopoietic changes as curdlan. I therefore injected SKG mice with IL-33 over 1 week (**Fig. 5.18A**); this treatment caused

marked reductions in the frequency and absolute number of erythroid progenitors, to a similar extent as observed with curdlan injection (**Fig. 5.18B-C**). Changes in BM cell numbers were also reflected in functional differences in colony formation, with an increased number of myeloid (CFU-GM) and decreased number of erythroid (BFU-E) colonies observed with addition of IL-33 to whole BM in methylcellulose medium (**Fig. 5.18C**).

Figure 5.18

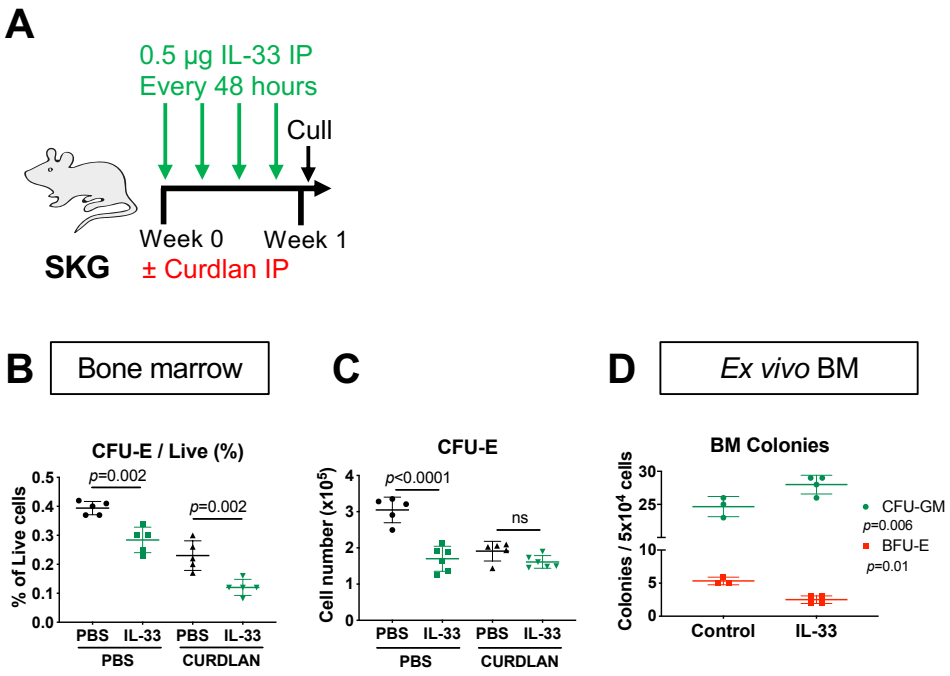

Figure 5.18: IL-33 suppresses erythropoiesis *in vivo*
(**A**) Schematic diagram showing injection of IL-33, with or without curdlan, in SKG before culling after 1 week to obtain data shown in (**B**)-(**C**).
(**B**) Frequency of CFU-Es among live BM cells. Points represent individual mice with mean and SD, one-way ANOVA with Tukey's test.
(**C**) Number of CFU-Es in 1 femur and 1 tibia. Points represent individual mice with mean and SD, one-way ANOVA with Tukey's test.
(**D**) Number of colonies derived from $5x10^4$ whole BM cells plated in methylcellulose medium with or without IL-33 for 10 days. Points indicate individual mice with mean and SD, two-way ANOVA with Sidak's test. CFU-GM: colony forming unit granulocyte macrophage, BFU-E: blast-forming unit erythroid.

Data representative of 4 (**A**)-(**C**) or 2 (**D**) independent experiments.

In mast cells and eosinophils, IL-33 causes production of other pro-inflammatory cytokines that may suppress erythropoiesis, including TNF-α and IL-6 [343, 512]. Accordingly, I found the concentration of TNF-α, but not IL-6, was increased in BM plasma of mice injected with IL-33 (**Fig. 5.19A**). To determine whether these cytokines were required, I injected IL-33 in mice lacking IL-6 or the receptors for TNF-α (TNFRI and TNFRII), but, in all three strains, IL-33 produced similar suppression of erythropoiesis, indicating they were dispensable for those effects (**Fig. 5.19B-D**). To establish definitively whether IL-33 was exerting direct effects on erythroid progenitors *in vivo*, I produced mixed BM chimeras, comprising a 1:1 mixture of $ST2^{-/-}$ and Ub-GFP WT BM injected into lethally irradiated Ub-GFP recipients (**Fig. 5.20A**). After 8 weeks, I injected these chimeras with PBS or curdlan and culled them after a further week to evaluate the BM. Among pre-CFU-Es, absence of ST2 provided a small advantage at steady state and after curdlan injection, indicating that IL-33 was affecting these cells directly *in vivo* (**Fig. 5.20B**). However, this effect was relatively minor compared to the reduction in pre-CFU-E frequency after curdlan injection, indicating that other cytokines induced by curdlan probably make a substantial contribution to suppression of erythropoiesis, as also suggested by my results when injecting curdlan in $IL\text{-}33^{-/-}$ mice. Although there was no difference between genotypes in the frequency of the more numerous CFU-E progenitors, a similar pattern was observed when analysing all $Ter119^{+}$ cells in BM (**Fig. 5.20B**), suggesting the effect of IL-33 on pre-CFU-Es translates into a reduced frequency of mature erythroid cells.

Figure 5.19

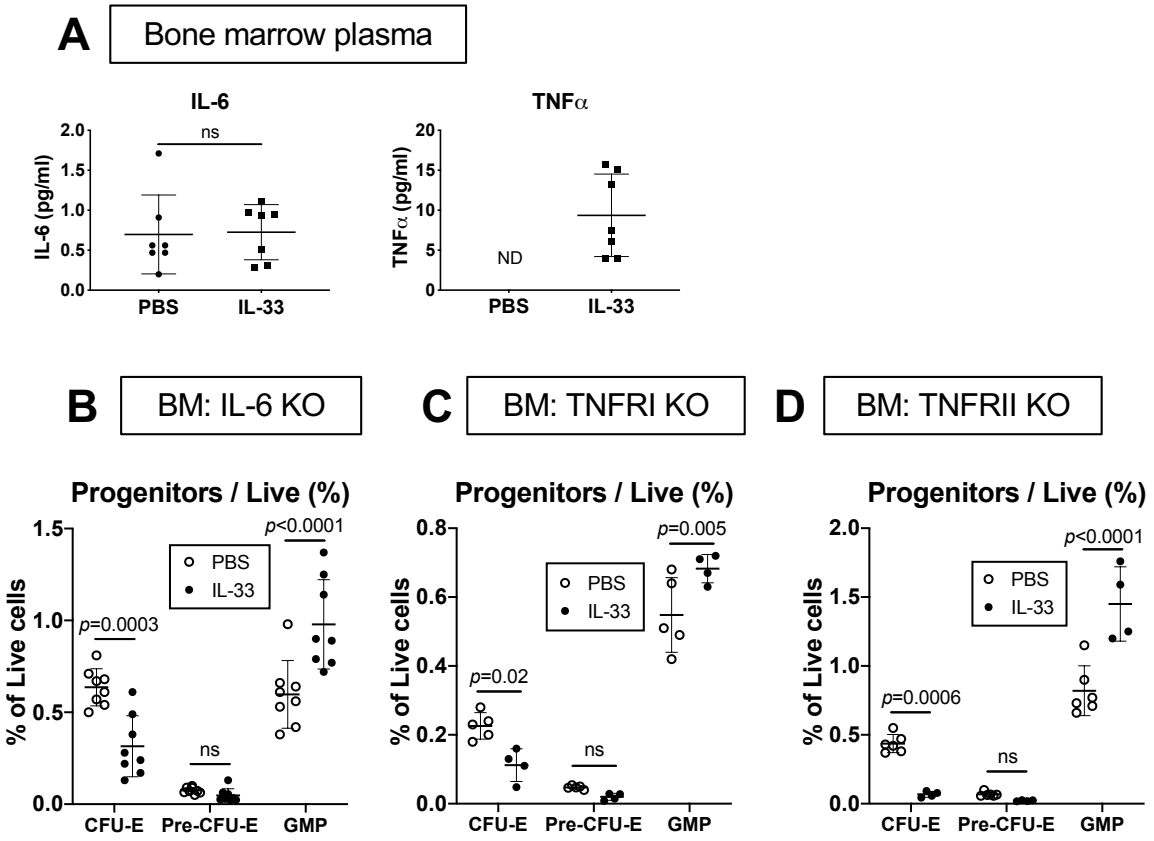

Figure 5.19: Effects of IL-33 are not dependent on IL-6 or TNFR signalling
(**A**) Concentrations of indicated cytokines measured by bead-based multiplex assay (IL-6) or ELISA (TNF-α) in BM plasma of healthy SKG mice injected with PBS or IL-33 for 1 week. Points indicate individual mice with mean and SD, Mann-Whitney U test. ND: not detected.
(**B**) Frequency of indicated progenitor populations among total live BM cells of IL-6$^{-/-}$ (IL-6 KO) mice injected with PBS or IL-33 for 1 week.
(**C**) Frequency of indicated progenitor populations among total live BM cells of TNFRI$^{-/-}$ (TNFRI KO) mice injected with PBS or IL-33 for 1 week.
(**D**) Frequency of indicated progenitor populations among total live BM cells of TNFRII$^{-/-}$ (TNFRII KO) mice injected with PBS or IL-33 for 1 week.
For (**B**)-(**D**), points represent individual mice with mean, two-way ANOVA with Sidak's test.

Data representative of 2 independent experiments.

Figure 5.20

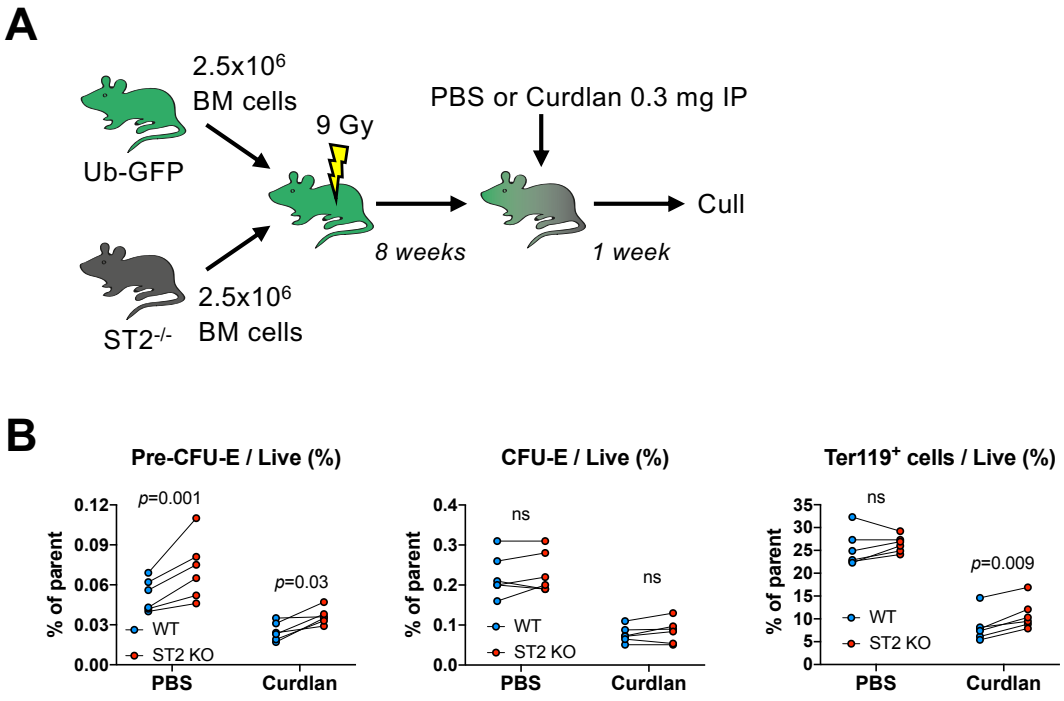

Figure 5.20: Effects of IL-33 on erythropoiesis *in vivo* are predominantly indirect
(**A**) Schematic diagram showing generation of mixed BM chimeras by injection of a 1:1 mixture whole BM from wild type Ub-GFP and ST2$^{-/-}$ mice in lethally irradiated Ub-GFP recipients. Mice were injected with PBS, curdlan, or IL-33 after 8 weeks then culled 1 week later to obtain data shown in (**B**).
(**B**) Frequency of indicated progenitors and of Ter119^{+} cells among parent BM populations in chimeras described in (**A**). Points represent genotypes in the same mouse linked by a line, two-way ANOVA with Sidak's test.

Data from a single experiment.

At a cellular level, I found the proportion of erythroid progenitors expressing Ki67 (**Fig. 5.21A**) and incorporating BrdU (**Fig. 5.21B**) was decreased when IL-33 was injected *in vivo* in healthy SKG mice, an effect that was not apparent in *ex vivo* cultures of the same cells (**Fig. 5.6C**). The proportion of cells in the early phase of apoptosis, indicated by expression of annexin V, was also decreased (**Fig. 5.21C**), which could have been a compensatory response, possibly mediated by increased

EPO production. In the transcriptome, there was a striking reduction in expression of the genes encoding the adult globin chains (*Hbb-b1* and *Hbb-a1*), forming the proteinaceous component of Hgb, in FACS-sorted pre-CFU-Es from mice exposed to IL-33 for 1 week compared to controls (**Fig. 5.22A**). There were similar reductions in expression of other genes required for production of mature RBCs, including those encoding the haem enzyme ALAS2 (*Alas2*) and the major surface proteins glycophorin A (*Gypa*), erythroid band protein 4.1 (*Epb41*), and aquaporin 1 (*Aqp1*) (**Fig. 5.22B**). Interleukin-33 exerted no significant effects on expression of genes encoding major erythroid transcription factors such as GATA1, GATA2, and KLF1 (**Fig. 5.22C**). With prolonged exposure to IL-33 over 4 weeks (**Fig. 5.23A**), these changes in cellular activity resulted in a decreased frequency of $Ter119^{+}$ erythroid cells in BM (**Fig. 5.23B**) and decreased Hgb concentrations and RBC counts in peripheral blood (**Fig. 5.23C**). These changes were dependent on inhibition of BM erythropoiesis because there was no significant change in the frequency of erythroid progenitors in the spleen (**Fig. 5.23D**).

Taken together, these observations demonstrate that IL-33 is both necessary and sufficient for the full extent of curdlan-induced suppression of erythropoiesis. Remarkably, injection of IL-33 alone decreased expression of globin and haem synthesis enzyme genes, resulting in decreased blood Hgb with prolonged exposure. *In vivo*, IL-33 caused decreased proliferation of erythroid progenitors, as assessed by Ki67 expression and BrdU incorporation, but this is likely to have been an indirect effect because it was not observed when the same cells were cultured with IL-33 *ex vivo*.

Figure 5.21

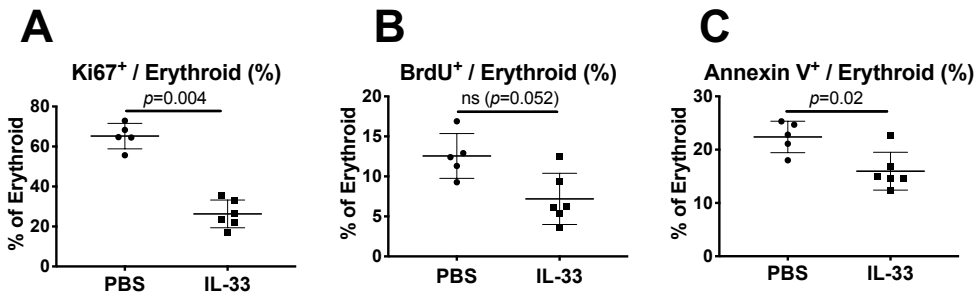

Figure 5.21: IL-33 inhibits proliferation of erythroid progenitors *in vivo*
(**A**) Frequency of erythroid progenitors (CFU-E and pre-CFU-E) expressing Ki67 by flow cytometry in BM of healthy SKG mice injected with PBS or IL-33 for 1 week.
(**B**) Frequency of erythroid progenitors incorporating bromodeoxyuridine (BrdU) by flow cytometry in BM of healthy SKG mice injected with PBS or IL-33 for 1 week. BrdU was injected 6 hours before culling.
(**C**) Frequency of erythroid progenitors expressing annexin V by flow cytometry in BM of healthy SKG mice injected with PBS or IL-33 for 1 week.
For (**A**)-(**C**), points represent individual mice with mean and SD, Mann-Whitney U test.

Data representative of 2 independent experiments.

Figure 5.22 Sorted erythroid progenitors

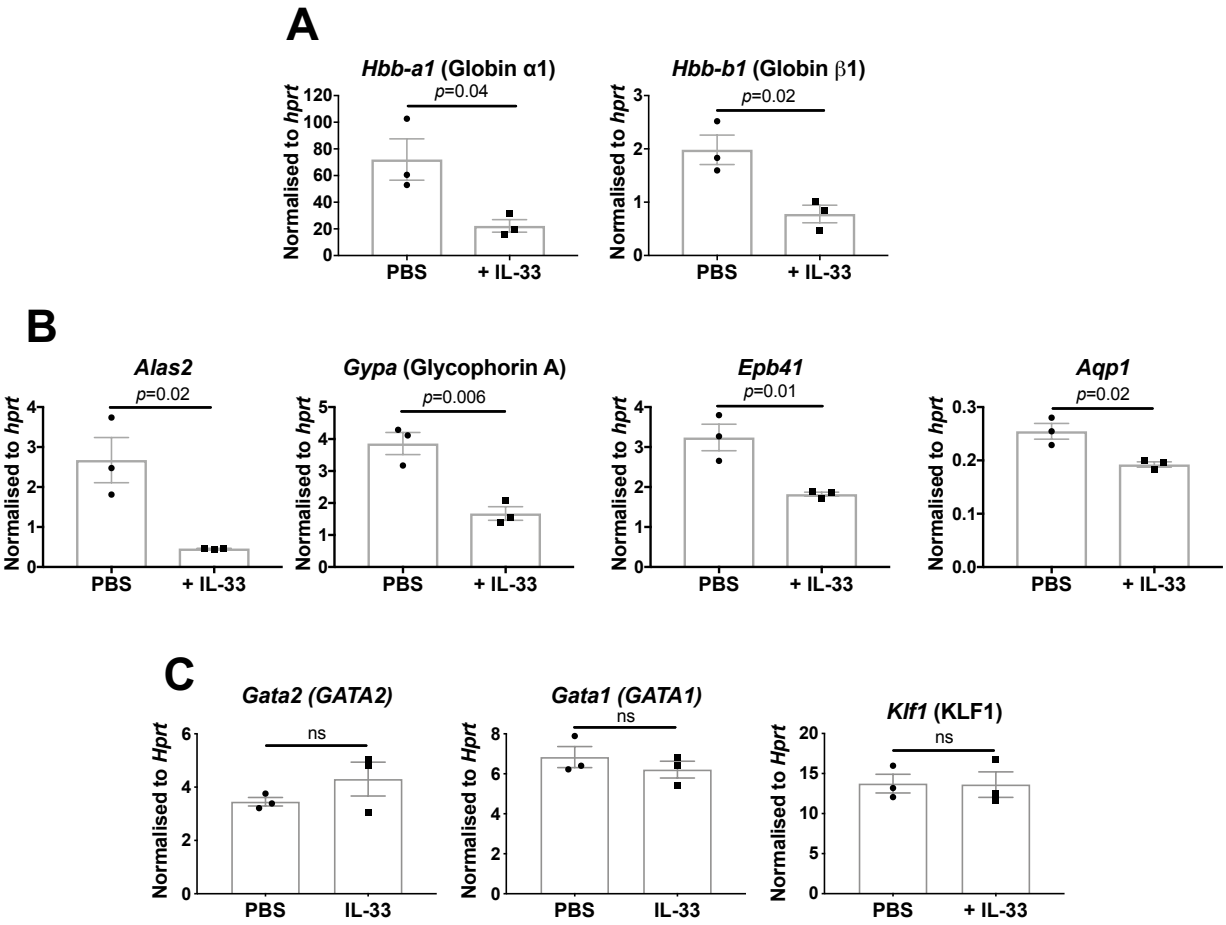

Figure 5.22: IL-33 decreases expression of globin genes *in vivo*
(**A**)-(**C**) Expression of indicated genes by RT-qPCR in pre-CFU-E cells sorted by FACS from healthy SKG mice injected with PBS or IL-33 for 1 week. Expression normalised to *Hprt*. Points represent biological replicates, each with n=2 mice, bars show mean with SEM, Student's t test.

Data from independent replicates.

Figure 5.23

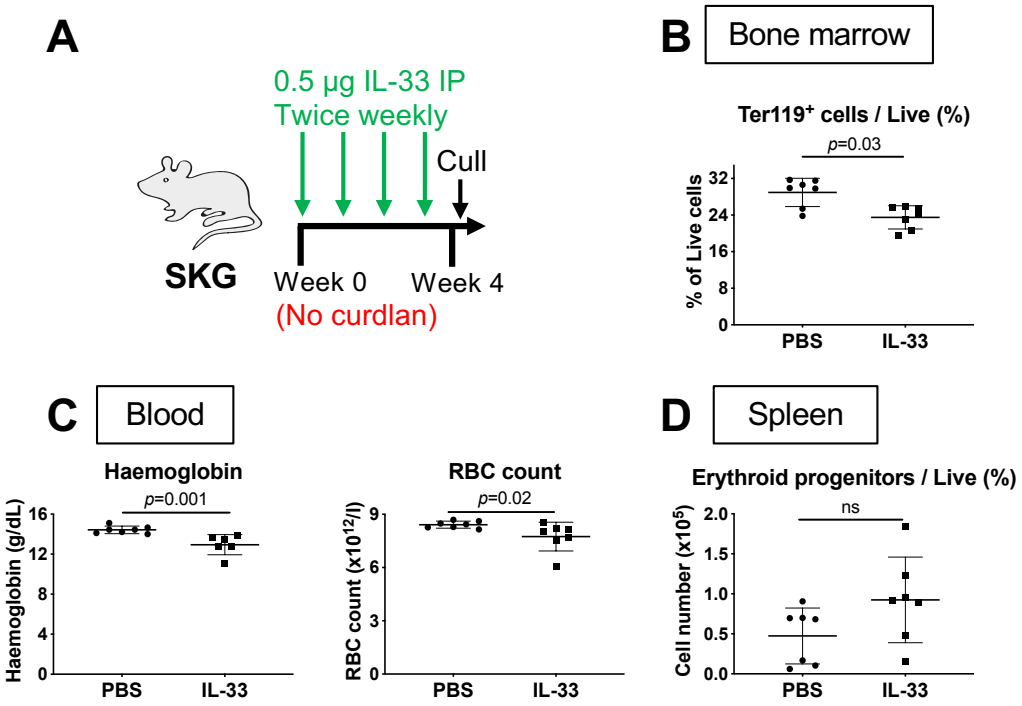

Figure 5.23: IL-33 causes anaemia when injected for 4 weeks
(**A**) Schematic diagram showing injection of PBS or IL-33 in healthy mice for 4 weeks before culling to obtain data shown in (**B**)-(**D**).
(**B**) Frequency of Ter119$^+$ cells among total live BM cells.
(**C**) Concentration of haemoglobin and red blood cell (RBC) count in blood.
(**D**) Frequency of erythroid progenitors among total live splenocytes.
For (**B**)-(**D**), points represent individual mice with mean and SD, Mann-Whitney U test.

Data representative of 2 independent experiments.

5.2.7 The effects of IL-33 in erythroid progenitors are dependent on NF-kB

To explore the transcriptomic events occurring after erythroid progenitors are exposed to IL-33, I sorted pre-CFU-Es from healthy mice and cultured them for 6 hours *ex vivo* before performing bulk RNA sequencing analysis (**Fig. 5.24A**). I chose to do bulk RNA sequencing because I was sorting cells already committed to the erythroid lineage for which surface marker expression is relatively homogeneous; single cell sequencing would have been of greater utility if investigating cells that were still multipotent. Control and IL-33-exposed pre-CFU-Es clustered separately based on differential expression of 482 genes, of which 388 were upregulated and 94 downregulated (**Fig. 5.24B**). Among those genes downregulated were several with known roles in erythroid differentiation, including vimentin (*Vim*) required for enucleation [513], the enzyme coproporphyrinogen III oxidase (*Cpox*) required for Hgb synthesis [514], cytidine deaminase (*Cda*) required for pyrimidine recycling in erythroid progenitors [515, 516], and the serine/threonine kinase Pim-1 (*Pim1*), of which deficiency causes microcytosis and anaemia in mice [193] (**Fig. 5.24C-D**). Conversely, CD69, which inhibits erythroid differentiation [517], was upregulated.

Figure 5.24

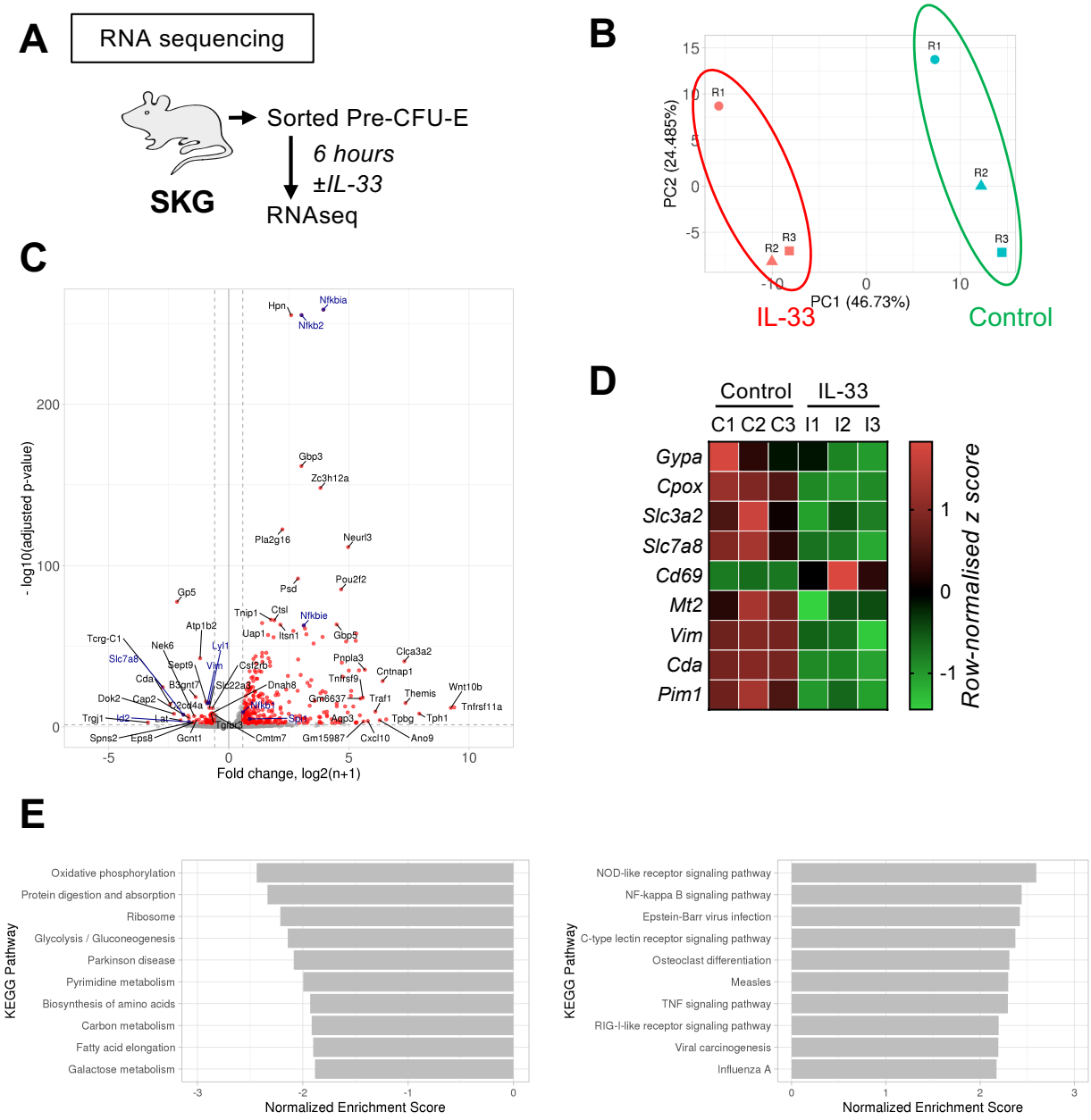

Figure 5.24: IL-33 changes gene expression in erythroid progenitors
(**A**) Schematic diagram showing incubation of pre-CFU-Es sorted by FACS from healthy SKG mice with IL-33 or control for 6 hours before extracting RNA for bulk sequencing to generate data shown in (**B**)-(**E**).
(**B**) Scatter plot showing largest principal components (PCs) for differentially regulated genes in pre-CFU-E cells exposed to IL-33 or control medium. Points represent biological replicates.
(**C**) Volcano plot showing differential expression of genes from cells described in (**A**). Genes marked in red are changed 1.5 fold with adjusted *p* value <0.01. Genes of interest are highlighted in blue.
(**D**) Heatmap showing expression of indicated genes of interest in cells described in (**A**), normalised to row means. Columns represent paired biological replicates.
(**E**) Bar charts showing enrichment of most significantly downregulated (Left) and upregulated (Right) KEGG pathways among differentially regulated genes for cells described in (**A**).

Data analysed by Dr Lada Koneva, University of Oxford, and reproduced here with her permission

Among the genes strikingly upregulated by IL-33 were many members of the NF-kB pathway, and a gene set encompassing known NF-kB targets was among the KEGG pathways most significantly enriched in the upregulated genes (**Fig. 5.24E**). Interleukin-33, in common with other members of the IL-1 cytokine family, is known to cause NF-kB activation in other cell types [518], and I found members of both canonical and non-canonical pathways were upregulated in erythroid progenitors (**Fig. 5.25A-B**). To confirm that transcriptional differences in NF-KB expression were reflected in functional changes inside the cell, I stimulated preparations of BM cells depleted of mature cells with IL-33 for 30 minutes and then assessed the localisation of the p65 subunit (encoded by *Rela* in the canonical pathway) by imaging flow cytometry (**Fig. 5.25C**). Under steady state conditions, p65 was chiefly located in the cytoplasm but, with IL-33 stimulation, the proportion of cells with predominantly nuclear localisation was significantly increased (**Fig. 5.25D**), indicating NF-kB complexes were translocating into the nucleus. To determine whether this effect was necessary for IL-33-induced suppression of differentiation, I inhibited the canonical NF-kB pathway using a NEMO-domain binding (NBD) peptide that inhibits IκB kinase (IKK)γ [462]. In cultures of sorted pre-CFU-Es, inclusion of this peptide inhibited the effect of IL-33, alleviating its suppression of development of $Ter119^{+}$ cells by ~50% (**Fig. 5.26A-B**). Collectively, these observations confirmed that activation of NF-kB signalling, which normally decreases with progressive erythroid maturation [519], was required for the suppressive action of IL-33.

Figure 5.25

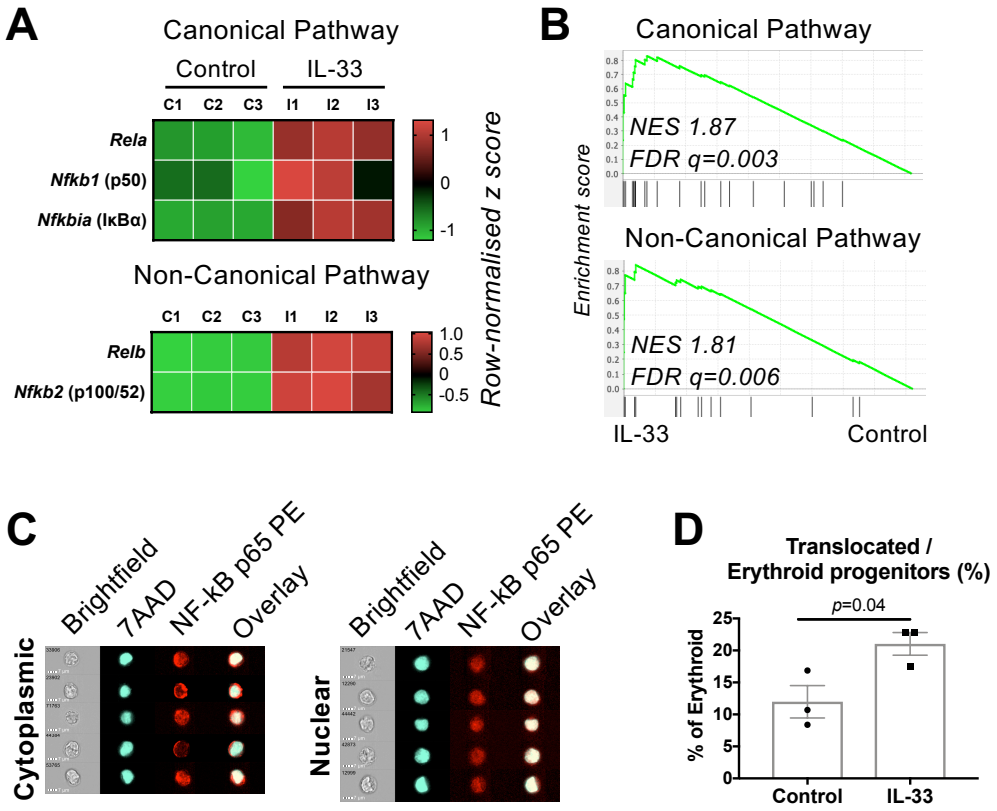

Figure 5.25: IL-33 upregulates NF-kB in erythroid progenitors
(**A**) Expression of selected members of NF-kB signalling pathways by RNA sequencing of FACS-sorted pre-CFU-E progenitors exposed to IL-33 or control medium for 6 hours *ex vivo*. Expression normalised to row means, columns show biological replicates.
(**B**) Enrichment of genesets incorporating NF-kB pathway members among genes differentially regulated by IL-33 in cells described in (**A**). NES: normalised enrichment score, FDR: false discovery rate.
(**C**) Representative images of erythroid progenitors from healthy BM of SKG mice by imaging flow cytometry, showing either cytoplasmic or nuclear localisation of the NF-kB p65 protein. Nuclear location is shown by 7AAD staining.
(**D**) Frequency of erythroid progenitors with predominantly nuclear localisation of p65 after exposure to PBS or IL-33 for 30 minutes. Points represent mean of replicates from independent experiments, bars shown mean with SEM, Student's t test.

Data from 3 independent experiments (**D**).

Figure 5.26

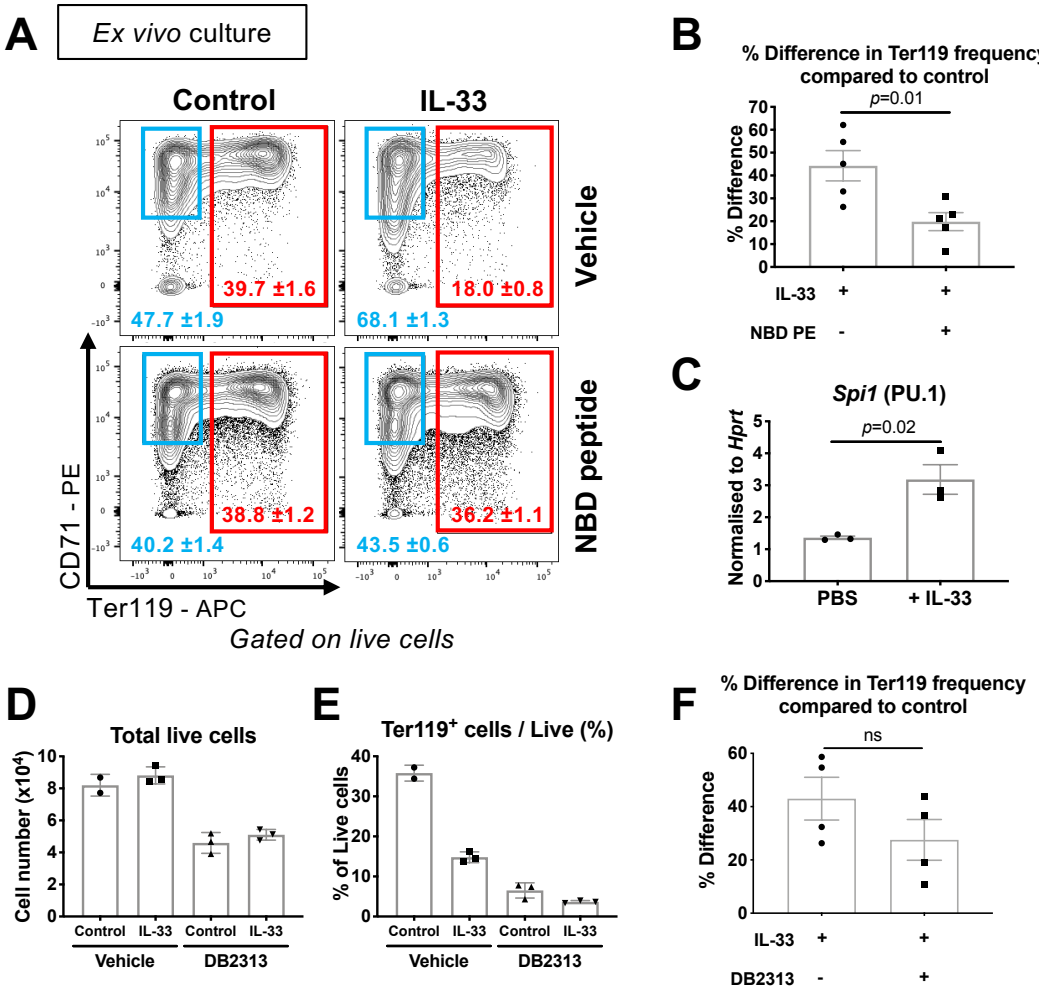

Figure 5.26: NF-kB activation is required but PU.1 activity is not for the effect of IL-33 in erythroid progenitors

(**A**) Representative flow cytometric images of cells derived from culture of FACS-sorted pre-CFU-Es for 4 days with or without IL-33 and NEMO binding domain (NBD) peptide, which inhibits the NF-Kb canonical pathway. Figures show mean and SD frequencies among total live cells for technical triplicates of a single experiment.

(**B**) Change in frequency of Ter119⁺ cells among total live cells derived from cultures described in (**A**), with or without the NBD peptide. Points represent mean of technical replicates from independent experiments, bars indicate mean with SEM, Mann-Whitney U test.

(**C**) Expression of *Spi1*, encoding PU.1, by RT-qPCR in pre-CFU-Es sorted by FACS from mice injected with PBS or IL-33 for 1 week. Expression normalised to Hprt. Points represent biological replicates, each with n=2 mice, bars indicate mean with SEM, Student's t test.

(**D**) Number of cells derived from FACS-sorted pre-CFU-Es cultured for 4 days with or without IL-33 or the PU.1 inhibitor DB2313. Points represent technical triplicates from a single experiment, bars indicate mean and SD.

(**E**) Frequency of Ter119⁺ cells among total live cells from cells described in (**D**). Points represent technical triplicates from a single experiment, bars indicate mean and SD.

(**F**) Change in frequency of Ter119⁺ cells among total live cells derived from cultures described in (**D**), with or without the PU.1 inhibitor DB2313. Points represent mean of technical replicates from independent experiments, bars indicate mean with SEM, Mann-Whitney U test.

Data from or representative of 4 (**D**)-(**F**) or 5 (**A**)-(**B**) independent experiments.

5.2.8 PU.1 is not required for the suppressive actions of IL-33 on erythropoiesis

Among the other genes significantly upregulated by IL-33 in the RNA sequencing analysis was *Spi1* (**Fig. 5.24C**), which encodes the transcription factor PU.1. I confirmed that *Spi1* was also upregulated in pre-CFU-Es sorted by FACS from mice injected with IL-33 for 1 week compared to controls (**Fig. 5.26C**). Previous studies show that PU.1 is not required for early specification of the erythroid lineage but is needed for terminal maturation, to the extent that PU.1 knockout mice die shortly after birth owing to severe anaemia [154, 520, 521]. However, PU.1 is normally downregulated as erythroid progenitors transition from the pre-CFU-E to CFU-E stage, and forced expression of PU.1 in these cells prevents terminal differentiation by arresting cells at the pre-CFU-E stage [162, 506]. At a molecular level, this effect is mediated partly by direct interaction between PU.1 and the critical erythroid transcription factor GATA1, with PU.1 preventing expression of important GATA1 targets required for erythroid differentiation [162, 522, 523]. Owing to these observations, I considered that PU.1 upregulation induced by IL-33 could be an important mechanism explaining the observed phenotype of inhibited differentiation in erythroid progenitors, as has been described recently for IFN-γ in human erythroid progenitors [269]. To test this, I used a newly described small molecule inhibitor of PU.1, DB2313 [463], in cultures with IL-33. Unlike the NF-kB inhibitory peptide, I found DB2313 1) resulted in a greatly reduced cell yield after 4 days of culture of primary pre-CFU-Es (**Fig. 5.26D**), and 2) significantly inhibited the emergence of $Ter119^{+}$ cells from pre-CFU-Es compared to control samples (**Fig. 5.26E**). Nevertheless, an inhibitory effect of IL-33 could still be appreciated against this background, with no significant change in

the suppression of development of Ter119^{+} cells across experiments (**Fig. 5.26F**). This showed that although the gene PU.1 was upregulated by IL-33 in erythroid progenitors, it did not appear to be necessary for the effect of IL-33 to suppress differentiation.

5.2.9 IL-33 inhibits phosphorylation events downstream of the EPO receptor, producing resistance to EPO-accelerated erythropoiesis

Analysing the genes downregulated by IL-33 in sorted pre-CFU-Es in more detail, I observed considerable overlap between these and a group of genes upregulated in equivalent progenitors by injection of EPO in mice in a previous study [17] (**Fig. 5.27A-B**). These genes were enriched in IL-33-naïve pre-CFU-Es in our analysis (**Fig. 5.27A**), leading me to hypothesize that IL-33 might interfere with the action of EPO in these cells. Exposure to IL-33 did not cause downregulation of the *Epor* gene (**Fig. 5.27C**), encoding the EPO receptor (EPO-R), or loss of the protein from the cell surface (**Fig. 5.27D**), nor did use of a tenfold greater concentration of EPO rescue IL-33-induced inhibition in culture (**Fig. 5.27E**). Collectively, this suggested any effect of IL-33 on EPO-R signalling would be downstream of the surface receptor itself.

Figure 5.27

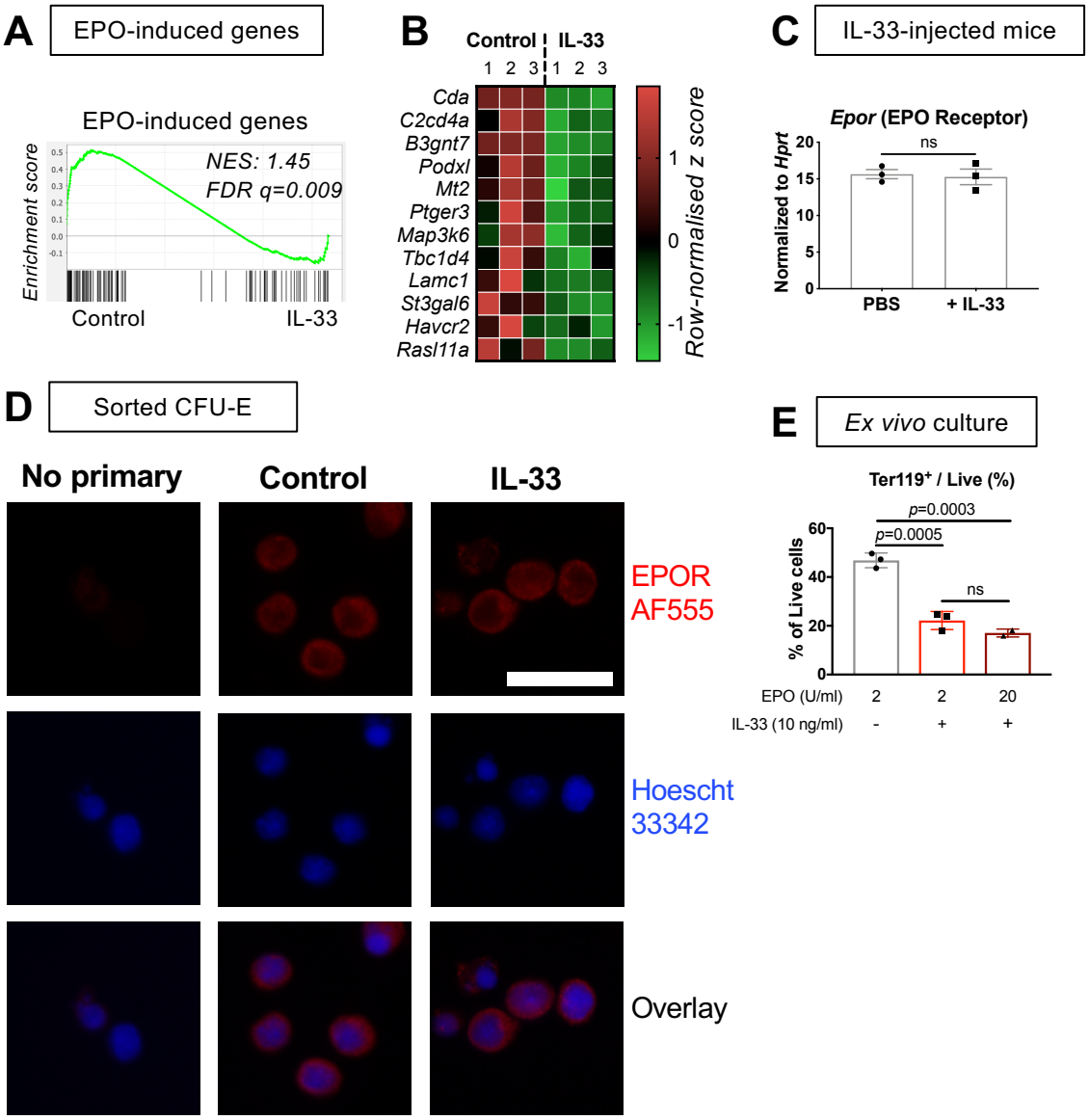

Figure 5.27: IL-33 inhibits EPO-induced gene expression
(**A**) Enrichment of genes upregulated by erythropoietin (EPO) in a previous study among the genes differentially regulated by IL-33 in pre-CFU-Es sorted by FACS and exposed to IL-33 or control medium for 6 hours before RNA sequencing. NES: normalised enrichment score, FDR: false discovery rate.
(**B**) Expression of selected genes by RNA sequencing in pre-CFU-Es described in (**A**). Expression normalised to row means. Columns represent paired biological replicates.
(**C**) Expression of *Epor*, encoding the EPO receptor (EPO-R), in pre-CFU-Es sorted by FACS from healthy SKG mice injected with PBS or IL-33 for 1 week. Expression normalised to *Hprt*. Points represent biological replicates, n=2 mice per group, bars indicate mean with SEM, Student's t test.
(**D**) Representative fluorescence microscopy images of CFU-Es sorted by FACS from healthy SKG mice and cultured overnight with or without IL-33 then stained for expression of EPO-R. Scale bar = 25 μm.
(**E**) Frequency of Ter119^{+} cells among total live cells derived from culture of pre-CFU-Es sorted by FACS from healthy SKG mice after 4 days and with indicated IL-33 and EPO dosages. Points represent technical replicates from a single experiment, bars indicate mean with SD, one-way ANOVA with Tukey's test.
Data representative of 2 (**D**)-(**E**) or 3 (**C**) independent experiments

Upon binding to EPO, the cell surface EPO-R dimerises and causes activation of several intracellular signalling cascades, including JAK2-STAT5, PI3K-ERK1/2, p38 MAPK, and PI3K-Akt [524]. Of these, JAK2-STAT5 activates Bcl-xL to prevent apoptosis of erythroid progenitors [176], whereas Akt promotes differentiation [183] by phosphorylating the essential erythroid transcription factor GATA1 [184] and by activating metabolic pathways via phosphorylation of the mTORC1 complex [186]. To assess the effect of IL-33 on these pathways, I incubated BM preparations depleted of mature cells with IL-33 or medium and then stimulated them with EPO before assessing phosphorylation of critical molecules in erythroid progenitors (i.e. CFU-Es and pre-CFU-Es) by phosphoflow cytometry. In control conditions, EPO activated all four pathways downstream of EPO-R but, with prior incubation with IL-33, there was consistent suppression of STAT5, ERK1/2, and, more strikingly, Akt phosphorylation in response to EPO (**Fig. 5.28A-B**). To demonstrate that these effects were not dependent on other cell types that would be present in BM preparations, I conducted the same experiments in purified CFU-Es sorted by FACS, opting to use CFU-Es because they are much more numerous in BM than pre-CFU-Es. In these sorted CFU-Es, although the baseline levels of phosphorylation of STAT5 and Akt differed from those of erythroid progenitors in BM preparations depleted of mature cells, the same effect of IL-33 was apparent (**Fig. 5.28C**). This indicated IL-33 is probably acting directly on erythroid progenitors to produce the observed changes in protein phosphorylation.

Figure 5.28

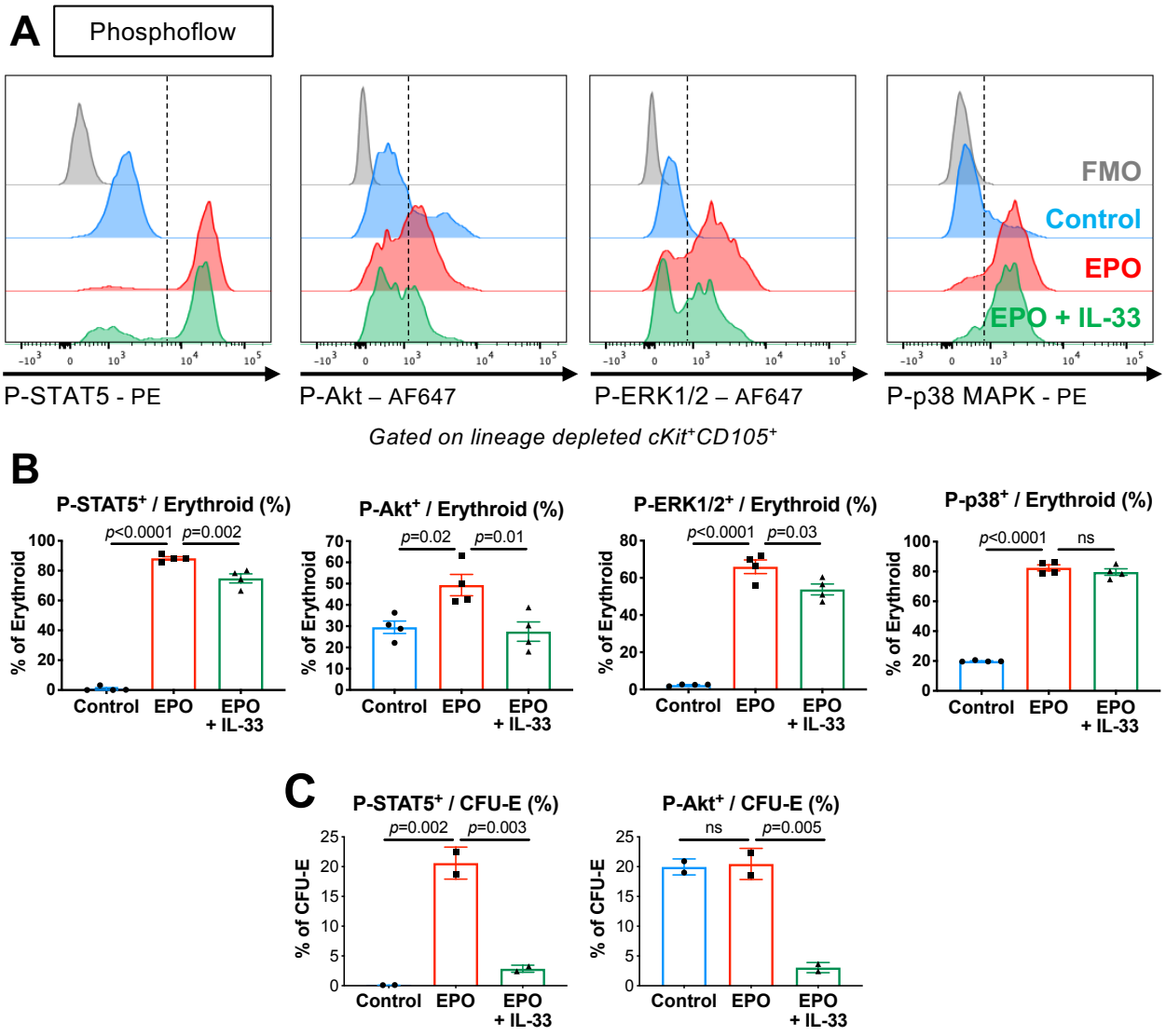

Figure 5.28: IL-33 inhibits EPO-induced Akt phosphorylation
(**A**) Representative flow cytometric images of expression of indicated phosphorylated proteins in erythroid progenitors from healthy SKG BM. Cells were incubated with IL-33 or control medium for 6 hours then stimulated with EPO or PBS before staining. FMO: fluorescence minus one control.
(**B**) Frequency of cells expressing indicated phosphorylated proteins among erythroid progenitors described in (**A**). Points represent mean of replicates from independent experiments, bars indicate mean with SEM, one-way ANOVA with Tukey's test.
(**C**) Expression of indicated phosphorylated proteins in CFU-E cells sorted by FACS from the BM of healthy SKG mice then incubated as described in (**A**). Points represent technical replicates, bars indicate mean with SD, one-way ANOVA with Tukey's test.

Data from 4 independent experiments (**A**)-(**B**) or a single experiment (**C**).

Focusing on Akt, I found the effect of IL-33 in inhibiting EPO-induced phosphorylation was confined to the serine (S)473 residue, and even caused a slight reduction in the proportion of cells with S473-phosphorylated Akt without EPO stimulation (**Fig. 5.29A**). Conversely, the tyrosine (T)308 residue appeared to be constitutively phosphorylated in erythroid progenitors, irrespective of EPO status, and was not affected by IL-33 (**Fig. 5.29A**). The decreased phosphorylation of Akt S473 also could not be rescued by stimulation with a tenfold greater concentration of EPO (**Fig. 5.29B**), indicating the effect was probably not attributable to decreased EPO sensitivity but to uncoupling of signalling events connecting the EPO-R to Akt, such as mTORC2. Among the substrates of Akt is the mTORC1 complex, which phosphorylates S6 kinase and other targets to enhance protein translation and cellular metabolism [186]. Activity of the mTORC1/S6 pathway is increased with and essential for progressive erythroid differentiation [196, 525], and, in murine erythroid progenitors, I found increased phosphorylation of mTOR and S6 kinase with EPO stimulation (**Fig. 5.29C**). However, phosphorylation of neither molecule was affected by IL-33 exposure, indicating IL-33-induced suppression of Akt phosphorylation did not impair EPO-induced mTORC1/S6 kinase activation.

Figure 5.29

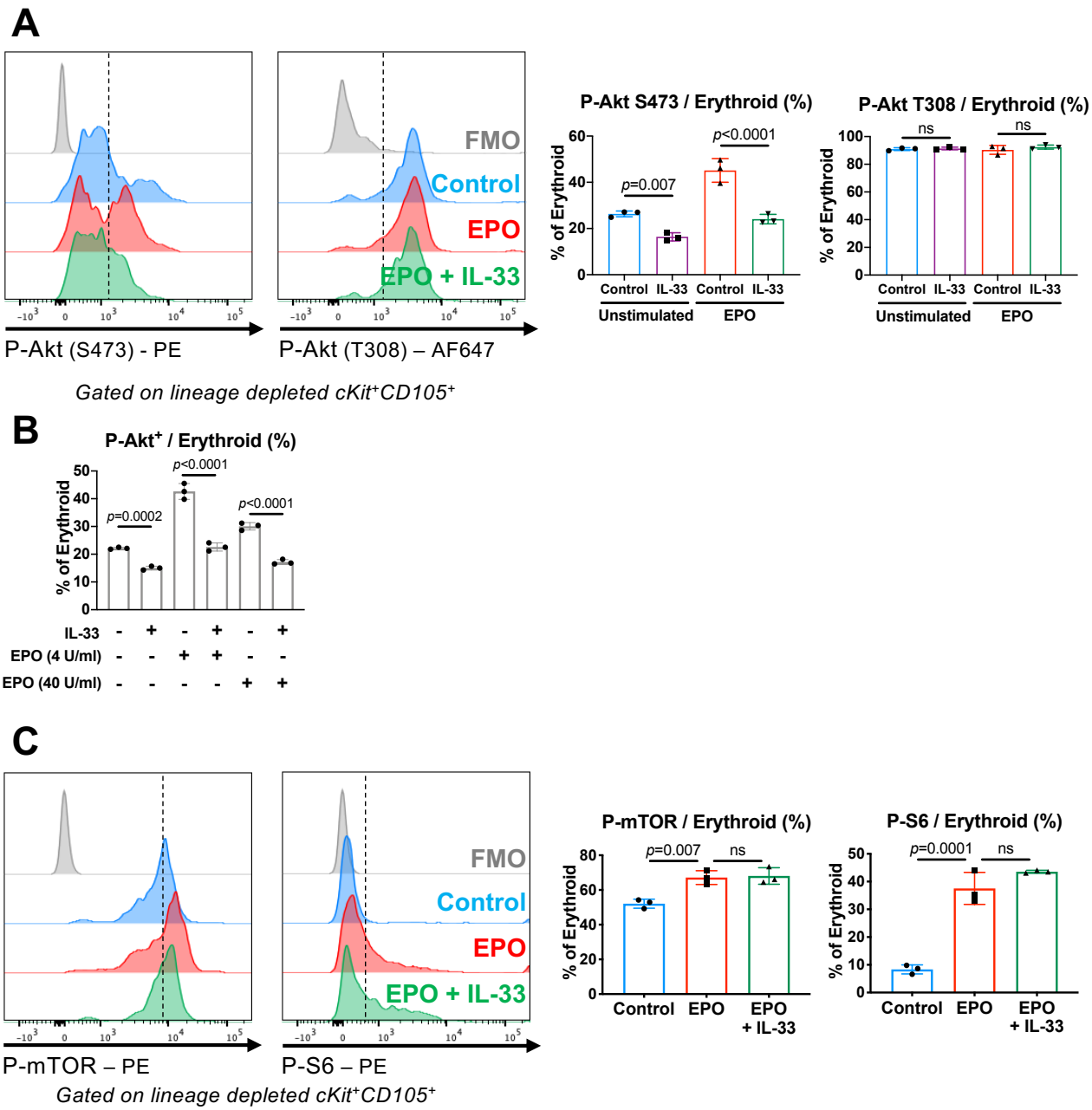

Figure 5.29: IL-33 specifically inhibits EPO-induced S473 Akt phosphorylation
(**A**) (Left) Representative flow cytometric images of expression of indicated phosphorylated proteins in erythroid progenitors from healthy SKG BM. Cells were incubated with IL-33 or control medium for 6 hours then stimulated with EPO or PBS before staining. FMO: fluorescence minus one control. (Right) Frequency of cells expressing indicated phosphorylated proteins among same cells. Points represent technical triplicates from a single experiment, bars indicate mean with SD, two-way ANOVA with Sidak's test.
(**B**) Frequency of erythroid progenitors expressing P-Akt S473 after incubation as in (**A**) but with indicated concentrations of EPO. Points represent technical triplicates from a single experiment, bars indicate mean with SD, one-way ANOVA with Tukey's test.
(**C**) (Left) Representative flow cytometric images of expression of indicated phosphorylated proteins in erythroid progenitors described in (**A**) (Right) Frequency of cells expressing indicated phosphorylated proteins among same cells. Points represent technical triplicates from a single experiment, bars indicate mean with SD, one-way ANOVA with Tukey's test.
Data representative of 2 independent experiments (**B**)-(**C**) or from a single experiment (**A**).

I wished to determine if the changes in Akt activity were required for the effect of IL-33 to suppress erythroid differentiation. I approached this question using a small molecule activator of Akt, SC-79, which caused constitutive phosphorylation of both S473 and T308 residues in a previous study [464]. However, inclusion of this activator in cultures of sorted pre-CFU-Es did not rescue the effect of IL-33 (**Fig. 5.30A**) and, in my hands, SC-79 did not increase phosphorylation of S473 as assessed by phosphoflow cytometry across a range of concentrations (**Fig. 5.30B**).

To try to determine if these changes in signalling events downstream of the EPO-R were related to increased NF-kB activity also caused by IL-33, I incubated BM preparations with the NBD peptide inhibitor, with or without IL-33, before stimulating with EPO. However, I found inhibition of the NF-kB canonical pathway did not prevent the effect of IL-33 on Akt (**Fig. 5.30C**), suggesting this was probably an independent effect mediated through a different cascade downstream of ST2.

Figure 5.30

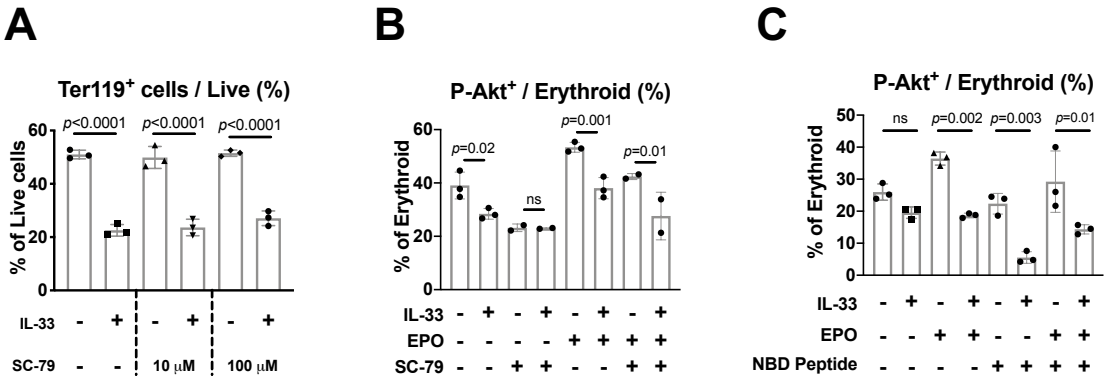

Figure 5.30: SC-79 does not cause phosphorylation of Akt S473
(**A**) Frequency of Ter119+ cells among total live cells derived from culture of pre-CFU-Es sorted by FACS from BM of healthy SKG mice for 4 days with indicated doses of the Akt activator SC-79. Points represent technical triplicates from a single experiment, bars indicate mean with SD, two-way ANOVA with Sidak's test.
(**B**) Frequency of erythroid progenitors expressing P-Akt S473 after incubation with IL-33 or control medium for 6 hours, with or without SC-79, then stimulation with EPO or PBS for 20 minutes. Points represent technical triplicates from a single experiment, bars indicate mean with SD, two-way ANOVA with Sidak's test.
(**C**) Frequency of erythroid progenitors expressing P-Akt S473 after incubation with IL-33 or control medium for 6 hours, with or without the NF-kB inhibiting NEMO binding domain (NBD) peptide, then stimulation with EPO or PBS for 20 minutes. Points represent technical triplicates from a single experiment, bars indicate mean with SD, two-way ANOVA with Sidak's test.

Data representative of 2 (**A**)-(**B**) or 3 (**C**) independent experiments.

Inflammation has been implicated as a factor causing resistance to therapeutic administration of EPO in patients with chronic anaemia [276]; I hypothesized that IL-33 could contribute to this effect owing to its impact on EPO-R signalling. Additional support for this hypothesis came from my observation that IL-33 injection in healthy SKG mice caused increases in serum EPO concentration in some individuals (**Fig. 5.31A**). This effect was not significant when groups were compared but suggested that erythroid suppression caused by IL-33 might be associated with an ineffective compensatory increase in EPO production. To

investigate the interaction between IL-33 and EPO further, I injected EPO in mice to produce a model of accelerated erythropoiesis (**Fig. 5.31B**), which occurs during severe anaemia to increase production of RBCs. Whereas injection of EPO alone caused marked increases in the numbers of BM erythroid progenitors (**Fig. 5.31C**), BM Ter119^{+} erythroid cells (**Fig. 5.31D**), and blood Hgb (**Fig. 5.31E**), concurrent administration of IL-33 largely abrogated these responses. To understand the relevance of this finding in the setting of inflammation (**Fig. 5.31F**), I injected EPO, with or without curdlan, in WT mice, finding that curdlan clearly suppressed the EPO-induced expansion of erythroid progenitors and Ter119^{+} cells in BM (**Fig. 5.31G-H**). However, this effect was partially inhibited in IL-33$^{-/-}$ mice (**Fig. 5.31G-H**), indicating IL-33 production contributed to the EPO resistance produced by curdlan.

Collectively, these results show that IL-33 inhibits EPO-induced erythropoiesis *ex* and *in vivo*, which may be attributable to decreased activity in the Akt and, to a lesser extent, ERK1/2 and STAT5 signalling pathways. Suppression of Akt phosphorylation by IL-33 was not dependent on the NF-kB pathway and did not cause decreased activation of mTOR and S6 kinase downstream of Akt, suggesting any role of decreased Akt activation in the phenotype produced by IL-33 is probably mediated by a different pathway, such as reduced GATA1 phosphorylation.

Figure 5.31

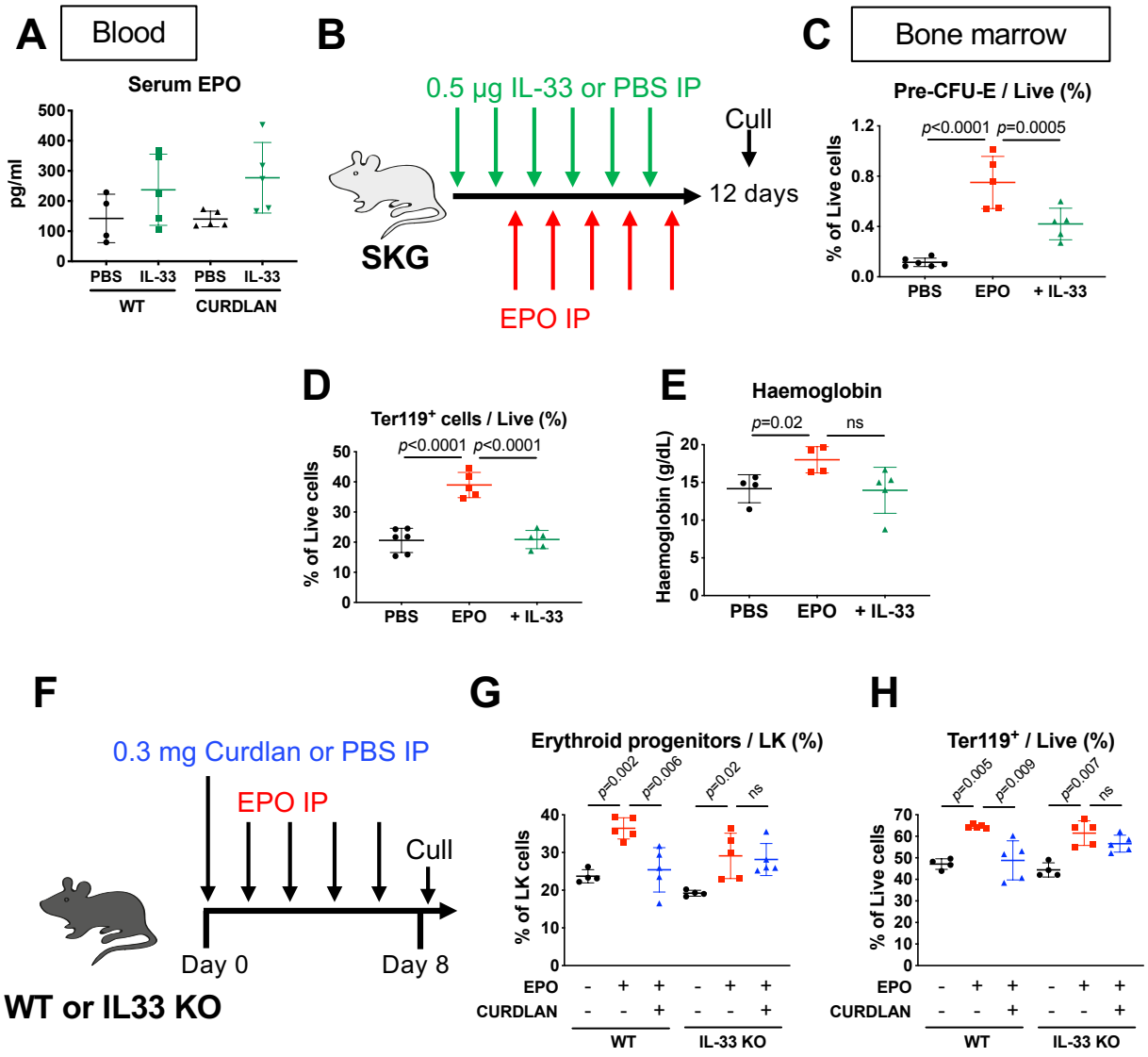

Figure 5.31: IL-33 inhibits EPO-accelerated erythropoiesis *in vivo*
(**A**) Concentration of erythropoietin (EPO) measured by bead-based multiplex assay in serum of mice injected with PBS or IL-33, with or without curdlan, for 1 week. Points represent individual mice with mean and SD, two-way ANOVA with Sidak's test.
(**B**) Schematic diagram showing injection of healthy SKG mice with EPO and IL-33 or PBS as indicated before culling to generate data shown in (**C**)-(**E**).
(**C**) Frequency of pre-CFU-E cells among total live BM cells.
(**D**) Frequency of Ter119$^+$ cells among total live BM cells.
(**E**) Blood haemoglobin concentration.
For (**C**)-(**E**), points represent individual mice with mean and SD, one-way ANOVA with Tukey's test.
(**F**) Schematic diagram showing injection of EPO in C57BL/6 wild type (WT) or IL-33$^{-/-}$ (IL33 KO) mice, with injection of curdlan or PBS, to generate data shown in (**G**)-(**H**).
(**G**) Frequency of erythroid progenitors (CFU-E and pre-CFU-E) among lineage$^-$, c-Kit$^+$ (LK) progenitors in BM.
(**H**) Frequency of Ter119$^+$ cells among total live BM cells.
For (**G**)-(**H**), points represent individual mice with mean and SD, one-way ANOVA with Tukey's test.

Data representative of 2 independent experiments (**B**)-(**H**) or from a single experiment (**A**).

5.3 Discussion

In this chapter, I show that IL-33 specifically inhibits differentiation of erythroid progenitors *ex vivo* and suppresses erythropoiesis *in vivo*, causing anaemia. This effect is dependent on NF-kB activation and is also associated with altered signalling events downstream of the EPO-R.

5.3.1 NF-kB activity and PU.1

I found the effects of IL-33 in erythroid progenitors are dependent on NF-kB activation, and NF-kB is a common pathway utilised by IL-1 cytokine family members [501]. However, in the context of erythropoiesis, this is important because activity of many NF-kB constituents, including p65, p50, and p52, decreases with progressive differentiation [519]. Studies of human and murine erythroid cell lines suggest high levels of NF-kB activity repress transcription at important loci required in differentiated cells, including the globin genes [526]. Based on this and my own observation that NF-kB inhibition rescued cells from IL-33-mediated inhibition *ex vivo*, I suggest IL-33 maintains inappropriately increased levels of NF-kB activity that prevent terminal differentiation of erythroid progenitors.

Although IL-33 caused increased expression of PU.1, which co-operates with NF-kB in transcriptional regulation of target genes [527], pharmacological inhibition did not prevent IL-33-induced inhibition of erythroid differentiation *ex vivo* (**Fig. 5.32**). I have encountered the suggestion that increased PU.1 expression could not be the explanation for my observations because others had reported that PU.1 and GATA1 were not expressed in the same cells [85, 86]. However, those studies described the initial myeloid/erythroid lineage decision of MPPs, which cells appear to express one or other of these transcription factors but never both [86]. However,

as others have reported and as I confirm, several types of more committed progenitor, including those for eosinophils, mast cells, and erythrocytes, do express PU.1 and GATA1 simultaneously. The apparent lack of effect of PU.1 in my system could have been related to the experimental strategy because I used the recently described DB2313 inhibitor, whereas others have approached this question by over- or under-expressing PU.1 by viral transfection [269]. However, I could see a clear effect of the PU.1 inhibitor to inhibit the development of pre-CFU-Es, consistent with its described role in early erythropoiesis [504], suggesting this was an effective means to study the role of PU.1 without the possible off-target effects of viral transfection. The effectiveness of the inhibitor could have been investigated further by assessing its ability to inhibit known functions in other cell types, such as macrophages, or by assessing its ability to inhibit expression of known PU.1 transcriptional targets. Collectively, my work suggests the mechanism by which IL-33 suppresses erythropoiesis is distinct from that of IFN-γ, for which PU.1-IRF1 activity was essential to prevent terminal differentiation of human erythroid progenitors [269, 270].

5.3.2 Changes in EPO signalling and EPO resistance

Serendipitously, I discovered that many genes upregulated by EPO in erythroid progenitors were downregulated by IL-33, and I show that IL-33 suppresses EPO-induced Akt phosphorylation (**Fig. 5.32**). This is important because EPO has a central and indispensable role in supporting erythroid cells during the final stages of differentiation, to the extent that EPO and EPO-R deficient mice suffer embryonic lethality [175]. Interestingly, the onset of EPO dependence occurs shortly after formation of CFU-E, coinciding with point at which IL-33

prevented further differentiation in cultures. At a molecular level, Akt, activated by EPO, causes phosphorylation and activation of GATA1, which is required for erythroid differentiation. Consequently, loss or inhibition of Akt activity prevents terminal differentiation of human and murine erythroid progenitors (see **chapter 1.1.7**).

Figure 5.32

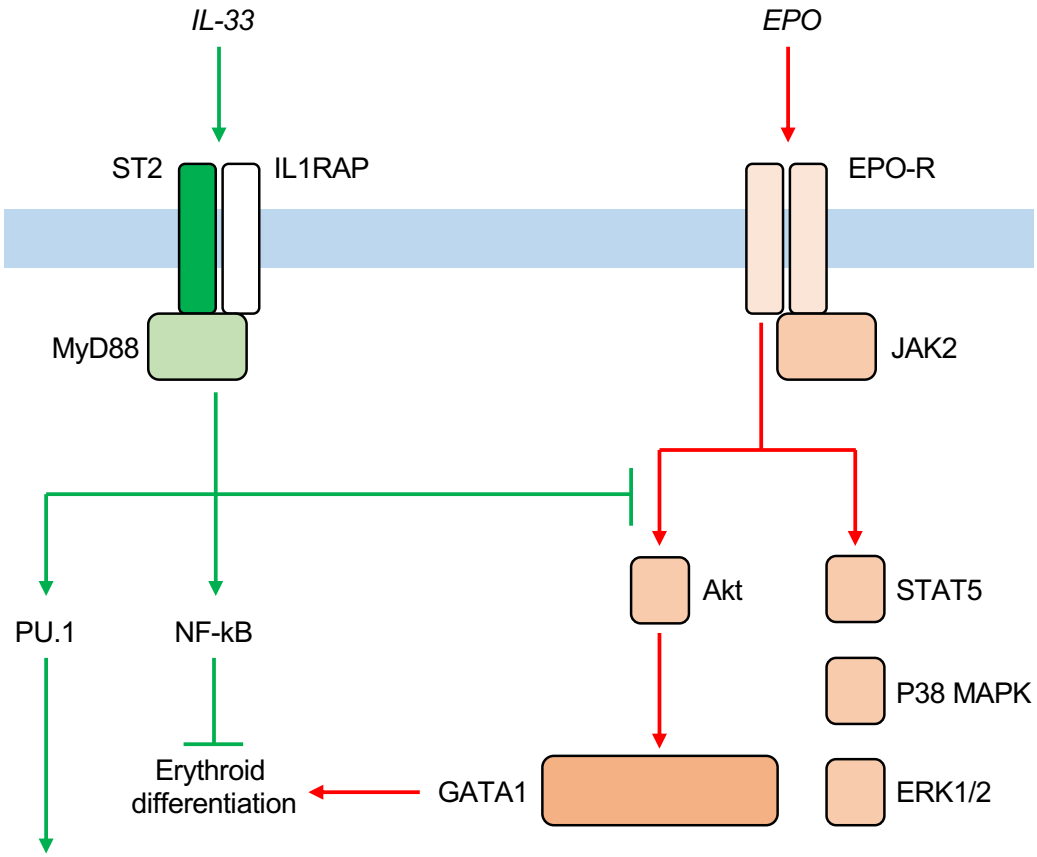

Figure 5.32: Model for the interaction of IL-33 and EPO signalling in erythroid progenitors
Schematic diagram showing proposed effect of IL-33 to increase activation of NF-kB, which inhibits erythroid differentiation, while simultaneously inhibiting EPO-induced phosphorylation of Akt, which has a role in GATA1 phosphorylation and activation of erythroid differentiation.

In my system, I found 1) S473, but not T308, phosphorylation of Akt in response to EPO was decreased by IL-33, with IL-33 also causing downregulation of the gene encoding Pim-1 in pre-CFU-Es in the RNA sequencing analysis, 2) there was no difference in mTOR or S6 phosphorylation downstream of Akt, and 3) the purported Akt activator SC-79 did not rescue the phenotype but also did not affect S473 phosphorylation of Akt. On the basis of these results, I suggest Akt activation is impaired after exposure to IL-33 because dual T308 and S473 phosphorylation is prevented, which could be related to changes in mTORC2 activity or Pim-1 expression [180] (**Fig. 5.33**). Conversely, the T308 residue appears to be constitutively phosphorylated, as described previously [528, 529], which probably explains why phosphorylation of the mTORC1 target S6 kinase is unaffected by IL-33. Instead, I suggest decreased S473 phosphorylation of Akt may prevent it from phosphorylating and activating GATA1, which is required for erythroid differentiation. Interestingly, a recent study comparing the substrate specificity of Akt with one or both phosphorylation events revealed that Akt phosphorylated at both T308 and S473 acts more effectively on GATA1 than T308 alone [530], which provides a possible explanation for how some pathways downstream of Akt may be unaffected by decreased S473 phosphorylation (i.e. mTORC1) whereas others, such as GATA1, could be impaired. However, in this work, I did not demonstrate that decreased Akt S473 phosphorylation was essential for the IL-33-induced phenotype in erythroid progenitors, nor that it results in decreased activity of GATA1. I tried to investigate the role of Akt using the small molecule activator SC-79, which is reported to cause constitutive phosphorylation of both T308 and S473 residues but to prevent translocation of Akt into the plasma membrane [464], which normally occurs before phosphorylation. However, by phosphoflow cytometry, I did

not see any change in S473 phosphorylation with SC-79. Therefore, I suspect the observed lack of effect of SC-79 in cultures of pre-CFU-Es was probably attributable to poor activity, highlighting the need for alternative approaches to investigate this question. This could be done by expressing a constitutively activated form of Akt in erythroid progenitors, as reported previously [184], to determine how it would affect the IL-33-induced phenotype and GATA1 phosphorylation. Furthermore, the effect of decreased Akt S473 phosphorylation on GATA1 could be investigated further by evaluating GATA1 S310 phosphorylation, or by performing electrophoretic mobility shift assays (EMSA) to determine whether DNA binding of GATA1 was impaired by IL-33.

Figure 5.33

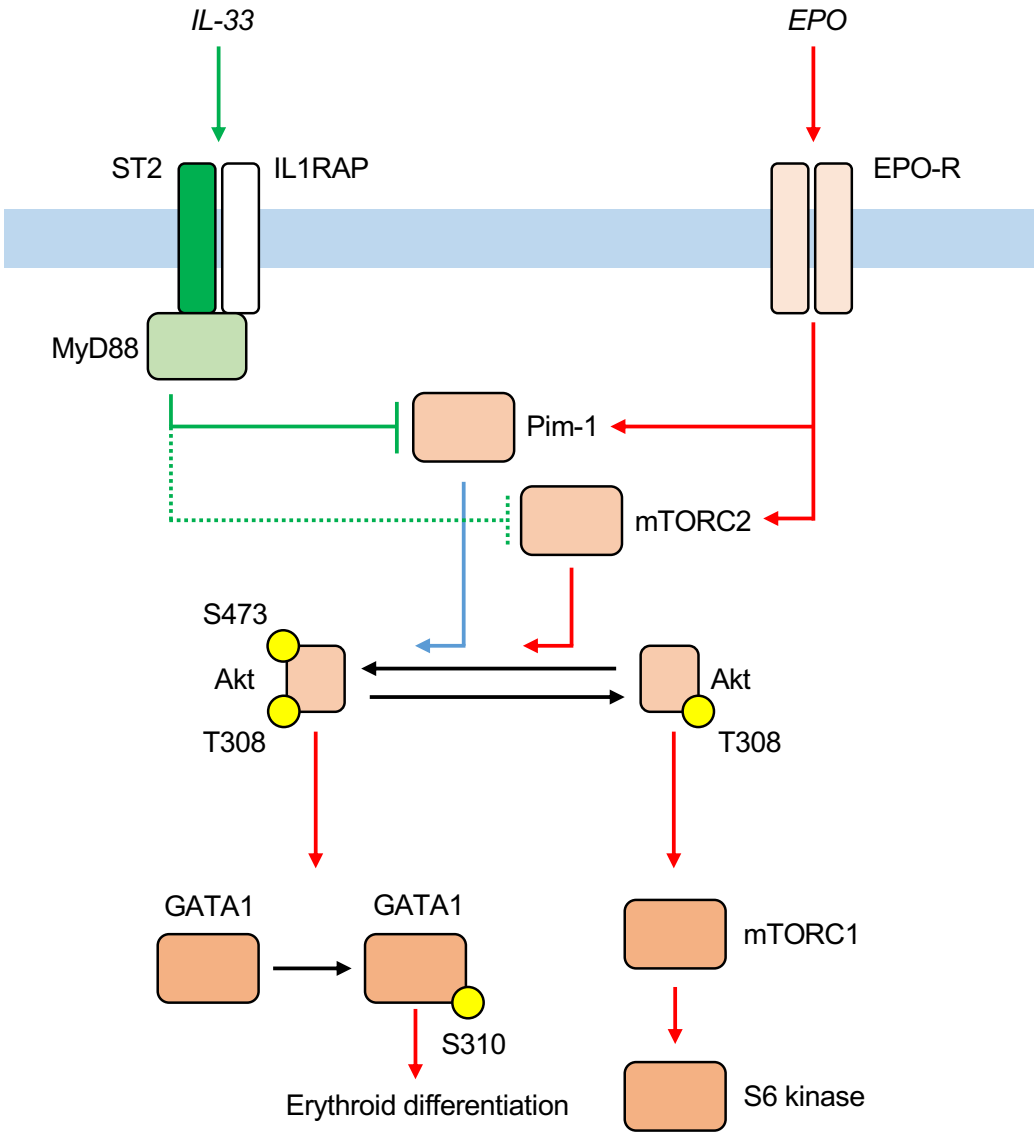

Figure 5.33: Model for proposed changes in Akt signalling caused by IL-33 in erythroid progenitors
When EPO binds to its receptor, mTORC2 is activated to phosphorylate Akt at the S473 residue, which enhances its ability to phosphorylate and activate GATA1. IL-33 decreases expression of Pim-1, which phosphorylates S473, by RNA sequencing, and, if this is not the mechanism by which it decreases Akt phosphorylation, it could also inhibit mTORC2. My data confirm that Akt T308 is constitutively phosphorylated in erythroid progenitors, which probably explains the lack of effect of IL-33 on phosphorylation of S6 kinase with EPO stimulation. Solid red lines show confirmed effects of EPO in previous studies, solid green lines show confirmed actions of IL-33 in this thesis, dashed green lines show speculated effects of IL-33, blue lines show confirmed effect of Pim-1 in previous studies, but it is unclear if this is mechanism by which IL-33 inhibits Akt S473 phosphorylation. Yellow circles indicate phosphorylation events.

I remain unsure how the increase in NF-kB activity and decrease in Akt phosphorylation might be related, if at all, and how these findings reconcile with wider understanding of ST2 signalling in cells. Indeed, in mast cells, IL-33-induced activation of Akt is required for IL-6 and IL-13 production [531], suggesting IL-33 might regulate Akt differently according to cell type and presence of other growth factors, such as EPO. I found that the NBD peptide inhibitor did not prevent IL-33-induced suppression of Akt phosphorylation in response to EPO, which would be expected because NF-kB regulation is normally downstream of Akt, possibly via mTORC1 [532]. Collectively, this suggests either that changes in NF-kB and Akt activity are linked, but with NF-kB downstream of Akt, or that NF-kB and Akt pathways are separate and could each produce inhibitory effects through distinct mechanisms. Accordingly, it would have been informative to investigate whether changes in Akt activity affect NF-kB translocation in erythroid progenitors. A further possibility is that early events in NF-kB activation might affect Akt phosphorylation upstream of the point of action of the NBD peptide. This might be investigated further using cells lacking myeloid differentiation primary response (MyD)88 or by pharmacological inhibition of IL-1 receptor associated kinase (IRAK)4, which act as early adaptors between ST2 receptor activation and NF-kB induction before IKKγ is recruited [518].

In some chronic inflammatory settings, including chronic kidney disease, attempts to treat anaemic patients with EPO or its synthetic derivatives have been unsuccessful, creating the clinical phenotype of ‘EPO resistance’ [276]. Like AID, the pathophysiology of this phenomenon is probably multifactorial [277], but I contribute to this area of investigation by showing that IL-33 interferes with EPO-R signalling. It was particularly striking that the effects of exogenous EPO,

administered to excess, could be almost entirely abrogated by concurrent administration of IL-33 *in vivo*, and that similar suppression of EPO-accelerated erythropoiesis by curdlan was less effective in IL-33$^{-/-}$ mice. I considered the possibility that IL-33 and EPO might form a mutually antagonistic relationship to inhibit or facilitate terminal differentiation of erythroid progenitors because EPO decreases activity of NF-kB members in macrophages [533]. However, use of a higher concentration of EPO in cultures of erythroid progenitors did not rescue IL-33-mediated inhibition, suggesting the effect of IL-33 is dominant.

5.3.3 IL-33 production by CD169^{+} macrophages

I showed that the gene encoding IL-33 was expressed by CD169^{+} erythroblastic island macrophages in the BM. Other have suggested that myeloid cells in mice do not produce the IL-33 protein, even if they express mRNA [327], and I did not confirm protein production in these macrophages by Western blot or flow cytometry. Indeed, although I attempted flow cytometry for intracellular IL-33 as others had reported [534, 535], I found this unrewarding owing to high background fluorescence, even preventing me from observing IL-33 in stromal cells despite using IL-33$^{-/-}$ mice as controls (data not shown). Nevertheless, others have also observed IL-33 production in a population of induced erythroblastic island macrophages created by overexpressing the transcription factor KLF-1 in human primary monocytes [536], suggesting my observation might be valid. A further modality that would have added considerably to my work is imaging of BM sections to determine whether IL-33-producing macrophages were directly apposed to erythroid progenitors. Without this, my suggestion that IL-33 is being produced in the ‘erythroid niche’ is based only on published descriptions of CD169^{+}

macrophages as forming the core of erythroblastic islands, rather than direct evidence.

With curdlan injection, expression of *Il33* was decreased in sorted BM macrophages while IL-33 concentration in the BM plasma was increased, suggesting local production in the BM might be superseded by release of IL-33 from damaged tissues in inflamed sites during disease, as discussed in **chapter 6**.

5.3.4 Role of IL-33 in erythropoiesis under homeostatic and disease conditions

What do my findings tell us about the role of IL-33 in health and disease (**Fig. 5.34**)? Its role in healthy mice is difficult to define: I did not observe any defect in the erythroid compartment when comparing IL-33$^{-/-}$ to WT mice. Constitutive IL-33$^{-/-}$ mice could have compensatory mechanisms that would obscure any difference, but the two strains had similar concentrations of serum EPO, which is a sensitive marker of the rate of erythropoiesis. Without *in situ* imaging or a functional readout, I cannot demonstrate that erythroid progenitors are ever exposed to IL-33 in healthy mice, even if it is being produced in adjacent macrophages. This would fit with the broader principles of IL-33 biology, which state that the cytokine is usually synthesised and stored in the nucleus but only released from damaged cells [332]. Additionally, GWAS studies in healthy people do not identify the *IL33* or *IL1RL1* loci as important associates of any RBC indices [537, 538], suggesting it is not a regulating factor for the erythroid compartment under homeostatic conditions.

Our laboratory and others have shown that IL-33 enhances myelopoiesis [368], which is the subject of **chapter 6** of the thesis. Teleologically, I suggest the simultaneous effects of IL-33 to permit myelopoiesis and suppress erythropoiesis

could enable organisms to respond to transient damage or infection, taking advantage of the long circulating time of mature RBCs to provide a buffer against the development of anaemia while BM output is diverted to meet other demands. During inflammatory diseases, this process would become detrimental if suppression of erythropoiesis were prolonged, resulting in AID as RBCs were lost but not replaced.

Figure 5.34

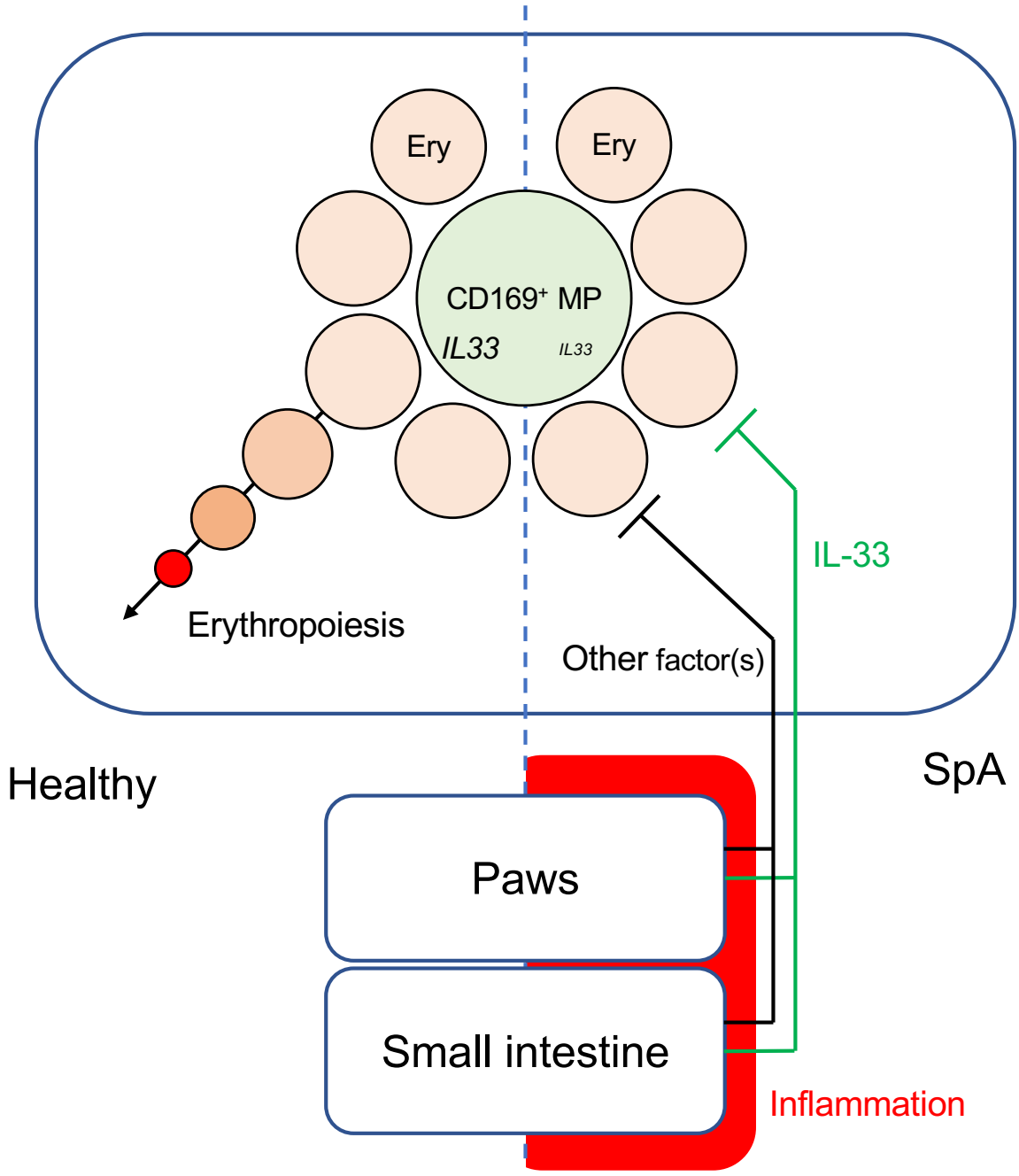

Figure 5.34: Proposed model for the actions of IL-33 in erythropoiesis in health and disease
Under healthy conditions, erythropoiesis progresses in the BM in erythroblastic islands. Island macrophages express *Il33* but it is unclear if they release it, and IL-33 does not appear to have any role in erythropoiesis under homeostatic conditions. With inflammation, IL-33 is produced in the paws and small intestine, causing an increased concentration in BM plasma early in disease. This appears to inhibit erythropoiesis, in combination with other factors, as demonstrated by the amelioratory effect of anti-IL-33 antibodies. Expression of *Il33* is decreased in island macrophages, possibly as a compensatory response to increased IL-33 in the local milieu. Ery: erythroid progenitor, MP: macrophage.

It is unclear whether the development of anaemia contributes to the progression of the inflammatory disease that caused it, or whether this is an incidental comorbidity. I suggest the anaemia is not important for progression of the arthritis and enteritis in SKG mice, though it could contribute to other aspects of the disease phenotype such as decreased mobility, but the diversion of BM output towards myelopoiesis is likely to contribute, as discussed in **chapter 6**. Previous data from our laboratory suggests EPO administration alone does not ameliorate disease severity in SpA despite expanding the erythroid compartment (T. Griseri, unpublished observations), supporting this assertion.

The effects caused by IL-33 on erythroid progenitors were clear when I conducted experiments *ex vivo*, but there were some important discrepancies with results obtained *in vivo*: 1) proliferation of (pre)-CFU-Es was decreased by IL-33 injection in mice but not *ex vivo*, and 2) IL-33 caused marked suppression of erythroid differentiation *in vitro* but the direct effect of IL-33 *in vivo* was less striking when injecting curdlan in mixed BM chimeras. The first effect could represent an indirect effect of IL-33 mediated by TNF-α or IL-6. Because erythroid progenitors did not express either cytokine under steady state or IL-33-exposed conditions by RNA sequencing (data not shown), this effect would not be observed *ex vivo*. The second discrepancy could be attributable to the effects of other inflammatory cytokines induced by curdlan injection that would be absent in cultures. My results from IL-33$^{-/-}$ mice and mixed BM chimeras indicate that curdlan injection must suppress erythropoiesis through other mechanisms, which could be related to production of other cytokines that affect erythroid progenitors directly or to effects on upstream MPPs to cause preferential production of myeloid progenitors. This investigation could be extended further by injecting IL-33 in the same mixed BM

chimeras to establish whether the suppression of erythropoiesis it causes *in vivo* is also mediated predominantly by direct or indirect effects on $ST2^+$ erythroid progenitors. So far, my data indicate that two major candidates induced by IL-33 (IL-6 and TNF-α) are not required for this effect. Any indirect effects of IL-33 *in vivo* could also have important implications for the application of the results of my RNA sequencing: I chose to expose cells to IL-33 *ex vivo* because I wished to focus on the direct effects of the cytokine, removing any indirect effects that might have occurred *in vivo*. To determine what direct effects of IL-33 might be occurring *in vivo*, I could have sorted pre-CFU-Es from mice injected with PBS or IL-33 for 1 week for RNA sequencing and then assessed those genes that were significantly differentially regulated in both *in vivo* and *ex vivo* settings.

5.4 Conclusions

- IL-33 suppresses differentiation of murine and human erythroid progenitors *ex vivo*.
- Injection of IL-33 *in vivo* suppresses erythropoiesis and causes anaemia, and IL-33 is one factor mediating curdlan-induced suppression of erythropoiesis in healthy mice and murine SpA; this identifies IL-33 as a factor mediating AID.
- Suppression of erythroid differentiation by IL-33 is dependent on upregulation of NF-kB pathways.
- IL-33 alters signalling events downstream of the EPO-R and causes resistance to the effects of EPO *in vivo*; this identifies IL-33 as a possible mediator of EPO resistance during chronic inflammation.

6 Interleukin-33 modulates myelopoiesis and has a role in development of spondyloarthritis in mice

6.1 Introduction

Interleukin-33 has pleiotropic effects, promoting type 2 immune responses [332, 335] and acting as an alarmin to signal the presence of tissue damage [342]. Its receptor is expressed principally on haematopoietic cells that participate in type 2 immune responses, including eosinophils, basophils, mast cells, ILC2s, and Th2 T cells. In response to IL-33, many of these cell types produce other cytokines, including the canonical type 2 cytokines IL-4, IL-5, and IL-13, but also non-type 2 pro-inflammatory molecules such as TNF-α, IL-6, and GM-CSF [343]. Owing to these features, IL-33 has been implicated as an important factor promoting inflammatory responses during disease: the serum concentration of IL-33 is increased in patients with AS [347, 348] and RA [349], and deficiency of IL-33 ameliorates disease in murine models of inflammatory arthritis [350, 351].

In **chapter 3**, I found development of SpA in SKG mice was associated with infiltration of mature myeloid cells into paws and small intestine and with flagrant myelopoiesis in BM and extramedullary sites. This was interesting because IL-33 causes leukocytosis in peripheral blood when injected into mice [205] and promotes infiltration of mature myeloid cells into the peritoneum when injected there [377]. In the BM, transgenic overexpression of IL-33 in mice causes marked expansion of myeloid cells [368], whereas IL-33 injection expands the population of LSK cells [367] and mobilises them from the BM in mice [370]. Additionally, IL-33 has a direct role in promoting early eosinophil development [323]. Taken together, this work suggested IL-33 has pro-myelopoietic effects owing to some combination of changes in the progenitor compartment, but the cellular pathways and molecular

mechanisms underlying this phenomenon were poorly understood. In particular, the relative contributions of direct effects of IL-33 and indirect effects mediated by other cytokines produced in response to it were unknown, and I considered this question was important in defining possible therapeutic targets in inflammatory diseases because, if all pro-myelopoietic effects of IL-33 could be attributed to another cytokine, it would be logical to designate that agent as a possible target for future therapies, rather than IL-33 itself.

Owing to the roles of IL-33 in other inflammatory diseases and as a possible regulator of myelopoiesis, I had the following aims in this chapter:

1. To determine whether IL-33 is implicated in development of SpA in mice
2. To determine whether IL-33 regulates myelopoiesis
3. To investigate whether any effects of IL-33 on myelopoiesis are mediated by direct effects or are dependent on production of other cytokines

6.2 Results

6.2.1 IL-33 is increased in SKG mice with SpA compared to controls

To determine whether development of SpA in SKG mice was associated with increased concentrations of IL-33, as reported in people with AS, I obtained explants of small intestine and paw from mice 4 weeks after injection of curdlan or PBS. I cultured these explants overnight and measured IL-33 in the supernatant, finding it was present at significantly greater concentrations at both sites in inflamed mice (**Fig. 6.1A**). To determine if this could be important for modulation of haematopoiesis, I also measured IL-33 in serum and BM plasma. Whereas IL-33 was not detectable in serum of healthy or inflamed mice (data not shown), its concentration increased rapidly after injection of curdlan in BM plasma (**Fig. 5.15A**).

However, by the time clinical features of SpA had developed at 4 weeks, the concentration was similar to that measured in healthy mice, which may have been attributable to production of the counter-regulatory soluble form of the ST2 receptor (sST2), which is induced rapidly in response to increased IL-33 concentrations [332].

6.2.2 IL-33 exacerbates clinical disease in SpA

To evaluate the importance of increased IL-33 production in SpA, I injected polyclonal anti-IL-33 antibodies ('αIL-33') or a polyclonal goat IgG1 preparation ('Control') in SKG mice after they were injected with curdlan (**Fig. 6.1B**). Because the concentration of IL-33 was increased in BM plasma in the first week after curdlan injection but not at 4 weeks, I opted to cull these mice after 10 days to evaluate BM changes. Treatment with anti-IL-33 antibodies slightly ameliorated clinical disease compared to controls, reducing the clinical arthritis score but not causing a significant difference in paw or tarsal swelling (**Fig. 6.1C**). However, anti-IL-33 treatment did decrease the number of neutrophils and Ly6C$^+$ monocytes but not eosinophils accumulating in the paws (**Fig. 6.1D**). To investigate the converse of this effect, I injected recombinant IL-33 or PBS in mice developing SpA (**Fig. 6.2A**), finding that IL-33 caused more marked swelling of the paws and tarsi and a higher clinical score of arthritis (**Fig. 6.2B**). Increased paw swelling was associated with greater infiltration of granulocytes (neutrophils and eosinophils) in those mice injected with IL-33 (**Fig. 6.2C**).

Figure 6.1

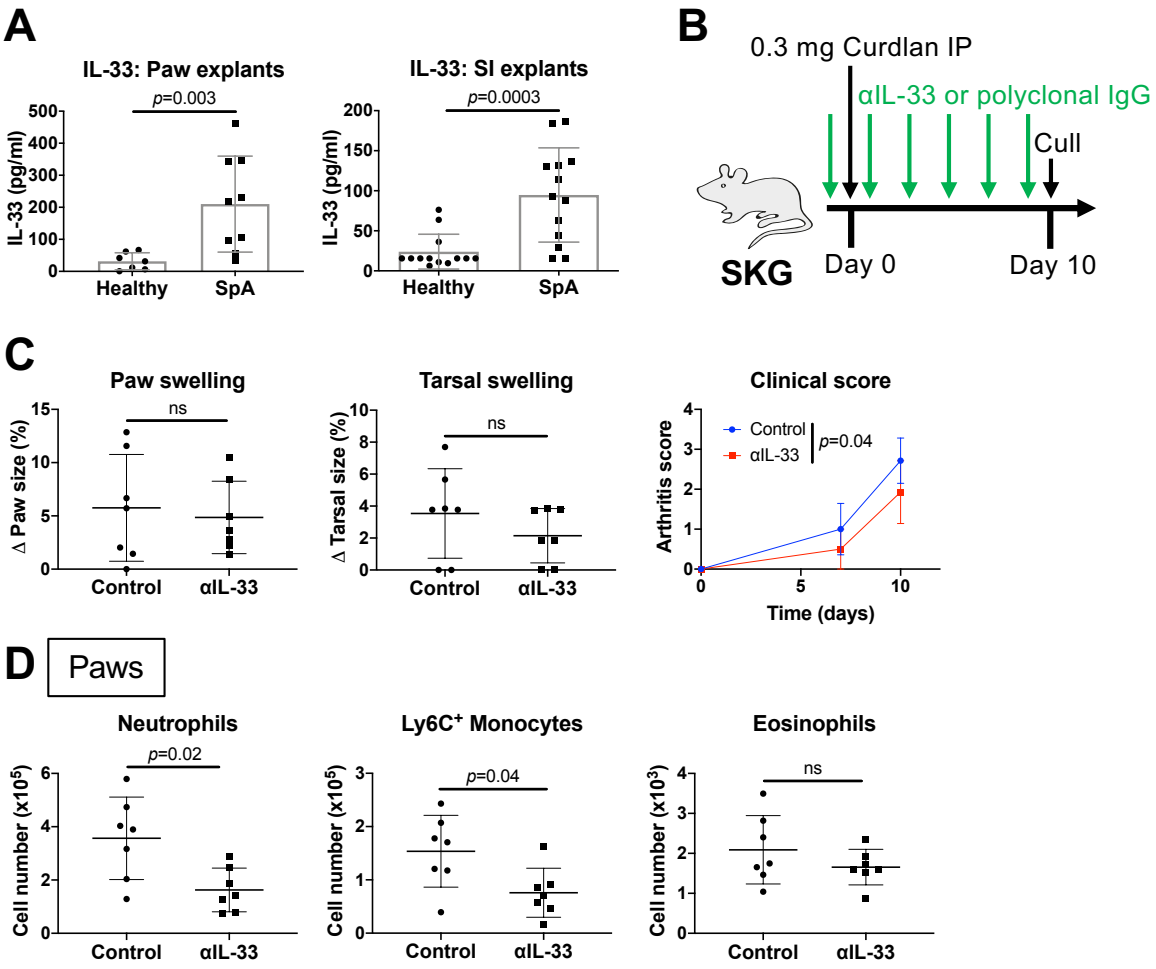

Figure 6.1: IL-33 is produced in inflamed sites during SpA
(**A**) Concentration of IL-33 measured by ELISA in supernatant of explants of paw and small intestine obtained from healthy mice and mice with SpA, 4 weeks after curdlan injection, and cultured overnight.
(**B**) Schematic diagram showing injection of curdlan in SKG mice followed by either polyclonal anti-IL-33 antibodies or a control goat IgG1 preparation until culled after 10 days to generate data shown in (**C**)-(**D**).
(**C**) Changes in paw and tarsal swelling and in clinical arthritis score. For clinical score, points represent mean with SD for n=7 mice per group, two-way ANOVA.
(**D**) Number of indicated mature myeloid cells in paws.
For (**A**), (**C**), and (**D**), points represent individual mice with mean and SD, Mann-Whitney U test.

Data pooled from 3 independent experiments (**A**) or from a single experiment (**B**)-(**D**).

Figure 6.2

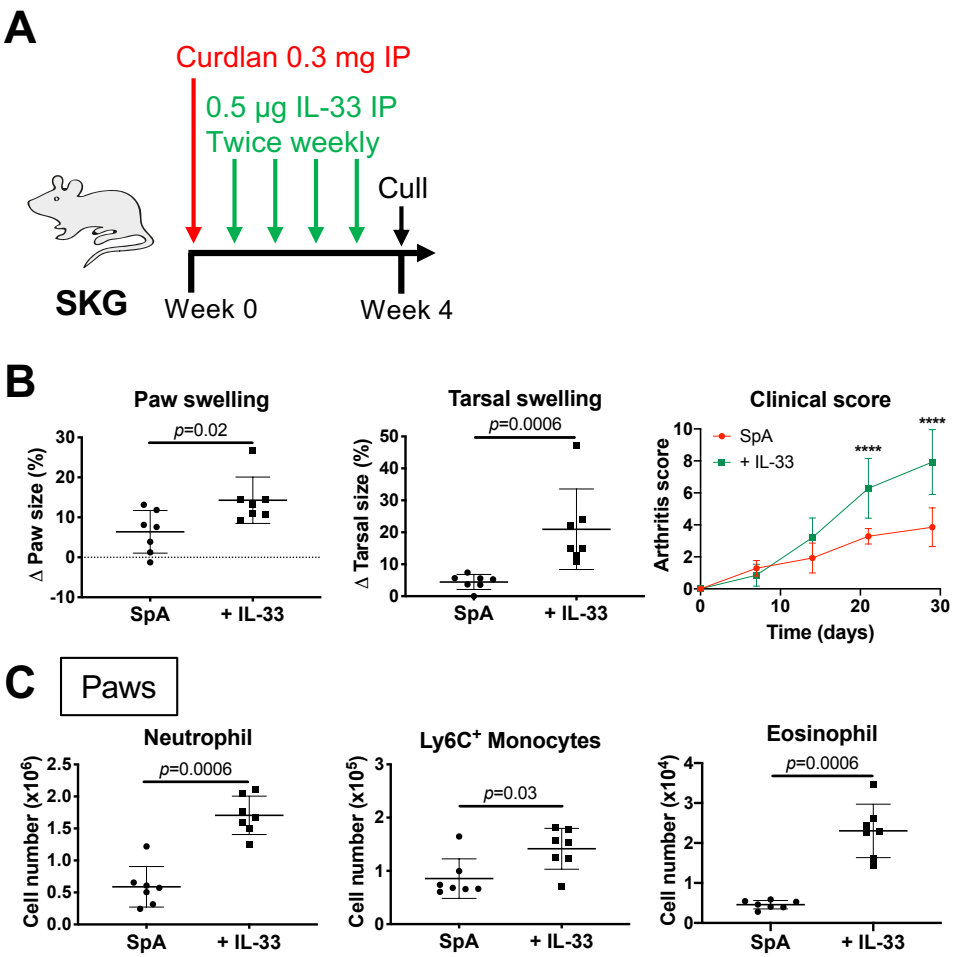

Figure 6.2: Recombinant IL-33 injections exacerbate SpA
(**A**) Schematic diagram showing injection of recombinant murine IL-33 or PBS three times weekly in male SKG mice injected with curdlan to induce SpA, before culling after 4 weeks to produce data shown in (**B**)-(**C**).
(**B**) Changes in paw and tarsal swelling and in clinical arthritis score. For clinical score, points represent mean with SD for n=7 mice per group, two-way ANOVA, **** $p<0.0001$.
(**C**) Number of indicated mature myeloid cells in paws.
For (**B**)-(**C**), points represent individual mice with mean and SD, Mann-Whitney U test.

Data representative of 3 independent experiments.

Interleukin-33 can cause production of GM-CSF from mast cells [343], and we and others have shown previously that GM-CSF is essential for development of inflammatory arthritis in SKG mice [394, 441]. To determine if IL-33-induced exacerbation of SpA might be related to increased production of GM-CSF, I injected

mice with IL-33 as they were developing SpA in combination with either anti-GM-CSF antibodies or an isotype control. In this way, I found that GM-CSF was partially or completely responsible for the IL-33-mediated exacerbation of the clinical features of SpA: with GM-CSF blockade, IL-33-injected mice no longer had a further increase in paw and tarsal swelling or clinical score of arthritis (**Fig. 6.3A**). Furthermore, GM-CSF blockade prevented the accumulation of neutrophils and $Ly6C^+$ monocytes (in frequency though not absolute number) in the paws caused by IL-33 (**Fig. 6.3B**).

Having observed changes in the numbers of mature myeloid cells in the paws of mice receiving recombinant IL-33 or anti-IL-33 antibodies during SpA, I asked whether this was associated with corresponding changes in myelopoiesis in the BM. Administration of anti-IL-33 antibodies did not cause significant changes in frequency or number of GMPs or mature neutrophils in BM compared to those receiving control antibodies (**Fig. 6.4A**). However, with IL-33 injection, there were marked increases in both types of cell compared to PBS-injected controls (**Fig. 6.4B**). Injection of anti-GM-CSF antibodies or isotype alongside IL-33 further showed that accumulation of GMPs was partially dependent on IL-33-induced GM-CSF production, though this effect was not statistically significant (**Fig. 6.4C**).

Figure 6.3

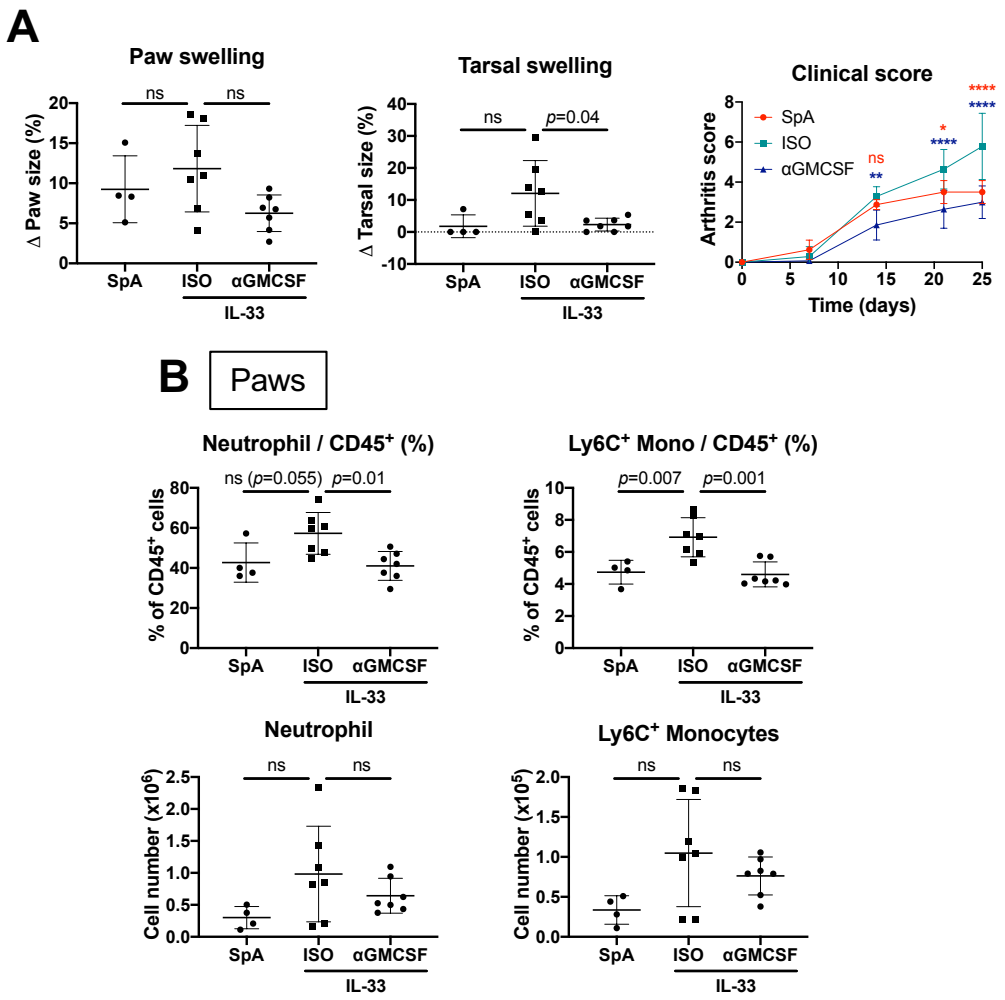

Figure 6.3: GM-CSF is responsible for some effects of IL-33 on clinical disease in SpA

(**A**) Change in paw and tarsal swelling and in clinical arthritis score in SKG mice injected with curdlan (SpA). Some mice were injected with IL-33 and either anti-GM-CSF antibodies (αGMCSF) or an isotype (ISO) until culled after 4 weeks. For clinical score, points represent mean and SD for n=4-7 mice per group, two-way ANOVA with Sidak's test, stars indicate difference between SpA or αGMCSF groups and the isotype group. *p<0.05, **p<0.01, ****p<0.0001.

(**B**) Frequency among CD45$^+$ leukocytes and absolute number of indicated cells in paws of mice described in (**A**). Mono: monocyte.

For all except clinical score, points represent individual mice with mean and SD, one-way ANOVA with Tukey's test.

Data representative of 2 independent experiments.

Figure 6.4

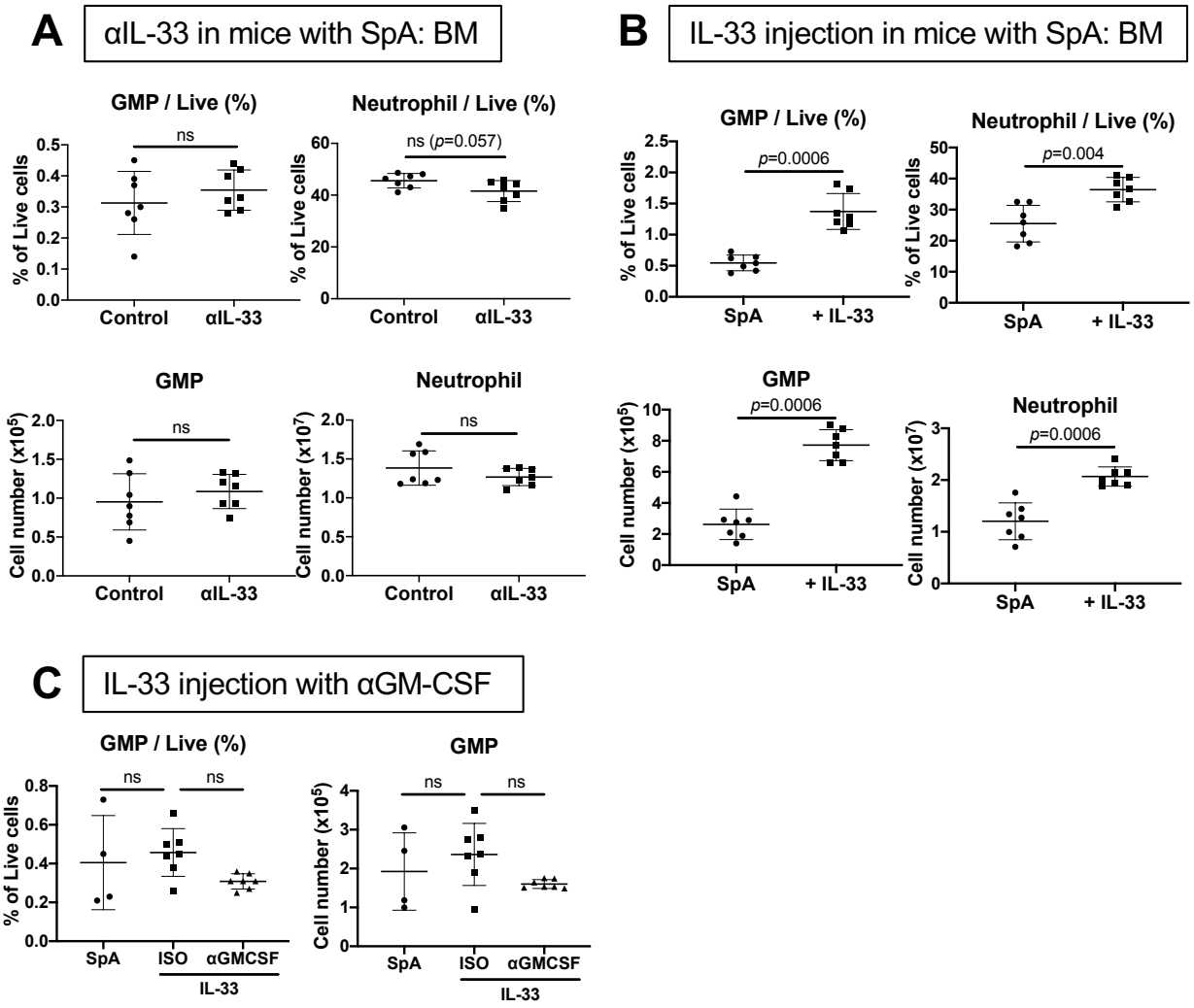

Figure 6.4: Recombinant IL-33 injections increase myelopoiesis in SpA
(**A**) Frequency among total live BM cells and absolute number in 1 femur and 1 tibia of GMPs and mature neutrophils of SKG mice injected with curdlan then either polyclonal anti-IL-33 antibodies of a goat IgG preparation before culling after 10 days.
(**B**) Frequency and absolute number of GMPs and mature neutrophils of SKG mice injected with curdlan then either PBS or IL-33 for 4 weeks until culled.
(**C**) Frequency and absolute number of GMPs in mice injected with curdlan. Some mice received IL-33 then either anti-GM-CSF antibodies(αGM-CSF) or isotype (ISO) for 4 weeks until culled. Points represent individual mice with mean and SD, one-way ANOVA with Tukey's test.
For (**A**)-(**B**), points represent individual mice with mean and SD, Mann-Whitney U test.

Data representative of 2 (**C**) or 3 (**B**) experiments or from a single experiment (**A**).

Collectively, this suggested that although IL-33 was implicated in accumulation of myeloid cells in the joints in early SpA, it was dispensable for expansion of the GMP population; in this setting, its effects might be superseded by those of other pro-myeloid cytokines such as TNF-α and GM-CSF. Conversely, injection of IL-33 caused expansion of BM myelopoiesis, with greater accumulation of mature myeloid progeny in the inflamed paws during disease, suggesting IL-33 can exert a pro-myelopoietic effect, which is partly attributable to induction of GM-CSF.

6.2.3 IL-33 enhances myelopoiesis by acting at multiple points in the haematopoietic system

The impact of IL-33 was difficult to separate from the complex immune background of SpA, which is associated with production of other cytokines that have a pro-myelopoietic effect, including GM-CSF [394], IL-1β, and TNF-α [393]. Consequently, I injected healthy SKG mice with IL-33 but not curdlan to determine if it would produce the same changes in myelopoiesis. When injected for 1 week, exposure to IL-33 alone was sufficient to expand the pool of GMPs in the BM (**Fig. 6.5A**), causing accumulation of BM neutrophils (**Fig. 6.5B**) and an increased white blood cell (WBC) count in peripheral blood (**Fig. 6.5C**). With prolonged exposure to IL-33 for 4 weeks, expansion of the GMP pool was still evident (**Fig. 6.6A**), but the number of neutrophils in the BM was similar when comparing IL-33 and PBS injected mice (**Fig. 6.6B**). Similarly, the WBC count in blood was still increased in mice injected with IL-33 for 4 weeks compared to controls (**Fig. 6.6C**), but the increase was of lesser magnitude than observed after IL-33 was injected for 1 week (**Fig. 6.5C**). Strikingly, with exposure to IL-33 for 4 weeks, mice also developed

mild infiltration of neutrophils into the perisynovial regions of the paw joints (**Fig. 6.6D**), indicating IL-33 alone could recapitulate some features of SpA without the additional innate immune stimulation of curdlan. However, these infiltrates did not cause measurable swelling of the paws or any change in their gross appearance (data not shown), indicating activation of autoreactive T cells by curdlan was necessary for disease progression.

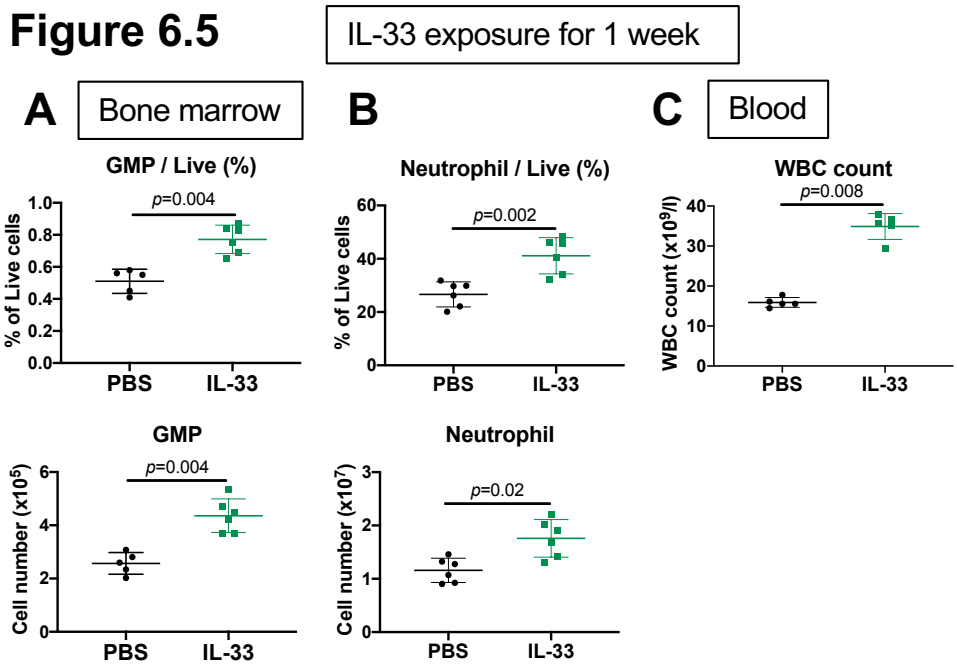

Figure 6.5: Recombinant IL-33 injections increase myelopoiesis in healthy mice
(**A**) Frequency among total live BM cells and absolute number in 1 femur and 1 tibia of GMPs in SKG mice injected with either PBS or IL-33 for 1 week.
(**B**) Frequency and absolute number of neutrophils for mice described in (**A**).
(**C**) Blood white blood cell (WBC) count for mice described in (**A**).
Points represent individual mice with mean and SD, Mann-Whitney U test.

Data representative of 3 independent experiments.

Figure 6.6 IL-33 exposure for 4 weeks

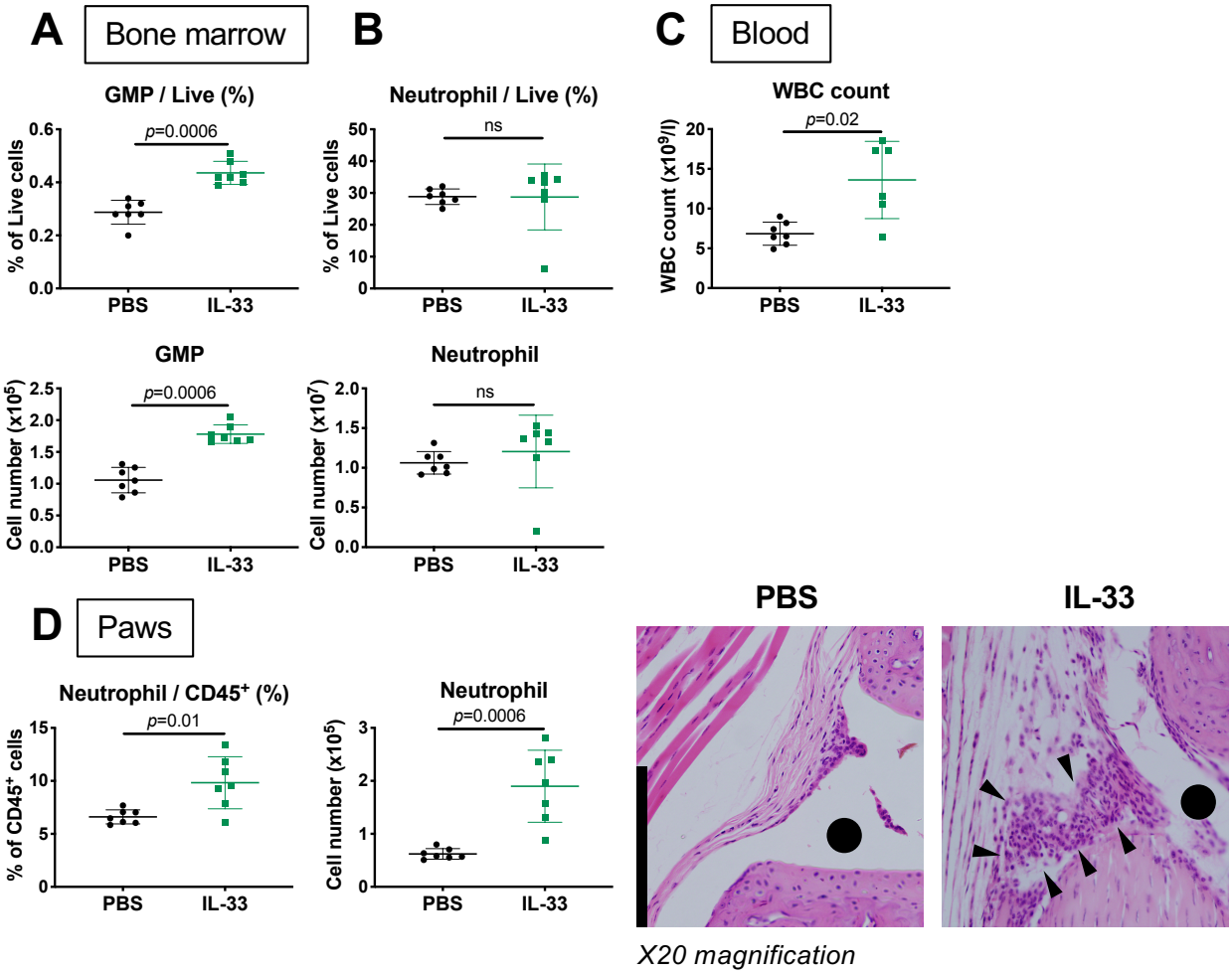

Figure 6.6: Exogenous IL-33 recapitulates some features of SpA
(**A**) Frequency among total live BM cells and absolute number in 1 femur and 1 tibia of GMPs of SKG mice injected with either PBS or IL-33 for 4 weeks.
(**B**) Frequency and absolute number of neutrophils for mice described in (**A**).
(**C**) Blood white blood cell (WBC) count for mice described in (**A**).
(**D**) (Left) Frequency among CD45⁺ leukocytes and absolute number of neutrophils in paws of mice described in (**A**). (Right) Representative photomicrographs of sagittal sections of the metatarsophalangeal joints of mice described in (**A**). Black dots indicate the joint space, blad arrowheads show infiltrating perisynovial leukocytes. Scale bar = 200 μm. Stained with haematoxylin and eosin.
Points represent individual mice with mean and SD, Mann-Whitney U test.

Data representative of 2 independent experiments.

These observations confirmed that IL-33 has a pro-myelopoietic effect, particularly in the first week of exposure, but I was concerned that the resolution of these investigations was too low to determine at which stage in the haematopoietic

system IL-33 might be acting. Previous studies suggested MPPs generate common myeloid progenitors (CMPs) with potential to produce megakaryoid/erythroid progenitors (MEPs) or GMPs. In this scheme, GMPs defined by conventional flow cytometric markers (LK, $CD34^+$, $CD16/32^+$) would give rise to all types of myeloid cell [15]. However, more recent work has developed this model by demonstrating that the 'CMP' designation is actually composed of a mixed population of progenitors that are already committed or predisposed to generate particular lineages [80, 140, 141]. According to this work, MPPs commit at an early stage to produce $GATA1^+$ myeloerythroid cells (red blood cells, platelets, mast cells/basophils, and eosinophils) or $GATA1^-$ cells (lymphocytes, neutrophils, and monocytes) [17, 80], departing from previous models by showing that basophils and eosinophils are linked more closely to erythroid/megakaryoid cells than to other types of myeloid cell. In these reports, some of the genes differentially expressed between $GATA1^+$ and $GATA1^-$ multipotent (pre-GM) progenitors were *Il1rl1*, which encodes ST2 (the specific receptor for IL-33), the high affinity IgE receptor FcεRI, and the complement inhibitory factor CD55, which has been proposed as the best surface marker to distinguish between these populations [80]. I confirmed the existence of different sub-populations of pre-GMs and GMPs in BM, finding that $CD55^+$ GMPs represented ~10% of the total and that approximately half of these cells co-expressed FcεRI (**Fig. 6.7A**).

Analysis of RNA sequencing data from our laboratory showed that *Il1rl1* was expressed at low levels in HSCs and MPPs, with slightly greater expression in GMPs (**Fig. 6.7B**). However, to refine these observations, I assessed ST2 expression by flow cytometry, using $ST2^{-/-}$ mice as controls. Whereas the expression of ST2 protein was low overall in the GMP pool and below the detection

threshold in pre-GM and LSK cells (**Fig. 6.7C**), as described before [358], it was preferentially expressed in CD55$^+$ GMPs, which correspond to the population of GATA1$^+$ GMPs (**Fig. 6.7D**). Therefore, I hypothesised that IL-33 might be exerting a selective stimulatory effect on GATA1$^+$ GMPs to cause increased production of mature myeloid cells. However, when I analysed the population of myeloid progenitors in more detail in SKG mice injected with IL-33 but not curdlan for 1 week, I found both CD55$^+$ and CD55$^-$ GMP populations were expanded (**Fig. 6.8A**). The CD55$^+$ GMPs were always less abundant than CD55$^-$ GMPs but their frequency in the GMP pool was increased with IL-33 injection (**Fig. 6.8B**). As might be expected with the expansion of CD55$^-$ GMPs, there was a corresponding increase in the frequency and number of BM neutrophils (**Fig. 6.8C**). However, among the expected progeny of CD55$^+$ GMPs, there was a striking expansion of eosinophils but not basophils with IL-33 (**Fig. 6.8D**). This suggested IL-33 might promote the production of eosinophils from CD55$^+$ progenitors to a greater extent than basophils, as has been suggested previously [358].

Figure 6.7

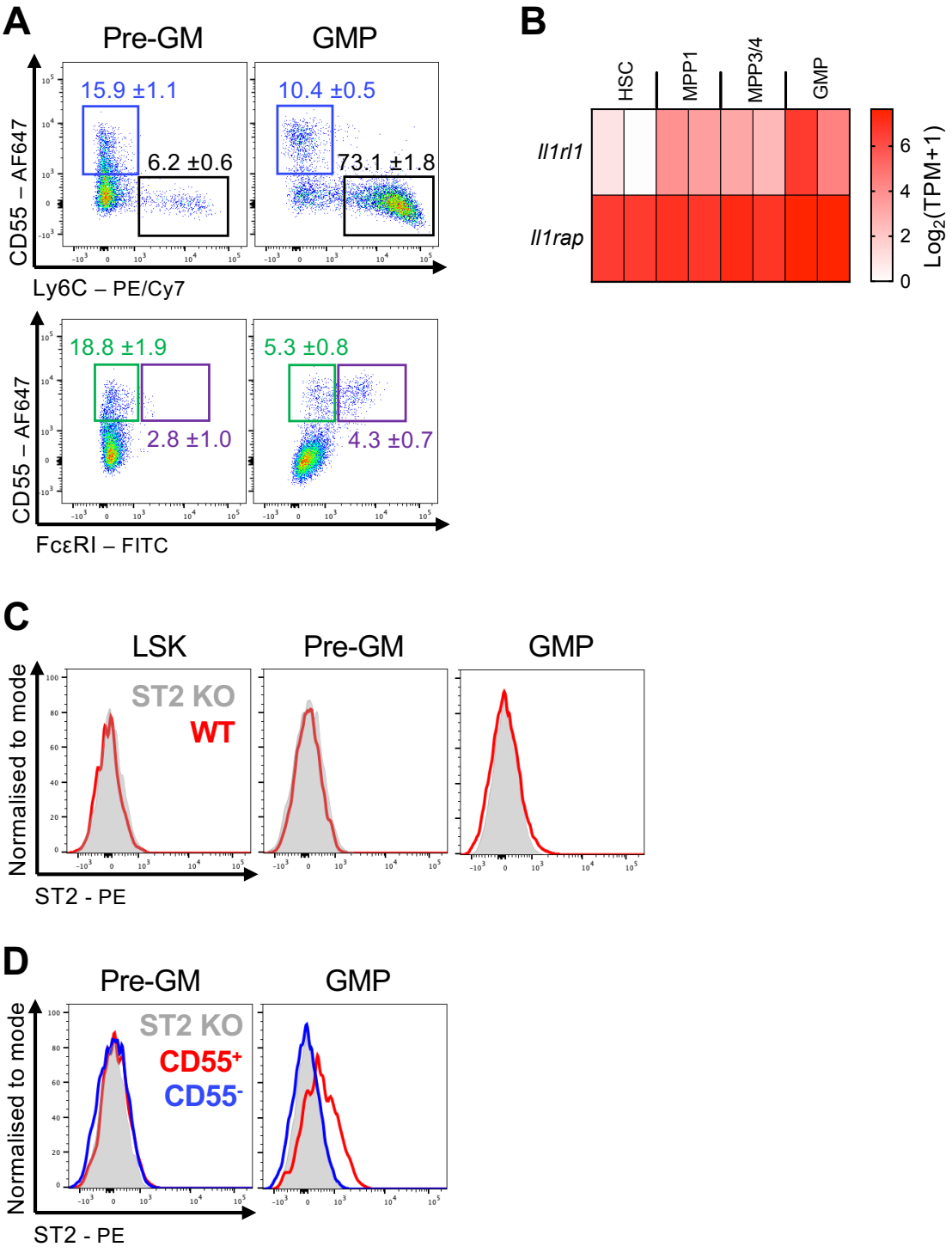

Figure 6.7: ST2 is expressed on CD55⁺ GMPs

(**A**) Representative flow cytometric images showing expression of CD55 and FcεRI in the pool of GMP and pre-granulocyte macrophage (pre-GM) progenitors from the healthy BM of SKG mice. Figure represent mean and SD frequencies among the progenitor populations for n=5 mice.

(**B**) Expression of genes encoding ST2 (*Il1rl1*) and IL1RAP (*Il1rap*) in indicated cell populations by RNA sequencing in transcripts per million (TPM). Columns represent biological replicates. Data derived from our laboratory.

(**C**) Representative flow cytometric images of indicated progenitor populations stained for ST2 in C57BL/6 wild type (WT) and ST2$^{-/-}$ (ST2 KO) mice.

(**D**) Representative flow cytometric images of indicated progenitor populations stained for ST2 according to CD55 expression in WT and ST2 KO mice.

Data representative of 2 independent experiments (**A**), (**C**), (**D**).

Figure 6.8

Bone marrow

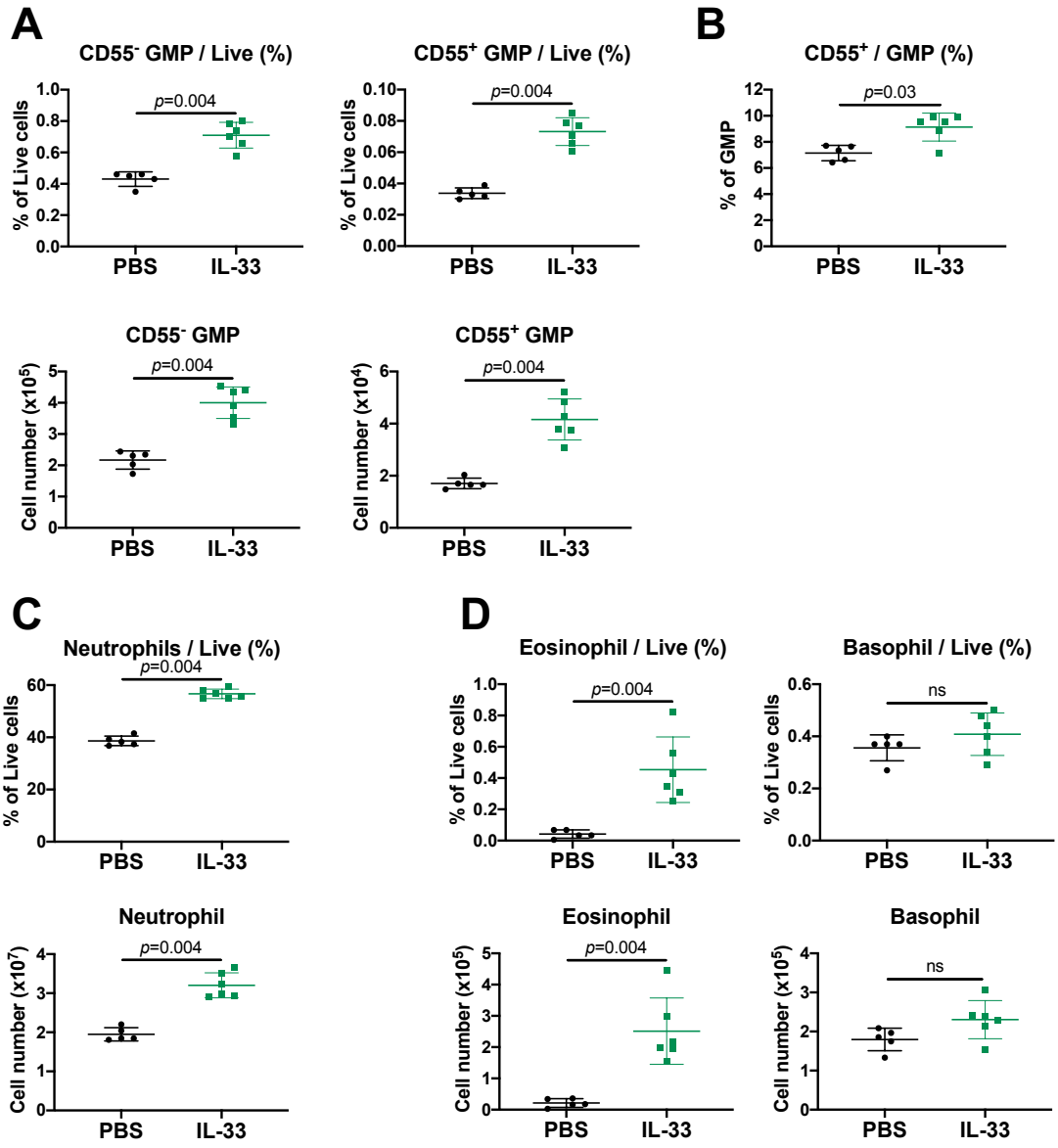

Figure 6.8: IL-33 expands both CD55⁻ and CD55⁺ GMPs

(**A**) Frequency among total live BM cells and absolute number in 1 femur and 1 tibia of CD55⁺ and CD55⁻ GMPs from SKG mice injected with PBS or IL-33 for 1 week.
(**B**) Frequency of CD55⁺ GMPs among the total GMP population for mice described in (**A**).
(**C**) Frequency and absolute number of neutrophils in mice described in (**A**).
(**D**) Frequency and absolute number of eosinophils and basophils in mice described in (**A**).
Points represent individual mice with mean and SD, Mann-Whitney U test.

Data representative of 3 independent experiments.

I wished to understand the relevance of these findings in the context of curdlan-induced inflammation. When injecting curdlan in SKG mice, I found similar expansion of both $CD55^+$ and $CD55^-$ GMPs after 1 week (**Fig. 6.9A**), as was observed with IL-33 injection. Curdlan also caused expansion of BM neutrophils and eosinophils after 1 week, but not basophils (**Fig. 6.9B**). To understand whether curdlan-induced expansion of different types of GMP and mature cell was dependent on IL-33, I injected curdlan in C57BL/6 WT mice and IL-$33^{-/-}$ or $ST2^{-/-}$ mice. This caused similar expansion of the total GMP pool and mature neutrophil population in BM of WT mice as observed in SKG mice (**Fig. 6.10A**), and these changes were similar in IL-$33^{-/-}$ (**Fig. 6.10A**) and $ST2^{-/-}$ mice (**Fig. 6.10B**). This suggested IL-33 was dispensable for accumulation of GMPs and neutrophils in response to curdlan, reconciling with similar findings in SKG mice injected with anti-IL-33 antibodies (**Fig. 6.4B**). In contrast, the frequency and number of eosinophils was increased in the BM with curdlan treatment in WT mice but not in IL-$33^{-/-}$ or $ST2^{-/-}$ mice (**Fig. 6.10C**), indicating IL-33 signalling through the ST2 receptor was required for this effect. When examining the GMP pool in more detail using the surface marker FcεRI, which is expressed only in the population of $CD55^+$ GMPs, I found both $Fc\varepsilon RI^+$ and $Fc\varepsilon RI^-$ GMPs were increased by curdlan in WT and IL-$33^{-/-}$ mice (**Fig. 6.10D**), suggesting expansion of these populations was not dependent on IL-33. With expansion of $Fc\varepsilon RI^+$ GMPs in response to curdlan but decreased accumulation of eosinophils in the absence of IL-33, I hypothesised that IL-33 might act indirectly to increase the number of these progenitors but directly to induce subsequent differentiation of eosinophils.

Figure 6.9

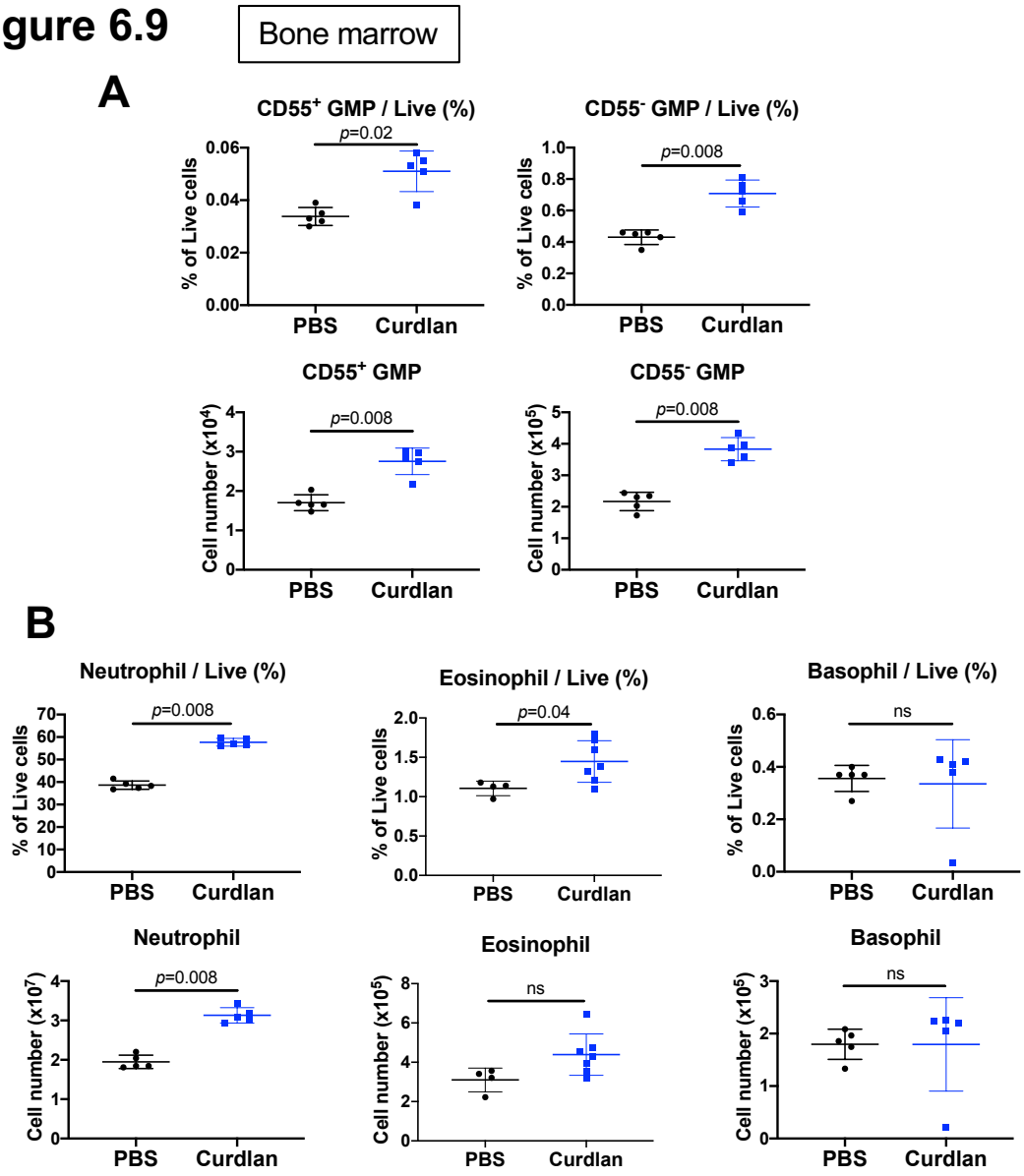

Figure 6.9: Curdlan expands both CD55$^-$ and CD55$^+$ GMPs
(**A**) Frequency among total live BM cells and absolute number in 1 femur and 1 tibia of CD55$^+$ and CD55$^-$ GMPs from SKG mice injected with PBS or curdlan then culled after 1 week.
(**B**) Frequency and absolute number of neutrophils, eosinophils and basophils in mice described in (**A**).
Points represent individual mice with mean and SD, Mann-Whitney U test.

Data representative of 4 independent experiments.

Figure 6.10

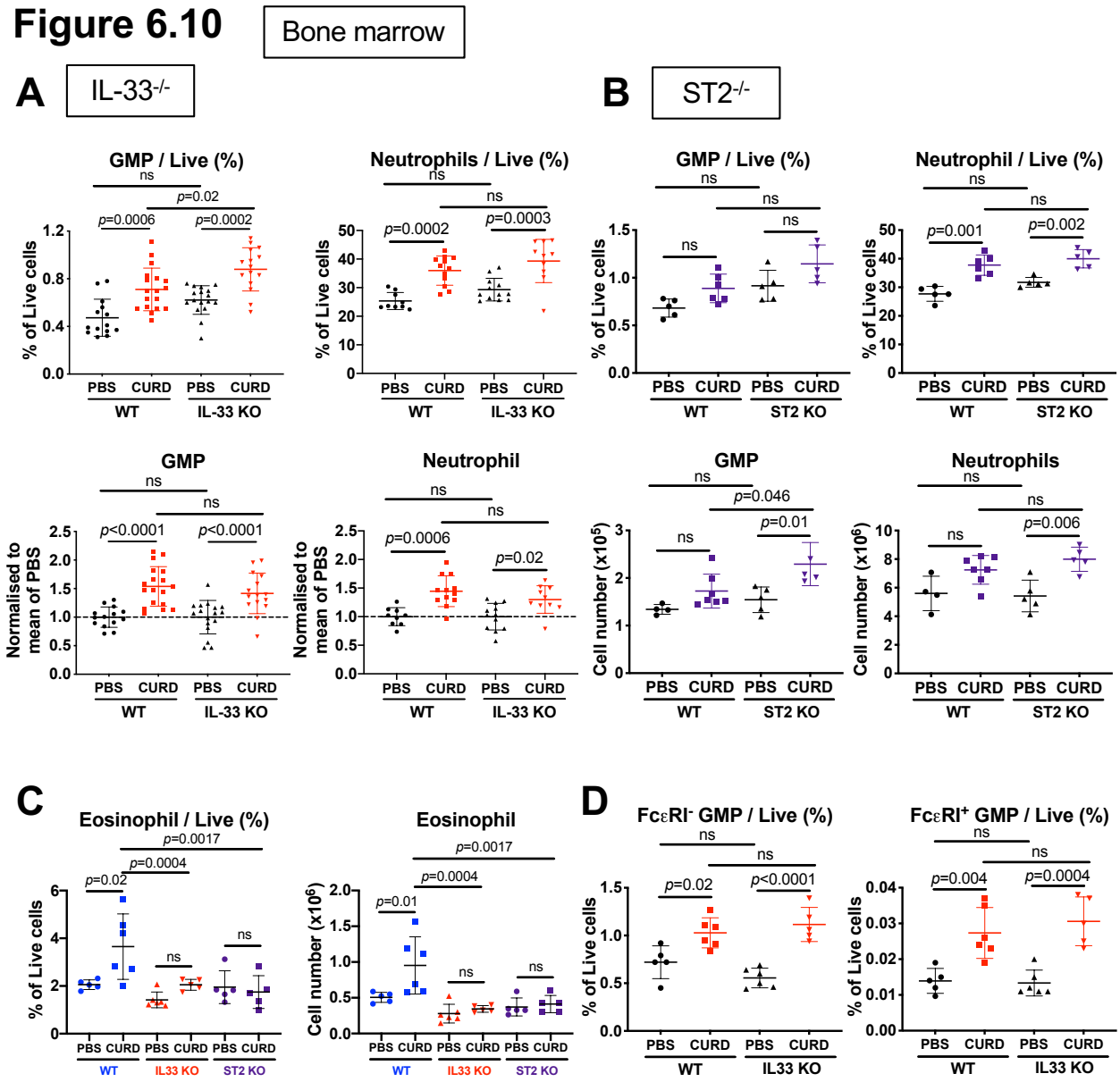

Figure 6.10: IL-33 is required for curdlan-induced expansion of eosinophils
(**A**) Frequency among total live BM cells and absolute number in 1 femur and 1 tibia of total GMPs and neutrophils from C57BL/6 wild type (WT) and IL-33$^{-/-}$ (IL33 KO) mice injected with PBS or curdlan then culled after 1 week.
(**B**) Frequency and absolute number of total GMPs and neutrophils from C57BL/6 wild type (WT) and ST2$^{-/-}$ (ST2 KO) mice injected with PBS or curdlan then culled after 1 week.
(**C**) Frequency and absolute number of eosinophils in BM of WT, IL-33$^{-/-}$, and ST2$^{-/-}$ mice injected with PBS or curdlan then culled after 1 week.
(**D**) Frequency of FcεRI^{-} and FcεRI^{+} GMPs among total live BM cells in WT and IL-33-/- mice injected with PBS or curdlan then culled after 1 week.
Points represent individual mice with mean and SD, two-way ANOVA with Sidak's test.

Data representative of 2 (**B**), (**C**), (**D**) or 4 (**A**) independent experiments.

To test this hypothesis, I sorted progenitors by FACS for culture *ex vivo* in medium supplemented with haematopoietic cytokines. Using $CD55^-$ pre-GM cells, IL-33 had little impact on the frequencies of cell types observed after 4 days of culture, except to cause a reduction in those with the surface phenotype of monocytes ($CD11b^+$, $CD115^+$) (**Fig. 6.11A**). Conversely, among $CD55^+$ pre-GMs, IL-33 increased the frequencies of cells resembling neutrophils ($CD11b^+$, $Ly6G^+$) and eosinophils ($CD11b^+$, $Ly6G^-$, $SiglecF^+$) but caused a striking reduction in $Fc\varepsilon RI^+$ cells (**Fig. 6.11B-C**). This was particularly apparent for those cells resembling basophils ($Fc\varepsilon RI^+$, $CD49b^+$), which were effectively absent when IL-33 was present (**Fig. 6.11B-C**). This recalled the selective effect of IL-33 when injected *in vivo*, where eosinophils were significantly increased in BM but basophils were not (**Fig. 6.8D**). Collectively, this suggested IL-33 might exert direct effects on $CD55^+$ pre-GM cells to promote granulopoiesis but not on $CD55^-$ counterparts.

Since both $CD55^+$ and $CD55^-$ GMPs were expanded by IL-33, I asked whether this could be attributable to an effect on upstream MPPs, producing an expanded pool for differentiation of all types of myeloid progenitor irrespective of GATA1 expression. I considered this plausible because, even though the ST2 receptor protein was not detected by flow cytometry on LSK cells, we and others have shown that *Il1rl1* is expressed in the same population, and others have demonstrated that ST2 has some functional role in HSCs [357], suggesting that the receptor might be able to regulate cell behaviour even if expressed at low levels. In our setting, I found IL-33 expanded the MPP pool to a similar extent as did curdlan after one week, but there was no change in the frequency or number of primitive HSCs (**Fig. 6.12**).

Figure 6.11

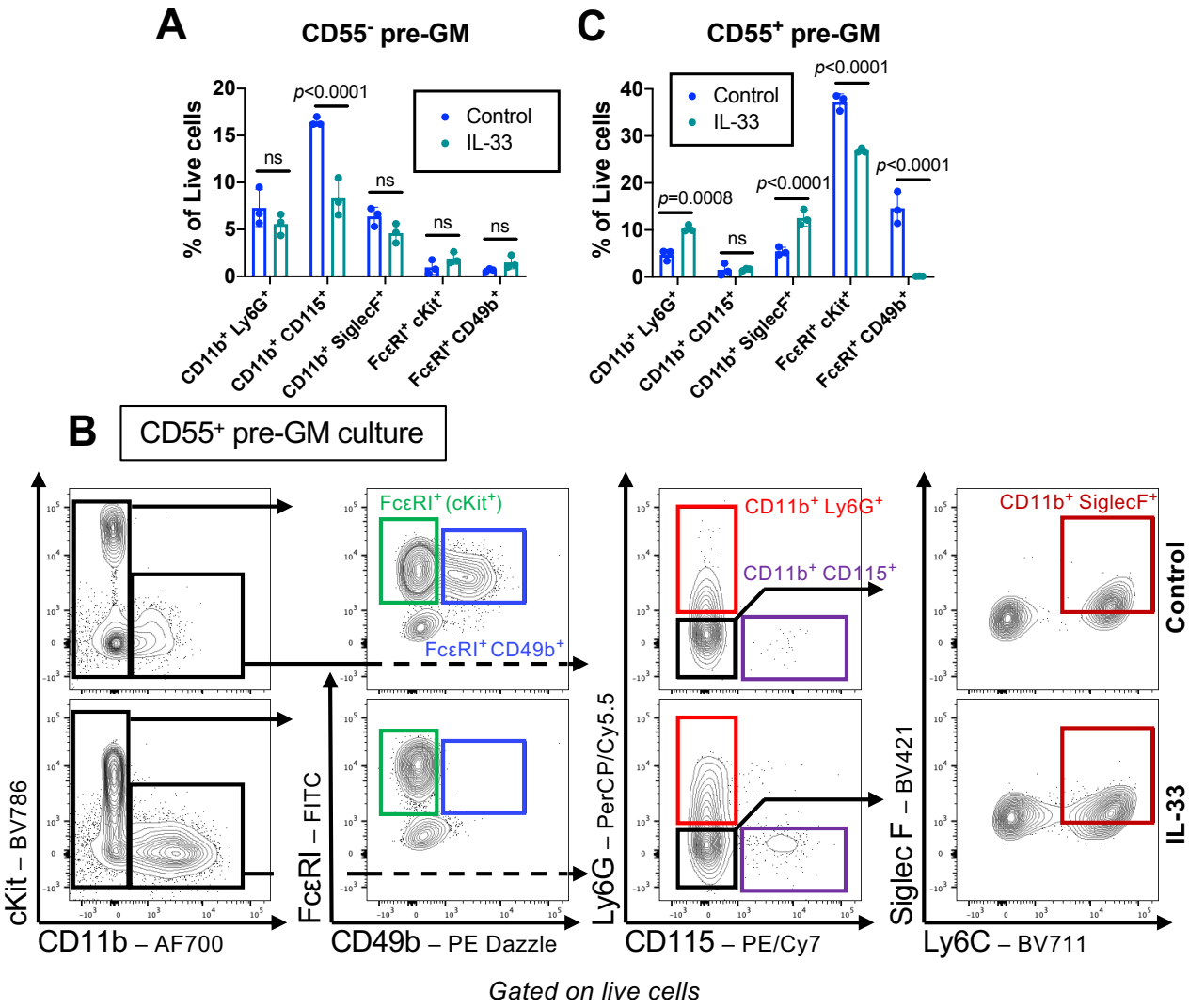

Figure 6.11: IL-33 has differential effects on CD55⁺ and CD55⁻ progenitors *ex vivo*

(**A**) Frequency of cells with indicated surface phenotypes among total live cells derived from culture of CD55⁻ pre-GM cells sorted by FACS from the BM of healthy SKG mice after 7 days.

(**B**) Representative flow cytometric images of cells derived from CD55⁺ pre-GMs isolated and cultured as described in (**A**). Figures represent mean and SD for technical triplicates of a single experiment.

(**C**) Frequency of cells with indicated surface phenotypes among total live cells derived from culture of CD55⁺ pre-GM cells sorted by FACS from the BM of healthy SKG mice after 7 days.

For (**A**) and (**C**), points represent technical replicates in a single experiment, bars indicate mean with SD, two-way ANOVA with Sidak's test.

Data representative of 2 independent experiments.

Figure 6.12

Bone marrow

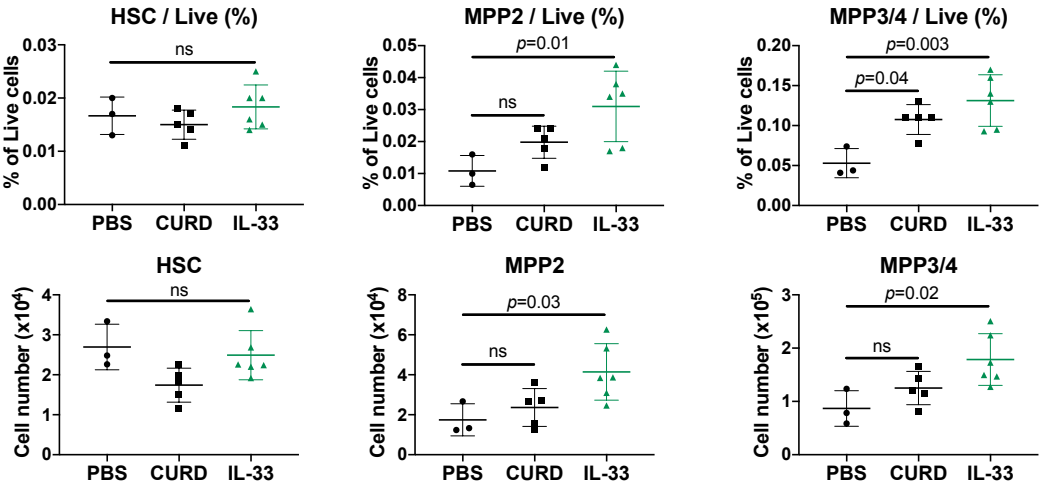

Figure 6.12: IL-33 expands cells in the LSK population
Frequency among total live BM cells and absolute number in 1 femur and 1 tibia of indicated LSK populations in healthy SKG mice injected with PBS or IL-33 for 1 week. Points represent individual mice with mean and SD, Mann-Whitney U test.

Data representative of 2 independent experiments.

6.2.4 IL-33 exerts a combination of direct and indirect effect on HSPCs

My results suggested IL-33 might exert a number of effects on HSPCs at different points in the myeloid differentiation trajectories extending from MPPs to the formation of mature neutrophils and eosinophils. However, it remained unclear which cells or processes were experiencing direct effects, and which were affected by indirect effects, including cytokines produced in response to IL-33. To investigate this, I produced mixed BM chimeras by reconstituting lethally irradiated CD45.1^{+} recipients with a 1:1 mixture of BM from WT (CD45.1^{+}) and ST2$^{-/-}$ donors (CD45.2^{+}, **Fig. 6.13A**). Presence or absence of the IL-33 receptor produced no effect on chimerism of blood cells 4 weeks after reconstitution (**Fig. 6.13B**), though others have reported that ST2$^{-/-}$ cells become less competitive by 6 months [357]. Five weeks after reconstitution, the chimeras were injected with curdlan or IL-33 and culled after 1 week to determine the frequency of cell types among CD45^{+} cells

of each genotype. Because mature erythroid cells and erythroid progenitors do not express CD45, they were effectively excluded from this analysis, meaning that values differ from other figures in this chapter where frequencies among total live BM cells are reported (see **coronavirus statement)**. This was complicated by the relative increase in frequency of all $CD45^+$ cells among live cells with curdlan or IL-33 injection (**Fig. 6.13C**), which I attribute to the expected increase in ($CD45^+$) myeloid cells and reduction in ($CD45^-$) erythroid cells under these conditions. However, differences between genotypes could still be assessed, with significant differences in frequency indicating probable direct effects of IL-33 acting through ST2.

Figure 6.13

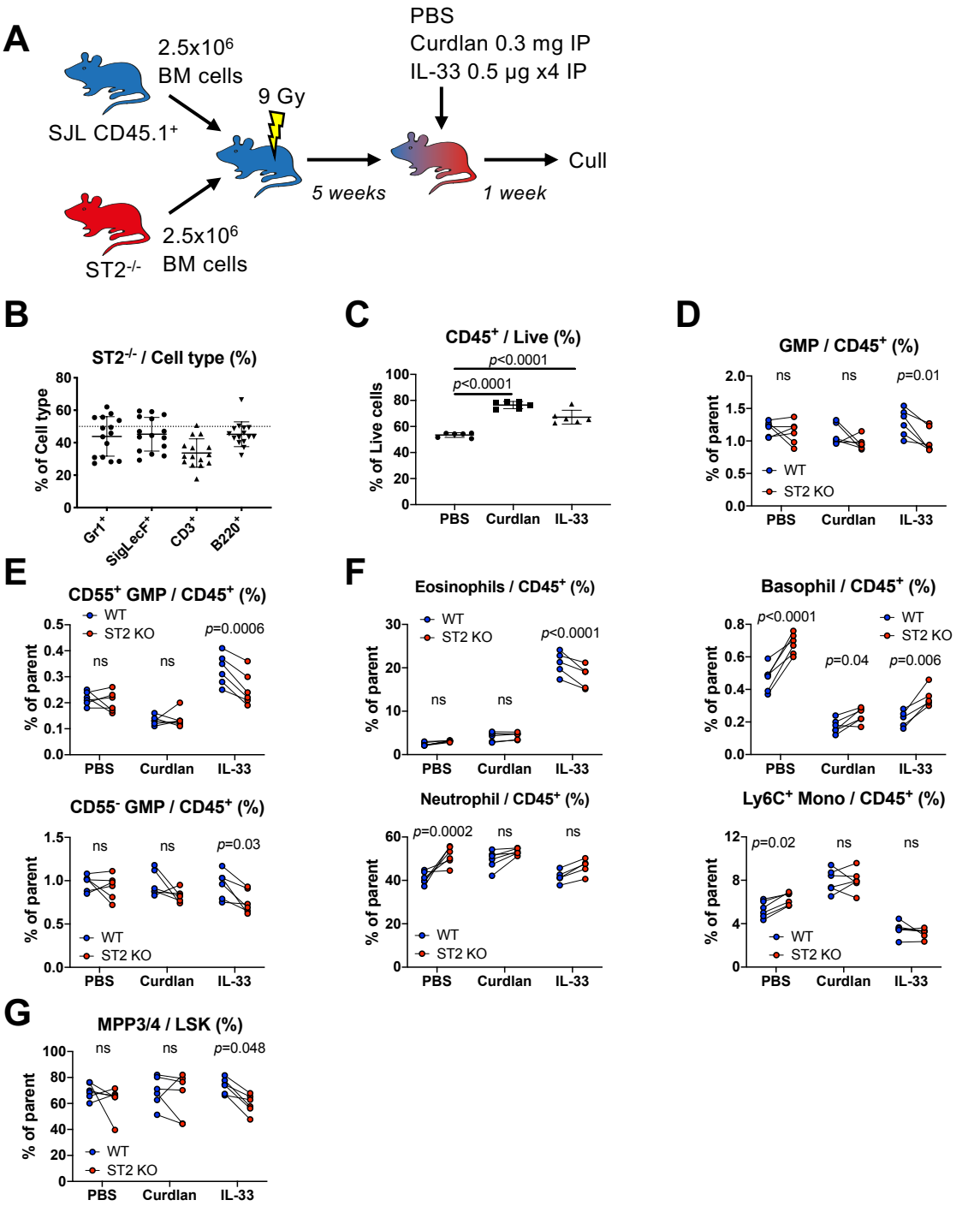

Figure 6.13: IL-33 has direct and indirect effects on haematopoiesis

(**A**) Schematic diagram showing reconstitution of lethally irradiated CD45.1⁺ recipients with a 1:1 mixture of whole BM from wild type (WT) CD45.1⁺ mice and ST2⁻/⁻ (ST2 KO) CD45.2⁺ mice. Mice were injected with PBS, curdlan or IL-33 for 1 week before culling to generate data shown in (**C**)-(**G**).

(**B**) Total blood chimerism in chimeras described in (**A**) after 5 weeks. Points represent individual mice with mean and SD.

(**C**) Frequency of CD45⁺ of both genotypes among total live cells. Points represent individual mice with mean and SD, one-way ANOVA with Tukey's test.

(**D**) Frequency of GMPs among parent BM types.

(**E**) Frequency of CD55⁺ and CD55⁻ GMPs among parent BM types.

(**F**) Frequency of indicated mature cell types among parent BM types.

(**G**) Frequency of MPP3/4 cells among parent BM types.

In (**B**), (**D**)-(**G**), points represent individual mice with mean and SD, two-way ANOVA with Sidak's test. Data from a single experiment.

Analysing results in this way, I found that IL-33 had direct effects on the GMP pool because there was a difference in frequency of GMPs between WT and $ST2^{-/-}$ BM of mice injected with IL-33 (**Fig. 6.13D**). Although this difference was detectable in both $CD55^{+}$ and $CD55^{-}$ GMPs, it was most striking in $CD55^{+}$ GMPs, which were increased by IL-33 to a greater extent in WT than in $ST2^{-/-}$ cells (**Fig. 6.13E**). Examining the cells produced by different types of GMP, there was no difference in the frequency of neutrophils or $Ly6C^{+}$ monocytes among BM genotypes of chimeras injected with curdlan or IL-33 (**Fig. 6.13F**), suggesting expansion of neutrophils when IL-33 is injected *in vivo* is not a direct effect of the cytokine. Conversely, the frequency of eosinophils was greater in WT cells than in $ST2^{-/-}$ (**Fig. 6.13F**), suggesting accumulation of eosinophils after IL-33 injection is mediated partly by a direct effect of the cytokine. In contrast, the frequency of basophils was decreased among WT cells under all conditions compared to $ST2^{-/-}$ cells (**Fig. 6.13F**), suggesting IL-33 was exerting a direct effect to decrease their numbers. Upstream of GMPs, the frequency of MPP3/4 cells was lower among $ST2^{-/-}$ LSK cells than WT LSK cells with injection of IL-33 (**Fig. 6.13G**), suggesting the expansion of MPPs observed after injection of IL-33 *in vivo* might be a direct effect of the cytokine.

Based on these data, I suggest IL-33 exerts a direct effect on MPPs to cause expansion, creating a pool of cells capable of pursuing myeloid differentiation along either $GATA1^{+}$ or $GATA1^{-}$ pathways. This effect is presumably attributable to expression of ST2 at levels below the detection threshold of flow cytometry. Accumulation of committed myeloid progenitors of both types is then dependent on a combination of direct and indirect effects of IL-33; direct effects may be more important in $GATA1^{+}$ than $GATA1^{-}$ GMPs, but the accumulation of $GATA1^{+}$ GMPs in response to IL-33 is still dependent on other indirect factors because their

frequency was still increased among ST2$^{-/-}$ cells with IL-33 injection, albeit to a lesser extent than in WT cells (**Fig. 6.13E**). Downstream of GMPs, accumulation of neutrophils caused by IL-33 is mediated predominantly by secondary factors. Conversely, numbers of GATA1^{+} myeloid cells are influenced by direct effects of IL-33 to permit accumulation of eosinophils but restrain the frequency of basophils, reconciling with similar effects seen with *ex vivo* culture of CD55^{+} pre-GMs with IL-33 (**Fig. 6.11C**) and with injection of IL-33 *in vivo* (**Fig. 6.8D**).

6.3 Discussion

In this chapter, I find that administration of anti-IL-33 antibodies to mice with SpA ameliorates myeloid infiltration into the joints whereas recombinant IL-33 injection exacerbates it. I further show that IL-33 exerts direct and indirect effects in different parts of the haematopoietic system, with direct effects on the frequency of MPP3/4s, GMPs, eosinophils, and basophils.

6.3.1 Role of IL-33 in the disease phenotype of SpA

Treatment of mice developing SpA with anti-IL-33 antibodies decreased the extent of neutrophil and monocyte accumulation in the paws but did not affect the BM GMP population. The latter finding was confirmed when curdlan was injected in IL-33$^{-/-}$ and ST2$^{-/-}$ mice, which suggests it was probably not attributable to inadequate blockade of IL-33 with antibody injection: these mice had similar expansions of the GMP population when compared to WT mice, indicating that neither IL-33 nor the ST2 receptor was required for this effect. Importantly, this differed from the effect of endogenous IL-33 on erythropoiesis in SpA, where control mice had lower CFU-E frequencies and blood Hgb concentrations than those

treated with anti-IL-33 antibodies (see **chapter 5.2.6**). The relative lack of effect of any curdlan-induced IL-33 on myelopoiesis was confirmed by analysis of mixed BM chimeras, where there were few differences between WT and $ST2^{-/-}$ populations in the same mice injected with curdlan. Collectively, this suggests IL-33 may have a more important role in regulating infiltration and survival of mature myeloid cells in the inflamed joints than in modulating BM myelopoiesis during SpA (**Fig. 6.14**). This notion is supported by other models of inflammatory arthritis in mice, where IL-33 affected local disease progression by attracting neutrophils directly and by causing local production of TNF-α, which also recruits myeloid cells [376]. This question could be investigated further by crossing $ST2^{-/-}$ mice onto the SKG background then producing mixed SKG/SKG.$ST2^{-/-}$ BM chimeras. When these mice were injected with curdlan, it would be possible to compare the accumulation of cells of different genotypes in BM and paws. According to my hypothesis, there would be little difference in myeloid populations in the BM, as seen with mixed BM chimeras in this chapter, but ST2 sufficient cells would accumulate preferentially in the joints. Conversely, I show that exogenous IL-33 can exacerbate disease in murine SpA, which could be attributable to a combined effect on BM myelopoiesis and local effects in the inflamed sites; the relative importance of these effects could again be established in SKG/SKG.$ST2^{-/-}$ chimeras injected with IL-33.

Figure 6.14

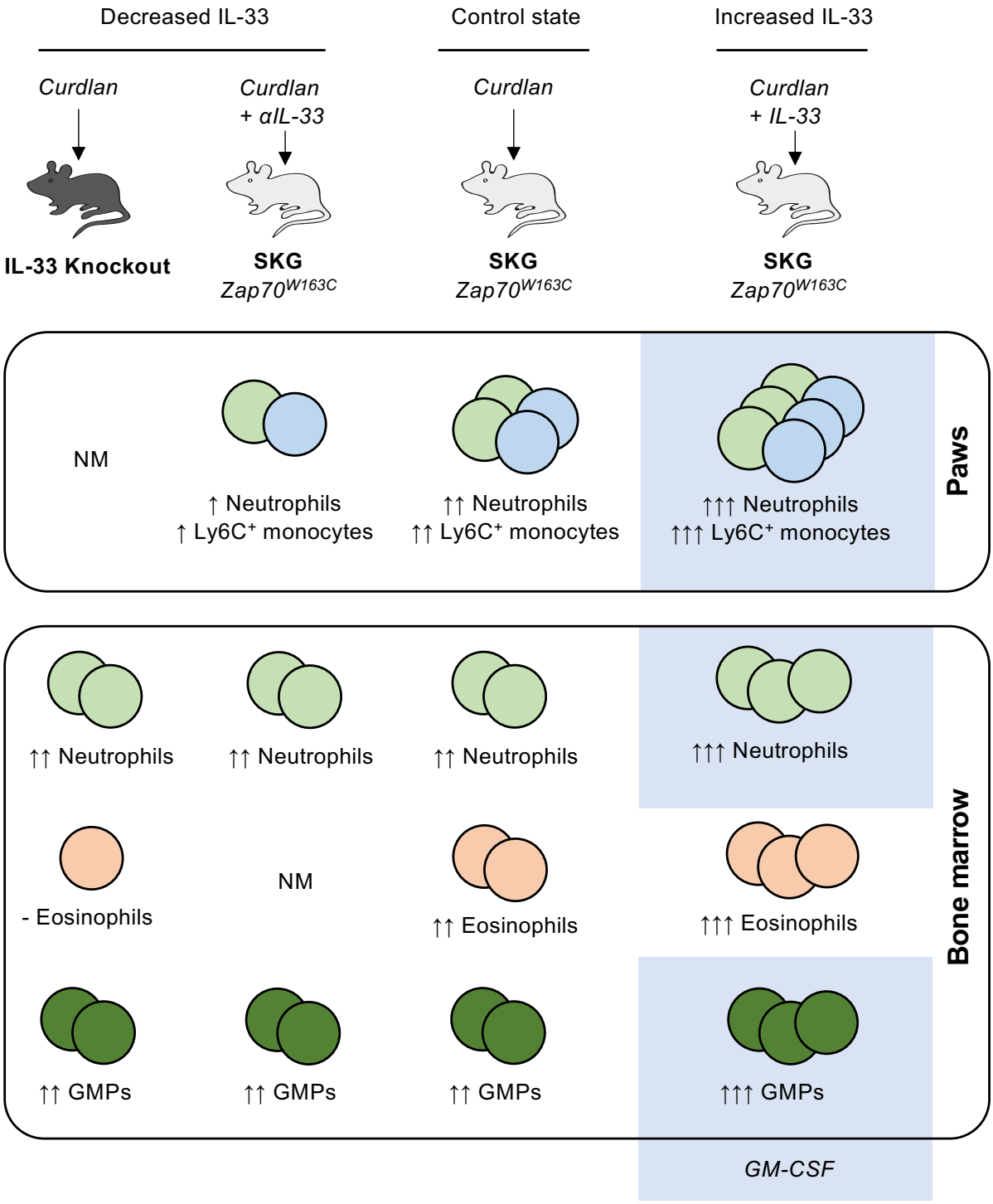

Figure 6.14: Summary of the effects of IL-33 on myelopoiesis in SpA
Schematic diagram showing the effect of increased or decreased amounts of IL-33 on the phenotype of mature myeloid cell infiltration of the inflamed paws and on bone marrow myelopoiesis in the context of SpA. Blue shading indicates those effects likely to be mediated indirectly by IL-33-induced production of GM-CSF. Differences among models suggest that IL-33 might promote entry of mature myeloid cells into the paws but that it is not required for expansion of granulocyte macrophage progenitor (GMP) numbers in the bone marrow during SpA. Conversely, IL-33 does appear to be required for eosinophil expansion in bone marrow during SpA. NM: not measured.

My work suggests systemic increases in endogenous IL-33 are an early event in SpA, detectable in BM plasma in the first week after curdlan injection but no longer apparent after 4 weeks, even though increased amounts of IL-33 were measured from explants of paw and small intestine at that time. This reduction in IL-33 in BM plasma could be related to production of the counter-regulatory soluble ST2 receptor, which is produced rapidly in response to increased IL-33 [330]. In accordance with this notion, it was interesting to note that some effects of exogenous IL-33 injection, such as expansion of BM neutrophils and increased blood leukocytes, also decreased in magnitude when IL-33 was injected for 4 weeks as opposed to 1 week, suggesting this treatment might also induce feedback mechanisms that moderate its biological effects. The early increase in IL-33 led me to hypothesise that any contribution it would make to development of SpA would occur before the onset of severe disease in a similar fashion to murine DSS colitis, where IL-33 is pathogenic early in disease but not later (see **chapter 1.3.4**). However, I have not investigated whether the effect of anti-IL-33 antibodies to decrease myeloid cell accumulation in the paws would be lost later, nor whether this treatment could alleviate myeloid cell infiltration in the paws if commenced after inflammation had already started to develop. Alternatively, if the major effect of IL-33 in SpA is in local recruitment of myeloid cells, anti-IL-33 treatment may remain effective throughout disease because I found IL-33 was increased in paw and small intestine explants from mice with advanced SpA.

I showed that some effects of IL-33 injection on disease are mediated by GM-CSF, which has a non-redundant role in development of arthritis in the SKG model [394, 441] that is probably related to its effects on the myeloid compartment [539, 540]. However, in the experiment where I injected IL-33 and anti-GM-CSF

antibodies in mice developing SpA, the mechanisms by which IL-33 exacerbates disease and anti-GM-CSF ameliorates it could be independent, rather than converging around GM-CSF. For example, in another study, IL-33 exacerbated murine arthritis induced by K/BxN serum transfer by increasing degranulation of mast cells and production of autoantibodies [351]. The same authors showed that IL-33 increased autoantibody production and caused mast cells to produce pro-inflammatory cytokines in arthritis induced by collagen immunisation [350]. In both cases, mast cells were essential for the effect of IL-33, but the authors did not demonstrate which effector mechanism of these cells was necessary. In our previous work, we showed that IL-33 alone does not induce degranulation of cultured BM mast cells but does cause them to produce GM-CSF *in vitro* and *in vivo*, suggesting this may be the more important role of IL-33-activated mast cells in disease [441], and that the major role of IL-33 might indeed be to increase GM-CSF production. This uncertainty about whether IL-33 is acting only through GM-CSF might be resolved by injecting IL-33 in SKG mice crossed onto a background deficient in GM-CSF or its receptor as they developed SpA, but this approach might not be successful because SKG mice are largely protected from development of arthritis in the absence of GM-CSF [394, 441].

6.3.2 Regulation of myelopoiesis during SpA

Accumulated evidence in this chapter suggests endogenous IL-33 makes little contribution to expansion of the GMP pool observed in SpA; we have shown previously that this effect is critically dependent on GM-CSF [441]. I refine this previous study of myelopoiesis in SKG mice by showing that curdlan causes expansion of both $CD55^+$ and $CD55^-$ GMPs, with corresponding increases in mature

myeloid cells thought to be derived from each (eosinophils and neutrophils, respectively). My analysis of these changes was complicated by a change in methodology during my thesis: initially, I identified GATA1$^+$ myeloid cells by their expression of FcεRI, but I later used CD55 after the publication of papers that described this as a more inclusive marker of the GATA1$^+$ population [17, 80]. My analysis shows that all FcεRI$^+$ GMPs also express CD55, but, when I assessed only FcεRI$^+$ GMPs, a number of CD55$^+$, FcεRI$^-$ cells will have been counted among the FcεRI$^-$ GMPs. This could be important because FcεRI$^+$ GMPs might represent the population partially or completely committed to generate basophils and mast cells, which express the same receptor [143].

Although the contribution of basophils to SpA has not been established in the SKG model, I suggest the increase in eosinophils presumably deriving from CD55$^+$ GMPs is largely incidental because I showed in **chapter 4.2.3** that eosinophil depletion using anti-IL-5 antibodies did not affect disease progression. This raises the interesting notion that expansion of myelopoiesis during chronic inflammatory disease may be relatively non-specific, causing accumulation of some cell types that may be redundant. Alternatively, these cells might have a role that has not been detected in my experiments. For example, eosinophils might contribute to fibrosis in chronically inflamed joints, but I have not investigated whether this occurs in SKG mice or whether eosinophils contribute to it.

6.3.3 Regulation of myelopoiesis by IL-33

The limited role for endogenous IL-33 in regulating myelopoiesis in SpA led me to rely on IL-33 injection to evaluate its effects, and the remainder of this discussion focuses on those results. Whereas this intervention produces a clear

phenotype, which has been helpful in my investigations, the physiological relevance of administering IL-33 to such excess is probably limited for this model. As with IL-4, discussed in **chapter 4**, it is possible that IL-33 might have a more important role in regulation of myelopoiesis in diseases where it is produced in larger quantities, such as allergic disease or parasite infestation.

6.3.3.1 HSPCs

I show that IL-33 exerts a number of actions at different stages in the production of mature myeloid cells (**Fig. 6.15A-B**). First, IL-33 exerted a direct effect to increase the relative abundance of myeloid-biased MPP3/4 progenitors among LSK cells. This refines previous findings showing that IL-33 causes expansion of the whole LSK population when injected *in vivo* [367], and I also confirm that IL-33 has no effect on the size of the more primitive HSC population [369]. Downstream of MPPs, I found IL-33 increased populations of both $CD55^+$ and $CD55^-$ GMPs when injected *in vivo*, which might be attributable to increased generation of all types of GMP from the expanded MPP pool. However, whereas IL-33 had no direct effect on the frequency of ($GATA1^-$) neutrophils in mixed BM chimeras, it caused accumulation of ($GATA1^+$) eosinophils while limiting the number of basophils. Therefore, my work contributes to newly proposed models of haematopoiesis [17, 80, 541] by showing that extrinsic cytokine regulation also differs according to GATA1 status. In previous work, *Il1rl1*, encoding ST2, was one of the most differentially regulated genes when comparing $GATA1^+$ and $GATA1^-$ pre-GM progenitors [80]. More broadly, the ST2 receptor is expressed by progenitors giving rise to most types of $GATA1^+$ cell at some stage, including mast cells, basophils, eosinophils ($CD55^+$ GMP), red blood cells (pre-CFU-E and CFU-E,

see **chapter 5**), and platelets (pre-MegE, at low levels). Conversely, *Il1rl1*/ST2 does not appear to be expressed in progenitors of any GATA1^{-} cells, although it is acquired in several types of mature cell deriving from those lineages, including Tregs, Th2 and Th9 T cells, activated Th1 and Th17 T cells, ILC2s, NKT cells, neutrophils, dendritic cells, and macrophages.

Figure 6.15

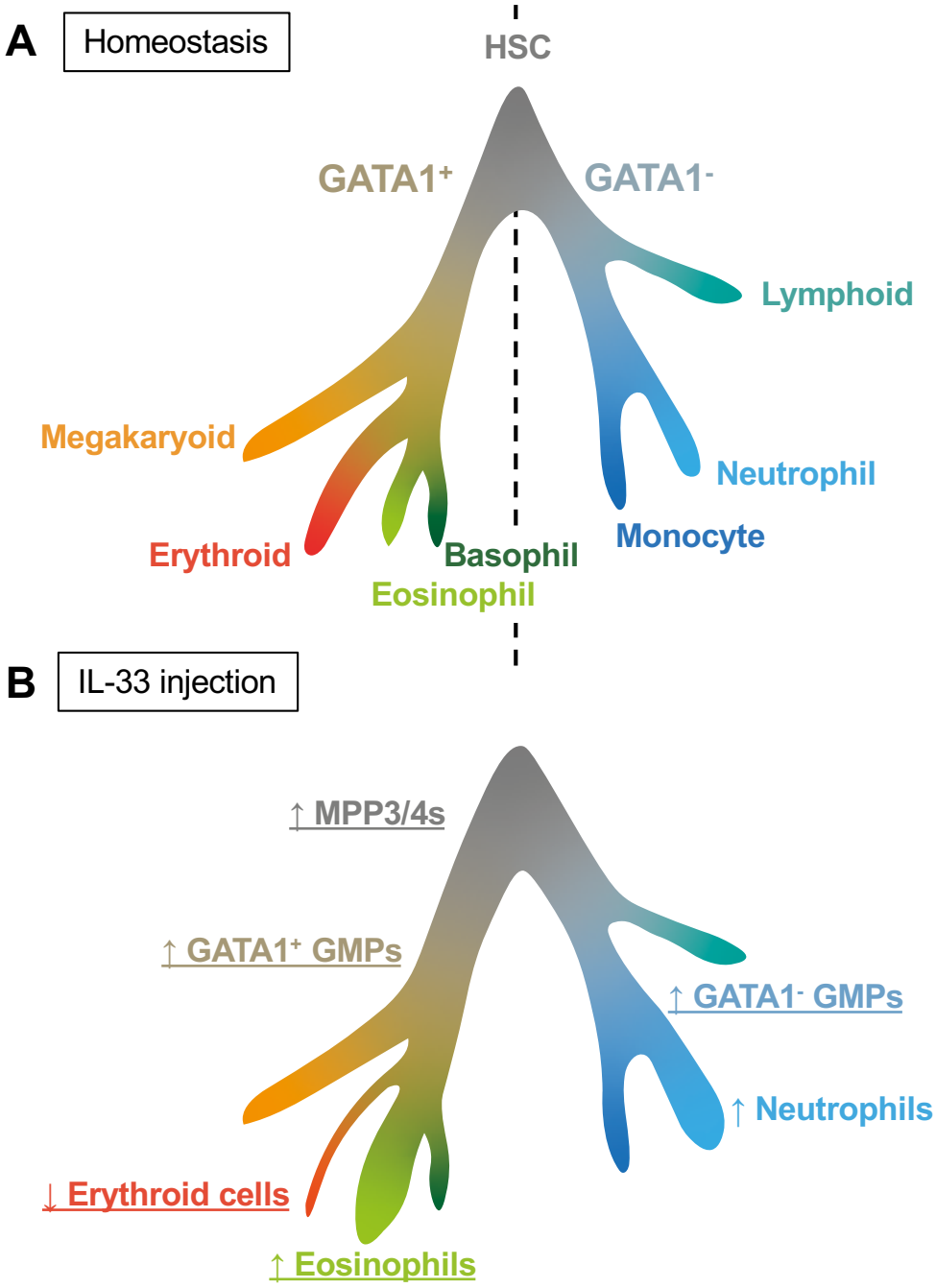

Figure 6.15: Model for the effects of IL-33 injection on haematopoiesis
(**A**) Under homeostatic conditions, haematopoiesis forms a continuum of differentiation from HSCs to various lineages, with a major branch occurring between cells that do or do not express GATA1.
(**B**) With IL-33 injection, the indicated changes occur, with underlined events indicating those in which a direct effect of IL-33 is entirely or partly implicated, based on the results of *ex vivo* cultures and mixed BM chimeras in this chapter.

In the GATA1$^+$ branch of haematopoiesis, I show that IL-33 produces highly variable effects on component lineages, inhibiting differentiation of erythroid progenitors (**chapter 5**), favouring accumulation of eosinophils, decreasing basophil output, while seeming to have little effect on the megakaryoid lineage (data not shown). Previous studies have also reported that IL-33 causes peripheral eosinophilia when injected in mice [368], and *Il33* and *Il1rl1* genes have been identified as loci affecting the basal eosinophil count, but not other blood cell counts, in humans in genome-wide association studies [542], suggesting IL-33 is an important physiological regulator of eosinophil survival and/or eosinopoiesis. In support of this, previous work had also shown that IL-33 has a role in murine BM eosinopoiesis by expanding a progenitor stage before the onset of IL-5 sensitivity [323], and my work builds on these observations by showing that the cells affected by IL-33 are in fact CD55$^+$ pre-GMs/GMPs, from which eosinophil progenitors are derived [80].

Although I find that IL-33 affects different GATA1$^+$ lineages selectively, I cannot infer the mechanism by which this is occurring because my observations are compatible with several possible mechanisms: 1) lineage-instructive effects on multipotent cells to promote one fate over another, 2) selective expansion or inhibition of apparently multipotent cells that are already committed to one, or a restricted number, of fates, 3) re-direction of apparently committed progenitors of one lineage to another, 4) differential lineage-reinforcing or inhibiting effects that affect terminal differentiation of some lineages to mature stages, even if they do not affect the emergence of committed progenitors, and 5) effects on mature cells to maintain survival or a differentiated state.

As I show in erythroid progenitors, IL-33, in common with other members of the IL-1 cytokine family, causes activation of NF-kB, and I speculate that the differential effects of IL-33 in different lineages could be related to the different consequences of NF-kB activation. The effect of NF-kB in haematopoiesis is complex and has been difficult to investigate using knockout models owing to the widespread expression of major members of the signalling complex within and without the haematopoietic system [543, 544]. Nevertheless, it seems that while sustained expression of NF-kB members inhibits erythroid differentiation in cell lines owing to their probable interference with GATA1 [526], some members, such as p50, promote differentiation of myeloid progenitors by activating PU.1 and the transcription factor C/EBP-α [545]. Thus, I suggest the activation of NF-kB induced by IL-33, which is probably common to all cell types expressing ST2, could exert lineage-specific effects dictated by the variable nature of interactions of NF-kB members with different lineage-defining transcription factors required for terminal differentiation. This hypothesis could be extended further to suggest that the variable effects of different IL-1 family cytokine members on haematopoietic progenitors may be related to their efficacy in activating NF-kB according to their receptor expression. For example, I found IL-1β was much less effective in inhibiting erythropoiesis in cultured pre-CFU-Es when compared to IL-33 (**chapter 5.2.2**), which may be related to greater expression of the IL-33 receptor and more effective activation of NF-kB. Conversely, I found IL-33 did not directly promote megakaryopoiesis or GATA1^{-} myelopoiesis *in vivo* whereas IL-1β, for which the receptor is expressed at higher levels in myeloid and megakaryocyte progenitors than that of IL-33, promoted myelopoiesis and megakaryopoiesis in previous studies, in a manner that was also dependent on NF-kB activation [247, 251, 546].

Further exploration of this hypothesis would require 1) over- and under-expression of NF-kB members with and without cytokine stimulation in a wider range of progenitor types and 2) investigation of the interactions between NF-kB members and lineage-defining transcription factors to determine whether the effects of IL-33 in various lineages could be attributable to a shared but non-instructive mechanism.

Instead of or as well as any effect on lineage-committed progenitors, IL-33 could have an instructive effect on GATA1$^+$ multipotent progenitors. If so, such an effect would probably be related to usage of transcription factors that are expressed differentially in the different GATA1$^+$ lineages (see **chapter 1.1.6**). Given the observed effects of IL-33 in haematopoiesis, I speculate that any lineage instructive effect among GATA1$^+$ multipotent progenitors would involve C/EBP-α and/or FOG-1. In particular, increased expression or activity of C/EBP-α would be expected to produce the observed increase in eosinophils but not basophils, while having little effect on the erythroid and megakaryoid lineages. This reconciles with the separate effect of IL-33 on erythropoiesis, which occurs after erythroid progenitors have already been specified. To my knowledge, the effect of IL-33 on C/EBP-α activity has not been investigated in any cell type, but it is interesting to note that IL-33 causes marked upregulation of the IL-5 receptor in EoPs [323], and that expression of the gene encoding this protein (*Il5ra*) is strongly regulated by C/EBP-α [547].

6.3.3.2 Mature cells

The ST2 receptor is not expressed on mature platelets and erythrocytes, suggesting it probably exerts little direct effect on these cells beyond their differentiation. However, ST2 is expressed by mature eosinophils and mast cells, and IL-33 enhances survival of eosinophils directly [548]. This effect was less

striking than that of IL-5, but IL-33 also causes production of IL-5 from various type 2 immune cells, including Th2 T cells and ILC2s [290], to the extent that IL-33 injection in mice causes a marked increase in the serum concentration of IL-5 [205]. Subsequently, it was shown that co-administration of an anti-IL-5 antibody with IL-33 in mice reduces the extent of peripheral eosinophilia caused by the latter [323], demonstrating that this effect of IL-33 is at least partly mediated by an effect on mature cells. This reconciles with my own data showing that IL-33 increased the frequency of eosinophils in $ST2^{-/-}$ cells in mixed BM chimeras but to a lesser extent than in WT cells, showing there was a considerable indirect effect alongside the direct effect on $CD55^{+}$ GMP frequency.

6.4 Conclusions

- In SpA, IL-33 promotes accumulation of mature myeloid cells in the paws; this effect is alleviated by concurrent GM-CSF blockade.
- IL-33 expands BM myelopoiesis when injected in healthy mice or mice with SpA by causing accumulation of both types of GMPs, neutrophils, and eosinophils; the same changes are observed with curdlan injection but only eosinophil expansion is dependent on IL-33 in this setting.
- IL-33 mediates direct effects on MPPs, GMPs, eosinophils, and basophils *in vivo*, but not neutrophils.
- The prevailing effect of IL-33 is to promote accumulation of eosinophils at the expense of basophils, suggesting it could affect the behaviour of $CD55^{+}$ myeloid progenitors from which both are derived: this effect is observed *ex vivo*.

7 Discussion

7.1 Summary

In common with other chronic inflammatory diseases, SpA in humans is associated with haematological abnormalities, of which the causes are largely unknown. Human and murine SpA are associated with type 17 immune responses, which play an important role in development of disease in the joints and enthesis. However, in human SpA, there was evidence of a concurrent type 2 immune module in the small intestine. Knowing that the type 2 cytokines IL-4, IL-5, and IL-33 have been suggested as possible regulators of haematopoiesis in our own work and in previous studies, I combined these areas of investigation to ask what role is played by these cytokine pathways in the remodelling of haematopoiesis that occurs in murine SpA, and whether this is of clinical importance in disease.

In this thesis (**Fig. 7.1**), I show that development of SpA in SKG mice causes perturbations in haematopoiesis, resulting in a marked bias in the BM towards myelopoiesis at the expense of erythropoiesis and lymphopoiesis (**chapter 3**). I find there is evidence of a type 2 immune module in the mesenteric lymph nodes and small intestine of mice with SpA, just as there is in humans, resulting in accumulation of IL-4$^+$ CD4$^+$ T cells. Although I show that IL-4 is capable of inducing early myeloid differentiation in murine HSCs *ex vivo* and *in vivo* (**Fig. 7.2A**), I find this pathway is not required for development of clinical disease in SpA (**chapter 4**). When comparing myeloid and erythroid progenitors, I find that the receptor for IL-33, ST2, is expressed preferentially among the latter. Interleukin-33 suppresses differentiation of erythroid progenitors *ex vivo* and *in vivo*, to the extent that repeated injection causes anaemia in healthy mice. This effect is dependent on NF-kB

activation and associated with decreased responsiveness to EPO. I therefore identify IL-33 as a novel mediator of anaemia of chronic inflammation and EPO resistance (**chapter 5**). Developing this topic further, I show that production of IL-33 in murine SpA promotes accumulation of myeloid cells in the joints, and that exogenous IL-33 can stimulate myelopoiesis. The latter effect is dependent on a combination of direct and indirect effects, with direct effects on the frequencies of myeloid-biased MPPs, GMPs, and eosinophils but not on neutrophils. My work therefore reveals IL-33 as a mediator of co-ordinated responses in multiple parts of the haematopoietic system (**chapter 6**) (**Fig. 7.2B**).

Figure 7.1

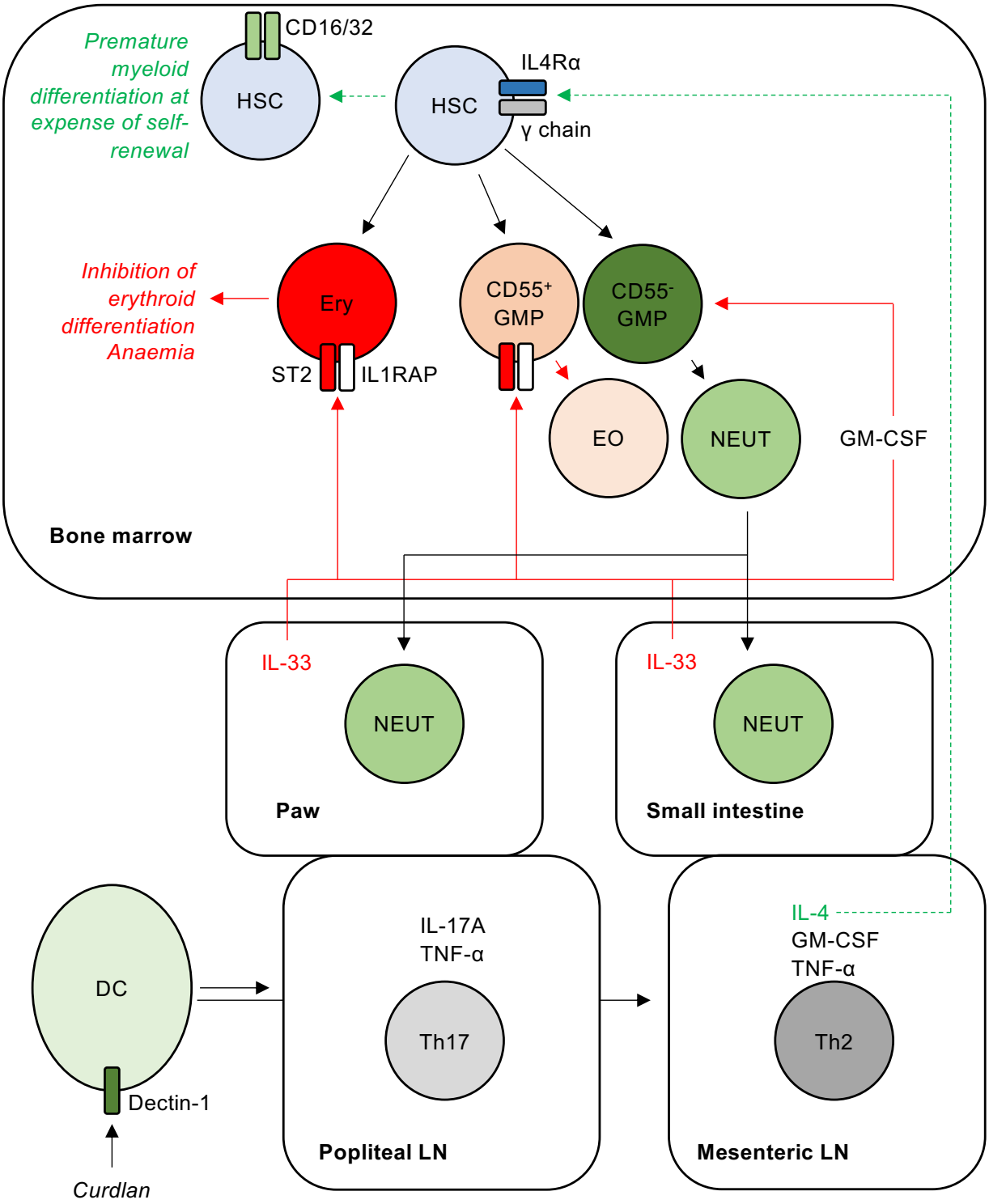

Figure 7.1: Summary of major findings of thesis

Schematic diagram showing major findings described in this thesis. During SpA, curdlan injection causes development of autoreactive T cells producing predominantly IL-17A in the popliteal lymph node (LN) but mainly IL-4 in the mesenteric LN. Although the receptor for IL-4 is expressed on HSCs and can induce early myeloid differentiation at the expense of self-renewal potential, this pathway does not appear to be important during murine SpA. Release of IL-33 in the inflamed paw and small intestine suppresses differentiation of erythroid progenitors, resulting in anaemia of inflammatory disease. Additionally, IL-33 stimulates eosinophil (EO) production directly from CD55$^+$ GMPs, but generation of eosinophils does not appear to play an important role in development of SpA, where accumulation of neutrophils (NEUT) in the inflamed sites is key to disease progression. Effects of IL-33 shown in red lines, potential effects of IL-4 shown with dashed green lines, though these are not apparently important in murine SpA.

Figure 7.2

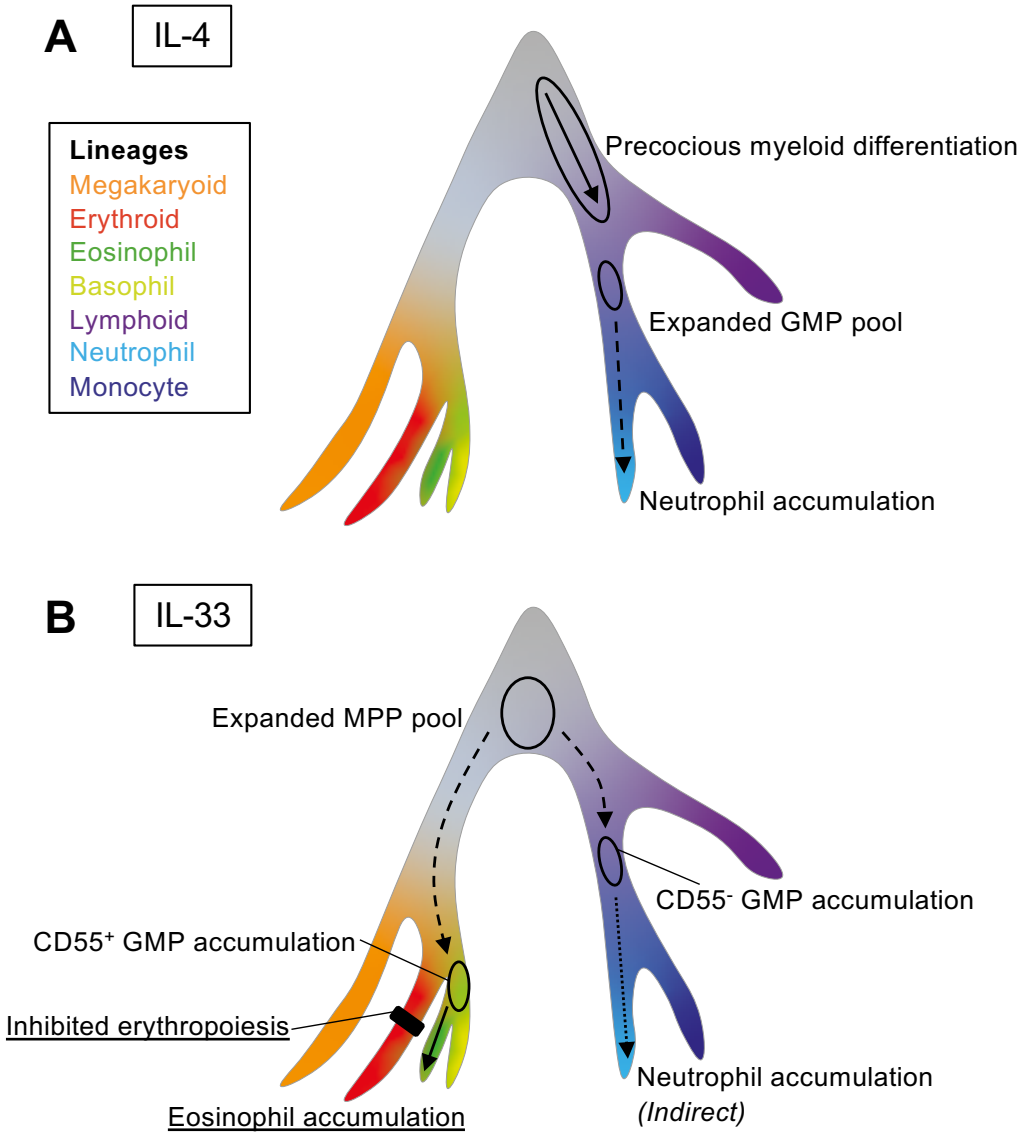

Figure 7.2: Summary of *in vivo* effects of IL-4 and IL-33 on haematopoiesis in bone marrow

(**A**) IL-4 caused HSCs to adopt features of myeloid differentiation *ex vivo* and *in vivo*, probably resulting in GMP expansion. *In vivo*, this was associated with neutrophil accumulation though, *ex vivo*, monocytes prevailed.

(**B**) IL-33 expanded the MPP pool and directly caused expansion of both types of GMP. It caused accumulation of eosinophils but not basophils, and increased neutrophils through an indirect effect. It also specifically inhibited differentiation of erythroid progenitors but did not prevent them from being specified from MPPs. Dashed lines indicate proposed effects; solid lines indicate observed direct effects in this thesis, and dotted lines indicate observed indirect effects. Underlined events indicate those occurring in SpA or with curdlan injection that are dependent on the relevant cytokine.

7.2 Context

My work contributes to a growing corpus showing that haematopoiesis is a dynamic process that may be affected by chronic inflammation [243, 256, 259]. Many different cytokine pathways have been implicated in this process, and I now identify IL-33 as a contributor to some aspects of the haematopoietic phenotype of murine SpA (**Fig. 7.3A-B**). Importantly, there appears to be considerable redundancy and overlap in the actions of different inflammatory cytokines to remodel haematopoiesis, with different mediators probably playing more or less important roles according to the type of immune response that dominates particular diseases. For example, mice infected with intracellular pathogens such as *Mycobacterium avium* develop comparable haematopoietic changes to those with SpA but, among the former, this is probably mediated more by IFN-γ than IL-33 [36, 37, 549]. This recalls a similar argument made about emergency granulopoietic responses to infection [219]: G-CSF, GM-CSF, and IL-3 all have similar effects on myelopoiesis, but each is required for beneficial responses to some types of pathogen infection and not others. This variability in the importance of individual cytokines in different diseases is also likely to explain my results investigating IL-4: I showed that IL-4 can affect myelopoiesis but that this pathway appeared to be unimportant in SpA (**Fig. 7.3A**). However, in a different disease setting characterised by more flagrant production of IL-4, such as allergic or parasitic disease, this pathway might be of considerable importance.

Figure 7.3

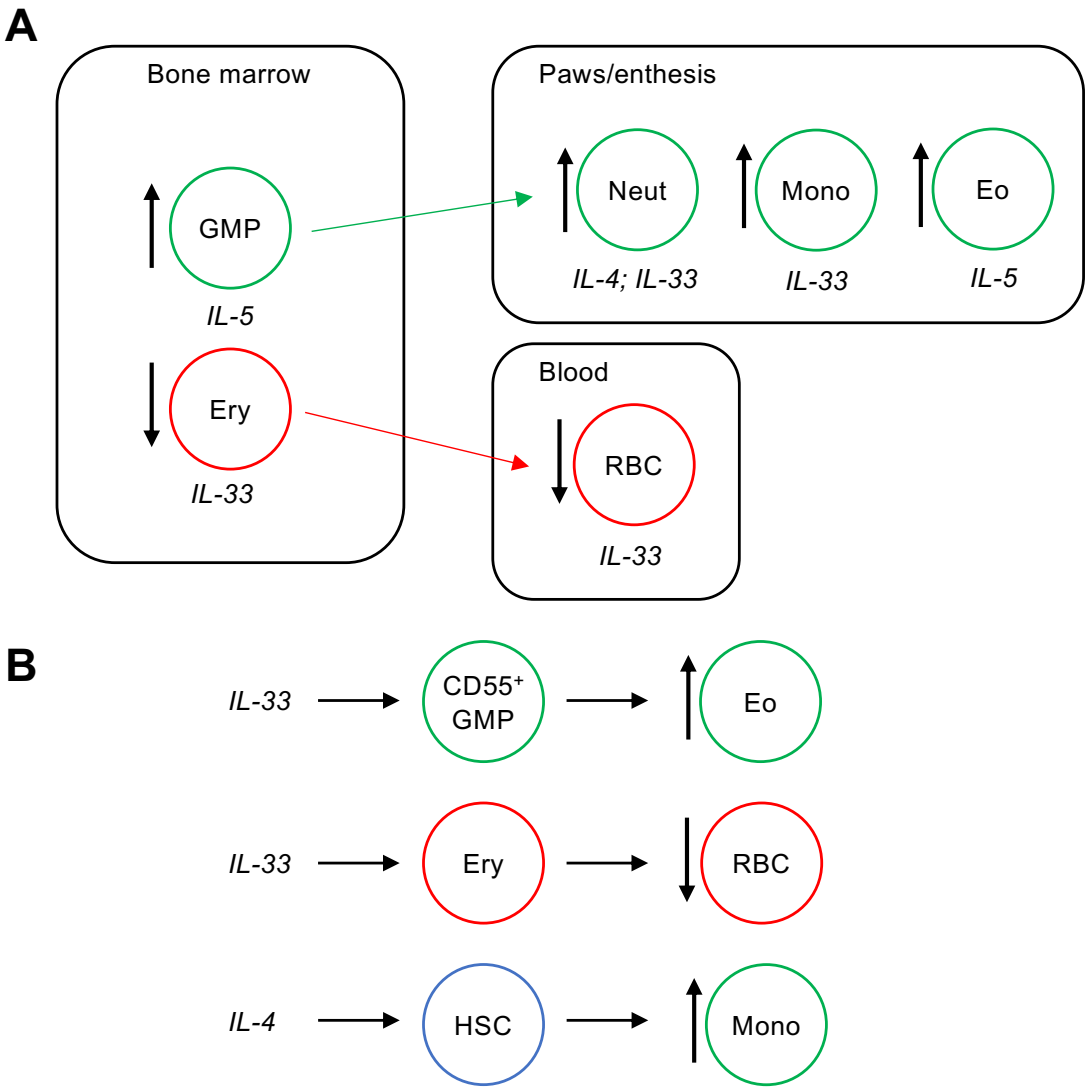

Figure 7.3: Effects of type 2 cytokines on haematopoiesis in SpA and *ex vivo*
(**A**) Schematic diagram showing changes occurring in SpA in BM, blood, and inflamed paws that were affected by one or more type 2 cytokines. Cytokines observed to have an effect on indicated events in this thesis are shown below schematic cell types. Neut: neutrophil, Mono: monocyte, Eo: eosinophil, RBC: red blood cell, Ery: erythroid progenitors.
(**B**) Summary of major ex vivo effects of indicated cytokines on different progenitor stages sorted from murine BM and cultured *ex vivo.*

The period of time over which the work described in this thesis has been conducted has coincided with some changes in the prevailing models and concepts used to understand haematopoiesis, which have been underwritten by advances in single cell technologies and studies of undisturbed haematopoiesis [13, 18, 21, 44, 67, 81, 483]. One important example is the discovery that erythroid, megakaryoid,

basophil, mast cell, and eosinophil lineages segregate from others at an early stage [17, 80]. My work adds to these developing concepts by showing that cytokine regulation also partitions along similar lines, with IL-33 affecting HSPCs predominantly in one branch of this scheme but less strikingly in the other. This contributes to a wider re-evaluation of the importance of extrinsic signals in the regulation of haematopoiesis under homeostatic conditions: HSPCs are known to express receptors for a considerable number of cytokines, hormones, and other soluble mediators, but the function of most of these molecules among these cells is unknown. Examples of newly described role for cytokines in haematopoiesis include IL-27 as a stimulator of HSC differentiation [204] and IL-17 as a promoter of erythropoiesis [17]. Conceptually, these findings highlight a need to move towards a more ecological framework that recognises the importance of all interactions of a cell, some of which may compete or contradict one another, in determining its behaviour. Thus, in future, it may become more common to consider the effects of inflammatory cytokines on HSPCs as an interacting web rather than as reductionist pathways, as I have done in this thesis.

7.3 Applications

I identify IL-33 as a novel mediator of AID and EPO resistance. Both conditions are prevalent comorbidities of common chronic inflammatory diseases [259, 276], and increased serum concentrations of IL-33 have been described in patients with RA and SpA [348, 349]. This suggests that therapies intended to inhibit the effects of IL-33 could have a considerable impact on human disease. In support of this, I show that anti-IL-33 antibodies alleviate anaemia in murine SpA when injected from the point of disease induction. Of greater importance for future

investigation is whether similar treatment could rescue patients that have already developed AID, or whether the effect of IL-33 must be inhibited as BM changes are first developing. At least two pharmaceutical companies have produced biological therapies to neutralise IL-33 [550][5], with one anti-ST2 antibody undergoing clinical trials for treatment of chronic obstructive pulmonary disease, meaning application of similar therapies to AID could be feasible if found to be safe. Conversely, a modified long-acting form of IL-33 has been proposed as a therapeutic product to mobilise HSPCs from BM into the blood in preparation for transplantation into other people [371]. If this product enters trials in humans, my data suggest a key concern should be whether this treatment might suppress erythropoiesis to the detriment of the donor or recipient.

7.4 Futurism

With rapid changes in methodology, a partial limitation of some work in this thesis is my reliance on whole animal or bulk cell assays. In some areas, this has complicated interpretation of results because cytokines may be acting in different cell types and locations simultaneously, making it difficult to separate their effects on mature cells from those on HSPCs. In future, new technologies, particularly single cell techniques, combined with growing numbers of cell type specific knockout mouse strains, are likely to facilitate analyses with a higher resolution. However, I suggest my approach has maximised the clinical applicability of my results by evaluating effects of interventions on clinical disease and haematopoiesis at the same time.

[5] https://clinicaltrials.gov/ct2/show/NCT03546907. Accessed 23rd September 2020.

I describe several effects of IL-4 on HSCs, and further investigation of this phenomenon is indicated. In particular, analysis of the transcriptomic changes occurring in HSCs after IL-4 exposure might provide insight on the molecular mechanisms underlying this effect, and blockade of IL-4 in other diseases might reveal whether it plays any role in regulation of haematopoiesis in a real world setting or whether this only occurs when it is administered to excess. A further question is whether the output of IL-4 exposed HSCs is qualitatively similar to that of IL-4 naïve cells. This is important because others have shown that exposure of HSCs to pathogen derivatives can induce epigenetic changes that are inherited by the progeny, producing a type of 'myeloid training' in progenitors rather than mature cells [551-553]. Because IL-4 can induce alternative activation of mature macrophages, I speculate that the myeloid output of IL-4 exposed HSCs could be predisposed to this type of differentiation, affecting the development of disease when mature cells reach the inflamed site.

7.5 Teleology

Immunology and haematopoiesis are frequently designated as separate areas of study, the latter only contributing to the former because the BM is the site of production of most immune cells. Instead, my work suggests haematopoiesis participates in the execution of integrated responses that have probably evolved to confront pathogens. In **chapter 5**, I suggested IL-33, acting as an alarmin, might temporarily suppress erythropoiesis to permit production of myeloid cells, taking advantage of the long circulating time of RBCs in the blood. In **chapter 6**, I developed this idea by suggesting IL-33 simultaneously promotes myelopoiesis through various means, recapitulating many of the haematopoietic features of SpA

that I described in **chapter 3** when it was injected in healthy mice. Here, I broaden this notion further to suggest that different types of immune response (e.g. 1, 2, 17) may each have cytokines that are critical modulators of haematopoiesis, prioritising BM output to supply the effector cells required for clearance of the pathogens they evolved to confront. For example, overproduction of IL-12, a classical type 1 cytokine, during intestinal *Toxoplasma gondii* infection causes BM NK cells to produce IFN-γ, which alters the nature of the mature myeloid cells reaching the intestine [554]. Conversely, I use my data to suggest IL-4 could be a counterpart during type 2 responses, promoting production of myeloid cells appropriate for responses to helminths and other parasites. The actions of IL-33 appear consistent with its suggested roles as type 2 cytokine and alarmin, promoting the formation of cells required to clear helminth infestation that can also respond to and repair damage. However, others have also shown that production of IL-33 is stimulated in myeloid cells by curdlan [328, 329], a β-1,3-glucan mainly encountered in fungal cell walls. Therefore, IL-33 might be of particular importance in haematopoietic responses to fungi, against which type 17 responses are often also directed [426]. These examples suggest that recruitment of haematopoiesis is a key feature of immune responses, which should perhaps be included in their conventional descriptions.

References

1. Silver, L. and J. Palis, *Initiation of murine embryonic erythropoiesis: a spatial analysis.* Blood, 1997. **89**(4): p. 1154-64.
2. Medvinsky, A., S. Rybtsov, and S. Taoudi, *Embryonic origin of the adult hematopoietic system: advances and questions.* Development, 2011. **138**(6): p. 1017-31.
3. Medvinsky, A. and E. Dzierzak, *Definitive hematopoiesis is autonomously initiated by the AGM region.* Cell, 1996. **86**(6): p. 897-906.
4. Muller, A.M., et al., *Development of hematopoietic stem cell activity in the mouse embryo.* Immunity, 1994. **1**(4): p. 291-301.
5. Johnson, G.R. and M.A. Moore, *Role of stem cell migration in initiation of mouse foetal liver haemopoiesis.* Nature, 1975. **258**(5537): p. 726-8.
6. Christensen, J.L., et al., *Circulation and chemotaxis of fetal hematopoietic stem cells.* PLoS Biol, 2004. **2**(3): p. E75.
7. Wagers, A.J., et al., *Little evidence for developmental plasticity of adult hematopoietic stem cells.* Science, 2002. **297**(5590): p. 2256-9.
8. Matsuzaki, Y., et al., *Unexpectedly efficient homing capacity of purified murine hematopoietic stem cells.* Immunity, 2004. **20**(1): p. 87-93.
9. Kiel, M.J., et al., *SLAM family receptors distinguish hematopoietic stem and progenitor cells and reveal endothelial niches for stem cells.* Cell, 2005. **121**(7): p. 1109-21.
10. Osawa, M., et al., *Long-term lymphohematopoietic reconstitution by a single CD34-low/negative hematopoietic stem cell.* Science, 1996. **273**(5272): p. 242-5.
11. Purton, L.E. and D.T. Scadden, *Limiting factors in murine hematopoietic stem cell assays.* Cell Stem Cell, 2007. **1**(3): p. 263-70.
12. Schoedel, K.B., et al., *The bulk of the hematopoietic stem cell population is dispensable for murine steady-state and stress hematopoiesis.* Blood, 2016. **128**(19): p. 2285-2296.
13. Busch, K., et al., *Fundamental properties of unperturbed haematopoiesis from stem cells in vivo.* Nature, 2015. **518**(7540): p. 542-6.
14. Orkin, S.H. and L.I. Zon, *Hematopoiesis: an evolving paradigm for stem cell biology.* Cell, 2008. **132**(4): p. 631-44.
15. Akashi, K., et al., *A clonogenic common myeloid progenitor that gives rise to all myeloid lineages.* Nature, 2000. **404**(6774): p. 193-7.
16. Kondo, M., I.L. Weissman, and K. Akashi, *Identification of clonogenic common lymphoid progenitors in mouse bone marrow.* Cell, 1997. **91**(5): p. 661-72.
17. Tusi, B.K., et al., *Population snapshots predict early haematopoietic and erythroid hierarchies.* Nature, 2018. **555**(7694): p. 54-60.
18. Giladi, A., et al., *Single-cell characterization of haematopoietic progenitors and their trajectories in homeostasis and perturbed haematopoiesis.* Nat Cell Biol, 2018. **20**(7): p. 836-846.
19. Nestorowa, S., et al., *A single-cell resolution map of mouse hematopoietic stem and progenitor cell differentiation.* Blood, 2016. **128**(8): p. e20-31.
20. Pina, C., et al., *Inferring rules of lineage commitment in haematopoiesis.* Nat Cell Biol, 2012. **14**(3): p. 287-94.

21. Haas, S., A. Trumpp, and M.D. Milsom, *Causes and Consequences of Hematopoietic Stem Cell Heterogeneity.* Cell Stem Cell, 2018. **22**(5): p. 627-638.
22. Cheshier, S.H., et al., *In vivo proliferation and cell cycle kinetics of long-term self-renewing hematopoietic stem cells.* Proc Natl Acad Sci U S A, 1999. **96**(6): p. 3120-5.
23. Passegue, E., et al., *Global analysis of proliferation and cell cycle gene expression in the regulation of hematopoietic stem and progenitor cell fates.* J Exp Med, 2005. **202**(11): p. 1599-611.
24. Kim, I., T.L. Saunders, and S.J. Morrison, *Sox17 dependence distinguishes the transcriptional regulation of fetal from adult hematopoietic stem cells.* Cell, 2007. **130**(3): p. 470-83.
25. Mohrin, M., et al., *Hematopoietic stem cell quiescence promotes error-prone DNA repair and mutagenesis.* Cell Stem Cell, 2010. **7**(2): p. 174-85.
26. Milyavsky, M., et al., *A distinctive DNA damage response in human hematopoietic stem cells reveals an apoptosis-independent role for p53 in self-renewal.* Cell Stem Cell, 2010. **7**(2): p. 186-97.
27. van Galen, P., et al., *The unfolded protein response governs integrity of the haematopoietic stem-cell pool during stress.* Nature, 2014. **510**(7504): p. 268-72.
28. Ho, T.T., et al., *Autophagy maintains the metabolism and function of young and old stem cells.* Nature, 2017. **543**(7644): p. 205-210.
29. Warr, M.R., et al., *FOXO3A directs a protective autophagy program in haematopoietic stem cells.* Nature, 2013. **494**(7437): p. 323-7.
30. Ito, K., et al., *Reactive oxygen species act through p38 MAPK to limit the lifespan of hematopoietic stem cells.* Nat Med, 2006. **12**(4): p. 446-51.
31. Miyamoto, K., et al., *Foxo3a is essential for maintenance of the hematopoietic stem cell pool.* Cell Stem Cell, 2007. **1**(1): p. 101-12.
32. Jorgensen, H.G., et al., *Intermittent exposure of primitive quiescent chronic myeloid leukemia cells to granulocyte-colony stimulating factor in vitro promotes their elimination by imatinib mesylate.* Clin Cancer Res, 2006. **12**(2): p. 626-33.
33. Wilson, A., et al., *Hematopoietic stem cells reversibly switch from dormancy to self-renewal during homeostasis and repair.* Cell, 2008. **135**(6): p. 1118-29.
34. Essers, M.A., et al., *IFNalpha activates dormant haematopoietic stem cells in vivo.* Nature, 2009. **458**(7240): p. 904-8.
35. Sato, T., et al., *Interferon regulatory factor-2 protects quiescent hematopoietic stem cells from type I interferon-dependent exhaustion.* Nat Med, 2009. **15**(6): p. 696-700.
36. Baldridge, M.T., et al., *Quiescent haematopoietic stem cells are activated by IFN-gamma in response to chronic infection.* Nature, 2010. **465**(7299): p. 793-7.
37. Matatall, K.A., et al., *Chronic Infection Depletes Hematopoietic Stem Cells through Stress-Induced Terminal Differentiation.* Cell Rep, 2016. **17**(10): p. 2584-2595.
38. Hartner, J.C., et al., *ADAR1 is essential for the maintenance of hematopoiesis and suppression of interferon signaling.* Nat Immunol, 2009. **10**(1): p. 109-15.
39. King, K.Y., et al., *Irgm1 protects hematopoietic stem cells by negative regulation of IFN signaling.* Blood, 2011. **118**(6): p. 1525-33.
40. Nagai, Y., et al., *Toll-like receptors on hematopoietic progenitor cells stimulate innate immune system replenishment.* Immunity, 2006. **24**(6): p. 801-12.

41. Esplin, B.L., et al., *Chronic exposure to a TLR ligand injures hematopoietic stem cells.* J Immunol, 2011. **186**(9): p. 5367-75.
42. Rodriguez, S., et al., *Dysfunctional expansion of hematopoietic stem cells and block of myeloid differentiation in lethal sepsis.* Blood, 2009. **114**(19): p. 4064-76.
43. Chen, C., et al., *Mammalian target of rapamycin activation underlies HSC defects in autoimmune disease and inflammation in mice.* J Clin Invest, 2010. **120**(11): p. 4091-101.
44. Laurenti, E. and B. Gottgens, *From haematopoietic stem cells to complex differentiation landscapes.* Nature, 2018. **553**(7689): p. 418-426.
45. Bernitz, J.M., et al., *Hematopoietic Stem Cells Count and Remember Self-Renewal Divisions.* Cell, 2016. **167**(5): p. 1296-1309 e10.
46. Cheng, T., et al., *Hematopoietic stem cell quiescence maintained by p21cip1/waf1.* Science, 2000. **287**(5459): p. 1804-8.
47. Ito, K., et al., *PML targeting eradicates quiescent leukaemia-initiating cells.* Nature, 2008. **453**(7198): p. 1072-8.
48. King, K.Y. and M.A. Goodell, *Inflammatory modulation of HSCs: viewing the HSC as a foundation for the immune response.* Nat Rev Immunol, 2011. **11**(10): p. 685-92.
49. Foudi, A., et al., *Analysis of histone 2B-GFP retention reveals slowly cycling hematopoietic stem cells.* Nat Biotechnol, 2009. **27**(1): p. 84-90.
50. van der Wath, R.C., et al., *Estimating dormant and active hematopoietic stem cell kinetics through extensive modeling of bromodeoxyuridine label-retaining cell dynamics.* PLoS One, 2009. **4**(9): p. e6972.
51. Zhao, M., et al., *N-Cadherin-Expressing Bone and Marrow Stromal Progenitor Cells Maintain Reserve Hematopoietic Stem Cells.* Cell Rep, 2019. **26**(3): p. 652-669 e6.
52. Takizawa, H., et al., *Dynamic variation in cycling of hematopoietic stem cells in steady state and inflammation.* J Exp Med, 2011. **208**(2): p. 273-84.
53. Cabezas-Wallscheid, N., et al., *Vitamin A-Retinoic Acid Signaling Regulates Hematopoietic Stem Cell Dormancy.* Cell, 2017. **169**(5): p. 807-823 e19.
54. Benveniste, P., et al., *Intermediate-term hematopoietic stem cells with extended but time-limited reconstitution potential.* Cell Stem Cell, 2010. **6**(1): p. 48-58.
55. Kiel, M.J., G.L. Radice, and S.J. Morrison, *Lack of evidence that hematopoietic stem cells depend on N-cadherin-mediated adhesion to osteoblasts for their maintenance.* Cell Stem Cell, 2007. **1**(2): p. 204-17.
56. Rabe, J.L., et al., *CD34 and EPCR coordinately enrich functional murine hematopoietic stem cells under normal and inflammatory conditions.* Exp Hematol, 2020. **81**: p. 1-15 e6.
57. Balazs, A.B., et al., *Endothelial protein C receptor (CD201) explicitly identifies hematopoietic stem cells in murine bone marrow.* Blood, 2006. **107**(6): p. 2317-21.
58. Wilson, A., et al., *Dormant and self-renewing hematopoietic stem cells and their niches.* Ann N Y Acad Sci, 2007. **1106**: p. 64-75.
59. Viatour, P., et al., *Hematopoietic stem cell quiescence is maintained by compound contributions of the retinoblastoma gene family.* Cell Stem Cell, 2008. **3**(4): p. 416-28.
60. Simsek, T., et al., *The distinct metabolic profile of hematopoietic stem cells reflects their location in a hypoxic niche.* Cell Stem Cell, 2010. **7**(3): p. 380-90.

61. Takubo, K., et al., *Regulation of glycolysis by Pdk functions as a metabolic checkpoint for cell cycle quiescence in hematopoietic stem cells.* Cell Stem Cell, 2013. **12**(1): p. 49-61.
62. Laurenti, E., et al., *CDK6 levels regulate quiescence exit in human hematopoietic stem cells.* Cell Stem Cell, 2015. **16**(3): p. 302-13.
63. Scheicher, R., et al., *CDK6 as a key regulator of hematopoietic and leukemic stem cell activation.* Blood, 2015. **125**(1): p. 90-101.
64. Wilson, A., et al., *c-Myc controls the balance between hematopoietic stem cell self-renewal and differentiation.* Genes Dev, 2004. **18**(22): p. 2747-63.
65. Laurenti, E., et al., *Hematopoietic stem cell function and survival depend on c-Myc and N-Myc activity.* Cell Stem Cell, 2008. **3**(6): p. 611-24.
66. Lu, R., et al., *Clonal-level lineage commitment pathways of hematopoietic stem cells in vivo.* Proc Natl Acad Sci U S A, 2019. **116**(4): p. 1447-1456.
67. Rodriguez-Fraticelli, A.E., et al., *Clonal analysis of lineage fate in native haematopoiesis.* Nature, 2018. **553**(7687): p. 212-216.
68. Yu, V.W.C., et al., *Epigenetic Memory Underlies Cell-Autonomous Heterogeneous Behavior of Hematopoietic Stem Cells.* Cell, 2016. **167**(5): p. 1310-1322 e17.
69. Pei, W., et al., *Polylox barcoding reveals haematopoietic stem cell fates realized in vivo.* Nature, 2017. **548**(7668): p. 456-460.
70. Carrelha, J., et al., *Hierarchically related lineage-restricted fates of multipotent haematopoietic stem cells.* Nature, 2018. **554**(7690): p. 106-111.
71. Grover, A., et al., *Single-cell RNA sequencing reveals molecular and functional platelet bias of aged haematopoietic stem cells.* Nat Commun, 2016. **7**: p. 11075.
72. Dykstra, B., et al., *Long-term propagation of distinct hematopoietic differentiation programs in vivo.* Cell Stem Cell, 2007. **1**(2): p. 218-29.
73. Muller-Sieburg, C.E., et al., *Myeloid-biased hematopoietic stem cells have extensive self-renewal capacity but generate diminished lymphoid progeny with impaired IL-7 responsiveness.* Blood, 2004. **103**(11): p. 4111-8.
74. Morita, Y., H. Ema, and H. Nakauchi, *Heterogeneity and hierarchy within the most primitive hematopoietic stem cell compartment.* J Exp Med, 2010. **207**(6): p. 1173-82.
75. Weksberg, D.C., et al., *CD150- side population cells represent a functionally distinct population of long-term hematopoietic stem cells.* Blood, 2008. **111**(4): p. 2444-51.
76. Yang, J., et al., *Single cell transcriptomics reveals unanticipated features of early hematopoietic precursors.* Nucleic Acids Res, 2017. **45**(3): p. 1281-1296.
77. Sanjuan-Pla, A., et al., *Platelet-biased stem cells reside at the apex of the haematopoietic stem-cell hierarchy.* Nature, 2013. **502**(7470): p. 232-6.
78. Yamamoto, R., et al., *Clonal analysis unveils self-renewing lineage-restricted progenitors generated directly from hematopoietic stem cells.* Cell, 2013. **154**(5): p. 1112-1126.
79. Pietras, E.M., et al., *Functionally Distinct Subsets of Lineage-Biased Multipotent Progenitors Control Blood Production in Normal and Regenerative Conditions.* Cell Stem Cell, 2015. **17**(1): p. 35-46.
80. Drissen, R., et al., *Distinct myeloid progenitor-differentiation pathways identified through single-cell RNA sequencing.* Nat Immunol, 2016. **17**(6): p. 666-676.
81. Paul, F., et al., *Transcriptional Heterogeneity and Lineage Commitment in Myeloid Progenitors.* Cell, 2015. **163**(7): p. 1663-77.

82. Waddington, C.H., *The strategy of the genes; a discussion of some aspects of theoretical biology*. 1957, London,: Allen & Unwin. ix, 262 p.
83. Graf, T. and T. Enver, *Forcing cells to change lineages.* Nature, 2009. **462**(7273): p. 587-94.
84. Arinobu, Y., et al., *Reciprocal activation of GATA-1 and PU.1 marks initial specification of hematopoietic stem cells into myeloerythroid and myelolymphoid lineages.* Cell Stem Cell, 2007. **1**(4): p. 416-27.
85. Strasser, M.K., et al., *Lineage marker synchrony in hematopoietic genealogies refutes the PU.1/GATA1 toggle switch paradigm.* Nat Commun, 2018. **9**(1): p. 2697.
86. Hoppe, P.S., et al., *Early myeloid lineage choice is not initiated by random PU.1 to GATA1 protein ratios.* Nature, 2016. **535**(7611): p. 299-302.
87. Mossadegh-Keller, N., et al., *M-CSF instructs myeloid lineage fate in single haematopoietic stem cells.* Nature, 2013. **497**(7448): p. 239-43.
88. Grover, A., et al., *Erythropoietin guides multipotent hematopoietic progenitor cells toward an erythroid fate.* J Exp Med, 2014. **211**(2): p. 181-8.
89. Uchida, N., et al., *Rapid and sustained hematopoietic recovery in lethally irradiated mice transplanted with purified Thy-1.1lo Lin-Sca-1+ hematopoietic stem cells.* Blood, 1994. **83**(12): p. 3758-79.
90. Ikuta, K. and I.L. Weissman, *Evidence that hematopoietic stem cells express mouse c-kit but do not depend on steel factor for their generation.* Proc Natl Acad Sci U S A, 1992. **89**(4): p. 1502-6.
91. Beaudin, A.E., S.W. Boyer, and E.C. Forsberg, *Flk2/Flt3 promotes both myeloid and lymphoid development by expanding non-self-renewing multipotent hematopoietic progenitor cells.* Exp Hematol, 2014. **42**(3): p. 218-229 e4.
92. Oguro, H., L. Ding, and S.J. Morrison, *SLAM family markers resolve functionally distinct subpopulations of hematopoietic stem cells and multipotent progenitors.* Cell Stem Cell, 2013. **13**(1): p. 102-16.
93. Yilmaz, O.H., M.J. Kiel, and S.J. Morrison, *SLAM family markers are conserved among hematopoietic stem cells from old and reconstituted mice and markedly increase their purity.* Blood, 2006. **107**(3): p. 924-30.
94. Warr, M.R., E.M. Pietras, and E. Passegue, *Mechanisms controlling hematopoietic stem cell functions during normal hematopoiesis and hematological malignancies.* Wiley Interdiscip Rev Syst Biol Med, 2011. **3**(6): p. 681-701.
95. Cabezas-Wallscheid, N., et al., *Identification of regulatory networks in HSCs and their immediate progeny via integrated proteome, transcriptome, and DNA methylome analysis.* Cell Stem Cell, 2014. **15**(4): p. 507-522.
96. Benveniste, P., et al., *Hematopoietic stem cells engraft in mice with absolute efficiency.* Nat Immunol, 2003. **4**(7): p. 708-13.
97. Ooi, A.G., et al., *The adhesion molecule esam1 is a novel hematopoietic stem cell marker.* Stem Cells, 2009. **27**(3): p. 653-61.
98. Yokota, T., et al., *The endothelial antigen ESAM marks primitive hematopoietic progenitors throughout life in mice.* Blood, 2009. **113**(13): p. 2914-23.
99. Gazit, R., et al., *Fgd5 identifies hematopoietic stem cells in the murine bone marrow.* J Exp Med, 2014. **211**(7): p. 1315-31.
100. Goodell, M.A., et al., *Isolation and functional properties of murine hematopoietic stem cells that are replicating in vivo.* J Exp Med, 1996. **183**(4): p. 1797-806.

101. Zhao, Y., et al., *Murine hematopoietic stem cell characterization and its regulation in BM transplantation.* Blood, 2000. **96**(9): p. 3016-22.
102. Santaguida, M., et al., *JunB protects against myeloid malignancies by limiting hematopoietic stem cell proliferation and differentiation without affecting self-renewal.* Cancer Cell, 2009. **15**(4): p. 341-52.
103. Adolfsson, J., et al., *Identification of Flt3+ lympho-myeloid stem cells lacking erythro-megakaryocytic potential a revised road map for adult blood lineage commitment.* Cell, 2005. **121**(2): p. 295-306.
104. Forsberg, E.C., et al., *New evidence supporting megakaryocyte-erythrocyte potential of flk2/flt3+ multipotent hematopoietic progenitors.* Cell, 2006. **126**(2): p. 415-26.
105. Pinho, S. and P.S. Frenette, *Haematopoietic stem cell activity and interactions with the niche.* Nat Rev Mol Cell Biol, 2019. **20**(5): p. 303-320.
106. Baccin, C., et al., *Combined single-cell and spatial transcriptomics reveal the molecular, cellular and spatial bone marrow niche organization.* Nat Cell Biol, 2020. **22**(1): p. 38-48.
107. Wei, Q. and P.S. Frenette, *Niches for Hematopoietic Stem Cells and Their Progeny.* Immunity, 2018. **48**(4): p. 632-648.
108. Morrison, S.J. and D.T. Scadden, *The bone marrow niche for haematopoietic stem cells.* Nature, 2014. **505**(7483): p. 327-34.
109. Mendez-Ferrer, S., et al., *Mesenchymal and haematopoietic stem cells form a unique bone marrow niche.* Nature, 2010. **466**(7308): p. 829-34.
110. Kunisaki, Y., et al., *Arteriolar niches maintain haematopoietic stem cell quiescence.* Nature, 2013. **502**(7473): p. 637-43.
111. Asada, N., et al., *Differential cytokine contributions of perivascular haematopoietic stem cell niches.* Nat Cell Biol, 2017. **19**(3): p. 214-223.
112. Arai, F., et al., *Tie2/angiopoietin-1 signaling regulates hematopoietic stem cell quiescence in the bone marrow niche.* Cell, 2004. **118**(2): p. 149-61.
113. Pinho, S., et al., *PDGFRalpha and CD51 mark human nestin+ sphere-forming mesenchymal stem cells capable of hematopoietic progenitor cell expansion.* J Exp Med, 2013. **210**(7): p. 1351-67.
114. Morikawa, S., et al., *Prospective identification, isolation, and systemic transplantation of multipotent mesenchymal stem cells in murine bone marrow.* J Exp Med, 2009. **206**(11): p. 2483-96.
115. Ding, L., et al., *Endothelial and perivascular cells maintain haematopoietic stem cells.* Nature, 2012. **481**(7382): p. 457-62.
116. Zhou, B.O., et al., *Leptin-receptor-expressing mesenchymal stromal cells represent the main source of bone formed by adult bone marrow.* Cell Stem Cell, 2014. **15**(2): p. 154-68.
117. Omatsu, Y., et al., *The essential functions of adipo-osteogenic progenitors as the hematopoietic stem and progenitor cell niche.* Immunity, 2010. **33**(3): p. 387-99.
118. Sugiyama, T., et al., *Maintenance of the hematopoietic stem cell pool by CXCL12-CXCR4 chemokine signaling in bone marrow stromal cell niches.* Immunity, 2006. **25**(6): p. 977-88.
119. Calvi, L.M., et al., *Osteoblastic cells regulate the haematopoietic stem cell niche.* Nature, 2003. **425**(6960): p. 841-6.

120. Zhang, J., et al., *Identification of the haematopoietic stem cell niche and control of the niche size.* Nature, 2003. **425**(6960): p. 836-41.
121. Lo Celso, C., et al., *Live-animal tracking of individual haematopoietic stem/progenitor cells in their niche.* Nature, 2009. **457**(7225): p. 92-6.
122. Ding, L. and S.J. Morrison, *Haematopoietic stem cells and early lymphoid progenitors occupy distinct bone marrow niches.* Nature, 2013. **495**(7440): p. 231-5.
123. Visnjic, D., et al., *Conditional ablation of the osteoblast lineage in Col2.3deltatk transgenic mice.* J Bone Miner Res, 2001. **16**(12): p. 2222-31.
124. Visnjic, D., et al., *Hematopoiesis is severely altered in mice with an induced osteoblast deficiency.* Blood, 2004. **103**(9): p. 3258-64.
125. Zhu, J., et al., *Osteoblasts support B-lymphocyte commitment and differentiation from hematopoietic stem cells.* Blood, 2007. **109**(9): p. 3706-12.
126. Terashima, A., et al., *Sepsis-Induced Osteoblast Ablation Causes Immunodeficiency.* Immunity, 2016. **44**(6): p. 1434-43.
127. Cordeiro Gomes, A., et al., *Hematopoietic Stem Cell Niches Produce Lineage-Instructive Signals to Control Multipotent Progenitor Differentiation.* Immunity, 2016. **45**(6): p. 1219-1231.
128. Schepers, K., et al., *Myeloproliferative neoplasia remodels the endosteal bone marrow niche into a self-reinforcing leukemic niche.* Cell Stem Cell, 2013. **13**(3): p. 285-99.
129. Winkler, I.G., et al., *Bone marrow macrophages maintain hematopoietic stem cell (HSC) niches and their depletion mobilizes HSCs.* Blood, 2010. **116**(23): p. 4815-28.
130. Komori, T., *Regulation of Proliferation, Differentiation and Functions of Osteoblasts by Runx2.* Int J Mol Sci, 2019. **20**(7).
131. Itkin, T., et al., *Distinct bone marrow blood vessels differentially regulate haematopoiesis.* Nature, 2016. **532**(7599): p. 323-8.
132. Kusumbe, A.P., et al., *Age-dependent modulation of vascular niches for haematopoietic stem cells.* Nature, 2016. **532**(7599): p. 380-4.
133. Bruns, I., et al., *Megakaryocytes regulate hematopoietic stem cell quiescence through CXCL4 secretion.* Nat Med, 2014. **20**(11): p. 1315-20.
134. Zhao, M., et al., *Megakaryocytes maintain homeostatic quiescence and promote post-injury regeneration of hematopoietic stem cells.* Nat Med, 2014. **20**(11): p. 1321-6.
135. Albiero, M., et al., *Bone Marrow Macrophages Contribute to Diabetic Stem Cell Mobilopathy by Producing Oncostatin M.* Diabetes, 2015. **64**(8): p. 2957-68.
136. Chow, A., et al., *CD169(+) macrophages provide a niche promoting erythropoiesis under homeostasis and stress.* Nat Med, 2013. **19**(4): p. 429-36.
137. Hettinger, J., et al., *Origin of monocytes and macrophages in a committed progenitor.* Nat Immunol, 2013. **14**(8): p. 821-30.
138. Schlitzer, A., et al., *Identification of cDC1- and cDC2-committed DC progenitors reveals early lineage priming at the common DC progenitor stage in the bone marrow.* Nat Immunol, 2015. **16**(7): p. 718-28.
139. Evrard, M., et al., *Developmental Analysis of Bone Marrow Neutrophils Reveals Populations Specialized in Expansion, Trafficking, and Effector Functions.* Immunity, 2018. **48**(2): p. 364-379 e8.

140. Kwok, I., et al., *Combinatorial Single-Cell Analyses of Granulocyte-Monocyte Progenitor Heterogeneity Reveals an Early Uni-potent Neutrophil Progenitor.* Immunity, 2020.
141. Yanez, A., et al., *Granulocyte-Monocyte Progenitors and Monocyte-Dendritic Cell Progenitors Independently Produce Functionally Distinct Monocytes.* Immunity, 2017. **47**(5): p. 890-902 e4.
142. Arinobu, Y., et al., *Developmental checkpoints of the basophil/mast cell lineages in adult murine hematopoiesis.* Proc Natl Acad Sci U S A, 2005. **102**(50): p. 18105-10.
143. Qi, X., et al., *Antagonistic regulation by the transcription factors C/EBPalpha and MITF specifies basophil and mast cell fates.* Immunity, 2013. **39**(1): p. 97-110.
144. Franco, C.B., et al., *Distinguishing mast cell and granulocyte differentiation at the single-cell level.* Cell Stem Cell, 2010. **6**(4): p. 361-8.
145. Dahlin, J.S., et al., *A single-cell hematopoietic landscape resolves 8 lineage trajectories and defects in Kit mutant mice.* Blood, 2018. **131**(21): p. e1-e11.
146. McNagny, K. and T. Graf, *Making eosinophils through subtle shifts in transcription factor expression.* J Exp Med, 2002. **195**(11): p. F43-7.
147. Tsai, F.Y. and S.H. Orkin, *Transcription factor GATA-2 is required for proliferation/survival of early hematopoietic cells and mast cell formation, but not for erythroid and myeloid terminal differentiation.* Blood, 1997. **89**(10): p. 3636-43.
148. Pevny, L., et al., *Development of hematopoietic cells lacking transcription factor GATA-1.* Development, 1995. **121**(1): p. 163-72.
149. Yu, C., et al., *Targeted deletion of a high-affinity GATA-binding site in the GATA-1 promoter leads to selective loss of the eosinophil lineage in vivo.* J Exp Med, 2002. **195**(11): p. 1387-95.
150. Zhang, D.E., et al., *Absence of granulocyte colony-stimulating factor signaling and neutrophil development in CCAAT enhancer binding protein alpha-deficient mice.* Proc Natl Acad Sci U S A, 1997. **94**(2): p. 569-74.
151. Iwasaki, H., et al., *The order of expression of transcription factors directs hierarchical specification of hematopoietic lineages.* Genes Dev, 2006. **20**(21): p. 3010-21.
152. Walsh, J.C., et al., *Cooperative and antagonistic interplay between PU.1 and GATA-2 in the specification of myeloid cell fates.* Immunity, 2002. **17**(5): p. 665-76.
153. McNagny, K.M., et al., *Regulation of eosinophil-specific gene expression by a C/EBP-Ets complex and GATA-1.* EMBO J, 1998. **17**(13): p. 3669-80.
154. McKercher, S.R., G.W. Henkel, and R.A. Maki, *The transcription factor PU.1 does not regulate lineage commitment but has lineage-specific effects.* J Leukoc Biol, 1999. **66**(5): p. 727-32.
155. Querfurth, E., et al., *Antagonism between C/EBPbeta and FOG in eosinophil lineage commitment of multipotent hematopoietic progenitors.* Genes Dev, 2000. **14**(19): p. 2515-25.
156. Cantor, A.B., et al., *Antagonism of FOG-1 and GATA factors in fate choice for the mast cell lineage.* J Exp Med, 2008. **205**(3): p. 611-24.
157. Mancini, E., et al., *FOG-1 and GATA-1 act sequentially to specify definitive megakaryocytic and erythroid progenitors.* EMBO J, 2012. **31**(2): p. 351-65.
158. Nerlov, C., et al., *Distinct C/EBP functions are required for eosinophil lineage commitment and maturation.* Genes Dev, 1998. **12**(15): p. 2413-23.

159. Pronk, C.J., et al., *Elucidation of the phenotypic, functional, and molecular topography of a myeloerythroid progenitor cell hierarchy.* Cell Stem Cell, 2007. **1**(4): p. 428-42.
160. Iscove, N.N., F. Sieber, and K.H. Winterhalter, *Erythroid colony formation in cultures of mouse and human bone marrow: analysis of the requirement for erythropoietin by gel filtration and affinity chromatography on agarose-concanavalin A.* J Cell Physiol, 1974. **83**(2): p. 309-20.
161. Pop, R., et al., *A key commitment step in erythropoiesis is synchronized with the cell cycle clock through mutual inhibition between PU.1 and S-phase progression.* PLoS Biol, 2010. **8**(9).
162. Zhang, P., et al., *PU.1 inhibits GATA-1 function and erythroid differentiation by blocking GATA-1 DNA binding.* Blood, 2000. **96**(8): p. 2641-8.
163. Stephenson, J.R., et al., *Induction of colonies of hemoglobin-synthesizing cells by erythropoietin in vitro.* Proc Natl Acad Sci U S A, 1971. **68**(7): p. 1542-6.
164. Liu, Y., et al., *Suppression of Fas-FasL coexpression by erythropoietin mediates erythroblast expansion during the erythropoietic stress response in vivo.* Blood, 2006. **108**(1): p. 123-33.
165. Kina, T., et al., *The monoclonal antibody TER-119 recognizes a molecule associated with glycophorin A and specifically marks the late stages of murine erythroid lineage.* Br J Haematol, 2000. **109**(2): p. 280-7.
166. Chen, K., et al., *Resolving the distinct stages in erythroid differentiation based on dynamic changes in membrane protein expression during erythropoiesis.* Proc Natl Acad Sci U S A, 2009. **106**(41): p. 17413-8.
167. Amireault, P., et al., *Ineffective erythropoiesis with reduced red blood cell survival in serotonin-deficient mice.* Proc Natl Acad Sci U S A, 2011. **108**(32): p. 13141-6.
168. Van Putten, L.M., *The life span of red cells in the rat and the mouse as determined by labeling with DFP32 in vivo.* Blood, 1958. **13**(8): p. 789-94.
169. Klei, T.R., et al., *From the Cradle to the Grave: The Role of Macrophages in Erythropoiesis and Erythrophagocytosis.* Front Immunol, 2017. **8**: p. 73.
170. Sadahira, Y., T. Yoshino, and Y. Monobe, *Very late activation antigen 4-vascular cell adhesion molecule 1 interaction is involved in the formation of erythroblastic islands.* J Exp Med, 1995. **181**(1): p. 411-5.
171. Fabriek, B.O., et al., *The macrophage CD163 surface glycoprotein is an erythroblast adhesion receptor.* Blood, 2007. **109**(12): p. 5223-9.
172. Li, W., et al., *Identification and transcriptome analysis of erythroblastic island macrophages.* Blood, 2019. **134**(5): p. 480-491.
173. Toda, S., K. Segawa, and S. Nagata, *MerTK-mediated engulfment of pyrenocytes by central macrophages in erythroblastic islands.* Blood, 2014. **123**(25): p. 3963-71.
174. Ebert, B.L. and H.F. Bunn, *Regulation of the erythropoietin gene.* Blood, 1999. **94**(6): p. 1864-77.
175. Wu, H., et al., *Generation of committed erythroid BFU-E and CFU-E progenitors does not require erythropoietin or the erythropoietin receptor.* Cell, 1995. **83**(1): p. 59-67.
176. Silva, M., et al., *Erythropoietin can induce the expression of bcl-x(L) through Stat5 in erythropoietin-dependent progenitor cell lines.* J Biol Chem, 1999. **274**(32): p. 22165-9.

177. Socolovsky, M., et al., *Fetal anemia and apoptosis of red cell progenitors in Stat5a-/-5b-/- mice: a direct role for Stat5 in Bcl-X(L) induction.* Cell, 1999. **98**(2): p. 181-91.
178. Hattangadi, S.M., et al., *From stem cell to red cell: regulation of erythropoiesis at multiple levels by multiple proteins, RNAs, and chromatin modifications.* Blood, 2011. **118**(24): p. 6258-68.
179. Jafari, M., et al., *PI3k/AKT signaling pathway: Erythropoiesis and beyond.* J Cell Physiol, 2019. **234**(3): p. 2373-2385.
180. Manning, B.D. and A. Toker, *AKT/PKB Signaling: Navigating the Network.* Cell, 2017. **169**(3): p. 381-405.
181. Hu, X.F., et al., *PIM-1-specific mAb suppresses human and mouse tumor growth by decreasing PIM-1 levels, reducing Akt phosphorylation, and activating apoptosis.* J Clin Invest, 2009. **119**(2): p. 362-75.
182. Sagar, V., et al., *PIM1 destabilization activates a p53-dependent response to ribosomal stress in cancer cells.* Oncotarget, 2016. **7**(17): p. 23837-49.
183. Ghaffari, S., et al., *AKT induces erythroid-cell maturation of JAK2-deficient fetal liver progenitor cells and is required for Epo regulation of erythroid-cell differentiation.* Blood, 2006. **107**(5): p. 1888-91.
184. Zhao, W., et al., *Erythropoietin stimulates phosphorylation and activation of GATA-1 via the PI3-kinase/AKT signaling pathway.* Blood, 2006. **107**(3): p. 907-15.
185. Kadri, Z., et al., *Phosphatidylinositol 3-kinase/Akt induced by erythropoietin renders the erythroid differentiation factor GATA-1 competent for TIMP-1 gene transactivation.* Mol Cell Biol, 2005. **25**(17): p. 7412-22.
186. Meng, D., A.R. Frank, and J.L. Jewell, *mTOR signaling in stem and progenitor cells.* Development, 2018. **145**(1).
187. Chen, W.S., et al., *Growth retardation and increased apoptosis in mice with homozygous disruption of the Akt1 gene.* Genes Dev, 2001. **15**(17): p. 2203-8.
188. Bavelloni, A., et al., *Inhibition of phosphoinositide 3-kinase impairs pre-commitment cell cycle traverse and prevents differentiation in erythroleukaemia cells.* Cell Death Differ, 2000. **7**(1): p. 112-7.
189. Kubota, Y., et al., *Src transduces erythropoietin-induced differentiation signals through phosphatidylinositol 3-kinase.* EMBO J, 2001. **20**(20): p. 5666-77.
190. Myklebust, J.H., et al., *Activation of phosphatidylinositol 3-kinase is important for erythropoietin-induced erythropoiesis from CD34(+) hematopoietic progenitor cells.* Exp Hematol, 2002. **30**(9): p. 990-1000.
191. Uddin, S., et al., *Activation of the Akt/FKHRL1 pathway mediates the antiapoptotic effects of erythropoietin in primary human erythroid progenitors.* Biochem Biophys Res Commun, 2000. **275**(1): p. 16-9.
192. Hammerman, P.S., et al., *Pim and Akt oncogenes are independent regulators of hematopoietic cell growth and survival.* Blood, 2005. **105**(11): p. 4477-83.
193. Laird, P.W., et al., *In vivo analysis of Pim-1 deficiency.* Nucleic Acids Res, 1993. **21**(20): p. 4750-5.
194. Kim, W.S., et al., *Erythropoiesis from human embryonic stem cells through erythropoietin-independent AKT signaling.* Stem Cells, 2014. **32**(6): p. 1503-14.
195. Rooke, H.M. and S.H. Orkin, *Phosphorylation of Gata1 at serine residues 72, 142, and 310 is not essential for hematopoiesis in vivo.* Blood, 2006. **107**(9): p. 3527-30.
196. Malik, N., et al., *mTORC1 activity is essential for erythropoiesis and B cell lineage commitment.* Sci Rep, 2019. **9**(1): p. 16917.

197. Chiu, S.C., et al., *Extramedullary hematopoiesis (EMH) in laboratory animals: offering an insight into stem cell research.* Cell Transplant, 2015. **24**(3): p. 349-66.
198. Johns, J.L. and M.M. Christopher, *Extramedullary hematopoiesis: a new look at the underlying stem cell niche, theories of development, and occurrence in animals.* Vet Pathol, 2012. **49**(3): p. 508-23.
199. Morita, Y., et al., *Functional characterization of hematopoietic stem cells in the spleen.* Exp Hematol, 2011. **39**(3): p. 351-359 e3.
200. Bayne, L.J., et al., *Tumor-derived granulocyte-macrophage colony-stimulating factor regulates myeloid inflammation and T cell immunity in pancreatic cancer.* Cancer Cell, 2012. **21**(6): p. 822-35.
201. Khaldoyanidi, S., et al., *Constitutive overexpression of IL-5 induces extramedullary hematopoiesis in the spleen.* Blood, 2003. **101**(3): p. 863-8.
202. Peters, M., et al., *Extramedullary expansion of hematopoietic progenitor cells in interleukin (IL)-6-sIL-6R double transgenic mice.* J Exp Med, 1997. **185**(4): p. 755-66.
203. Lai, Y.H., et al., *Continuous administration of Il-13 to mice induces extramedullary hemopoiesis and monocytosis.* J Immunol, 1996. **156**(9): p. 3166-73.
204. Seita, J., et al., *Interleukin-27 directly induces differentiation in hematopoietic stem cells.* Blood, 2008. **111**(4): p. 1903-12.
205. Schmitz, J., et al., *IL-33, an interleukin-1-like cytokine that signals via the IL-1 receptor-related protein ST2 and induces T helper type 2-associated cytokines.* Immunity, 2005. **23**(5): p. 479-90.
206. Canonne-Hergaux, F., et al., *Characterization of the iron transporter DMT1 (NRAMP2/DCT1) in red blood cells of normal and anemic mk/mk mice.* Blood, 2001. **98**(13): p. 3823-30.
207. Loukov, D., et al., *Tumor necrosis factor drives increased splenic monopoiesis in old mice.* J Leukoc Biol, 2016. **100**(1): p. 121-9.
208. Kaufman, R.M., et al., *Origin of Pulmonary Megakaryocytes.* Blood, 1965. **25**: p. 767-75.
209. Lefrancais, E., et al., *The lung is a site of platelet biogenesis and a reservoir for haematopoietic progenitors.* Nature, 2017. **544**(7648): p. 105-109.
210. Saenz, S.A., et al., *IL25 elicits a multipotent progenitor cell population that promotes T(H)2 cytokine responses.* Nature, 2010. **464**(7293): p. 1362-6.
211. Mendez-Ferrer, S., et al., *Haematopoietic stem cell release is regulated by circadian oscillations.* Nature, 2008. **452**(7186): p. 442-7.
212. Massberg, S., et al., *Immunosurveillance by hematopoietic progenitor cells trafficking through blood, lymph, and peripheral tissues.* Cell, 2007. **131**(5): p. 994-1008.
213. Wright, D.E., et al., *Physiological migration of hematopoietic stem and progenitor cells.* Science, 2001. **294**(5548): p. 1933-6.
214. Shatry, A.M., M. Jones, and R.B. Levy, *The effect of the spleen on compartmental levels and distribution of donor progenitor cells after syngeneic and allogeneic bone marrow transplants.* Stem Cells Dev, 2004. **13**(1): p. 51-62.
215. Wolber, F.M., et al., *Roles of spleen and liver in development of the murine hematopoietic system.* Exp Hematol, 2002. **30**(9): p. 1010-9.
216. Robbins, C.S., et al., *Extramedullary hematopoiesis generates Ly-6C(high) monocytes that infiltrate atherosclerotic lesions.* Circulation, 2012. **125**(2): p. 364-74.

217. Bugl, S., et al., *Steady-state neutrophil homeostasis is dependent on TLR4/TRIF signaling.* Blood, 2013. **121**(5): p. 723-33.
218. Bennett, L.F., C. Liao, and R.F. Paulson, *Stress Erythropoiesis Model Systems.* Methods Mol Biol, 2018. **1698**: p. 91-102.
219. Manz, M.G. and S. Boettcher, *Emergency granulopoiesis.* Nat Rev Immunol, 2014. **14**(5): p. 302-14.
220. Boettcher, S., et al., *Cutting edge: LPS-induced emergency myelopoiesis depends on TLR4-expressing nonhematopoietic cells.* J Immunol, 2012. **188**(12): p. 5824-8.
221. Boettcher, S., et al., *Endothelial cells translate pathogen signals into G-CSF-driven emergency granulopoiesis.* Blood, 2014. **124**(9): p. 1393-403.
222. Takizawa, H., et al., *Pathogen-Induced TLR4-TRIF Innate Immune Signaling in Hematopoietic Stem Cells Promotes Proliferation but Reduces Competitive Fitness.* Cell Stem Cell, 2017. **21**(2): p. 225-240 e5.
223. Liu, A., et al., *Cutting Edge: Hematopoietic Stem Cell Expansion and Common Lymphoid Progenitor Depletion Require Hematopoietic-Derived, Cell-Autonomous TLR4 in a Model of Chronic Endotoxin.* J Immunol, 2015. **195**(6): p. 2524-8.
224. Mitroulis, I., et al., *Myelopoiesis in the Context of Innate Immunity.* J Innate Immun, 2018. **10**(5-6): p. 365-372.
225. Lieschke, G.J., et al., *Mice lacking granulocyte colony-stimulating factor have chronic neutropenia, granulocyte and macrophage progenitor cell deficiency, and impaired neutrophil mobilization.* Blood, 1994. **84**(6): p. 1737-46.
226. Stanley, E., et al., *Granulocyte/macrophage colony-stimulating factor-deficient mice show no major perturbation of hematopoiesis but develop a characteristic pulmonary pathology.* Proc Natl Acad Sci U S A, 1994. **91**(12): p. 5592-6.
227. Zhan, Y., et al., *Essential roles for granulocyte-macrophage colony-stimulating factor (GM-CSF) and G-CSF in the sustained hematopoietic response of Listeria monocytogenes-infected mice.* Blood, 1998. **91**(3): p. 863-9.
228. Basu, S., et al., *"Emergency" granulopoiesis in G-CSF-deficient mice in response to Candida albicans infection.* Blood, 2000. **95**(12): p. 3725-33.
229. Basu, S., et al., *Candida albicans can stimulate stromal cells resulting in enhanced granulopoiesis.* Stem Cells Dev, 2004. **13**(1): p. 39-50.
230. Wang, H., et al., *C/EBPalpha arrests cell proliferation through direct inhibition of Cdk2 and Cdk4.* Mol Cell, 2001. **8**(4): p. 817-28.
231. Zhang, H., et al., *STAT3 controls myeloid progenitor growth during emergency granulopoiesis.* Blood, 2010. **116**(14): p. 2462-71.
232. Hirai, H., et al., *C/EBPbeta is required for 'emergency' granulopoiesis.* Nat Immunol, 2006. **7**(7): p. 732-9.
233. Satake, S., et al., *C/EBPbeta is involved in the amplification of early granulocyte precursors during candidemia-induced "emergency" granulopoiesis.* J Immunol, 2012. **189**(9): p. 4546-55.
234. Herault, A., et al., *Myeloid progenitor cluster formation drives emergency and leukaemic myelopoiesis.* Nature, 2017. **544**(7648): p. 53-58.
235. Jelkmann, W. and G. Wiedemann, *Serum erythropoietin level: relationships to blood hemoglobin concentration and erythrocytic activity of the bone marrow.* Klin Wochenschr, 1990. **68**(8): p. 403-7.

236. Perry, J.M., O.F. Harandi, and R.F. Paulson, *BMP4, SCF, and hypoxia cooperatively regulate the expansion of murine stress erythroid progenitors.* Blood, 2007. **109**(10): p. 4494-502.
237. Bennett, L.F., et al., *Inflammation induces stress erythropoiesis through heme-dependent activation of SPI-C.* Sci Signal, 2019. **12**(598).
238. Socolovsky, M., *Molecular insights into stress erythropoiesis.* Curr Opin Hematol, 2007. **14**(3): p. 215-24.
239. Harandi, O.F., et al., *Murine erythroid short-term radioprotection requires a BMP4-dependent, self-renewing population of stress erythroid progenitors.* J Clin Invest, 2010. **120**(12): p. 4507-19.
240. Perry, J.M., et al., *Maintenance of the BMP4-dependent stress erythropoiesis pathway in the murine spleen requires hedgehog signaling.* Blood, 2009. **113**(4): p. 911-8.
241. Jackson, A., et al., *Innate immune activation during Salmonella infection initiates extramedullary erythropoiesis and splenomegaly.* J Immunol, 2010. **185**(10): p. 6198-204.
242. Millot, S., et al., *Erythropoietin stimulates spleen BMP4-dependent stress erythropoiesis and partially corrects anemia in a mouse model of generalized inflammation.* Blood, 2010. **116**(26): p. 6072-81.
243. Pietras, E.M., *Inflammation: a key regulator of hematopoietic stem cell fate in health and disease.* Blood, 2017. **130**(15): p. 1693-1698.
244. Takizawa, H., S. Boettcher, and M.G. Manz, *Demand-adapted regulation of early hematopoiesis in infection and inflammation.* Blood, 2012. **119**(13): p. 2991-3002.
245. Schuettpelz, L.G., et al., *G-CSF regulates hematopoietic stem cell activity, in part, through activation of Toll-like receptor signaling.* Leukemia, 2014. **28**(9): p. 1851-60.
246. Weisser, M., et al., *Hyperinflammation in patients with chronic granulomatous disease leads to impairment of hematopoietic stem cell functions.* J Allergy Clin Immunol, 2016. **138**(1): p. 219-228 e9.
247. Pietras, E.M., et al., *Chronic interleukin-1 exposure drives haematopoietic stem cells towards precocious myeloid differentiation at the expense of self-renewal.* Nat Cell Biol, 2016. **18**(6): p. 607-18.
248. Pietras, E.M., et al., *Re-entry into quiescence protects hematopoietic stem cells from the killing effect of chronic exposure to type I interferons.* J Exp Med, 2014. **211**(2): p. 245-62.
249. Hernandez, G., et al., *Pro-inflammatory cytokine blockade attenuates myeloid expansion in a murine model of rheumatoid arthritis.* Haematologica, 2020. **105**(3): p. 585-597.
250. Griseri, T., et al., *Dysregulated hematopoietic stem and progenitor cell activity promotes interleukin-23-driven chronic intestinal inflammation.* Immunity, 2012. **37**(6): p. 1116-29.
251. Etzrodt, M., et al., *Inflammatory signals directly instruct PU.1 in HSCs via TNF.* Blood, 2019. **133**(8): p. 816-819.
252. Kang, Y.A., E.M. Pietras, and E. Passegue, *Deregulated Notch and Wnt signaling activates early-stage myeloid regeneration pathways in leukemia.* J Exp Med, 2020. **217**(3).

253. Reynaud, D., et al., *IL-6 controls leukemic multipotent progenitor cell fate and contributes to chronic myelogenous leukemia development.* Cancer Cell, 2011. **20**(5): p. 661-73.
254. Niu, H., et al., *The function of hematopoietic stem cells is altered by both genetic and inflammatory factors in lupus mice.* Blood, 2013. **121**(11): p. 1986-94.
255. Leuschner, F., et al., *Rapid monocyte kinetics in acute myocardial infarction are sustained by extramedullary monocytopoiesis.* J Exp Med, 2012. **209**(1): p. 123-37.
256. Paulson, R.F., et al., *Stress Erythropoiesis is a Key Inflammatory Response.* Cells, 2020. **9**(3).
257. Granick, J.L., et al., *Staphylococcus aureus recognition by hematopoietic stem and progenitor cells via TLR2/MyD88/PGE2 stimulates granulopoiesis in wounds.* Blood, 2013. **122**(10): p. 1770-8.
258. Weiss, G. and L.T. Goodnough, *Anemia of chronic disease.* N Engl J Med, 2005. **352**(10): p. 1011-23.
259. Nemeth, E. and T. Ganz, *Anemia of inflammation.* Hematol Oncol Clin North Am, 2014. **28**(4): p. 671-81, vi.
260. Ratajczak, M.Z., J. Ratajczak, and T. Skorski, *[In vitro studies on anemia in chronic inflammatory disease: influence of interleukin-6 on human erythropoietin].* Pol Merkur Lekarski, 1997. **2**(9): p. 172-5.
261. Tracey, K.J., et al., *Cachectin/tumor necrosis factor induces cachexia, anemia, and inflammation.* J Exp Med, 1988. **167**(3): p. 1211-27.
262. Zermati, Y., et al., *Transforming growth factor inhibits erythropoiesis by blocking proliferation and accelerating differentiation of erythroid progenitors.* Exp Hematol, 2000. **28**(8): p. 885-94.
263. Dybedal, I. and S.E. Jacobsen, *Transforming growth factor beta (TGF-beta), a potent inhibitor of erythropoiesis: neutralizing TGF-beta antibodies show erythropoietin as a potent stimulator of murine burst-forming unit erythroid colony formation in the absence of a burst-promoting activity.* Blood, 1995. **86**(3): p. 949-57.
264. Wang, C.Q., K.B. Udupa, and D.A. Lipschitz, *Interferon-gamma exerts its negative regulatory effect primarily on the earliest stages of murine erythroid progenitor cell development.* J Cell Physiol, 1995. **162**(1): p. 134-8.
265. Thawani, N., et al., *Interferon-gamma mediates suppression of erythropoiesis but not reduced red cell survival following CpG-ODN administration in vivo.* Exp Hematol, 2006. **34**(11): p. 1451-61.
266. McCranor, B.J., et al., *Interleukin-6 directly impairs the erythroid development of human TF-1 erythroleukemic cells.* Blood Cells Mol Dis, 2014. **52**(2-3): p. 126-33.
267. Ferry, A.E., et al., *Globin gene silencing in primary erythroid cultures. An inhibitory role for interleukin-6.* J Biol Chem, 1997. **272**(32): p. 20030-7.
268. Wang, C.Y. and J.L. Babitt, *Hepcidin regulation in the anemia of inflammation.* Curr Opin Hematol, 2016. **23**(3): p. 189-97.
269. Libregts, S.F., et al., *Chronic IFN-gamma production in mice induces anemia by reducing erythrocyte life span and inhibiting erythropoiesis through an IRF-1/PU.1 axis.* Blood, 2011. **118**(9): p. 2578-88.
270. Wang, W., et al., *Interferon-gamma exerts dual functions on human erythropoiesis via interferon regulatory factor 1 signal pathway.* Biochem Biophys Res Commun, 2020. **521**(2): p. 326-332.

271. Felli, N., et al., *Multiple members of the TNF superfamily contribute to IFN-gamma-mediated inhibition of erythropoiesis.* J Immunol, 2005. **175**(3): p. 1464-72.
272. Xiao, W., et al., *Tumor necrosis factor-alpha inhibits generation of glycophorin A+ cells by CD34+ cells.* Exp Hematol, 2002. **30**(11): p. 1238-47.
273. Johnson, C.S., et al., *In vivo hematopoietic effects of recombinant interleukin-1 alpha in mice: stimulation of granulocytic, monocytic, megakaryocytic, and early erythroid progenitors, suppression of late-stage erythropoiesis, and reversal of erythroid suppression with erythropoietin.* Blood, 1989. **73**(3): p. 678-83.
274. Ratajczak, J., et al., *Effect of Interleukin-1 alpha and Interleukin-1 beta on Erythroid Progenitor Cell Growth in Serum Free Cultures: An In Vitro Study Relevant to the Pathogenesis of the Anemia of Chronic Disease.* Hematology, 1997. **2**(1): p. 21-8.
275. Johnson, C.S., C.A. Cook, and P. Furmanski, *In vivo suppression of erythropoiesis by tumor necrosis factor-alpha (TNF-alpha): reversal with exogenous erythropoietin (EPO).* Exp Hematol, 1990. **18**(2): p. 109-13.
276. Macdougall, I.C. and A.C. Cooper, *Erythropoietin resistance: the role of inflammation and pro-inflammatory cytokines.* Nephrol Dial Transplant, 2002. **17 Suppl 11**: p. 39-43.
277. Casadevall, N., *Cellular mechanism of resistance to erythropoietin.* Nephrol Dial Transplant, 1995. **10 Suppl 6**: p. 27-30.
278. Mosmann, T.R., et al., *Two types of murine helper T cell clone. I. Definition according to profiles of lymphokine activities and secreted proteins.* J Immunol, 1986. **136**(7): p. 2348-57.
279. Abbas, A.K., K.M. Murphy, and A. Sher, *Functional diversity of helper T lymphocytes.* Nature, 1996. **383**(6603): p. 787-93.
280. Gieseck, R.L., 3rd, M.S. Wilson, and T.A. Wynn, *Type 2 immunity in tissue repair and fibrosis.* Nat Rev Immunol, 2018. **18**(1): p. 62-76.
281. Wynn, T.A., *Type 2 cytokines: mechanisms and therapeutic strategies.* Nat Rev Immunol, 2015. **15**(5): p. 271-82.
282. Maizels, R.M., et al., *Regulation of pathogenesis and immunity in helminth infections.* J Exp Med, 2009. **206**(10): p. 2059-66.
283. Robinette, M.L. and M. Colonna, *Immune modules shared by innate lymphoid cells and T cells.* J Allergy Clin Immunol, 2016. **138**(5): p. 1243-1251.
284. Maloy, K.J. and F. Powrie, *Intestinal homeostasis and its breakdown in inflammatory bowel disease.* Nature, 2011. **474**(7351): p. 298-306.
285. Junttila, I.S., *Tuning the Cytokine Responses: An Update on Interleukin (IL)-4 and IL-13 Receptor Complexes.* Front Immunol, 2018. **9**: p. 888.
286. Seder, R.A., et al., *Mouse splenic and bone marrow cell populations that express high-affinity Fc epsilon receptors and produce interleukin 4 are highly enriched in basophils.* Proc Natl Acad Sci U S A, 1991. **88**(7): p. 2835-9.
287. Gessner, A., K. Mohrs, and M. Mohrs, *Mast cells, basophils, and eosinophils acquire constitutive IL-4 and IL-13 transcripts during lineage differentiation that are sufficient for rapid cytokine production.* J Immunol, 2005. **174**(2): p. 1063-72.
288. Stetson, D.B., et al., *Constitutive cytokine mRNAs mark natural killer (NK) and NK T cells poised for rapid effector function.* J Exp Med, 2003. **198**(7): p. 1069-76.
289. Mohrs, K., et al., *A two-step process for cytokine production revealed by IL-4 dual-reporter mice.* Immunity, 2005. **23**(4): p. 419-29.

290. Neill, D.R., et al., *Nuocytes represent a new innate effector leukocyte that mediates type-2 immunity.* Nature, 2010. **464**(7293): p. 1367-70.
291. LaPorte, S.L., et al., *Molecular and structural basis of cytokine receptor pleiotropy in the interleukin-4/13 system.* Cell, 2008. **132**(2): p. 259-72.
292. Paul, W.E., *History of interleukin-4.* Cytokine, 2015. **75**(1): p. 3-7.
293. McKenzie, G.J., et al., *Simultaneous disruption of interleukin (IL)-4 and IL-13 defines individual roles in T helper cell type 2-mediated responses.* J Exp Med, 1999. **189**(10): p. 1565-72.
294. Isakson, P.C., et al., *T cell-derived B cell differentiation factor(s). Effect on the isotype switch of murine B cells.* J Exp Med, 1982. **155**(3): p. 734-48.
295. Gordon, S., *Alternative activation of macrophages.* Nat Rev Immunol, 2003. **3**(1): p. 23-35.
296. Kaplan, M.H., et al., *Stat6 is required for mediating responses to IL-4 and for development of Th2 cells.* Immunity, 1996. **4**(3): p. 313-9.
297. Takeda, K., et al., *Essential role of Stat6 in IL-4 signalling.* Nature, 1996. **380**(6575): p. 627-30.
298. Gordon, S. and F.O. Martinez, *Alternative activation of macrophages: mechanism and functions.* Immunity, 2010. **32**(5): p. 593-604.
299. Sonoda, Y., *Interleukin-4--a dual regulatory factor in hematopoiesis.* Leuk Lymphoma, 1994. **14**(3-4): p. 231-40.
300. Sonoda, Y., et al., *Actions of human interleukin-4/B-cell stimulatory factor-1 on proliferation and differentiation of enriched hematopoietic progenitor cells in culture.* Blood, 1990. **75**(8): p. 1615-21.
301. Broxmeyer, H.E., et al., *Synergistic effects of purified recombinant human and murine B cell growth factor-1/IL-4 on colony formation in vitro by hematopoietic progenitor cells. Multiple actions.* J Immunol, 1988. **141**(11): p. 3852-62.
302. Peschel, C., et al., *Effects of B cell stimulatory factor-1/interleukin 4 on hematopoietic progenitor cells.* Blood, 1987. **70**(1): p. 254-63.
303. Ferrajoli, A., et al., *Growth factors controlling interleukin-4 action on hematopoietic progenitors.* Ann Hematol, 1993. **67**(6): p. 277-84.
304. Ferrajoli, A., et al., *Interleukin 4 alters human bone marrow stroma and modulates its interaction with hematopoietic progenitors.* Stem Cells, 1994. **12**(6): p. 638-49.
305. Jacobsen, S.E., et al., *Interleukin 13: novel role in direct regulation of proliferation and differentiation of primitive hematopoietic progenitor cells.* J Exp Med, 1994. **180**(1): p. 75-82.
306. Broxmeyer, H.E., et al., *Th1 cells regulate hematopoietic progenitor cell homeostasis by production of oncostatin M.* Immunity, 2002. **16**(6): p. 815-25.
307. Sallusto, F. and A. Lanzavecchia, *Efficient presentation of soluble antigen by cultured human dendritic cells is maintained by granulocyte/macrophage colony-stimulating factor plus interleukin 4 and downregulated by tumor necrosis factor alpha.* J Exp Med, 1994. **179**(4): p. 1109-18.
308. Xu, Y., et al., *Differential development of murine dendritic cells by GM-CSF versus Flt3 ligand has implications for inflammation and trafficking.* J Immunol, 2007. **179**(11): p. 7577-84.
309. Bunting, K.D., et al., *Increased numbers of committed myeloid progenitors but not primitive hematopoietic stem/progenitors in mice lacking STAT6 expression.* J Leukoc Biol, 2004. **76**(2): p. 484-90.

310. Matsukawa, A., et al., *Pivotal role of signal transducer and activator of transcription (Stat)4 and Stat6 in the innate immune response during sepsis.* J Exp Med, 2001. **193**(6): p. 679-88.
311. Kaplan, M.H., et al., *Distinct requirements for Stat4 and Stat6 in hematopoietic progenitor cell responses to growth factors and chemokines.* J Hematother Stem Cell Res, 2003. **12**(4): p. 401-8.
312. Thawani, N., M. Tam, and M.M. Stevenson, *STAT6-mediated suppression of erythropoiesis in an experimental model of malarial anemia.* Haematologica, 2009. **94**(2): p. 195-204.
313. Milner, J.D., et al., *Sustained IL-4 exposure leads to a novel pathway for hemophagocytosis, inflammation, and tissue macrophage accumulation.* Blood, 2010. **116**(14): p. 2476-83.
314. Jenkins, S.J., et al., *IL-4 directly signals tissue-resident macrophages to proliferate beyond homeostatic levels controlled by CSF-1.* J Exp Med, 2013. **210**(11): p. 2477-91.
315. Pena-Martinez, P., et al., *Interleukin 4 induces apoptosis of acute myeloid leukemia cells in a Stat6-dependent manner.* Leukemia, 2018. **32**(3): p. 588-596.
316. Dougan, M., G. Dranoff, and S.K. Dougan, *GM-CSF, IL-3, and IL-5 Family of Cytokines: Regulators of Inflammation.* Immunity, 2019. **50**(4): p. 796-811.
317. Kopf, M., et al., *IL-5-deficient mice have a developmental defect in CD5+ B-1 cells and lack eosinophilia but have normal antibody and cytotoxic T cell responses.* Immunity, 1996. **4**(1): p. 15-24.
318. Shen, Z.J. and J.S. Malter, *Determinants of eosinophil survival and apoptotic cell death.* Apoptosis, 2015. **20**(2): p. 224-34.
319. Kouro, T. and K. Takatsu, *IL-5- and eosinophil-mediated inflammation: from discovery to therapy.* Int Immunol, 2009. **21**(12): p. 1303-9.
320. Warringa, R.A., et al., *Modulation of eosinophil chemotaxis by interleukin-5.* Am J Respir Cell Mol Biol, 1992. **7**(6): p. 631-6.
321. Yoshida, T., et al., *Defective B-1 cell development and impaired immunity against Angiostrongylus cantonensis in IL-5R alpha-deficient mice.* Immunity, 1996. **4**(5): p. 483-94.
322. Johnston, L.K. and P.J. Bryce, *Understanding Interleukin 33 and Its Roles in Eosinophil Development.* Front Med (Lausanne), 2017. **4**: p. 51.
323. Johnston, L.K., et al., *IL-33 Precedes IL-5 in Regulating Eosinophil Commitment and Is Required for Eosinophil Homeostasis.* J Immunol, 2016. **197**(9): p. 3445-3453.
324. Iwasaki, H., et al., *Identification of eosinophil lineage-committed progenitors in the murine bone marrow.* J Exp Med, 2005. **201**(12): p. 1891-7.
325. Cayrol, C. and J.P. Girard, *The IL-1-like cytokine IL-33 is inactivated after maturation by caspase-1.* Proc Natl Acad Sci U S A, 2009. **106**(22): p. 9021-6.
326. Rickard, J.A., et al., *RIPK1 regulates RIPK3-MLKL-driven systemic inflammation and emergency hematopoiesis.* Cell, 2014. **157**(5): p. 1175-88.
327. Cayrol, C. and J.P. Girard, *Interleukin-33 (IL-33): A nuclear cytokine from the IL-1 family.* Immunol Rev, 2018. **281**(1): p. 154-168.
328. Wang, D., et al., *Dectin-1 stimulates IL-33 expression in dendritic cells via upregulation of IRF4.* Lab Invest, 2018. **98**(6): p. 708-714.
329. Zhu, X., et al., *Dectin-1 signaling inhibits osteoclastogenesis via IL-33-induced inhibition of NFATc1.* Oncotarget, 2017. **8**(32): p. 53366-53374.

330. Griesenauer, B. and S. Paczesny, *The ST2/IL-33 Axis in Immune Cells during Inflammatory Diseases.* Front Immunol, 2017. **8**: p. 475.
331. Baumann, C., et al., *T-bet- and STAT4-dependent IL-33 receptor expression directly promotes antiviral Th1 cell responses.* Proc Natl Acad Sci U S A, 2015. **112**(13): p. 4056-61.
332. Liew, F.Y., J.P. Girard, and H.R. Turnquist, *Interleukin-33 in health and disease.* Nat Rev Immunol, 2016. **16**(11): p. 676-689.
333. Komai-Koma, M., et al., *IL-33 is a chemoattractant for human Th2 cells.* Eur J Immunol, 2007. **37**(10): p. 2779-86.
334. Piehler, D., et al., *T1/ST2 promotes T helper 2 cell activation and polyfunctionality in bronchopulmonary mycosis.* Mucosal Immunol, 2013. **6**(2): p. 405-14.
335. Townsend, M.J., et al., *T1/ST2-deficient mice demonstrate the importance of T1/ST2 in developing primary T helper cell type 2 responses.* J Exp Med, 2000. **191**(6): p. 1069-76.
336. Moritz, D.R., et al., *The IL-1 receptor-related T1 antigen is expressed on immature and mature mast cells and on fetal blood mast cell progenitors.* J Immunol, 1998. **161**(9): p. 4866-74.
337. Suzukawa, M., et al., *An IL-1 cytokine member, IL-33, induces human basophil activation via its ST2 receptor.* J Immunol, 2008. **181**(9): p. 5981-9.
338. Cherry, W.B., et al., *A novel IL-1 family cytokine, IL-33, potently activates human eosinophils.* J Allergy Clin Immunol, 2008. **121**(6): p. 1484-90.
339. Moffatt, M.F., et al., *A large-scale, consortium-based genomewide association study of asthma.* N Engl J Med, 2010. **363**(13): p. 1211-1221.
340. Queiroz, G.A., et al., *IL33 and IL1RL1 variants are associated with asthma and atopy in a Brazilian population.* Int J Immunogenet, 2017. **44**(2): p. 51-61.
341. Smith, D., et al., *A rare IL33 loss-of-function mutation reduces blood eosinophil counts and protects from asthma.* PLoS Genet, 2017. **13**(3): p. e1006659.
342. Martin, N.T. and M.U. Martin, *Interleukin 33 is a guardian of barriers and a local alarmin.* Nat Immunol, 2016. **17**(2): p. 122-31.
343. Lunderius-Andersson, C., M. Enoksson, and G. Nilsson, *Mast Cells Respond to Cell Injury through the Recognition of IL-33.* Front Immunol, 2012. **3**: p. 82.
344. Schiering, C., et al., *The alarmin IL-33 promotes regulatory T-cell function in the intestine.* Nature, 2014. **513**(7519): p. 564-568.
345. Zdravkovic, N., et al., *Regulatory T cells and ST2 signaling control diabetes induction with multiple low doses of streptozotocin.* Mol Immunol, 2009. **47**(1): p. 28-36.
346. Vasanthakumar, A., et al., *The transcriptional regulators IRF4, BATF and IL-33 orchestrate development and maintenance of adipose tissue-resident regulatory T cells.* Nat Immunol, 2015. **16**(3): p. 276-85.
347. Li, G.X., et al., *Serum levels of IL-33 and its receptor ST2 are elevated in patients with ankylosing spondylitis.* Scand J Rheumatol, 2013. **42**(3): p. 226-31.
348. Han, G.W., et al., *Serum levels of IL-33 is increased in patients with ankylosing spondylitis.* Clin Rheumatol, 2011. **30**(12): p. 1583-8.
349. Tang, S., et al., *Increased IL-33 in synovial fluid and paired serum is associated with disease activity and autoantibodies in rheumatoid arthritis.* Clin Dev Immunol, 2013. **2013**: p. 985301.
350. Xu, D., et al., *IL-33 exacerbates antigen-induced arthritis by activating mast cells.* Proc Natl Acad Sci U S A, 2008. **105**(31): p. 10913-8.

351. Xu, D., et al., *IL-33 exacerbates autoantibody-induced arthritis.* J Immunol, 2010. **184**(5): p. 2620-6.
352. Palmer, G., et al., *Inhibition of interleukin-33 signaling attenuates the severity of experimental arthritis.* Arthritis Rheum, 2009. **60**(3): p. 738-49.
353. Sedhom, M.A., et al., *Neutralisation of the interleukin-33/ST2 pathway ameliorates experimental colitis through enhancement of mucosal healing in mice.* Gut, 2013. **62**(12): p. 1714-23.
354. Zhu, J., et al., *IL-33 Aggravates DSS-Induced Acute Colitis in Mouse Colon Lamina Propria by Enhancing Th2 Cell Responses.* Mediators Inflamm, 2015. **2015**: p. 913041.
355. Duan, L., et al., *Interleukin-33 ameliorates experimental colitis through promoting Th2/Foxp3(+) regulatory T-cell responses in mice.* Mol Med, 2012. **18**: p. 753-61.
356. Zhu, J., et al., *IL-33 alleviates DSS-induced chronic colitis in C57BL/6 mice colon lamina propria by suppressing Th17 cell response as well as Th1 cell response.* Int Immunopharmacol, 2015. **29**(2): p. 846-853.
357. Capitano, M.L., et al., *The IL-33 Receptor/ST2 acts as a positive regulator of functional mouse bone marrow hematopoietic stem and progenitor cells.* Blood Cells Mol Dis, 2020. **84**: p. 102435.
358. Tsuzuki, H., et al., *Functional interleukin-33 receptors are expressed in early progenitor stages of allergy-related granulocytes.* Immunology, 2017. **150**(1): p. 64-73.
359. Le, H., et al., *Interleukin-33: a mediator of inflammation targeting hematopoietic stem and progenitor cells and their progenies.* Front Immunol, 2013. **4**: p. 104.
360. Brickshawana, A., et al., *Lineage(-)Sca1+c-Kit(-)CD25+ cells are IL-33-responsive type 2 innate cells in the mouse bone marrow.* J Immunol, 2011. **187**(11): p. 5795-804.
361. Hoyler, T., et al., *The transcription factor GATA-3 controls cell fate and maintenance of type 2 innate lymphoid cells.* Immunity, 2012. **37**(4): p. 634-48.
362. Wong, S.H., et al., *Transcription factor RORalpha is critical for nuocyte development.* Nat Immunol, 2012. **13**(3): p. 229-36.
363. Stolarski, B., et al., *IL-33 exacerbates eosinophil-mediated airway inflammation.* J Immunol, 2010. **185**(6): p. 3472-80.
364. Schneider, E., et al., *IL-33 activates unprimed murine basophils directly in vitro and induces their in vivo expansion indirectly by promoting hematopoietic growth factor production.* J Immunol, 2009. **183**(6): p. 3591-7.
365. Stier, M.T., et al., *IL-33 promotes the egress of group 2 innate lymphoid cells from the bone marrow.* J Exp Med, 2018. **215**(1): p. 263-281.
366. Mager, L.F., et al., *IL-33 signaling contributes to the pathogenesis of myeloproliferative neoplasms.* J Clin Invest, 2015. **125**(7): p. 2579-91.
367. Huang, P., et al., *Interleukin-33 regulates hematopoietic stem cell regeneration after radiation injury.* Stem Cell Res Ther, 2019. **10**(1): p. 123.
368. Talabot-Ayer, D., et al., *Severe neutrophil-dominated inflammation and enhanced myelopoiesis in IL-33-overexpressing CMV/IL33 mice.* J Immunol, 2015. **194**(2): p. 750-60.
369. Kenswil, K.J.G., et al., *Characterization of Endothelial Cells Associated with Hematopoietic Niche Formation in Humans Identifies IL-33 As an Anabolic Factor.* Cell Rep, 2018. **22**(3): p. 666-678.

370. Kim, J., et al., *IL-33-induced hematopoietic stem and progenitor cell mobilization depends upon CCR2.* J Immunol, 2014. **193**(7): p. 3792-802.
371. Alt, C., et al., *Long-Acting IL-33 Mobilizes High-Quality Hematopoietic Stem and Progenitor Cells More Efficiently Than Granulocyte Colony-Stimulating Factor or AMD3100.* Biol Blood Marrow Transplant, 2019. **25**(8): p. 1475-1485.
372. Saenz, S.A., et al., *IL-25 simultaneously elicits distinct populations of innate lymphoid cells and multipotent progenitor type 2 (MPPtype2) cells.* J Exp Med, 2013. **210**(9): p. 1823-37.
373. Kurowska-Stolarska, M., et al., *IL-33 amplifies the polarization of alternatively activated macrophages that contribute to airway inflammation.* J Immunol, 2009. **183**(10): p. 6469-77.
374. Van Dyken, S.J. and R.M. Locksley, *Interleukin-4- and interleukin-13-mediated alternatively activated macrophages: roles in homeostasis and disease.* Annu Rev Immunol, 2013. **31**: p. 317-43.
375. Sun, B., et al., *Characterization and allergic role of IL-33-induced neutrophil polarization.* Cell Mol Immunol, 2018. **15**(8): p. 782-793.
376. Verri, W.A., Jr., et al., *IL-33 induces neutrophil migration in rheumatoid arthritis and is a target of anti-TNF therapy.* Ann Rheum Dis, 2010. **69**(9): p. 1697-703.
377. Enoksson, M., et al., *Intraperitoneal influx of neutrophils in response to IL-33 is mast cell-dependent.* Blood, 2013. **121**(3): p. 530-6.
378. Lee, J.J., et al., *Eosinophils in health and disease: the LIAR hypothesis.* Clin Exp Allergy, 2010. **40**(4): p. 563-75.
379. Loke, P., et al., *Alternative activation is an innate response to injury that requires CD4+ T cells to be sustained during chronic infection.* J Immunol, 2007. **179**(6): p. 3926-36.
380. Sieper, J., et al., *Axial spondyloarthritis.* Nat Rev Dis Primers, 2015. **1**: p. 15013.
381. Ranganathan, V., et al., *Pathogenesis of ankylosing spondylitis - recent advances and future directions.* Nat Rev Rheumatol, 2017. **13**(6): p. 359-367.
382. De Vos, M., et al., *Ileocolonoscopy in seronegative spondylarthropathy.* Gastroenterology, 1989. **96**(2 Pt 1): p. 339-44.
383. De Vos, M., et al., *Long-term evolution of gut inflammation in patients with spondyloarthropathy.* Gastroenterology, 1996. **110**(6): p. 1696-703.
384. Braun, J., et al., *Prevalence of spondylarthropathies in HLA-B27 positive and negative blood donors.* Arthritis Rheum, 1998. **41**(1): p. 58-67.
385. Sakaguchi, N., et al., *Altered thymic T-cell selection due to a mutation of the ZAP-70 gene causes autoimmune arthritis in mice.* Nature, 2003. **426**(6965): p. 454-60.
386. Weiss, A. and D.R. Littman, *Signal transduction by lymphocyte antigen receptors.* Cell, 1994. **76**(2): p. 263-74.
387. Sakaguchi, S., et al., *T-cell receptor signaling and the pathogenesis of autoimmune arthritis: insights from mouse and man.* Immunol Cell Biol, 2012. **90**(3): p. 277-87.
388. Tanaka, S., et al., *Graded attenuation of TCR signaling elicits distinct autoimmune diseases by altering thymic T cell selection and regulatory T cell function.* J Immunol, 2010. **185**(4): p. 2295-305.
389. Yoshitomi, H., et al., *A role for fungal {beta}-glucans and their receptor Dectin-1 in the induction of autoimmune arthritis in genetically susceptible mice.* J Exp Med, 2005. **201**(6): p. 949-60.

390. Kim, H.S., et al., *Curdlan activates dendritic cells through dectin-1 and toll-like receptor 4 signaling.* Int Immunopharmacol, 2016. **39**: p. 71-78.
391. Ruutu, M., et al., *beta-glucan triggers spondylarthritis and Crohn's disease-like ileitis in SKG mice.* Arthritis Rheum, 2012. **64**(7): p. 2211-22.
392. Rahman, M.A. and R. Thomas, *The SKG model of spondyloarthritis.* Best Pract Res Clin Rheumatol, 2017. **31**(6): p. 895-909.
393. Hata, H., et al., *Distinct contribution of IL-6, TNF-alpha, IL-1, and IL-10 to T cell-mediated spontaneous autoimmune arthritis in mice.* J Clin Invest, 2004. **114**(4): p. 582-8.
394. Hirota, K., et al., *Autoimmune Th17 Cells Induced Synovial Stromal and Innate Lymphoid Cell Secretion of the Cytokine GM-CSF to Initiate and Augment Autoimmune Arthritis.* Immunity, 2018. **48**(6): p. 1220-1232 e5.
395. Hirota, K., et al., *T cell self-reactivity forms a cytokine milieu for spontaneous development of IL-17+ Th cells that cause autoimmune arthritis.* J Exp Med, 2007. **204**(1): p. 41-7.
396. Bowness, P., *Hla-B27.* Annu Rev Immunol, 2015. **33**: p. 29-48.
397. Braem, K. and R.J. Lories, *Insights into the pathophysiology of ankylosing spondylitis: contributions from animal models.* Joint Bone Spine, 2012. **79**(3): p. 243-8.
398. Schittenhelm, R.B., et al., *Human Leukocyte Antigen (HLA) B27 Allotype-Specific Binding and Candidate Arthritogenic Peptides Revealed through Heuristic Clustering of Data-independent Acquisition Mass Spectrometry (DIA-MS) Data.* Mol Cell Proteomics, 2016. **15**(6): p. 1867-76.
399. Duchmann, R., et al., *CD4+ and CD8+ clonal T cell expansions indicate a role of antigens in ankylosing spondylitis; a study in HLA-B27+ monozygotic twins.* Clin Exp Immunol, 2001. **123**(2): p. 315-22.
400. Dulphy, N., et al., *Common intra-articular T cell expansions in patients with reactive arthritis: identical beta-chain junctional sequences and cytotoxicity toward HLA-B27.* J Immunol, 1999. **162**(7): p. 3830-9.
401. Kollnberger, S., et al., *Cell-surface expression and immune receptor recognition of HLA-B27 homodimers.* Arthritis Rheum, 2002. **46**(11): p. 2972-82.
402. Gaur, P., R. Misra, and A. Aggarwal, *Natural killer cell and gamma delta T cell alterations in enthesitis related arthritis category of juvenile idiopathic arthritis.* Clin Immunol, 2015. **161**(2): p. 163-9.
403. Chan, A.T., et al., *Expansion and enhanced survival of natural killer cells expressing the killer immunoglobulin-like receptor KIR3DL2 in spondylarthritis.* Arthritis Rheum, 2005. **52**(11): p. 3586-95.
404. Ridley, A., et al., *Activation-Induced Killer Cell Immunoglobulin-like Receptor 3DL2 Binding to HLA-B27 Licenses Pathogenic T Cell Differentiation in Spondyloarthritis.* Arthritis Rheumatol, 2016. **68**(4): p. 901-14.
405. Deveci, H., et al., *Serum Interleukin-23/17 Levels in Ankylosing Spondylitis Patients Treated with Nonsteroidal Anti-Inflammatory Drugs: A Prospective Cohort Study.* J Interferon Cytokine Res, 2019. **39**(9): p. 572-576.
406. Ciccia, F., et al., *Type 3 innate lymphoid cells producing IL-17 and IL-22 are expanded in the gut, in the peripheral blood, synovial fluid and bone marrow of patients with ankylosing spondylitis.* Ann Rheum Dis, 2015. **74**(9): p. 1739-47.

407. Jansen, D.T., et al., *IL-17-producing CD4+ T cells are increased in early, active axial spondyloarthritis including patients without imaging abnormalities.* Rheumatology (Oxford), 2015. **54**(4): p. 728-35.
408. Kenna, T.J., et al., *Enrichment of circulating interleukin-17-secreting interleukin-23 receptor-positive gamma/delta T cells in patients with active ankylosing spondylitis.* Arthritis Rheum, 2012. **64**(5): p. 1420-9.
409. Menon, B., et al., *Interleukin-17+CD8+ T cells are enriched in the joints of patients with psoriatic arthritis and correlate with disease activity and joint damage progression.* Arthritis Rheumatol, 2014. **66**(5): p. 1272-81.
410. Shen, H., J.C. Goodall, and J.S. Hill Gaston, *Frequency and phenotype of peripheral blood Th17 cells in ankylosing spondylitis and rheumatoid arthritis.* Arthritis Rheum, 2009. **60**(6): p. 1647-56.
411. Soare, A., et al., *Cutting Edge: Homeostasis of Innate Lymphoid Cells Is Imbalanced in Psoriatic Arthritis.* J Immunol, 2018. **200**(4): p. 1249-1254.
412. Venken, K., et al., *RORgammat inhibition selectively targets IL-17 producing iNKT and gammadelta-T cells enriched in Spondyloarthritis patients.* Nat Commun, 2019. **10**(1): p. 9.
413. Gaston, J.S.H. and D.R. Jadon, *Th17 cell responses in spondyloarthritis.* Best Pract Res Clin Rheumatol, 2017. **31**(6): p. 777-796.
414. McGonagle, D.G., et al., *The role of IL-17A in axial spondyloarthritis and psoriatic arthritis: recent advances and controversies.* Ann Rheum Dis, 2019. **78**(9): p. 1167-1178.
415. International Genetics of Ankylosing Spondylitis, C., et al., *Identification of multiple risk variants for ankylosing spondylitis through high-density genotyping of immune-related loci.* Nat Genet, 2013. **45**(7): p. 730-8.
416. Australo-Anglo-American Spondyloarthritis, C., et al., *Genome-wide association study of ankylosing spondylitis identifies non-MHC susceptibility loci.* Nat Genet, 2010. **42**(2): p. 123-7.
417. Yu, J.J., et al., *An essential role for IL-17 in preventing pathogen-initiated bone destruction: recruitment of neutrophils to inflamed bone requires IL-17 receptor-dependent signals.* Blood, 2007. **109**(9): p. 3794-802.
418. Ye, P., et al., *Requirement of interleukin 17 receptor signaling for lung CXC chemokine and granulocyte colony-stimulating factor expression, neutrophil recruitment, and host defense.* J Exp Med, 2001. **194**(4): p. 519-27.
419. McGonagle, D., et al., *Histological assessment of the early enthesitis lesion in spondyloarthropathy.* Ann Rheum Dis, 2002. **61**(6): p. 534-7.
420. Appel, H., et al., *Analysis of IL-17(+) cells in facet joints of patients with spondyloarthritis suggests that the innate immune pathway might be of greater relevance than the Th17-mediated adaptive immune response.* Arthritis Res Ther, 2011. **13**(3): p. R95.
421. Noordenbos, T., et al., *Interleukin-17-positive mast cells contribute to synovial inflammation in spondylarthritis.* Arthritis Rheum, 2012. **64**(1): p. 99-109.
422. Tamassia, N., et al., *A Reappraisal on the Potential Ability of Human Neutrophils to Express and Produce IL-17 Family Members In Vitro: Failure to Reproducibly Detect It.* Front Immunol, 2018. **9**: p. 795.
423. Noordenbos, T., et al., *Human mast cells capture, store, and release bioactive, exogenous IL-17A.* J Leukoc Biol, 2016. **100**(3): p. 453-62.

424. Harrington, L.E., et al., *Interleukin 17-producing CD4+ effector T cells develop via a lineage distinct from the T helper type 1 and 2 lineages.* Nat Immunol, 2005. **6**(11): p. 1123-32.
425. Bettelli, E., et al., *Induction and effector functions of T(H)17 cells.* Nature, 2008. **453**(7198): p. 1051-7.
426. Korn, T., et al., *IL-17 and Th17 Cells.* Annu Rev Immunol, 2009. **27**: p. 485-517.
427. Aggarwal, S., et al., *Interleukin-23 promotes a distinct CD4 T cell activation state characterized by the production of interleukin-17.* J Biol Chem, 2003. **278**(3): p. 1910-4.
428. McGeachy, M.J., et al., *The interleukin 23 receptor is essential for the terminal differentiation of interleukin 17-producing effector T helper cells in vivo.* Nat Immunol, 2009. **10**(3): p. 314-24.
429. Fragoulis, G.E., S. Siebert, and I.B. McInnes, *Therapeutic Targeting of IL-17 and IL-23 Cytokines in Immune-Mediated Diseases.* Annu Rev Med, 2016. **67**: p. 337-53.
430. Cuthbert, R.J., et al., *Brief Report: Group 3 Innate Lymphoid Cells in Human Enthesis.* Arthritis Rheumatol, 2017. **69**(9): p. 1816-1822.
431. Cuthbert, R.J., et al., *Evidence that tissue resident human enthesis gammadeltaT-cells can produce IL-17A independently of IL-23R transcript expression.* Ann Rheum Dis, 2019. **78**(11): p. 1559-1565.
432. Sherlock, J.P., et al., *IL-23 induces spondyloarthropathy by acting on ROR-gammat+ CD3+CD4-CD8- entheseal resident T cells.* Nat Med, 2012. **18**(7): p. 1069-76.
433. Bridgewood, C., et al., *Interleukin-23 pathway at the enthesis: The emerging story of enthesitis in spondyloarthropathy.* Immunol Rev, 2020. **294**(1): p. 27-47.
434. Bridgewood, C., et al., *Identification of myeloid cells in the human enthesis as the main source of local IL-23 production.* Ann Rheum Dis, 2019. **78**(7): p. 929-933.
435. Gracey, E., et al., *Revisiting the gut-joint axis: links between gut inflammation and spondyloarthritis.* Nat Rev Rheumatol, 2020. **16**(8): p. 415-433.
436. Kobayashi, K., et al., *Cytokine production profile of splenocytes derived from zymosan A-treated SKG mice developing arthritis.* Inflamm Res, 2006. **55**(8): p. 335-41.
437. Benham, H., et al., *Interleukin-23 mediates the intestinal response to microbial beta-1,3-glucan and the development of spondyloarthritis pathology in SKG mice.* Arthritis Rheumatol, 2014. **66**(7): p. 1755-67.
438. Rehaume, L.M., et al., *ZAP-70 genotype disrupts the relationship between microbiota and host, leading to spondyloarthritis and ileitis in SKG mice.* Arthritis Rheumatol, 2014. **66**(10): p. 2780-92.
439. Ciccia, F., et al., *Overexpression of interleukin-23, but not interleukin-17, as an immunologic signature of subclinical intestinal inflammation in ankylosing spondylitis.* Arthritis Rheum, 2009. **60**(4): p. 955-65.
440. Ciccia, F., et al., *Macrophage phenotype in the subclinical gut inflammation of patients with ankylosing spondylitis.* Rheumatology (Oxford), 2014. **53**(1): p. 104-13.
441. Regan-Komito, D., et al., *GM-CSF drives dysregulated hematopoietic stem cell activity and pathogenic extramedullary myelopoiesis in experimental spondyloarthritis.* Nat Commun, 2020. **11**(1): p. 155.

442. Al-Mossawi, M.H., et al., *Unique transcriptome signatures and GM-CSF expression in lymphocytes from patients with spondyloarthritis.* Nat Commun, 2017. **8**(1): p. 1510.
443. Shi, H., et al., *GM-CSF Primes Proinflammatory Monocyte Responses in Ankylosing Spondylitis.* Front Immunol, 2020. **11**: p. 1520.
444. Mercan, R., et al., *The Association Between Neutrophil/Lymphocyte Ratio and Disease Activity in Rheumatoid Arthritis and Ankylosing Spondylitis.* J Clin Lab Anal, 2016. **30**(5): p. 597-601.
445. Furst, D.E., et al., *The effect of golimumab on haemoglobin levels in patients with rheumatoid arthritis, psoriatic arthritis or ankylosing spondylitis.* Rheumatology (Oxford), 2013. **52**(10): p. 1845-55.
446. Braun, J., et al., *Improvement in hemoglobin levels in patients with ankylosing spondylitis treated with infliximab.* Arthritis Rheum, 2009. **61**(8): p. 1032-6.
447. Niccoli, L., et al., *Frequency of anemia of inflammation in patients with ankylosing spondylitis requiring anti-TNFalpha drugs and therapy-induced changes.* Int J Rheum Dis, 2012. **15**(1): p. 56-61.
448. Finkelman, F.D., et al., *Anti-cytokine antibodies as carrier proteins. Prolongation of in vivo effects of exogenous cytokines by injection of cytokine-anti-cytokine antibody complexes.* J Immunol, 1993. **151**(3): p. 1235-44.
449. Haak-Frendscho, M., et al., *Administration of anti-IL-4 monoclonal antibody 11B11 increases the resistance of mice to Listeria monocytogenes infection.* J Immunol, 1992. **148**(12): p. 3978-85.
450. Bagley, J., et al., *A critical role for interleukin 4 in activating alloreactive CD4 T cells.* Nat Immunol, 2000. **1**(3): p. 257-61.
451. Bitton, A., et al., *A key role for IL-13 signaling via the type 2 IL-4 receptor in experimental atopic dermatitis.* Sci Immunol, 2020. **5**(44).
452. Griseri, T., et al., *Granulocyte Macrophage Colony-Stimulating Factor-Activated Eosinophils Promote Interleukin-23 Driven Chronic Colitis.* Immunity, 2015. **43**(1): p. 187-99.
453. Liu, B., et al., *IL-33/ST2 signaling excites sensory neurons and mediates itch response in a mouse model of poison ivy contact allergy.* Proc Natl Acad Sci U S A, 2016. **113**(47): p. E7572-E7579.
454. Peng, G., et al., *Anti-IL-33 Antibody Has a Therapeutic Effect in an Atopic Dermatitis Murine Model Induced by 2, 4-Dinitrochlorobenzene.* Inflammation, 2018. **41**(1): p. 154-163.
455. Govatati, S., et al., *NFATc1-E2F1-LMCD1-Mediated IL-33 Expression by Thrombin Is Required for Injury-Induced Neointima Formation.* Arterioscler Thromb Vasc Biol, 2019. **39**(6): p. 1212-1226.
456. Maguire, O., et al., *Quantifying nuclear p65 as a parameter for NF-kappaB activation: Correlation between ImageStream cytometry, microscopy, and Western blot.* Cytometry A, 2011. **79**(6): p. 461-9.
457. Uchida, N., et al., *Serum-free Erythroid Differentiation for Efficient Genetic Modification and High-Level Adult Hemoglobin Production.* Mol Ther Methods Clin Dev, 2018. **9**: p. 247-256.
458. Shuga, J., et al., *In vitro erythropoiesis from bone marrow-derived progenitors provides a physiological assay for toxic and mutagenic compounds.* Proc Natl Acad Sci U S A, 2007. **104**(21): p. 8737-42.

459. England, S.J., et al., *Immature erythroblasts with extensive ex vivo self-renewal capacity emerge from the early mammalian fetus.* Blood, 2011. **117**(9): p. 2708-17.
460. Zhao, B., et al., *Mouse fetal liver culture system to dissect target gene functions at the early and late stages of terminal erythropoiesis.* J Vis Exp, 2014(91): p. e51894.
461. An, X. and L. Chen, *Flow Cytometric Analysis of Erythroblast Enucleation.* Methods Mol Biol, 2018. **1698**: p. 193-203.
462. May, M.J., et al., *Selective inhibition of NF-kappaB activation by a peptide that blocks the interaction of NEMO with the IkappaB kinase complex.* Science, 2000. **289**(5484): p. 1550-4.
463. Antony-Debre, I., et al., *Pharmacological inhibition of the transcription factor PU.1 in leukemia.* J Clin Invest, 2017. **127**(12): p. 4297-4313.
464. Jo, H., et al., *Small molecule-induced cytosolic activation of protein kinase Akt rescues ischemia-elicited neuronal death.* Proc Natl Acad Sci U S A, 2012. **109**(26): p. 10581-6.
465. Golde, D.W., N. Bersch, and M.J. Cline, *Potentiation of erythropoiesis in vitro by dexamethasone.* J Clin Invest, 1976. **57**(1): p. 57-62.
466. Sjogren, S.E., et al., *Glucocorticoids improve erythroid progenitor maintenance and dampen Trp53 response in a mouse model of Diamond-Blackfan anaemia.* Br J Haematol, 2015. **171**(4): p. 517-29.
467. Mori, Y., et al., *Prospective isolation of human erythroid lineage-committed progenitors.* Proc Natl Acad Sci U S A, 2015. **112**(31): p. 9638-43.
468. Marks, P.A., et al., *Inducing differentiation of transformed cells with hybrid polar compounds: a cell cycle-dependent process.* Proc Natl Acad Sci U S A, 1994. **91**(22): p. 10251-4.
469. Profous-Juchelka, H.R., et al., *Transcriptional and post-transcriptional regulation of globin gene accumulation in murine erythroleukemia cells.* Mol Cell Biol, 1983. **3**(2): p. 229-32.
470. Kim, D., B. Langmead, and S.L. Salzberg, *HISAT: a fast spliced aligner with low memory requirements.* Nat Methods, 2015. **12**(4): p. 357-60.
471. Liao, Y., G.K. Smyth, and W. Shi, *featureCounts: an efficient general purpose program for assigning sequence reads to genomic features.* Bioinformatics, 2014. **30**(7): p. 923-30.
472. Patro, R., et al., *Salmon provides fast and bias-aware quantification of transcript expression.* Nat Methods, 2017. **14**(4): p. 417-419.
473. Love, M.I., W. Huber, and S. Anders, *Moderated estimation of fold change and dispersion for RNA-seq data with DESeq2.* Genome Biol, 2014. **15**(12): p. 550.
474. Sergushichev, A.A., *An algorithm for fast preranked gene set enrichment analysis using cumulative statistic calculation.* bioRxiv, 2016.
475. Hanson, W.R., et al., *Comparison of intestine and bone marrow radiosensitivity of the BALB/c and the C57BL/6 mouse strains and their B6CF1 offspring.* Radiat Res, 1987. **110**(3): p. 340-52.
476. Choi, J., et al., *Haemopedia RNA-seq: a database of gene expression during haematopoiesis in mice and humans.* Nucleic Acids Res, 2019. **47**(D1): p. D780-D785.
477. Sun, J., et al., *Clonal dynamics of native haematopoiesis.* Nature, 2014. **514**(7522): p. 322-7.

478. Misharin, A.V., et al., *Nonclassical Ly6C(-) monocytes drive the development of inflammatory arthritis in mice.* Cell Rep, 2014. **9**(2): p. 591-604.
479. Sunderkotter, C., et al., *Subpopulations of mouse blood monocytes differ in maturation stage and inflammatory response.* J Immunol, 2004. **172**(7): p. 4410-7.
480. Cook, A.D., et al., *Regulation of systemic and local myeloid cell subpopulations by bone marrow cell-derived granulocyte-macrophage colony-stimulating factor in experimental inflammatory arthritis.* Arthritis Rheum, 2011. **63**(8): p. 2340-51.
481. Seeling, M., et al., *Inflammatory monocytes and Fcgamma receptor IV on osteoclasts are critical for bone destruction during inflammatory arthritis in mice.* Proc Natl Acad Sci U S A, 2013. **110**(26): p. 10729-34.
482. Schulz, C., U.H. Von Andrian, and S. Massberg, *Trafficking of murine hematopoietic stem and progenitor cells in health and vascular disease.* Microcirculation, 2009. **16**(6): p. 497-507.
483. McRae, H.M., A.K. Voss, and T. Thomas, *Are transplantable stem cells required for adult hematopoiesis?* Exp Hematol, 2019. **75**: p. 1-10.
484. Sanchez, M., et al., *An SCL 3' enhancer targets developing endothelium together with embryonic and adult haematopoietic progenitors.* Development, 1999. **126**(17): p. 3891-904.
485. Choi, Y.J., et al., *D-cyclins repress apoptosis in hematopoietic cells by controlling death receptor Fas and its ligand FasL.* Dev Cell, 2014. **30**(3): p. 255-67.
486. Domen, J., S.H. Cheshier, and I.L. Weissman, *The role of apoptosis in the regulation of hematopoietic stem cells: Overexpression of Bcl-2 increases both their number and repopulation potential.* J Exp Med, 2000. **191**(2): p. 253-64.
487. Domen, J. and I.L. Weissman, *Hematopoietic stem cells need two signals to prevent apoptosis; BCL-2 can provide one of these, Kitl/c-Kit signaling the other.* J Exp Med, 2000. **192**(12): p. 1707-18.
488. Yamashita, M. and E. Passegue, *TNF-alpha Coordinates Hematopoietic Stem Cell Survival and Myeloid Regeneration.* Cell Stem Cell, 2019. **25**(3): p. 357-372 e7.
489. Akagi, T., et al., *Impaired response to GM-CSF and G-CSF, and enhanced apoptosis in C/EBPbeta-deficient hematopoietic cells.* Blood, 2008. **111**(6): p. 2999-3004.
490. Dent, L.A., et al., *Eosinophilia in transgenic mice expressing interleukin 5.* J Exp Med, 1990. **172**(5): p. 1425-31.
491. Foster, P.S., et al., *Interleukin 5 deficiency abolishes eosinophilia, airways hyperreactivity, and lung damage in a mouse asthma model.* J Exp Med, 1996. **183**(1): p. 195-201.
492. Bamias, G. and F. Cominelli, *Role of type 2 immunity in intestinal inflammation.* Curr Opin Gastroenterol, 2015. **31**(6): p. 471-6.
493. Fuss, I.J., et al., *Nonclassical CD1d-restricted NK T cells that produce IL-13 characterize an atypical Th2 response in ulcerative colitis.* J Clin Invest, 2004. **113**(10): p. 1490-7.
494. Grinenko, T., et al., *Hematopoietic stem cells can differentiate into restricted myeloid progenitors before cell division in mice.* Nat Commun, 2018. **9**(1): p. 1898.
495. Heney, D. and J.T. Whicher, *Factors affecting the measurement of cytokines in biological fluids: implications for their clinical measurement.* Ann Clin Biochem, 1995. **32 (Pt 4)**: p. 358-68.

496. Girard, D., R. Paquin, and A.D. Beaulieu, *Responsiveness of human neutrophils to interleukin-4: induction of cytoskeletal rearrangements, de novo protein synthesis and delay of apoptosis.* Biochem J, 1997. **325 (Pt 1)**: p. 147-53.
497. Bes, C., A. Yazici, and M. Soy, *Monoclonal anti-TNF antibodies can elevate hemoglobin level in patients with ankylosing spondylitis.* Rheumatol Int, 2013. **33**(6): p. 1415-8.
498. Hashimoto, M., et al., *Increase of hemoglobin levels by anti-IL-6 receptor antibody (tocilizumab) in rheumatoid arthritis.* PLoS One, 2014. **9**(5): p. e98202.
499. Song, S.N., et al., *Comparative evaluation of the effects of treatment with tocilizumab and TNF-alpha inhibitors on serum hepcidin, anemia response and disease activity in rheumatoid arthritis patients.* Arthritis Res Ther, 2013. **15**(5): p. R141.
500. Papadaki, H.A., et al., *Anemia of chronic disease in rheumatoid arthritis is associated with increased apoptosis of bone marrow erythroid cells: improvement following anti-tumor necrosis factor-alpha antibody therapy.* Blood, 2002. **100**(2): p. 474-82.
501. Fields, J.K., S. Gunther, and E.J. Sundberg, *Structural Basis of IL-1 Family Cytokine Signaling.* Front Immunol, 2019. **10**: p. 1412.
502. Zhao, J.L., et al., *Conversion of danger signals into cytokine signals by hematopoietic stem and progenitor cells for regulation of stress-induced hematopoiesis.* Cell Stem Cell, 2014. **14**(4): p. 445-459.
503. Moreau-Gachelin, F., *Multi-stage Friend murine erythroleukemia: molecular insights into oncogenic cooperation.* Retrovirology, 2008. **5**: p. 99.
504. Back, J., et al., *PU.1 determines the self-renewal capacity of erythroid progenitor cells.* Blood, 2004. **103**(10): p. 3615-23.
505. Nutt, S.L., et al., *Dynamic regulation of PU.1 expression in multipotent hematopoietic progenitors.* J Exp Med, 2005. **201**(2): p. 221-31.
506. Rimmele, P., et al., *Spi-1/PU.1 participates in erythroleukemogenesis by inhibiting apoptosis in cooperation with Epo signaling and by blocking erythroid differentiation.* Blood, 2007. **109**(7): p. 3007-14.
507. Andrews, N.C. and S.H. Orkin, *Transcriptional control of erythropoiesis.* Curr Opin Hematol, 1994. **1**(2): p. 119-24.
508. Nishigaki, K., et al., *Erythroid cells rendered erythropoietin independent by infection with Friend spleen focus-forming virus show constitutive activation of phosphatidylinositol 3-kinase and Akt kinase: involvement of insulin receptor substrate-related adapter proteins.* J Virol, 2000. **74**(7): p. 3037-45.
509. Stankovic, M.S., et al., *Effects of Il-33/St2 pathway on alteration of iron and hematological parameters in acute inflammation.* Exp Mol Pathol, 2015. **99**(3): p. 687-92.
510. Wei, J., et al., *Red Blood Cells Store and Release Interleukin-33.* J Investig Med, 2015. **63**(6): p. 806-10.
511. Jacobsen, R.N., et al., *Mobilization with granulocyte colony-stimulating factor blocks medullar erythropoiesis by depleting F4/80(+)VCAM1(+)CD169(+)ER-HR3(+)Ly6G(+) erythroid island macrophages in the mouse.* Exp Hematol, 2014. **42**(7): p. 547-61 e4.
512. Moulin, D., et al., *Interleukin (IL)-33 induces the release of pro-inflammatory mediators by mast cells.* Cytokine, 2007. **40**(3): p. 216-25.

513. Xue, S.P., et al., *The role of cytoskeletal elements in the two-phase denucleation process of mammalian erythroblasts in vitro observed by laser confocal scanning microscope.* Cell Mol Biol (Noisy-le-grand), 1997. **43**(6): p. 851-60.
514. Taketani, S., T. Furukawa, and K. Furuyama, *Expression of coproporphyrinogen oxidase and synthesis of hemoglobin in human erythroleukemia K562 cells.* Eur J Biochem, 2001. **268**(6): p. 1705-11.
515. Reem, G.H. and C. Friend, *Purine metabolism in murine virus-induced erythroleukemic cells during differentiation in vitro.* Proc Natl Acad Sci U S A, 1975. **72**(4): p. 1630-4.
516. Rothman, I.K., et al., *Nucleoside deaminase: an enzymatic marker for stress erythropoiesis in the mouse.* J Clin Invest, 1970. **49**(11): p. 2051-67.
517. Huang, S.Y., et al., *CD69 partially inhibits apoptosis and erythroid differentiation via CD24, and their knockdown increase imatinib sensitivity in BCR-ABL-positive cells.* J Cell Physiol, 2018. **233**(9): p. 7467-7479.
518. Pinto, S.M., et al., *A network map of IL-33 signaling pathway.* J Cell Commun Signal, 2018. **12**(3): p. 615-624.
519. Zhang, M.Y., et al., *NF-kappaB transcription factors are involved in normal erythropoiesis.* Blood, 1998. **91**(11): p. 4136-44.
520. McKercher, S.R., et al., *Targeted disruption of the PU.1 gene results in multiple hematopoietic abnormalities.* EMBO J, 1996. **15**(20): p. 5647-58.
521. Scott, E.W., et al., *Requirement of transcription factor PU.1 in the development of multiple hematopoietic lineages.* Science, 1994. **265**(5178): p. 1573-7.
522. Choe, K.S., et al., *Reversal of tumorigenicity and the block to differentiation in erythroleukemia cells by GATA-1.* Cancer Res, 2003. **63**(19): p. 6363-9.
523. Rekhtman, N., et al., *PU.1 and pRB interact and cooperate to repress GATA-1 and block erythroid differentiation.* Mol Cell Biol, 2003. **23**(21): p. 7460-74.
524. Watowich, S.S., *The erythropoietin receptor: molecular structure and hematopoietic signaling pathways.* J Investig Med, 2011. **59**(7): p. 1067-72.
525. Liu, X., et al., *Regulation of mitochondrial biogenesis in erythropoiesis by mTORC1-mediated protein translation.* Nat Cell Biol, 2017. **19**(6): p. 626-638.
526. Liu, J.J., S.C. Hou, and C.K. Shen, *Erythroid gene suppression by NF-kappa B.* J Biol Chem, 2003. **278**(21): p. 19534-40.
527. Bhatt, D. and S. Ghosh, *Regulation of the NF-kappaB-Mediated Transcription of Inflammatory Genes.* Front Immunol, 2014. **5**: p. 71.
528. Jacinto, E., et al., *SIN1/MIP1 maintains rictor-mTOR complex integrity and regulates Akt phosphorylation and substrate specificity.* Cell, 2006. **127**(1): p. 125-37.
529. Guertin, D.A., et al., *Ablation in mice of the mTORC components raptor, rictor, or mLST8 reveals that mTORC2 is required for signaling to Akt-FOXO and PKCalpha, but not S6K1.* Dev Cell, 2006. **11**(6): p. 859-71.
530. Balasuriya, N., et al., *Phosphorylation-dependent substrate selectivity of protein kinase B (AKT1).* J Biol Chem, 2020. **295**(24): p. 8120-8134.
531. Drube, S., et al., *MK2/3 Are Pivotal for IL-33-Induced and Mast Cell-Dependent Leukocyte Recruitment and the Resulting Skin Inflammation.* J Immunol, 2016. **197**(9): p. 3662-3668.
532. Dan, H.C., et al., *Akt-dependent regulation of NF-{kappa}B is controlled by mTOR and Raptor in association with IKK.* Genes Dev, 2008. **22**(11): p. 1490-500.

533. Nairz, M., et al., *Erythropoietin contrastingly affects bacterial infection and experimental colitis by inhibiting nuclear factor-kappaB-inducible immune pathways.* Immunity, 2011. **34**(1): p. 61-74.
534. Spallanzani, R.G., et al., *Distinct immunocyte-promoting and adipocyte-generating stromal components coordinate adipose tissue immune and metabolic tenors.* Sci Immunol, 2019. **4**(35).
535. Gadani, S.P., et al., *The glia-derived alarmin IL-33 orchestrates the immune response and promotes recovery following CNS injury.* Neuron, 2015. **85**(4): p. 703-9.
536. Lopez-Yrigoyen, M., et al., *Genetic programming of macrophages generates an in vitro model for the human erythroid island niche.* Nat Commun, 2019. **10**(1): p. 881.
537. Ganesh, S.K., et al., *Multiple loci influence erythrocyte phenotypes in the CHARGE Consortium.* Nat Genet, 2009. **41**(11): p. 1191-8.
538. Soranzo, N., et al., *A genome-wide meta-analysis identifies 22 loci associated with eight hematological parameters in the HaemGen consortium.* Nat Genet, 2009. **41**(11): p. 1182-90.
539. Becher, B., S. Tugues, and M. Greter, *GM-CSF: From Growth Factor to Central Mediator of Tissue Inflammation.* Immunity, 2016. **45**(5): p. 963-973.
540. Lang, R.A., et al., *Transgenic mice expressing a hemopoietic growth factor gene (GM-CSF) develop accumulations of macrophages, blindness, and a fatal syndrome of tissue damage.* Cell, 1987. **51**(4): p. 675-86.
541. Olsson, A., et al., *Single-cell analysis of mixed-lineage states leading to a binary cell fate choice.* Nature, 2016. **537**(7622): p. 698-702.
542. Gudbjartsson, D.F., et al., *Sequence variants affecting eosinophil numbers associate with asthma and myocardial infarction.* Nat Genet, 2009. **41**(3): p. 342-7.
543. Zhang, J., et al., *Loss of IKKbeta but Not NF-kappaB p65 Skews Differentiation towards Myeloid over Erythroid Commitment and Increases Myeloid Progenitor Self-Renewal and Functional Long-Term Hematopoietic Stem Cells.* PLoS One, 2015. **10**(6): p. e0130441.
544. Stein, S.J. and A.S. Baldwin, *Deletion of the NF-kappaB subunit p65/RelA in the hematopoietic compartment leads to defects in hematopoietic stem cell function.* Blood, 2013. **121**(25): p. 5015-24.
545. Wang, D., I. Paz-Priel, and A.D. Friedman, *NF-kappa B p50 regulates C/EBP alpha expression and inflammatory cytokine-induced neutrophil production.* J Immunol, 2009. **182**(9): p. 5757-62.
546. Beaulieu, L.M., et al., *Interleukin 1 receptor 1 and interleukin 1beta regulate megakaryocyte maturation, platelet activation, and transcript profile during inflammation in mice and humans.* Arterioscler Thromb Vasc Biol, 2014. **34**(3): p. 552-64.
547. Ackerman, S.J., Du, J., Xin, F., Dekoter, R., McKercher, S., Maki, R., Singh, H., Yamaguchi, Y., *To be or not to be (an eosinophil)?That is the question: transcriptionalmechanisms regulating eosinophilgenes and development.* Respiratory Medicine, 2000. **94**: p. 1135-1140.
548. Willebrand, R. and D. Voehringer, *IL-33-Induced Cytokine Secretion and Survival of Mouse Eosinophils Is Promoted by Autocrine GM-CSF.* PLoS One, 2016. **11**(9): p. e0163751.

549. Gomes, A.C., et al., *IFN-gamma-Dependent Reduction of Erythrocyte Life Span Leads to Anemia during Mycobacterial Infection.* J Immunol, 2019. **203**(9): p. 2485-2496.
550. Chen, Y.L., et al., *Proof-of-concept clinical trial of etokimab shows a key role for IL-33 in atopic dermatitis pathogenesis.* Sci Transl Med, 2019. **11**(515).
551. de Laval, B., et al., *C/EBPbeta-Dependent Epigenetic Memory Induces Trained Immunity in Hematopoietic Stem Cells.* Cell Stem Cell, 2020. **26**(5): p. 657-674 e8.
552. Kaufmann, E., et al., *BCG Educates Hematopoietic Stem Cells to Generate Protective Innate Immunity against Tuberculosis.* Cell, 2018. **172**(1-2): p. 176-190 e19.
553. Mitroulis, I., et al., *Modulation of Myelopoiesis Progenitors Is an Integral Component of Trained Immunity.* Cell, 2018. **172**(1-2): p. 147-161 e12.
554. Askenase, M.H., et al., *Bone-Marrow-Resident NK Cells Prime Monocytes for Regulatory Function during Infection.* Immunity, 2015. **42**(6): p. 1130-42.